



KOREAN SOCIETY OF
ULTRASOUND IN MEDICINE



KSUM *Open* 2017

The 48th Annual Congress of
Korean Society of Ultrasound in Medicine

May 26 (Fri) - 27 (Sat), 2017
Coex, Seoul, Korea

Abstract Book

<http://2017.ksum.or.kr>

Day 1 (Friday, 26 May)

Meet the Professor 1,2,3

Thyroid Cutting Edge of Head and Neck US

07:50-08:20 **GBR 101**

Chairperson:

Ji-Hoon Kim *Seoul National University Hospital, Korea*

MP 1 THY

07:50-08:20

US Elastography in the Head and Neck: Current Status and Future Perspectives **19**

Kunwar Bhatia

Department of Radiology, Imperial College Healthcare NHS Trust, UK

Musculoskeletal

07:50-08:20 **GBR 102**

Chairperson:

Sungjun Kim *Gangnam Severance Hospital, Korea*

MP 2 MSK

07:50-08:20

Musculoskeletal Soft Tissue Lesions: How to Make a Diagnosis **20**

Min Hee Lee

Department of Radiology, Asan Medical Center, Korea

Abdomen CEUS: Past and Current Status

07:50-08:20 **GBR 103**

Chairperson:

Jae Young Lee *Seoul National University Hospital, Korea*

MP 3 ABD-1

07:50-08:05

CEUS: Past and Current Status in Asia **21**

Byung Ihn Choi

Department of Radiology, Chung-Ang University Hospital, Korea

MP 3 ABD-2

08:05-08:20

Integration of CEUS and Elastography in Clinical Liver Patient Management **22**

Giovanna Ferraioli

Department of Internal Medicine-Infection, Fondazione IRCCS Policlinico San Matteo, University of Pavia, Italy

Scientific Sessions 1

Head & Neck, Thyroid

08:30-10:00 **GBR 101**

Chairpersons:

So Lyung Jung *The Catholic University of Korea, Seoul St. Mary's Hospital, Korea*

Jeong Hyun Lee *Asan Medical Center, Korea*

SS 1 HN-1

08:30-08:40

Ultrasonographic Determination of the Location of Parotid Gland Tumor Relative to the Facial Nerve **127**

Jeong Kyu Kim, Ho-Jin Son

Department of Otorhinolaryngology, Daegu Catholic University Medical Center, Korea

SS 1 THY-1

08:40-08:50

Comparison Between Benign & Malignant Mass **127**

Kalpana Tayade

Department of Otorhinolaryngology, MCI, India

SS 1 THY-2

08:50-09:00

The Implication of Doppler Ultrasonography in Thyroid Nodules Showing Intermediate Features on Gray-Scale US **128**

Ilah Shin

Department of Radiology, Severance Hospital, Korea

SS 1 THY-3

09:00-09:10

Different Impact of Nodule Size on Malignancy Risk According to Ultrasonography Pattern of Thyroid Nodule **128**

Min Ji Hong¹, Dong Gyu Na², Jung Hwan Baek³, Jin Yong Sung⁴, Ji-Hoon Kim⁵

¹Department of Radiology, Gachon University Gil Medical Center, Korea

²Department of Radiology, GangNeung Asan Hospital, Korea

³Department of Radiology, Asan Medical Center, Korea

⁴Department of Radiology, Daerim St. Marys Hospital, Korea

⁵Department of Radiology, Seoul National University Hospital, Korea

SS 1 THY-4

09:10-09:20

Role of Ultrasound in Predicting Tumor Invasiveness in Follicular Variant of Papillary Thyroid Carcinoma **129**

Soo Yeon Hahn¹, Jung Hee Shin¹, Young Lyun Oh², Tae Hyuk Kim³

¹Department of Radiology, Samsung Medical Center, Korea

²Department of Pathology, Samsung Medical Center, Korea

³Department of Internal Medicine-Endocrine, Samsung Medical Center, Korea

SS 1 THY-5

09:20-09:30

Thyroid Incidentalomas Detected on 18F-FDG PET/CT: Malignant Risk Stratification Using US Features According to the Guidelines **129**

Saerom Chung, Young Jun Choi, Jeong Hyun Lee, Jung Hwan Baek

Department of Radiology, Asan Medical Center, Korea

SS 1 THY-6

09:30-09:40

Indeterminate Lymph Nodes in Thyroid Cancer Patients: Rate of Lymph Node Metastasis and US Findings Predictive of the Metastasis **130**

Roh-Eul Yoo, Ji-Hoon Kim

Department of Radiology, Seoul National University Hospital, Korea

- SS 1 THY-7** **09:40-09:50**
- Computer-Aided Diagnosis System for Thyroid Nodules on Ultrasound: Initial Experience** 130
 Young Jin Yoo, Eun Ju Ha, Yoon Joo Cho, Miran Han
 Department of Radiology, Ajou University Hospital, Korea
- SS 1 THY-8** **09:50-10:00**
- Growth Rate and Size of Large Thyroid Nodules of 2 cm or Larger: Be Useful to Differentiate Malignancy from Benignity?** 131
 Song Lee, So Lyung Jung, Jinhee Jang, Hyunsuk Choi, Kookjin Ahn, Bum-Soo Kim
 Department of Radiology, The Catholic University of Korea, Seoul St. Mary's Hospital, Korea

Categorical Course 1

Musculoskeletal Upper Extremity

- 08:30-10:00** **GBR 102**
- Chairperson:**
Jung-Ah Choi Hallym University Dongtan Sacred Heart Hospital, Korea
-
- CC 1 MSK-1** **08:30-09:00**
- Shoulder** 23
 Jee Won Chai
 Department of Radiology, SMG-SNU Boramae Medical Center, Korea
- CC 1 MSK-2** **09:00-09:30**
- Elbow Ultrasound** 24
 Yusuhn Kang
 Department of Radiology, Seoul National University Bundang Hospital, Korea
- CC 1 MSK-3** **09:30-10:00**
- Ultrasound of the Wrist and Hand** 26
 Eun Hae Park
 Department of Radiology, Chonbuk National University Hospital, Korea

Special Focus Session 1

Abdomen CEUS: Hepatic & Extrahepatic Application

- 08:30-10:00** **GBR 103**
- Chairpersons:**
Won Jae Lee Samsung Medical Center, Korea
Chang Hee Lee Korea University Guro Hospital, Korea
-
- SFS 1 ABD-1** **08:30-9:00**
- CEUS for the Liver using Sonovue** 28
 Giovanna Ferraioli
 Department of Internal Medicine-Infection, Fondazione IRCCS Policlinico San Matteo, University of Pavia, Italy
- SFS 1 ABD-2** **09:00-9:30**
- CEUS for the Liver using Sonazoid** 29
 Mi-Suk Park
 Department of Radiology, Severance Hospital, Korea
- SFS 1 ABD-3** **09:30-10:00**
- Contrast Enhanced EUS for Extrahepatic Application** 30
 Dong Wan Seo
 Department of Gastroenterology, Asan Medical Center, Korea

Categorical Course 2

Physics Physics in Emerging Ultrasound Imaging Technologies

- 08:30-10:00** **Room 201**
- Chairpersons:**
Dong-Guk Paeng Jeju National University, Korea
Yangmo Yoo Sogang University, Korea
-
- CC 2 PHY-1** **08:30-9:00**
- Photoacoustic Imaging: Toward Clinical Translation** 32
 Changhan Yoon
 Department of Biomedical Engineering, Inje University, Korea
- CC 2 PHY-2** **09:00-9:30**
- Present and Future Technology for Intravascular Ultrasound Imaging** 33
 Jinhyung Park
 Department of Biomedical Engineering, Sungkyunkwan University, Korea
- CC 2 PHY-3** **09:30-10:00**
- High Frequency Ultrasound Transducers for High Definition Imaging** 34
 Hyung Ham Kim
 Department of Creative IT Engineering, Pohang University of Science and Technology, Korea

Series Course 1

Thyroid

- 10:20-11:50** **GBR 101**
- Chairpersons:**
Eun-Kyung Kim Severance Hospital, Korea
Younghen Lee Korea University Ansan Hospital, Korea
-
- SC 1 THY-1** **10:20-10:40**
- US for Thyroid Nodules: Technical Advances and Future Horizons** 35
 Kunwar Bhatia
 Department of Radiology, Imperial College Healthcare NHS Trust, UK
- SC 1 THY-2** **10:40-10:50**
- Application of the 2015 ATA Guidelines on Thyroid Nodules with Atypia of Undetermined Significance / Follicular Lesion of Undetermined Significance (AUS/FLUS) Cytology** 131
 Ji Hye Lee, Kyunghwa Han, Eun-Kyung Kim, Hee Jung Moon, Jung Hyun Yoon, Youngjean Park, Jin Young Kwak
 Department of Radiology, Severance Hospital, Korea
- SC 1 THY-3** **10:50-11:00**
- Validation of the 2015 American Thyroid Association Management Guidelines for Repeat Fine-Needle Aspiration Biopsy in Thyroid Nodules with Benign Cytology** 132
 Yeun-Yoon Kim, Kyunghwa Han, Eun-Kyung Kim, Hee Jung Moon, Jung Hyun Yoon, Youngjean Park, Jin Young Kwak
 Department of Radiology, Severance Hospital, Korea

SC 1 THY-4	11:00-11:10	133
Diagnostic Performance of Ultrasound-Based Fine Needle Aspiration Biopsy Criteria for Thyroid Malignancy: A Comparative Study Based on Six International Society Guidelines		
Eun Ju Ha ¹ , Dong Gyu Na ² , Jung Hwan Baek ³ , Jin Yong Sung ⁴ , Ji-Hoon Kim ⁵		
¹ Department of Radiology, Ajou University Hospital, Korea		
² Department of Radiology, Human Medical Imaging and Intervention Center, Korea		
³ Department of Radiology, Asan Medical Center, Korea		
⁴ Department of Radiology, Thyroid Center, Daerim St. Marys Hospital, Korea		
⁵ Department of Radiology, Seoul National University Hospital, Korea		
SC 1 THY-5	11:10-11:20	133
Ultrasound Guided Core Needle Biopsy for Intermediate or Low Suspicion Thyroid Nodules: Which Method is Effective for Diagnosis?		
Soo Yeon Hahn, Jung Hee Shin		
Department of Radiology, Samsung Medical Center, Korea		
SC 1 THY-6	11:20-11:30	134
Web-Based Thyroid Imaging Reporting and Data System: Malignant Risk Calculated by a Combination of Ultrasonography Features and Biopsy Results		
Young Jun Choi ¹ , Jung Hwan Baek ¹ , Jung Hee Shin ² , Jeong Hyun Lee ¹		
¹ Department of Radiology, Asan Medical Center, Korea		
² Department of Radiology, Samsung Medical Center, Korea		
SC 1 THY-7	11:30-11:40	134
Radiofrequency Ablation of Small Follicular Neoplasms: Initial Clinical Outcomes		
Su Min Ha ¹ , Jin Yong Sung ² , Jung Hwan Baek ³ , Dong Gyu Na ⁴ , Ji-Hoon Kim ⁵ , Hyunju Yoo ² , Ducky Lee ² , Dong Whan Choi ²		
¹ Department of Radiology, Chung-Ang University Hospital, Korea		
² Department of Radiology, Daerim St. Mary's Hospital, Korea		
³ Department of Radiology, Asan Medical Center, Korea		
⁴ Department of Radiology, GangNeung Asan Hospital, Korea		
⁵ Department of Radiology, Seoul National University Hospital, Korea		
SC 1 THY-8	11:40-11:50	135
US-Guided Radiofrequency Ablation for Primary Thyroid Cancer: Efficacy and Safety of Long-Term Follow-Up in a Large Population		
Hyun Kyung Lim ¹ , Seon Mi Baek ² , Jung Hwan Baek ³		
¹ Department of Radiology, Soonchunhyang University Seoul Hospital, Korea		
² Department of Radiology, Haeundae Sharing and Happiness Hospital, Korea		
³ Department of Radiology, Asan Medical Center, Korea		

Scientific Session 2

Musculoskeletal

10:20-11:10	GBR 102
Chairpersons:	
Won-Hee Jee The Catholic University of Korea, Seoul St. Mary's Hospital, Korea	
Ik Yang Hallym University Kangnam Sacred Heart Hospital, Korea	
SS 2 MSK-1	10:20-10:30
Acoustic Radiation Force Impulse in Peripheral Lymph Nodes Assessment 135	
Chau Tran, Quyen Vo, Hai Phan	
Department of Radiology, Medic Medical Center, Vietnam	
SS 2 MSK-2	10:30-10:40
Ultrasonographic Measurement of the Axillary Recess Thickness in Unilateral Shoulder Pain 136	
Gi-Young Park, Dong Rak Kwon, Dae-Gil Kwon, Won-Bin Jung	
Department of Rehabilitation Medicine, Daegu Catholic University Medical Center, Korea	
SS 2 MSK-3	10:40-10:50
Sonoelastography in Evaluation of Various Benign Soft Tissue Lesions 136	
Eunjin Hwang, Eun-Kyung Khil, Seun-Ah Lee, Jung-Ah Choi	
Department of Radiology, Dongtan Sacred Heart Hospital, Korea	
SS 2 MSK-4	10:50-11:00
Feasibility of Shear Wave Ultrasound Elastography in Diagnosis of Superficial Benign Soft Tissue Tumor 137	
Hyun Jung Yeoh, Tae-Yoon Kim, Jeong Ah Ryu	
Department of Radiology, Hanyang University Guri Hospital, Korea	
SS 2 MSK-5	11:00-11:10
Ultrasonographic Findings of Scleroderma Adulorum 137	
Dong-Ho Ha ¹ , Sujin Kim ²	
¹ Department of Radiology, Dong-A University Hospital, Korea	
² Department of Pathology, Dong-A University Hospital, Korea	

Case Based Review

Musculoskeletal

11:10-11:50	GBR 102
Chairperson:	
Sun Joo Lee Inje University Busan Paik Hospital, Korea	
CR -1	11:10-11:20
Musculoskeletal Case Based Reviews 138	
Hee-Dong Chae	
Department of Radiology, Seoul National University Hospital, Korea	
CR -2	11:20-11:30
Hand Disease 139	
Sekyoung Park	
Department of Radiology, Kosin University Gospel Hospital, Korea	

- CR-3** **11:30-11:40**
Trigger Finger (Pulley Thickening) / What You See is Not Everything; Venous Malformation 139
 Esther Koh
 Department of Radiology, Chonbuk National University Hospital, Korea
- CR-4** **11:40-11:50**
Elastography of Fat Necrosis / Sonography of Atypical Pulled Elbow 140
 Yura Kim
 Department of Radiology, Korea University Anam Hospital, Korea

- HI-4** **10:50-11:00**
 국내초음파기술 경쟁력-치료 초음파 분야
 최민주
 제주대학교 교수
- HI-5** **11:00-11:10**
 국내초음파기술 경쟁력-인력양성
 팽동국
 초음파의료기기연구회 총무이사
- 패널토의:** **11:10-11:50**
 사회자: 유양모 (초음파의료기기연구회 학술이사)
 패 널: 허 영 (한국산업기술평가원)
 허성오 (한국연구재단)
 윤경식 (한국보건산업진흥원)
 김철안 (Samsung Medison)
 박진웅 (Alpinion Medical System)
 최승무 (GE Healthcare)
 백창훈 (Siemens Korea)

Categorical Course 3

Abdomen US-CT/MRI Correlation

10:20-11:50 **GBR 103**

Chairpersons:

Jae-Joon Chung Gangnam Severance Hospital, Korea
Jong Young Oh Dong-A University Hospital, Korea

- CC 3 ABD-1** **10:20-10:50**
US-CT/MRI Correlation of Liver Disease 36
 Yangshin Park
 Department of Radiology, Korea University Guro Hospital, Korea
- CC 3 ABD-2** **10:50-11:10**
US-CT/MRI Correlation of Gallbladder Disease 38
 Soo Jin Kim
 Department of Radiology, National Cancer Center, Korea
- CC 3 ABD-3** **11:10-11:30**
US-CT/MRI Correlation of Pancreas Disease 39
 Yedaun Lee
 Department of Radiology, Haeundae Paik Hospital, Korea
- CC 3 ABD-4** **11:30-11:50**
US-CT/MRI Correlation of Bowel Disease 41
 Yoon Jin Lee
 Department of Radiology, Seoul National University Bundang Hospital, Korea

Hot Issues

KOR

Korean Medical Ultrasound Link Strategic Meeting for Technological Advances in Domestic Medical Ultrasound Industries via R&D Collaboration

10:20-11:50 **Room 201**

- HI-1** **10:20-10:30**
 인사말
 송태경
 초음파의료기기연구회 회장
- HI-2** **10:30-10:40**
 국내초음파기술 경쟁력-진단 시스템 분야
 송태경
 초음파의료기기연구회 회장
- HI-3** **10:40-10:50**
 국내초음파기술 경쟁력-프로브 분야
 김형함
 포항공과대학교 교수

Luncheon Symposium 1

Samsung Medison

12:00-13:10 **GBR101-102**

Chairperson:

Byung Ihn Choi Chung-Ang University Hospital, Korea

- LS 1 Samsung Medison-1** **12:00~12:20**
Hepatocellular Carcinoma: The Advantages of Imaging with CEUS
 Stephanie Wilson
 University of Calgary, Canada
- LS 1 Samsung Medison-2** **12:20~12:40**
S-Detect, a Very Smart Intelligent Assistant for Assessing Thyroid Nodules on US IA (Intelligent Assistant) or AI (Artificial Intelligence) in the Future? or in the Near Future? No Right Now!
 Jin Young Kwak
 Severance Hospital, Korea

KSUM General Assembly

KOR

12:00-13:10 **GBR 103**

KMUL General Assembly

KOR

12:00-13:10 **Room 201**

Categorical Course 4

Thyroid Thyroid Imaging Reporting and Data System (TI-RADS)

13:10-14:40 GBR 101

Chairpersons:

Joon Hyung Lee Dong-A University Hospital, Korea

Jung Hwan Baek Asan Medical Center, Korea

CC 4 THY-1 13:10-13:40

K-TIRADS - Lexicon & Risk Stratification 43

Jung Hee Shin

Department of Radiology, Samsung Medical Center, Korea

CC 4 THY-2 13:40-14:10

K-TIRADS - Comparison with Guidelines of Other Societies 45

Dong Gyu Na

Department of Radiology, GangNeung Asan Hospital, Korea

CC 4 THY-3 14:10-14:40

K-TIRADS - Current Issues and Future Directions 47

Eun Ju Ha

Department of Radiology, Ajou University Hospital, Korea

Special Focus Session 2

Musculoskeletal Advanced Musculoskeletal US

13:10-14:10 GBR 102

Chairperson:

Kil-Ho Cho Yeungnam University Medical Center, Korea

SFS 2 MSK-1 13:10-13:40

Ankle Ultrasound around the Lateral Malleolus 49

Carlo Martinoli

Department of Radiology, DISSAL University of Genova, Italy

SFS 2 MSK-2 13:40-14:10

Ultrasound of the Anterolateral Hip 50

Carlo Martinoli

Department of Radiology, DISSAL University of Genova, Italy

Young Investigator Award Session

Young Investigator Award

14:10-14:40 GBR 102

Chairperson:

Joon Koo Han Seoul National University Hospital, Korea

YIA-1 14:10-14:20

Difference in Applicability, and Reproducibility, and Elasticity Value Between Transient 140

Elastography, Point Shear Wave Elastography, and Two-Dimensional Shear Wave Elastography: A Phantom Study

Sang Min Lee¹, Jeong Min Lee², Won Chang Chang³, Hyo-Jin Kang², Su Joa An², Jeong-Hoon Lee⁴

¹Department of Radiology, Hallym University Sacred Heart Hospital, Korea

²Department of Radiology, Seoul National University Hospital, Korea

³Department of Radiology, Seoul National University Bundang Hospital, Korea

⁴Department of Internal Medicine-G-I/Hepatology, Seoul National University Hospital, Korea

YIA-2 14:20-14:30

Comparison of Diagnostic Performance Between 141

3 Modes of CAD System and an Expert Radiologist for Diagnosis of Breast Mass Detected with US

Seung Mi Ha, Boo-Kyung Han, Ji Soo Choi,

Eun Young Ko, Eun Sook Ko

Department of Radiology, Samsung Medical Center, Korea

YIA-3 14:30-14:40

Differentiation of Thyroid Malignant Lymph Node 141

from Benign Lymph Node Using Artificial Intelligence

Jeonghoon Lee¹, Sueyoung Oh², Eunsol Lee³,

Jung Hwan Baek⁴

¹Department of Computer Science and Information Engineering, Seoul National University, Korea

²Department of Computer Science and Information Engineering, Pohang University of Science and Technology, Korea

³Department of Radiology, Gyeonggi-do Public Health Care Center, Korea

⁴Department of Radiology, Asan Medical Center, Korea

Scientific Sessions 3

Abdomen

13:10-14:40 GBR 103

Chairpersons:

Seung Yon Baek Ewha Women's University Hospital, Korea

Joon-Il Choi The Catholic University of Korea, Seoul St. Mary's Hospital, Korea

SS 3 ABD-1 13:10-13:20

Ultrasound Guided Percutaneous Microwave 142

Ablation Liver Partition and Portal Vein Embolization for Planned Hepatectomy: A Promising Tool to Replace the First Step of ALPPS

Zeng Zeng, Xiaoming Fan

Department of Ultrasound, Zhejiang Provincial People's Hospital, China



- SS 3 ABD-2 13:20-13:30 142**
Manual Versus Full-Automatic Image Fusion of Real-Time Ultrasound and MR/CT Images for Radiofrequency Ablation of Hepatic Tumors: An Interim Report of a Randomized Prospective Trial
 Moon Hyung Choi, Joon-Il Choi, Young Jonn Lee, Jae Young Byun, Sung Eun Rha
Department of Radiology, The Catholic University of Korea, Seoul St. Mary's Hospital, Korea
- SS 3 ABD-3 13:30-13:40 143**
Liver Stiffness Evaluation by ARFI Imaging in Type 2 Diabetes Mellitus Patients
 Anh Nguyen, Hung Nguyen, Hai Phan
Department of Radiology, Medic Medical Center, Vietnam
- SS 3 ABD-4 13:40-13:50 144**
Additional Value of Contrast Enhanced Ultrasonography on Fusion Guided Percutaneous Biopsies of Focal Liver Lesions: Prospective Feasibility Study
 Hyo-Jin Kang¹, Jung Hoon Kim¹, Sang Min Lee², Hyun Kyung Yang¹, Joon Koo Han¹
¹Department of Radiology, Seoul National University Hospital, Korea
²Department of Radiology, Hallym University Sacred Heart Hospital, Korea
- SS 3 ABD-5 13:50-14:00 144**
What I See on Ultrasound, I Treat it with Ultrasound: Feasibility and Efficacy of Ultrasound Guided Percutaneous Glue Embolization in the Management of Iatrogenic Bleed in Cirrhotics
 Sudheer Pargewar¹, Saloni Desai², Somsharan Betgeri³, S Rajesh⁴, Amar Mukund⁵
¹Department of Radiology, Gleneagles Global Hospitals, Mumbai, India
²Department of Radiology, SIR H.N. Reliance Foundation Hospital and Research Centre, Mumbai, India
³Department of Radiology, Caritas Hospital, Kottayam, Kerala, India
⁴Department of Radiology, Renai Medicity, Kochin, India
⁵Department of Radiology, Institute of Liver and Biliary Sciences (ILBS), New Delhi, India
- SS 3 ABD-6 14:00-14:10 145**
A Deep Convolutional Neural Network for Prediction of METAVIR Score Using B-Mode Ultrasonography Images
 Tae Wook Kang¹, Jung Hyun Lee¹, Dong Hyun Sinn², Sang Yun Ha³, Chung Hwan Choi⁴, Gun Woo Lee⁴, Jong Hyon Lee⁴
¹Department of Radiology, Samsung Medical Center, Korea
²Department of Internal Medicine-G-I/Hepatology, Samsung Medical Center, Korea
³Department of Pathology, Samsung Medical Center, Korea
⁴Department of Medical Imaging Group, Samsung Electronics, Korea
- SS 3 ABD-7 14:10-14:20 146**
Prospective Comparison of Two Point Shear Wave Elastographic Techniques by Acoustic Radiation Force Impulse Quantification for Assessing Liver Stiffness in Patients with Chronic Liver Disease
 Su Joa Ahn, Jeong Min Lee, Won Chang, Sang Min Lee, Hyo-Jin Kang, Hyun Kyung Yang, Jeong Hee Yoon, Sae Jin Park, Joon Koo Han
Department of Radiology, Seoul National University Hospital, Korea
- SS 3 ABD-8 14:20-14:30 146**
Monitoring of Hepatic Steatosis Using Ultrasound: Usefulness of Acoustic Structure Quantification
 Dong Ho Lee, Jae Young Lee
Department of Radiology, Seoul National University Hospital, Korea

- SS 3 ABD-9 14:30-14:40 147**
Shear Wave Velocity Measurement Using Acoustic Radiation Force Impulse Elastography for Colorectal Cancer Liver Metastasis: Assessment of Reproducibility
 Dong Ho Lee, Jae Young Lee
Department of Radiology, Seoul National University Hospital, Korea

Special Focus Session 3

The Korean Society for Therapeutic Ultrasound Therapeutic Ultrasound

- 13:10-14:40 Room 201**
Chairpersons:
Tai-Kyong Song Sogang University, Korea
Jinwoo Chang Yonsei University, Korea
- SFS 3 KSTU-1 13:10-13:40 51**
Fundamentals of Ultrasonic Contrast Agent
 Jongbum Seo
Department of Biomedical Engineering, Yonsei University, Korea
- SFS 3 KSTU-2 13:40-14:00 59**
Clinical Applications Using Therapeutic Ultrasound
 Jae Young Lee
Department of Radiology, Seoul National University Hospital, Korea
- SFS 3 KSTU-3 14:00-14:20 60**
Histotripsy (Mechanical Tissue Fractionation) Using Therapeutic Ultrasound
 Ki Joo Pahk
Department of Biomedical Research Institute, Korea Institute of Science and Technology, Korea
- SFS 3 KSTU-4 14:20-14:40 62**
Emerging Technologies in Therapeutic Ultrasound
 Dong-Guk Paeng
Department of Biomedical Engineering, Jeju National University, Korea

Jisan Lecture

- 15:10-16:20 GBR 103**
Chairperson:
Hae Jeong Jeon Konkuk University Medical Center, Korea
- JS 1 15:15-16:00 63**
Microbubble Pumps: Ultrasound Theragnostic Agents
 Christy Holland
Department of Internal Medicine-Cardiology, University of Cincinnati, USA

Interactive Case Review-Golden Bell Quiz

- 16:20-17:40 GBR 103**
Director:
So Yeon Kim Asan Medical Center, Korea
- MC:** Mye Sun Park (Asan Medical Center, Korea)
 Ki Chang Han (Severance Hospital, Korea)

Day 2 (Saturday, 27 May)

Meet the Professor 4,5,6

Pediatric

07:50-08:20 **GBR 101**

Chairperson:

Gye Yeon Lim *The Catholic University of Korea, Yeouido St. Mary's Hospital, Korea*

MP 4 PED **07:50-08:20** **64**

Contrast Enhanced Ultrasound in Pediatrics

M Beth McCarville

Department of Radiology, St. Jude Children's Research Hospital, USA

Genitourinary

07:50-08:20 **GBR 102**

Chairpersons:

Byung Chul Kang *Ewha Womans University Mokdong Hospital, Korea*

Hak Jong Lee *Seoul National University Bundang Hospital, Korea*

MP 5 GU **07:50-08:20** **65**

PI-RADS Based Transrectal US Biopsy of the Prostate

Byung Kwan Park

Department of Radiology, Samsung Medical Center, Korea

Breast Screening with Automated Breast (ABUS)

07:50-08:20 **GBR 103**

Chairperson:

Hak Hee Kim *Asan Medical Center, Korea*

MP 6 BR **07:50-08:20** **66**

Screening with Automated Breast (ABUS) Coronal Imaging: How to Reduce Call Backs

Beverly Hashimoto

Department of Radiology, Virginia Mason Medical Center, USA

Categorical Course 5

Cardiovascular Carotid US

08:30-10:00 **GBR 101**

Chairperson:

Bae Young Lee *The Catholic University of Korea, St. Paul's Hospital, Korea*

CC 5 CV-1 **08:30-08:50** **67**

US Evaluation of Carotid Artery: How to Do and How to Report

Eun-Ah Park

Department of Radiology, Seoul National University Hospital, Korea

CC 5 CV-2 **08:50-09:10** **68**

US Evaluation of Lower Extremity Artery:

How to Do and How to Report

Jeonghyun Jo

Department of Radiology, Dong-A University Hospital, Korea

CC 5 CV-3 **09:10-09:30** **72**

US Evaluation of Lower Extremity Vein:

How to Do and How to Report

You Seon Song

Department of Radiology, Pusan National University Hospital, Korea

CC 5 CV-4 **09:30-09:50** **74**

US Evaluation of Procedure Related Complication

Eun Ju Chun

Department of Radiology, Seoul National University Bundang Hospital, Korea

Scientific Sessions 4

Genitourinary

08:30-08:50 **GBR 102**

Chairperson:

Eun Ju Lee *Ajou University Hospital, Korea*

SS 4 GU-1 **08:30-08:40** **147**

Renal Cortical Elastography: Normal Values and Variations

Harsh Singh¹, Om Biju Panta², Umesh Khanal³, Ram Kumar Ghimire⁴

¹Department of Radiology, King George Medical University, Lucknow, India

²Department of Radiology, Siriraj Hospital, Thailand

³Department of Radiology, Tribhuvan University Teaching Hospital, Nepal

SS 4 GU-2 **08:40-08:50** **148**

Mimics of Renal Calculi

Prakash Tayade

Department of Radiology, MCI, India

Pediatric

08:50-10:00 **GBR 102**

Chairpersons:

Young Seok Lee *Dankook University Hospital, Korea*

Hye-Kyung Yoon *Kangwon National University Hospital, Korea*

SS 4 PED-1 **08:50-09:00** **148**

Accurate Measurement of Liver Stiffness Using Shear Wave Elastography in Children and the Role of Stability Index

Eun Kyoung Hong¹, Young Hun Choi¹,

Jung-Eun Cheon¹, Woo Sun Kim¹, In-One Kim¹,

Sun Young Kang²

¹Department of Radiology, Seoul National University Hospital, Korea

²Department of Clinical Ultrasound, DongSeo Medicare Co., Ltd. and SuperSonic Imagine, Korea

SS 4 PED-2	09:00-09:10	149
Ultrasonography of Normal Filum Terminale		
Myoungae Kwon, Bo-Kyung Je, Doran Hong Department of Radiology, Korea University Ansan Hospital, Korea		
SS 4 PED-3	09:10-09:20	149
Normal Change Limit of Pediatric Testicular Volume and Elasticity on Ultrasonography Including Shear Wave Elastography		
Hyun Joo Shin ¹ , Myung-Joon Kim ¹ , Haesung Yoon ¹ , Yong Seung Lee ² , Sang Won Han ² , Yun Ho Roh ³ , Mi-Jung Lee ¹		
¹ Department of Radiology, Severance Hospital, Korea		
² Department of Urology, Severance Hospital, Korea		
³ Department of Statistics, Yonsei University College of Medicine, Korea		
SS 4 PED-4	09:20-09:30	150
Localized Cystic Disease of the Kidney in Children: US Findings		
Haesung Yoon, Myung-Joon Kim, Mi-Jung Lee, Hyun Joo Shin Department of Radiology, Severance Hospital, Korea		
SS 4 PED-5	09:30-09:40	150
A Preliminary Study of Shear Wave Elastography for the Evaluation of Varicocele in Adolescent and Young Adults		
Young Jin Ryu ¹ , Young Hun Choi ² , Jung-Eun Cheon ² , Woo Sun Kim ² , In-One Kim ² , Ji Eun Park ³		
¹ Department of Radiology, Seoul National University Bundang Hospital, Korea		
² Department of Radiology, Seoul National University Hospital, Korea		
³ Department of Radiology, Kyungpook National University Hospital, Korea		
SS 4 PED-6	09:40-09:50	151
Risk Estimation for Biliary Atresia in Neonatal Cholestasis: Development and Validation of a Predictive Score		
Jeong Rye Kim, Hee Mang Yoon, Young Ah Cho, Jin Seong Lee, Ah Young Jung Department of Radiology, Asan Medical Center, Korea		
SS 4 PED-7	09:50-10:00	151
Diagnostic Value of the Renal Doppler Ultrasound for Detecting Renovascular Hypertension in Children		
Seunghyun Lee, Young Hun Choi, Yeon Jin Cho, Ji Young Ha, Jung-Eun Cheon, Woo Sun Kim, In-One Kim Department of Radiology, Seoul National University Hospital, Korea		

Special Focus Session 4,5

Breast Automated Breast (ABUS)

08:30-10:00	GBR 103
Chairpersons:	
Beverly Hashimoto Virginia Mason Medical Center, USA	
Woo Kyung Moon Seoul National University Hospital, Korea	
SFS 4 BR-1	08:30-09:00
Introduction to Automated Breast Ultrasound (ABUS) Coronal Imaging: Normal and Abnormal Findings	
Beverly Hashimoto Department of Radiology, Virginia Mason Medical Center, USA	

SFS 4 BR-2	09:00-09:30	76
ABUS: Image Quality and Artifact		
Sung Hun Kim Department of Radiology, The Catholic University of Korea, Seoul St. Mary's Hospital, Korea		
SFS 4 BR-3	09:30-10:00	77
Clinical Experience and Future of Automated Breast Ultrasound		
Joo Hee Cha Department of Radiology, Asan Medical Center, Korea		

Pediatric US for Pediatric Oncology

10:20-11:50	GBR 101
Chairperson:	
Kwan Seop Lee Hallym University Sacred Heart Hospital, Korea	
SFS 5 PED-1	10:20-10:45
US for Pediatric Liver Tumors	
Mi-Jung Lee Department of Radiology, Severance Hospital, Korea	
SFS 5 PED-2	10:45-11:10
US for Pediatric Retroperitoneal Tumors	
Tae Yeon Jeon Department of Radiology, Samsung Medical Center, Korea	
SFS 5 PED-3	11:10-11:35
Problem Solving Abdomen Ultrasound for Pediatric Oncology Patients	
M Beth McCarville Department of Radiology, St. Jude Children's Research Hospital, USA	

Categorical Course 6

Genitourinary Genitourinary Emergency US

10:20-11:50	GBR 102
Chairpersons:	
Sung Il Jung Konkuk University Medical Center, Korea	
Seong Kuk Yoon Dong-A Medical Center, Korea	
CC 6 GU-1	10:20-10:40
US for Acute Pelvic Pain	
Moon Hyung Choi Department of Radiology, The Catholic University of Korea, Seoul St. Mary's Hospital, Korea	
CC 6 GU-2	10:40-11:00
US of Acute Flank Pain	
Ki Choon Sim Department of Radiology, Korea University Anam Hospital, Korea	
CC 6 GU-3	11:00-11:20
US of Acute Scrotal Pain	
Young Sup Shim Department of Radiology, Gachon University Gil Medical Center, Korea	
CC 6 GU-4	11:20-11:40
US of Acute Abdominal Pain in Pregnancy	
Sung Kyoung Moon Department of Radiology, Kyung Hee University Hospital, Korea	

Series Course 2

Breast

10:20-11:50

GBR 103

Chairpersons:

Boo-Kyung Han Samsung Medical Center, Korea

Eun-Kyung Kim Severance Hospital, Korea

SC 2 BR-1

10:20-10:40

Artificial Intelligence in Breast US

94

Bong Joo Kang

Department of Radiology, The Catholic University of Korea,
Seoul St. Mary's Hospital, Korea

SC 2 BR-2

10:40-10:50

The Value of 3D Automated Breast Volume Scanner (ABVS) as a Breast Screening Tool

152

Yi Li (Grace) Wong, Sharifah Majedah Idrus Alhabshi

Department of Radiology, Hospital University Kebangsaan
Malaysia (HUKM), KL, Malaysia

SC 2 BR-3

10:50-11:00

Value of Ultrasound-Guided Fine Needle Aspiration in Diagnosing Axillary Lymph Node Recurrence After Breast Cancer Surgery

153

Youngjean Park, Eun-Kyung Kim, Hee Jung Moon,
Jung Hyun Yoon, Min Jung Kim

Department of Radiology, Severance Hospital, Korea

SC 2 BR-4

11:00-11:10

The Usefulness of Breast Ultrasound CAD to Diagnose Breast Cancer Based on the BIRADS Lexicon and Quantitative Characteristics

153

Yumi Kim¹, Bong Joo Kang², Sung Hun Kim²,
Jung Min Lee²

¹Department of Radiology, The Catholic University of
Korea, Bucheon St. Mary's Hospital, Korea

²Department of Radiology, The Catholic University of
Korea, Seoul St. Mary's Hospital, Korea

SC 2 BR-5

11:10-11:20

Application of Computer Aided Diagnosis (CAD) on Breast US: Evaluation of Diagnostic Performances and Agreement of Radiologists According to Different Levels of Experiences

154

Eun Cho¹, Eun-Kyung Kim², Min Jung Kim²,
Hee Jung Moon², Youngjean Park²,
Jung Hyun Yoon²

¹Department of Radiology, Dong-A University Hospital,
Korea

²Department of Radiology, Severance Hospital, Korea

SC 2 BR-6

11:20-11:30

Two-View Scanning Technique of Automated Breast Ultrasound System (ABUS) for Breast Cancer Screening: Comparison on the Diagnostic Performance with Three-View Scan Technique

154

Soo-Yeon Kim, Jung Min Chang, Woo Kyung Moon
Department of Radiology, Seoul National University
Hospital, Korea

SC 2 BR-7

11:30-11:40

The Benefits and Harms of Breast Ultrasound CAD; Focused on the Borderline Lesions

155

Yumi Kim¹, Bong Joo Kang², Na Young Jung¹,
Sung Hun Kim², Jung Min Lee²

¹Department of Radiology, The Catholic University of
Korea, Bucheon St. Mary's Hospital, Korea

²Department of Radiology, The Catholic University of
Korea, Seoul St. Mary's Hospital, Korea

SC 2 BR-8

11:40-11:50

Significance of Microvascular Evaluation in the Dilatation of Mammary Ducts: Influence on Diagnostic Performance

155

Eun Sil Kim¹, Bo Kyoung Seo¹, Ah Young Park²,
Ok Hee Woo³, Kyoonsoon Jung⁴, Kyu Ran Cho⁵,
Jaehyung Cha⁶

¹Department of Radiology, Korea University Ansan
Hospital, Korea

²Department of Radiology, Bundang CHA Medical Center,
Korea

³Department of Radiology, Korea University Guro Hospital,
Korea

⁴Department of Diagnostic Radiology, Hallym University
Sacred Heart Hospital, Korea

⁵Department of Radiology, Korea University Anam Hospital,
Korea

⁶Department of Medical Science Research Center, Korea
University Ansan Hospital, Korea

Luncheon Symposium 2

Bracco

CEUS in Abdominal Imaging

12:00-13:10

GBR 101

Chairperson:

Won Jae Lee Samsung Medical Center, Korea

LS 2 Bracco-1

12:00-12:30

Doppler US and CEUS for Assessing Renal Artery Stenosis

Byung Kwan Park

Samsung Medical Center, Korea

LS 2 Bracco-2

12:30-13:00

Contrast-Enhanced US: Extra-Hepatic Application in the Abdomen

Se Hyung Kim

Seoul National University Hospital, Korea

Luncheon Symposium 3

Philips

EPIQ, Evolution 3.0

12:00-13:10

GBR 102

Chairperson:

Joon Koo Han Seoul National University Hospital, Korea

LS 3 Philips

12:00-13:00

Liver Elastography: Recent Progress

Jae Young Lee

Seoul National University Hospital, Korea

Luncheon Symposium 4

Toshiba

Vascularity and Variance

12:00-13:10

GBR 103

Chairperson:

Byung Ihn Choi Chung-Ang University Hospital, Korea

LS 4 Toshiba-1 12:00-12:25

Vascularity in Breast

Bo Kyoung Seo

Korea University Ansan Hospital, Korea

LS 4 Toshiba-2 12:25-12:50

Variance in Abdomen

Dong Ho Lee

Seoul National University Hospital, Korea

Categorical Course 7

Pediatrics US for Pediatrics Endocrine Imaging

13:10-14:40

GBR 101

Chairperson:

Hee Jung Lee Keimyung University Dongsan Medical Center, Korea

CC 7 PED-1 13:10-13:35

US for Precocious Puberty

Jung-Eun Cheon

Department of Radiology, Seoul National University Hospital, Korea

95

CC 7 PED-2 13:35-14:00

Thyroid US in Children and Adolescents

Hyun Sook Hong

Department of Radiology, Soonchunhyang University Bucheon Hospital, Korea

98

CC 7 PED-3 14:00-14:25

Breast US in Children and Adolescents

Yun-Woo Chang

Department of Radiology, Soonchunhyang University Seoul Hospital, Korea

102

Special Focus Session 6

Genitourinary Recent Issues in Genitourinary US

13:10-14:40

GBR 102

Chairpersons:

Min Hoan Moon SMG-SNU Boramae Medical Center, Korea

Young Taik Oh Severance Hospital, Korea

SFS 6 GU-1 13:10-13:35

An Update on the Value of Elastography in the Diagnosis of Prostate Cancer

Trong Nguyen Quang

Department of Radiologist at Imaging, Franco-Vietnamese Hospital, Vietnam

106

SFS 6 GU-2 13:35-14:00

MR US Fusion Imaging

Sung Il Hwang

Department of Radiology, Seoul National University Bundang Hospital, Korea

112

SFS 6 GU-3

14:00-14:25

Multiparametric US for Focal Testicular Lesions

114

Trong Nguyen Quang

Department of Radiologist at Imaging, Franco-Vietnamese Hospital, Vietnam

Categorical Course 8

Breast Advanced Techniques and Interventions in Breast US

13:10-14:40

GBR 103

Chairpersons:

Eun Suk Cha Ewha Womans University Mokdong Hospital, Korea

Sun Mi Kim Seoul National University Bundang Hospital, Korea

CC 8 BR-1 13:10-13:40

Advanced Techniques in Breast Ultrasound

119

Ah Young Park

Department of Radiology, Bundang CHA Medical Center, Korea

CC 8 BR-2 13:40-14:10

Intervention in Breast US

122

Eun Young Ko

Department of Radiology, Samsung Medical Center, Korea

CC 8 BR-3 14:10-14:40

Image-Pathology Concordance/Discordance Evaluation after US Guided Intervention

126

Youngjean Park

Department of Radiology, Severance Hospital, Korea

Hands-on Session

Hands-on Session 1

15:10-16:10

GBR 101-102

HS 1 Abdomen-Liver Elastography

Ji Eun Kim

Gyeongsang National University Hospital, Korea

Genitourinary-Kidney, bladder US & Doppler

Sung Yoon Park

Severance Hospital, Korea

Abdomen-General

Eun Sun Lee

Chung-Ang University Hospital, Korea

Abdomen-Liver Intervention (Biopsy & Fusion)

Moon Hyung Choi

The Catholic University of Korea, Seoul St. Mary's Hospital, Korea

Abdomen-Liver Intervention (Biopsy & Fusion)

Tae Wook Kang

Samsung Medical Center, Korea

Abdomen-Radiofrequency Ablation

Dong Ho Lee

Seoul National University Hospital, Korea

Breast-Intervention

Soo-Yeon Kim

Seoul National University Hospital, Korea

Pediatric-Developmental Dysplasia of the Hip

Jung-Eun Cheon

Seoul National University Hospital, Korea

Cardiovascular-Carotid

Ki Seok Choo

Pusan National University Hospital, Korea

Head&Neck / Thyroid-Radiofrequency Ablation

Eun Ju Ha

Ajou University Hospital, Korea

Musculoskeletal-Shoulder

Min A Yoon

Korea University Guro Hospital, Korea

Musculoskeletal-Nerve

Hyejung Choo

Inje University Busan Paik Hospital, Korea

Abdomen-Liver Intervention (Biopsy & Fusion)

Moon Hyung Choi

The Catholic University of Korea, Seoul St. Mary's Hospital, Korea

Abdomen-Liver Intervention (Biopsy & Fusion)

Tae Wook Kang

Samsung Medical Center, Korea

Abdomen-Radiofrequency Ablation

Dong Ho Lee

Seoul National University Hospital, Korea

Breast-Intervention

Su Min Ha

Chung-Ang University Hospital, Korea

Pediatric-Developmental Dysplasia of the Hip

So-Young Yoo

Samsung Medical Center, Korea

Cardiovascular-Carotid

Ki Seok Choo

Pusan National University Hospital, Korea

Head&Neck / Thyroid-Radiofrequency Ablation

Eun Ju Ha

Ajou University Hospital, Korea

Musculoskeletal-Shoulder

Min A Yoon

Korea University Guro Hospital, Korea

Musculoskeletal-Nerve

Hyejung Choo

Inje University Busan Paik Hospital, Korea

Hands-on Session 2

16:10-17:10

GBR 101-102

HS 2 Abdomen-Liver Elastography

Ji Eun Kim

Gyeongsang National University Hospital, Korea

Genitourinary-Kidney, bladder US & Doppler

Sung Yoon Park

Severance Hospital, Korea

Abdomen-General

Eun Sun Lee

Chung-Ang University Hospital, Korea

Scientific Exhibition

Abdomen

SE 001

Is Contrast-Enhanced Ultrasound with Sonazoid Helpful for Percutaneous Biopsies of Focal Hepatic Lesions?: Prospective Feasibility Study 157
Sang Min Lee¹, Jung Hoon Kim², Hyun Kyung Yang²,
Hyo-Jin Kang², Joon Koo Han²
¹Department of Radiology, Hallym University Sacred Heart Hospital, Korea
²Department of Radiology, Seoul National University Hospital, Korea

SE 002

Contrast Enhanced Ultrasound for the Characterization of Hepatocellular Carcinoma 157
Hoang Nguyen Huy, Hanh Tuong Thi Hong,
Riep Tran Van
Department of Radiology, 108 Military Central Hospital, Vietnam

SE 003

The 100 Most-Cited Articles Focused on Ultrasound Imaging: A Bibliometric Analysis 158
Eun Joo Yun, Ji Yoon Moon, Chul Soon Choi,
Dae Young Yoon
Department of Radiology, Kangdong Sacred Heart Hospital, Korea

SE 004

A Study of Ultrasound Signs in Acute Pancreatitis, Swelling Form 158
Narantungalag Nyamkhuu¹, Badamsed Tserendorj²
¹Department of Radiology, Mongolian National University of Medical Sciences, Mongolia
²Department of Radiology, Shastin Hospital in Ulaanbaatar, Mongolia

SE 005

Ultrasonographic Atlas of Spleen 159
Gayoung Choi, Kyeong Ah Kim, Jeong Woo Kim,
Yang Shin Park, Jongmee Lee, Jae Woong Choi,
Chang Hee Lee, Cheol Min Park
Department of Radiology, Korea University Guro Hospital, Korea

SE 006

Determination of Hepatic Segment in Intrahepatic Tumor Using Ultrasound Contrast Agent (Sonazoid): Can it Help the Surgeon Decide Hepatic Segmentectomy or Sectionectomy? 159
Sangyun Lee, Jinhan Cho, Heejin Kwon,
Jongyoung Oh, Younghoon Roh
Department of Radiology, Dong-A University Hospital, Korea

SE 007

The Study and Characterization of Indefinite Spleen Lesions in Primary Ultrasound after Oncoming by Emergency as Abdominal Trauma: Capability of MRI 159
Undarmaa Dorjpalam, Enkhbold Sereejav
Department of Radiology, The First Central Hospital of Mongolia, Mongolia

SE 008

Pictorial Review of Ultrasound and Doppler in Diagnosis and Post Endovascular Intervention Surveillance of Patients with Budd-Chiari Syndrome 160
Saloni Desai¹, Sudheer Pargewar², Nitesh Agrawal³,
S Rajesh⁴, Amar Mukund⁵
¹Department of Radiology, SIR H.N. Reliance Foundation Hospital and Research Centre, Mumbai, India
²Department of Radiology, Gleneagles Global Hospital, Mumbai, India
³Department of Radiology, Fortis Escorts Heart Institute and Research Centre, Okhla, New Delhi, India
⁴Department of Radiology, Renai Medicity, Kochin, India
⁵Department of Radiology, Institute of Liver and Biliary Sciences (ILBS), New Delhi, India

SE 009

Competency of Ultrasound Diagnosis of Acute Appendicitis with Histo-Pathological Findings 161
Soyolmaa Erdenebaatar¹, Sarnaitsetseg Munkhbat²,
Baigalmaa Jantsansengee³, Bilegt Altangerel³
¹Department of Radiology, National Center for Communicable Diseases, Mongolia
²Department of Radiology, Intermed Hospital of Mongolia, Mongolia
³Department of Epidemiology, Field Epidemiology Training, National Center for Communicable Diseases, Mongolia

SE 010

Diagnosing Necrotic Type of Acute Pancreatitis 161
Saruulzaya Rentsensambuu, Badamsed Tserendorj
Department of Radiology, ACH Medical Institute of Mongolia, Mongolia

SE 011

Ultrasound Characteristics of Stomach Cancer 162
Amartuvshin Bor, Tuvshinjargal Tsendjav,
Tsetsegee J., Erdembileg Tsevegmid
Department of Radiology, Tsetsjin Clinic, Mongolia

SE 012

Ultrasonic Characterization of Chronic Constipation 162
Tuvshinjargal Tsendjav¹, Amartuvshin Bor¹, Tsetsegee J.¹,
Erdembileg Tsevegmid²
¹Department of Radiology, Tsetsjin Clinic, Mongolia
²Department of Radiology, Gurvan Gal Teaching Hospital, School of Medicine, Mongolian National University of Medical Sciences, Mongolia

SE 013

From Basics to Clinical Practice of Abdominal Ultrasonography for Beginners: To be an Expert! 163
Jeong Woo Kim, Chang Hee Lee, Yang Shin Park,
Jongmee Lee, Jae Woong Choi, Kyeong Ah Kim,
Cheol Min Park
Department of Radiology, Korea University Guro Hospital, Korea

SE 014

Typical and Atypical Paradoxical Hepatic Tumors 163
Sudheer Pargewar¹, Saloni Desai², Nitesh Agrawal³,
S Rajesh⁴
¹Department of Radiology, Gleneagles Global Hospital, Mumbai, India
²Department of Radiology, SIR H.N. Reliance Foundation Hospital and Research Centre, Mumbai, India
³Department of Radiology, Fortis Escorts Heart Institute and Research Centre, Okhla, New Delhi, India
⁴Department of Radiology, Renai Medicity, Kochin, India

SE 015

Focal Intrasplenic Extramedullary Hematopoiesis Masquerading as Tubercular Abscess 164

Saloni Desai¹, Sudheer Pargewar², Nitesh Agrawal³, S Rajesh⁴, Chhagan Bihari⁵, Ankur Arora⁶
¹Department of Radiology, SIR H.N. Reliance Foundation Hospital and Research Centre, Mumbai, India
²Department of Radiology, Gleneagles Global Hospital, Mumbai, India
³Department of Radiology, Fortis Escorts Heart Institute and Research Centre, Okhla, New Delhi, India
⁴Department of Radiology, Renai Medicity, Kochin, India
⁵Department of Pathology, Institute of Liver and Biliary Sciences (ILBS), New Delhi, India
⁶Department of Radiology, Worthing Hospital, Western Sussex Hospital, Nhs Foundation Trust, United Kingdom

SE 016

Correlation between Thigh Fat Content Measured on MRI and Fatty Change of the Liver on Ultrasound 165

Hee Jin Park
Department of Radiology, Kangbuk Samsung Medical Center, Korea

SE 017

Degree of Hepatic Steatosis in Chronic Hepatitis C Patient: Comparison with Healthy and Chronic Hepatitis B Patients 165

Chul Soon Choi, Eun Joo Yun, Kyoung Ja Lim, Young Lan Seo, Dae Young Yoon
Department of Radiology, Kangdong Sacred Heart Hospital, Korea

SE 018

Clinical Utility of Real-Time Fusion Guidance for Percutaneous Biopsy of Focal Hepatic Lesions 166

Su Joa Ahn, Jeong Min Lee, Won Chang, Sang Min Lee, Hyo-Jin Kang, Hyun Kyung Yang, Joon Koo Han
Department of Radiology, Seoul National University Hospital, Korea

Breast

SE 019

Near-Infrared Photothermal Therapy of Triple Negative Breast Cancer Using Anti-EGFR Antibody-Conjugated Gold Nanorods 166

Meihua Zhang, Hoe Suk Kim, Tiefeng Jin, Woo Kyung Moon
Department of Radiology, Seoul National University Hospital, Korea

SE 020

Differentiation of Benign and Metastatic Axillary Lymph Nodes in Breast Cancer: Additive Value of Shear Wave Elastography to B-mode Ultrasound 167

Yu-Mee Sohn, Mirinae Seo
Department of Radiology, Kyung Hee University Medical Center, Korea

SE 021

Ultrasonography Findings of Male Breast Disease, with Pathological Correlation: A Pictorial Essay 167

Youngseon Kim, Mi Soo Hwang
Department of Radiology, Yeungnam University Medical Center, Korea

SE 022

Interobserver Agreements of Breast Ultrasound Categorization Modified by the ABCS-K for the Mammography and Ultrasonography Study for Breast Cancer Screening Effectiveness (Must Be) Trial 168

Eun Jung Choi¹, Eun Hye Lee², You Me Kim³, Sung Hun Kim⁴, Jae Kwan Jun⁵
¹Department of Radiology, Chonbuk National University Hospital, Korea
²Department of Radiology, Soonchunhyang University Bucheon Hospital, Korea
³Department of Radiology, Dankook University Hospital, Korea
⁴Department of Radiology, The Catholic University of Korea, Seoul St. Mary's Hospital, Korea
⁵Department of National Cancer Control Institute, Korea Cancer Center Hospital, Korea

SE 023

Value of Combination of Shear-Wave Elastography and Color Doppler US for Preventing Unnecessary Excision of Equivocal Fibroepithelial Lesions Diagnosed by Core Needle Biopsy 168

Ji Soo Choi, Eun Young Ko, Boo-Kyung Han, Eun Sook Ko
Department of Radiology, Samsung Medical Center, Korea

SE 024

Early Prediction of Response to Neoadjuvant Chemotherapy in Breast Cancer: Quantitative Analysis of Dynamic Contrast-Enhanced Ultrasound 169

Yun Ju Kim¹, Sung Hun Kim², Byung Joo Song³, Ahwon Lee², Bong Joo Kang²
¹Department of Radiology, National Cancer Center, Korea
²Department of Radiology, The Catholic University of Korea, Seoul St. Mary's Hospital, Korea
³Department of Surgery, The Catholic University of Korea, Bucheon St. Mary's Hospital, Korea

SE 025

Development and Estimation of the Quality Control Program for Breast Ultrasound in Must-Be Trial: Initial Results 169

Hye Won Kim¹, Sun Hye Jeong², You Me Kim³, Keum Won Kim⁴, Jin Hwa Lee⁵, Eun Jung Choi⁶, Minseo Bang⁷, Yun Woo Chang⁸, Jae Kwan Jun⁹, Eun Hye Lee²
¹Department of Radiology, Wonkwang University School of Medicine & Hospital, Korea
²Department of Radiology, Soonchunhyang University Bucheon Hospital, Korea
³Department of Radiology, Dankook University Hospital, Korea
⁴Department of Radiology, Konyang University Hospital, Korea
⁵Department of Radiology, Dong-A University Hospital, Korea
⁶Department of Radiology, Chonbuk National University Hospital, Korea
⁷Department of Radiology, Ulsan University Hospital, Korea
⁸Department of Radiology, Soonchunhyang University Seoul Hospital, Korea
⁹Department of Preventive Medicine, National Cancer Center, Korea

SE 026

Imaging Findings of Medullary Carcinoma of the Breast 170

Hyeon Ji Jang, Bo Bae Choi
Department of Radiology, Chungnam National University Hospital, Korea

SE 027	Breast Lesions Correlation of the Ultrasound BI-RADS Classification with Pathologic Results	171	SE 034	Efficacy of Doppler Ultrasonography to Detect and Differentiate MR-Detected Breast Lesions	174
	Sarnaitsetseg Munkhbat, Khulan Khurelsukh, Zaya Duisyenbi, Altantsetseg Adiya, Chantsalsuren Galbaatar Department of Radiology, Intermed Hospital, Mongolia			Hankyul Kim, Boo-Kyung Han, Eun Young Ko, Eun Sook Ko, Ji Soo Choi, Joo Hyun Park Department of Radiology, Samsung Medical Center, Korea	
SE 028	Breast Augmentation: Pictorial Review of Ultrasonographic, Mammographic, and Magnetic Resonance Imaging Findings	171	SE 035	Contrast-Enhanced US Parameters in Breast Cancer: Correlations with Prognostic Factors	175
	Sang Soo Roh, Young Mi Park, Gi Won Shin, Sun Joo Lee, Hye Jung Choo, Dong Wook Kim, Yoo Jin Lee, Hae Woong Jeong Department of Radiology, Inje University Busan Paik Hospital, Korea			Youn Joo Lee ¹ , Sung Hun Kim ² , Bong Joo Kang ² , Yun Ju Kim ³ ¹ Department of Radiology, The Catholic University of Korea, Daejeon St. Mary's Hospital, Korea ² Department of Radiology, The Catholic University of Korea, Seoul St. Mary's Hospital, Korea ³ Department of Radiology, National Cancer Center, Korea	
SE 029	Sonographic Findings of Radial Scar Detected on Screening Breast US	172	SE 036	Doppler Ultrasonography Features of Breast Cancer	175
	Jin Hwa Lee ¹ , Jae Hong Yoon ¹ , Eun Cho ¹ , Sujin Kim ² ¹ Department of Radiology, Dong-A University Hospital, Korea ² Department of Pathology, Dong-A University Hospital, Korea			Fatima Kakhkharova ¹ , Jamoliddin Kahhorov ¹ , Alisher Kakhkharov ² ¹ Department of Radiology, National Oncologic Scientific Center, Uzbekistan ² Department of Oncology and Radiology, Tashkent Medical Academy, Uzbekistan	
SE 030	Role of Ultrasound: Hypoxia-Angiogenesis Pathway in Breast Cancer	172	SE 037	Breast Diseases Involving the Whole Breast: Clinicopathologic and Imaging Features	176
	Myoungae Kwon ¹ , Bo Kyoung Seo ¹ , Kyu Ran Cho ² , Ok Hee Woo ³ , Ju-Han Lee ⁴ , Jaehyung Cha ⁵ ¹ Department of Radiology, Korea University Ansan Hospital, Korea ² Department of Radiology, Korea University Anam Hospital, Korea ³ Department of Radiology, Korea University Guro Hospital, Korea ⁴ Department of Pathology, Korea University Ansan Hospital, Korea ⁵ Department of Medical Science Research Center, Korea University Ansan Hospital, Korea			Gi Won Shin ¹ , Young Mi Park ¹ , Suk Jung Kim ² , Hyun Kyung Jung ² ¹ Department of Radiology, Inje University Busan Paik Hospital, Korea ² Department of Radiology, Inje University Haeundae Paik Hospital, Korea	
SE 031	Breast Parenchymal Echogenicity and Neoadjuvant Chemotherapy in Postmenopausal Breast Cancer	173	SE 038	Silicone Injection of Breasts and Gluteal Region: Correlation of Ultrasound and Computed Tomography Scan Findings	176
	Alisher Kakhkharov ¹ , Jamoliddin Kahhorov ² , Fatima Kakhkharova ² ¹ Department of Oncology and Radiology, Tashkent Medical Academy, Uzbekistan ² Department of Radiology, National Scientific Oncologic Center, Uzbekistan			Ming Huan Cheng, Yin Eie Teo Department of Radiology, Keningau Hospital, Malaysia	
SE 032	Ultrasound Signs of Breast Cancer as Risk Factors of Further Metastases Development	173	SE 039	Complication after Breast Implants	176
	Nigora Atakhanova ¹ , Alisher Kakhkharov ¹ , Jamoliddin Kahhorov ² ¹ Department of Oncology and Radiology, Tashkent Medical Academy, Uzbekistan ² Department of Radiology, National Scientific Oncologic Center, Uzbekistan			Otgontuya Tserenjav ¹ , Tumendemberel Danga ² , Ul-Oldokh Sumya ² ¹ Department of Radiology, National Second Hospital of Mongolia, Mongolia ² Department of Radiology, Khovd Province Hospital, Mongolia	
SE 033	Imaging Features of Lobular Neoplasia in the Breast Diagnosed at Ultrasound-Guided Biopsies	174	SE 040	Spontaneous Infarction of Phyllodes Tumor of the Breast in a Postpartum Woman: A Case Report	177
	Ik Jung Hwang, Young Mi Park, Gi Won Shin, Sun Joo Lee, Hye Jung Choo, Dong Wook Kim, Yoo Jin Lee, Hae Woong Jeong Department of Radiology, Inje University Busan Paik Hospital, Korea			Yoogi Cha, Hye Won Kim Department of Radiology, Wonkwang University School of Medicine & Hospital, Korea	
			SE 041	Benign Skin Lesion in Premammary Zone of the Breast Mimicking Malignant Breast Parenchymal Lesion: A Case Report	177
				Jae Hong Yoon ¹ , Jin Hwa Lee ¹ , Eun Cho ¹ , Sujin Kim ² ¹ Department of Radiology, Dong-A University Hospital, Korea ² Department of Pathology, Dong-A University Hospital, Korea	

- SE 042**
A Rare Case of Solitary Fibrous Tumor of the Breast: Radiologic Findings and a Brief Review 177
So Yeon Park¹, Ok Hee Woo¹, Hye Seon Shin¹,
Kyu Ran Cho², Bo Kyoung Seo³
¹Department of Radiology, Korea University Guro Hospital, Korea
²Department of Radiology, Korea University Anam Hospital, Korea
³Department of Radiology, Korea University Ansan Hospital, Korea
- SE 043**
Breast Cancers with Unusual Site Presentation 178
Hye Seon Kang, Bo Bae Choi
Department of Radiology, Chungnam National University Hospital, Korea
- SE 044**
Breast Cancer 178
Tumenjargal Lkhagvasuren, Gonchigsuren Lkhagvasuren
Department of Radiology, National Trauma Center, Mongolia
- SE 045**
Diagnostic Benefits of Ultrasonography-Guided Biopsy Compared with Mammography-Guided Biopsy for Suspicious Microcalcifications without Definite Mass 178
Ji Youn Kim, Min Jae Yoon, Keum Won Kim, Yoong Joong Kim, Jae Young Seo, Chul Mok Hwang
Department of Radiology, Konyang University Hospital, Korea

Cardiovascular

- SE 046**
The Correlation of Epicardial Adipose Tissue by Echocardiography to Acute Coronary Syndrome 179
Uranzaya Ganbold, Enkhbold Sereejav
Department of Radiology, The First Central Hospital of Mongolia, Mongolia
- SE 047**
Sonographic Evaluation of Caval Index(C.I) for Prevention of Volume Overload Induced Lung Edema in Intensive Care Unit; Noninvasive Examination of Intravascular Volume Status 180
Heung Cheol Kim, Ko Eun Yang, Sook Namkung, Myung Sun Hong
Department of Radiology, Chuncheon Sacred Heart Hospital, Korea

Genitourinary

- SE 048**
First Trimester Biometric Differences in Ethnic Mongolian Population 180
Bayanjargal Ochirpurev, Mendsaikhan Gochoo, Erdembileg Tsegmed, Munkhtsetseg Davaasuren
Department of Obstetrics and Gynecology, Mongolian National University of Medical Science, Mongolia

- SE 049**
Retrospective Comparison of Renal Ultrasonographic and Clinical Findings in Patients with Rhabdomyolysis 181
Jae-Joon Chung, Eun-Suk Cho, Joo Hee Kim, Jeong-Sik Yu
Department of Radiology, Gangnam Severance Hospital, Korea
- SE 050**
Ultrasonographic Appearance of Tumors of the Testis; Radiologic-Pathologic Correlation 181
Yongsoo Kim, Young Seo Cho, Sanghyeok Lim
Department of Radiology, Hanyang University Guri Hospital, Korea
- SE 051**
Value of Renal RFA with CEUS as a Problem Solving Tool for a RCC in a Solitary Kidney and with Chronic Renal Disease 182
Shenaz Momin¹, Asif Momin¹, Avinash Gutte²
¹Department of Radiology, Prince Aly Khan Hospital, Mumbai, India
²Department of Radiology, Sir J J Hospital, Mumbai, India
- SE 052**
US of Prostate Masses 182
Dong Won Kim, Seong Kuk Yoon
Department of Radiology, Dong-A University Hospital, Korea
- SE 053**
Contrast-Enhanced Ultrasonography (CEUS) Findings of Solid and Cystic Lesions in Kidney 182
Jung Hun Lee, Young Hwan Lee
Department of Radiology, Wonkwang University School of Medicine & Hospital, Korea
- SE 054**
Intratesticular Focal Hypoechoic Lesions: Sonographic and Clinical Findings 183
Dal Mo Yang, Hyun Cheol Kim, Sang Won Kim, Ji Su Kim
Department of Radiology, Kyung Hee University Hospital at Gangdong, Korea
- SE 056**
Prenatal Ultrasound of Multiple Gestations: Check Points and Common Abnormalities 183
Seonghwan Byun, Boem Ha Yi, Hae Kyung Lee, Min Hee Lee, Seo-Youn Choi, Ji Eun Lee
Department of Radiology, Soonchunhyang University Bucheon Hospital, Korea
- SE 057**
Churg-Strauss Syndrome Involving Testis and Epididymis 183
Yongsoo Kim, Young Seo Cho, Sanghyeok Lim
Department of Radiology, Hanyang University Guri Hospital, Korea
- SE 058**
Cellular Angiofibroma of the Scrotum 184
Young Seo Cho
Department of Radiology, Hanyang University Guri Hospital, Korea

Head & Neck

SE 059

Superficially Palpable Masses in Head and Neck: Sonographic Features and Pathologic Correlations 184
 Hyoung Seop Kim, Jin Kyung An, Jeong Joo Woo, Yoon Young Jung, Myung Won You, Eui Chul Jung
Department of Radiology, Eulji Hospital, Eulji University, Korea

SE 060

Ultrasonographic Features of Pyriform Sinus Fistula-Related Suppurative Thyroiditis 184
 Dongbin Ahn¹, Jeong Kyu Kim²
¹*Department of Otorhinolaryngology, Kyungpook National University Hospital, Korea*
²*Department of Otorhinolaryngology, Daegu Catholic University Medical Center, Korea*

SE 061

Comparison of Ultrasonography (US) and Computed Tomography (CT) Features of Calcified Thyroid Nodules (CTNs): Histopathologic Correlation 185
 Yoo Jin Lee, Dong Wook Kim
Department of Radiology, Busan Paik Hospital, Korea

SE 062

Life Saving Chemical Ablation of Large Acute Onset Parotid Space Neck Lymphangioma 185
 Asif Momin, Shenaz Momin
Department of Radiology, B Y L Nair Hospital, Mumbai, India

SE 063

Merkel Cell Carcinoma, a Potential Mimicker of Lymphoma on Ultrasonography 186
 Soo Young Chae, Jung Hye Na, Inseon Ryoo, Sangil Suh, Hae Young Seol
Department of Radiology, Korea University Guro Hospital, Korea

Musculoskeletal

SE 064

Botulinum Toxin a Injection with Radial Extracorporeal Shock Wave Therapy in Spastic Cerebral Palsy 186
 Dong Rak Kwon, Gi-Young Park
Department of Rehabilitation Medicine, Daegu Catholic University Medical Center, Korea

SE 065

Do the Findings of Magnetic Resonance Imaging, Arthrography, and Ultrasonography Reflect Clinical Impairment in Patients with Adhesive Capsulitis of the Shoulder? 186
 Gi-Young Park¹, Dong Rak Kwon¹, Dae-Gil Kwon¹, Jung Hyun Park²
¹*Department of Rehabilitation Medicine, Daegu Catholic University Medical Center, Korea*
²*Department of Rehabilitation Medicine, Severance Hospital, Korea*

SE 066

Variable Sonographic Findings of the Subungual Glomus Tumor 187
 Ga Young Lee¹, Sun Joo Lee¹, Hye Jung Choo¹, Sung Moon Lee²
¹*Department of Radiology, Inje University Busan Paik Hospital, Korea*
²*Department of Radiology, Keimyung University Dongsan Medical Center, Korea*

SE 067

Ultrasonographic Finding of Joplins Neuroma: a Case Report 188
 Sumin Lee¹, Sunjoo Lee¹, Hyejung Choo¹, Sung Moon Lee²
¹*Department of Radiology, Inje University Busan Paik Hospital, Korea*
²*Department of Radiology, Keimyung University Dongsan Medical Center, Korea*

SE 068

Sonoelastography Findings in Evaluation of Various Benign Soft Tissue Lesions 188
 Eunjin Hwang, Eun-Kyung Khil, Seun-Ah Lee, Jung-Ah Choi
Department of Radiology, Dongtan Sacred Heart Hospital, Korea

SE 069

Imaging Findings of Digital and Extradigital Glomus Tumor 189
 Jungwon Park¹, Sunjoo Lee¹, Hyejung Choo¹, Sung Moon Lee²
¹*Department of Radiology, Inje University Busan Paik Hospital, Korea*
²*Department of Radiology, Keimyung University Dongsan Medical Center, Korea*

SE 070

High-Resolution Sonography of Cutaneous Branches: Upper Extremity 189
 Sung Kwan Kim¹, Sun Joo Lee¹, Hye Jung Choo¹, Sung Moon Lee²
¹*Department of Radiology, Inje University Busan Paik Hospital, Korea*
²*Department of Radiology, Keimyung University Dongsan Medical Center, Korea*

SE 071

Muskuloskeletal Ultrasound Finding in Disseminated Tuberculosis 190
 Maria Goretti Ametembun
Department of Internal Medicine, Lukas Government Hospital, Stella Maris Hospital, Fanayama Health Centre South Nias, North Sumatera, Indonesia

SE 072

Fibroma of Tendon Sheath of the Hand: Ultrasonographic and MRI Findings 190
 Yeon Soo Lee¹, Hae Joung Sul²
¹*Department of Radiology, The Catholic University of Korea, Daejeon St. Mary's Hospital, Korea*
²*Department of Pathology, The Catholic University of Korea, Daejeon St. Mary's Hospital, Korea*

Pediatric

SE 073

Quantifying Stenocleidomastoid Muscle Intrinsic Stiffness Difference Using Dynamic Sonoelastography in Congenital Muscular Torticollis 191
Dong Rak Kwon, Gi-Young Park
Department of Rehabilitation Medicine, Daegu Catholic University Medical Center, Korea

SE 074

Ultrasound Diagnosis of Development Dysplasia of the Hip and the Congenital Hip Dislocation in Children 191
Norjmaa Sereenendorj
Department of Radiology, Mongolian Radiological Society, Mongolia

SE 075

The Report about Ultrasonic Examination of a Hip Joint of Newborns in Delivery Room of a Hospital of Huvsgul Aimag 192
Enkhtaivan Namuuntsetseg, Enkhbold Sereejav
Department of Radiology, The First Central Hospital of Mongolia, Mongolia

SE 076

Is it Acceptable Not to Perform Voiding Cystourethrography in Infants with Low-Grade Hydronephrosis? 192
Sun Kyoung You, Seongsu Kang
Department of Radiology, Chungnam National University Hospital, Korea

SE 077

The Vomiting Neonates and Infants: Operation or Observation?-the Decision Algorithm Navigating the Radiologic Diagnosis of a Surgical Emergency 193
Yongsang Kim, Myung Won You, Yoon Young Jung
Department of Radiology, Eulji University Hospital, Korea

SE 078

Cervical Thymus Mimicking Metastatic Recurrence on PET/CT: Diagnosis with Ultrasound 193
Saelin Oh, So-Young Yoo, Ji Hye Kim, Tae Yeon Jeon
Department of Radiology, Samsung Medical Center, Korea

Physics

SE 079

A New High Definition Voxel Based Reconstruction Method for Three-Dimensional Ultrasound MPR Imaging 194
Sungchan Kim, Jinbum Kang, Ilseob Song, Yangmo Yoo
Department of Medical Solution Institute, Sogang University, Korea

SE 080

An Efficient Transmit Delay Calculation Method for Coherent Plane-Wave Compounding in Convex Array Transducer 194
Dooyoung Go, Jinbum Kang, Yangmo Yoo
Department of Medical Solution Institute, Sogang University, Korea

SE 081

A Modified Homographic Transform-Based Image Registration Method for 3-D Automatic Breast Ultrasound System with Dual Wide Field-of-View Imaging 195
Hojung Lee, Ilseob Song, Jinbum Kang, Yangmo Yoo
Department of Medical Solution Institute, Sogang University, Korea

SE 082

Characteristic Responses of Neuronal Cells to Ultrasound Under the Variable Heights of Culture Medium in the Well 195
Gwansuk Kang¹, Tsengel Bayarsaikhan¹, Su-Yong Eun², Min Joo Choi²
¹Department of Interdisciplinary Postgraduate Program in Biomedical Engineering, Jeju National University, Korea
²Department of Medicine, Jeju National University, Korea

Thyroid

SE 083

Detection of Malignancy among Suspicious Thyroid Nodules Less than 1 cm with Various Thyroid Image Reporting and Data Systems 196
Su Min Ha¹, Jae Kyun Kim¹, Jung Hwan Baek²
¹Department of Radiology, Chung-Ang University Hospital, Korea
²Department of Radiology, Asan Medical Center, Korea

SE 084

Columnar Cell Variant of Papillary Thyroid Carcinoma; Differentiation between Indolent and Aggressive Types 197
Jooyeon Cho¹, Jung Hee Shin¹, Soo Yeun Hahn¹, Young Lyun Oh²
¹Department of Radiology, Samsung Medical Center, Korea
²Department of Pathology, Samsung Medical Center, Korea

SE 085

Efficacy and Safety of Ethanol Ablation for Branchial Cleft Cysts 197
Eun Ju Ha¹, Seon Mi Baek², Jung Hwan Baek³, Su Young Shin², Miran Han¹, Chul-Ho Kim⁴
¹Department of Radiology, Ajou University Hospital, Korea
²Department of Radiology, Sharing and Happiness Hospital, Korea
³Department of Radiology, Asan Medical Center, Korea
⁴Department of Otolaryngology, Ajou University Hospital, Korea

SE 086

The Relationship between Thyroid Nodule Size and Malignancy Risk 198
Saerom Chung, Jung Hwan Baek, Young Jun Choi, Jeong Hyun Lee
Department of Radiology, Asan Medical Center, Korea

SE 087

Safety of Radiofrequency Ablation of Benign Thyroid Nodules and Recurrent Thyroid Cancers: A Systematic Review and Meta-Analysis 198
Saerom Chung, Chong Hyun Suh, Jung Hwan Baek, Hye Sun Park, Young Jun Choi, Jeong Hyun Lee
Department of Radiology, Asan Medical Center, Korea

- SE 089** **Ultrasound in Non Palpable Thyroid Masses** 199
Diagnostics
Nozima Khodjaeva
Department of Radiology, Medifarm Private Clinic, Uzbekistan
- SE 090** **Intra- and Inter-Observer Variability in** 199
Ultrasound Measurements of Thyroid Nodules
Hyung Jin Lee, Dae Young Yoon, Young Lan Seo, Jin Ho Kim, Sora Baek, Kyoung Ja Lim, Young Kwon Cho, Eun Joo Yun
Department of Radiology, Kangdong Sacred Heart Hospital, Korea
- SE 091** **US-Guided Ablations of Primary and Recurrent** 199
Thyroid Cancers
Soyeong Jeong, Jung Hwan Baek, Young Jun Choi, Jeong Hyun Lee
Department of Radiology, Asan Medical Center, Korea
- SE 092** **Diagnostic Efficacy of Core Needle Biopsy as a** 200
First-Line Diagnostic Tool for Low or Intermediate Suspicion Thyroid Nodules: Comparison with Fine Needle Aspiration Using Propensity Score Analysis
Hye Shin Ahn¹, Inyoung Youn², Dong Gyu Na³, Soo Jin Kim⁴
¹*Department of Radiology, Chung-Ang University Hospital, Korea*
²*Department of Radiology, Kangbuk Samsung Medical Center, Korea*
³*Department of Radiology, GangNeung Asan Hospital, Korea*
⁴*Department of Radiology, New Korea Hospital/Human Medical Imaging and Intervention Center, Korea*
- SE 093** **Comparison of Diagnostic Efficacy with** 201
18-Gauge and 20-Gauge Ultrasound-Guided Core Needle Biopsy for Thyroid Nodules
Hye Shin Ahn¹, Mirinae Seo², Su Min Ha¹, Hee Sung Kim³
¹*Department of Radiology, Chung-Ang University Hospital, Korea*
²*Department of Radiology, Kyung Hee University Medical Center, Korea*
³*Department of Pathology, Chung-Ang University Hospital, Korea*
- SE 094** **Comparison of Core Needle Biopsy and Fine** 201
Needle Aspiration as a First-Line Diagnostic Tool in High Suspicion Thyroid Nodules Using Propensity Score Analysis
Inyoung Youn¹, Hye Shin Ahn², Dong Gyu Na³, Soo Jin Kim⁴
¹*Department of Radiology, Kangbuk Samsung Medical Center, Korea*
²*Department of Radiology, Chung-Ang University Hospital, Korea*
³*Department of Radiology, GangNeung Asan Hospital, Korea*
⁴*Department of Radiology, New Korea Hospital/Human Medical Imaging and Intervention Center, Korea*
- SE 095** **Tuberculosis in Thyroid** 202
Munkhdul Altankhuyag
Department of Radiology, UB Songdo Hospital, Mongolia
- SE 096** **Radiofrequency Ablation for Nonfunctioning** 202
Benign Thyroid Nodules in Children and Adolescents
Jin Yong Sung
Department of Radiology, Daerim St. Mary's Hospital, Korea

MP 1 THY

Cutting Edge of Head and Neck US

07:50-08:20

GBR 101

Chairperson: Ji-Hoon Kim *Seoul National University Hospital, Korea*

US Elastography in the Head and Neck: Current Status and Future Perspectives

Kunwar Bhatia

Department of Radiology, Imperial College Healthcare NHS Trust, UK

US elastography is a collective term for several US-based techniques that measure tissue elasticity or stiffness non-invasively. Over the last decade, USE has undergone continued advances to optimize quality assurance and capabilities. There are different types of USE depending on the exciting stimulus and deformation measured but these can be broadly subdivided into strain elastography and shear wave elastography.

In the head and neck, most USE research has focused on characterization of thyroid nodules, where over 100 pilot studies and several meta-analysis reveal that malignant thyroid nodules, in particular papillary carcinomas, are firmer than benign nodules. However, the discriminatory performance of thyroid USE is controversial, partly due to discrepancies in reported diagnostic performance results. Recently, some investigators

have proposed that thyroid USE is a useful adjunct to conventional US by raising the negative predictive value for malignancy, which may reduce the rate of needle aspiration biopsies performed in otherwise sonographically indeterminate nodules.

USE has also been explored for characterization of cervical lymph nodes, salivary masses, as well as diffuse diseases in salivary glands and the thyroid, and post radiation complications in the neck.

This talk outlines the basic principles of elastography and technical aspects relevant to the head and neck. The latest evidence and future directions for USE for tissue characterization in several head and neck tissues will be summarized. The main focus will be on thyroid USE although the evidence for other head and neck tissues will be discussed.

MP 2 MSK

07:50-08:20

GBR 102

Chairperson: Sungjun Kim Gangnam Severance Hospital, Korea

Musculoskeletal Soft Tissue Lesions: How to Make a Diagnosis**Min Hee Lee***Department of Radiology, Asan Medical Center, Korea*

High resolution ultrasonography is now being widely used for the assessment of musculoskeletal soft tissue lesions. Non-invasiveness, easy accessibility and cost effectiveness have rendered ultrasonography to be the preferred imaging modality for the initial evaluation of soft tissue masses that present as palpable soft tissue lesions.

At the initial evaluation, ultrasound can confirm the presence of a mass and may characterize whether the mass is cystic or solid. In certain cases, specific diagnoses could be made on the basis of selected

imaging features, particularly in characteristic location, however, MR imaging are further required for more detailed information about soft tissue composition in many cases. The concern for a potential malignancy necessitates tissue biopsy for final diagnosis. In such a situation, ultrasonography can serve as a useful imaging guidance.

In this talk, the sequential steps leading to the final diagnosis of musculoskeletal soft tissue lesions are discussed with various cases focusing on the appropriate use of ultrasonography.

MP 3 ABD-1

CEUS: Past and Current Status

07:50-08:05

GBR 103

Chairperson: Jae Young Lee *Seoul National University Hospital, Korea*

CEUS: Past and Current Status in Asia

Byung Ihn Choi

Department of Radiology, Chung-Ang University Hospital, Korea

In this session, chronology of CEUS, contrast agents CEUS technology, congress in Asia, development of guidelines for CEUS, and statistics of publication in field of CEUS will be presented.

In 1969, Gramiak and Shah performed echocardiography after injection of mixture of fluid and patient's blood. Since then, many US contrast agents have been developed including Albunex, Echovist, Levovist, Definity, Sonovist, Echogen, Optison, SonoVue, Imagent, Quantison and Sonazoid. SonoVue is widely available in Europe and Asia and recently in America. Sonazoid is available in Japan, Korea and Norway, and will probably be available in China, Taiwan, Singapore and Europe in near future.

US contrast agents are coated microbubbles composed of gas such as air (Nitrogen, PFC, SF) and capsule consisting of phospholipid, albumin or high molecule. Microbubbles are air or nitrogen or perfluorocarbon or sulfur hexafluoride.

There are two techniques of contrast-enhanced US. One is high MI imaging and the other is low MI imaging. High MI imaging with a first generation contrast agent, Levovist, is disruptive bubble imaging and is no longer used. Low MI imaging using second generation contrast agents such as SonoVue or Definity, is a continuous bubble imaging and is useful in vascularity assessment.

Various contrast specific imaging software is now available by many US vendors, such as Siemens, Phillips, GE, Toshiba, Esaote, Aloka, Hitachi, BK Medical, Supersonics and Samsung.

In Asia, International Symposium on US Contrast Imaging (ISUCI) was organized by two professors, Dr. Moriyasu and Beppu. 1st meeting was held in Kyoto in 1999. This meeting was held annually until 2008 in Tokyo or Osaka, Japan. 1st ACUCI (Asian congress of ultrasound contrast imaging) was held in 2009 in Kunming hosted by China. This meeting is held annually.

CEUS was developed and has been widely used in Europe. So, EFSUMB guideline was published in 2004 and revised in 2008, (published revised guideline and good clinical practice recommendation for CE US update 2008,) and this guideline was propagated to Asia.

WFUMB started revision project of CEUS guideline in 2010. Final version of this WFUMB guideline was published simultaneously in two journals including UMB, official journal of WFUMB, and Ultraschall journal of EFSUMB in Feb, 2013.

The number of publication in the field of CEUS is increasing rapidly. According to PubMed search in 2016, total number of article is more than 5400. By organ, proportion of Nonhepatic organ is 70%, Cardiac (16%) and Hepatic (14%). By product, SonoVue is the 1st in rank, 42%, followed by Levovist, and Optison (13%), Definity (10%) and Sonazoid (9%).

Chairperson: Jae Young Lee *Seoul National University Hospital, Korea*

Integration of CEUS and Elastography in Clinical Liver Patient Management

Giovanna Ferraioli

Department of Internal Medicine-Infection, Fondazione IRCCS Policlinico San Matteo, University of Pavia, Italy

Contrast-enhanced ultrasound (CEUS) is useful for the characterization of an incidentally detected liver mass or a mass detected in a cirrhotic liver during the surveillance. Contrast US has also been used for the diagnosis of liver cirrhosis. The rationale is that in cirrhotic livers there is both a capillarization of the sinusoids and the development of arteriovenous and portovenous shunts. These changes lead to a decrease of the arrival of the contrast in the hepatic veins after the injection.

However, the most accurate method for staging liver fibrosis in patients with chronic liver disease is shear wave elastography. Elastography can be used not only for the staging of the disease, but also to follow up patients and to assess the risk of complication of cirrhosis, such as portal hypertension and hepatocellular carcinoma.

CC 1 MSK-1

Upper Extremity

08:30-09:00

GBR 102

Chairperson: Jung-Ah Choi Hallym University Dongtan Sacred Heart Hospital, Korea

Shoulder

Jee Won Chai

Department of Radiology, SMG-SNU Boramae Medical Center, Korea

Ultrasonography (US) is a useful diagnostic method that can be easily performed to find the cause of shoulder pain. Relatively low cost, excellent diagnostic accuracy, capability of dynamic evaluation are also advantages of the shoulder US. But the greatest value of the ultrasound is that we can communicate directly with the patient and can correlate ultrasonographic findings with symptoms and physical examinations. To assess all possible causes of shoulder pain, it is better to develop a systematic sequence of routine shoulder US rather than a focused examination. When the patient has localized symptoms, spending the last sequence to evaluate the painful site will enable thorough assessment without missing a true pathology.

Typically, the shoulder joint is evaluated from the anterior to superior, and to the posterior aspects. Anterior structures that require evaluation are the long head of biceps brachii tendon, tendon sheath and

pulley system, subscapularis tendon. Supraspinatus tendon, rotator interval, acromioclavicular joint and acromion, subacromial-subdeltoid bursa and dynamic evaluation for subacromial impingement can be evaluated on the superior aspect of the shoulder. Posterior structures to evaluate are infraspinatus tendon, teres minor tendon, posterior glenohumeral joint and spinoglenoid notch.

Knowledge of frequently encountered artifacts, pitfalls and its solutions are necessary to prevent false positive and false negative results. The evaluation of each structure should be done without artifacts on both short axis and long axis in the entire range of the structures. The accuracy of ultrasonography varies greatly depending on the operator, so the radiologists should be familiar with the detailed anatomy and routine scanning protocol for a sufficient and accurate US of the shoulder.

Elbow Ultrasound

Yusuhn Kang

Department of Radiology, Seoul National University Bundang Hospital, Korea

1. Anatomy of the elbow joint

Bones

Humerus (capitellum, trochlea, coronoid fossa, radial fossa, olecranon fossa)

Ulna (olecranon process, coronoid process, trochlear notch, radial notch)

Radius (radial head, neck, radial tuberosity)

Articulations

Ulnohumeral joint (hinge joint, flexion-extension)

Radiohumeral joint (gliding joint, flexion-extension)

Proximal radioulnar joints (pivot joint, flexion-extension, pronation-supination)

Synovial pouches: anterior coronoid recess, radial recess, posterior joint recess in the olecranon fossa

Ligaments

Medial collateral ligament complex (anterior, posterior, transverse bundle)

Lateral collateral ligament complex (radial collateral ligament, lateral ulnar collateral ligament, annular ligament, accessory annular ligament)

Muscles and tendons

Anterior: biceps brachii distal tendon, brachialis muscle

Posterior: triceps brachii, anconeus

Medial: common flexor tendon, pronator teres

Lateral: common extensor tendon, extensor carpi radialis longus, brachioradialis, supinator.

2. Scanning technique and normal US anatomy

Probe selection: Linear high-frequency transducer. (> 10MHz)

Patient positioning: patient seated with arm on the examination table.

General rule: Scan in both transverse and longitudinal planes.

Beware of anisotropy.

Compare with the contralateral side.

(1) Anterior elbow

- Position: patient with elbow fully extended resting on a table

- Check list

A. Distal biceps muscle and tendon

B. Brachialis tendon

C. Median nerve and anterior interosseous nerve.

D. Anterior synovial recess and anterior fat pad

E. Radio-capitellar and trochlea-ulnar joints.

(2) Medial elbow

- Position: Elbow extended and externally rotated resting on table

- Check list

A. Common flexor tendon: inserts on the medial aspect of the epitrochlear

B. Medial collateral ligament: epitrochlea - sublime tubercle of ulna, fibrillar pattern, fanlike shape

(3) Lateral elbow

- Position: Elbow in extension, thumbs up, palms

of the hands together

- Check list
 - A. Common extensor tendon:
 - B. Lateral ulnar collateral ligament
 - C. Radial nerve and posterior interosseous nerve

(4) Posterior elbow

- Position: elbow flexed 90 degrees with the palm resting on the table
- Check list
 - A. Triceps muscle and tendon
 - B. Posterior fossa with the posterior fat pad
 - C. Cubital tunnel and the ulnar nerve
 - D. Olecranon bursa

3. Pathology

(1) Tendon - overuse

- Lateral epicondylitis (Tennis elbow, m/c), Medial epicondylitis (Golfer's elbow)
- Degeneration or tearing of the common extensor/flexor tendon due to chronic microtrauma, resulting from overuse of the tendon.
- US findings: Hypoechoic areas within the tendon with loss of normal internal fibrillar pattern, Decreased echogenicity and thickening of tendon. Bony irregularity and small calcifications indicating enthesopathy

(2) Traumatic tendon tears

- Partial or complete rupture of tendons
- Distal biceps tendon tear, distal triceps tendon tear
- US finding: A fluid-filled gap or focal hypoechoic area in the substance of tendon
Wavy, retracted tendon stump surrounded by fluid (acute complete tear)

(3) Neuropathy

A. Cubital tunnel syndrome

- Cubital tunnel: Osborne ligament (roof), posterior band of medial collateral ligament (floor), humerus, ulna
- Ulnar nerve entrapment neuropathy
- US finding: Abrupt narrowing and displacement of the nerve within the tunnel, possibly in association with a thickened retinaculum or a space-occupying lesion.
Swelling of the nerve proximal to the constriction point, with loss of normal fascicular pattern.

B. Posterior interosseous syndrome

- Compressive neuropathy of the posterior interosseous nerve, just near or behind the supinator muscle
- Arcade of Frohse
- US Finding: Impingement of the posterior interosseous nerve in the supinator area, Swollen and hypoechoic proximal to or inside the supinator muscle.

References

1. De Maeseneer M, Marcelis S, Cattrysse E, Shahabpour M, De Smet K, De Mey J. Ultrasound of the elbow: a systematic approach using bony landmarks. *European journal of radiology*. 2012;81(5):919-22.
2. Lee KS, Rosas HG, Craig JG. Musculoskeletal ultrasound: elbow imaging and procedures. *Seminars in musculoskeletal radiology*. 2010;14(4):449-60.
3. Tagliafico AS, Bignotti B, Martinoli C. Elbow US: Anatomy, Variants, and Scanning Technique. *Radiology*. 2015;275(3):636-50.
4. Bianchi S, Martinoli C. *Ultrasound of the musculoskeletal system*. Berlin ; New York: Springer; 2007. xiv, 974 p. p.

Ultrasound of the Wrist and Hand

Eun Hae Park

Department of Radiology, Chonbuk National University Hospital, Korea

Technical Strategy

Transducers ideally suited for the detail work required in the hand are linear array transducers with a small foot print (only a few centimeters in width) that have a broad bandwidth from 4 ~ 15 MHz. A more focused examinations of superficially located structures is performed with transducers having a center frequency higher than 14 MHz. Ideal transducers focus the sound beam on the near field, i.e. the area of the clinically detectable abnormality, which in the hand can be in the order of millimeters.

Often a standoff pad must be utilized to visualize lesions close to the skin surface. Generous use of sonographic gel facilitates transverse imaging of the tendons of the fingers as a group. Transverse imaging of the tendons is performed first. This is essential for the identification of swelling of individual tendons and tendons sheaths. Measurement of the transverse diameters of tendons allows easy identification of tendon swelling.

Examination of the dorsal wrist, which starts in hand pronation, may require a wedge to sequentially lift the radial and ulnar aspects of the wrist depending upon whether the focus of the study is more radial or ulnar sided. Transverse visualization of the dorsal scapholunate joint and the dorsal scapholunate ligament requires right left comparison for diagnosis of injury.

The volar aspect of the wrist on a transverse image through the carpal tunnel, the flexor retinaculum is seen as a hyperechoic line. The rows of superficial and deep flexor tendons are identified within the carpal tunnel. The median nerve is an ovoid structure

on the radial side of the carpal tunnel immediately beneath the flexor retinaculum. It is slightly less echogenic than the surrounding tendons and flatter in appearance. The median nerve rests on the deep flexor tendon of the middle and index fingers. Flexion and extension of the fingers during real-time examination will demonstrate which structure is the median nerve.

In evaluation of collateral ligaments, the transducer must be aligned along medial and lateral joint capsules. Lesions are diagnosed easily with varus and valgus stress. The ulnar collateral ligament of the thumb can be assessed longitudinally by pressing the transducer into the soft tissue of the medial first web space. A metacarpal ridge and the origin of the ligament form a groove just distal to this ridge that can be used as internal landmark.

- Van Holsbeeck MT, Introcaso JH. Musculoskeletal ultrasound. 3rd ed.

References

1. Van Holsbeeck MT, Introcaso JH. Musculoskeletal ultrasound. 3rd ed.
2. Lee JC, Healy JC. Normal sonographic anatomy of the wrist and hand. *Radiographics*. 2005;25(6):1577-90.
3. Bianchi S, Martinoli C, Abdelwahab IF. High-frequency ultrasound examination of the wrist and hand. *Skeletal Radiol*. 1999;28(3):121-9.
4. Olchowy C, Lasecki M, Zaleska-Dorobisz U. Wrist ultrasound examination - scanning technique and ultrasound anatomy. Part 1: Dorsal wrist. *J Ultrason*. 2015;15(61):172-88.
5. Veziridis PS, Yoshioka H, Han R, Blazar P. Ulnar-sided wrist pain. Part I: anatomy and physical examination. *Skeletal Radiol*. 2010;39(8):733-45.

6. Watanabe A, Souza F, Vezeridis PS, Blazar P, Yoshioka H. Ulnar-sided wrist pain. II. Clinical imaging and treatment. *Skeletal Radiol.* 2010;39(9):837-57.
7. Baek HJ, Lee SJ, Cho KH, Choo HJ, Lee SM, Lee YH, et al. Subungual tumors: clinicopathologic correlation with US and MR imaging findings. *Radiographics.* 2010;30(6):1621-36.
8. Chiavaras MM, Jacobson JA, Yablon CM, Brigido MK, Girish G. Pitfalls in wrist and hand ultrasound. *AJR Am J Roentgenol.* 2014;203(3):531-40.
9. Olubaniyi BO, Bhatnagar G, Vardhanabhuti V, Brown SE, Gafoor A, Suresh PS. Comprehensive musculoskeletal sonographic evaluation of the hand and wrist. *J Ultrasound Med.* 2013;32(6):901-14.
10. Tagliafico A, Rubino M, Autuori A, Bianchi S, Martinoli C. Wrist and hand ultrasound. *Semin Musculoskelet Radiol.* 2007;11(2):95-104.
11. Daenen B, Houben G, Bauduin E, Debry R, Magotteaux P. Sonography in wrist tendon pathology. *J Clin Ultrasound.* 2004;32(9):462-9.
12. Robertson BL, Jamadar DA, Jacobson JA, Kalume-Brigido M, Caoili EM, Margalio Z, et al. Extensor retinaculum of the wrist: sonographic characterization and pseudotenosynovitis appearance. *AJR Am J Roentgenol.* 2007;188(1):198-202.

Chairpersons: **Won Jae Lee** *Samsung Medical Center, Korea*
Chang Hee Lee *Korea University Guro Hospital, Korea*

CEUS for the Liver using Sonovue

Giovanna Ferraioli

Department of Internal Medicine-Infection, Fondazione IRCCS Policlinico San Matteo, University of Pavia, Italy

Liver malignancies are among the most common tumors in the world, but there is also a high prevalence of benign focal liver lesions (FLLs). Thus, lesion characterization at imaging is of utmost importance. Arriving at a fast, definitive diagnosis of a benign FLL with minimal imaging studies can help reducing risks to patients, including radiation risks, and costs. Contrast-enhanced ultrasound (CEUS) is able to show the enhancement pattern of a FLL relative to the adjacent liver parenchyma.

SonoVue® (Bracco Imaging, Milan, Italy), is the US contrast used in Europe and some parts of Asia. Unlike other contrast agents, SonoVue® is a purely intravascular agent, allowing the dynamic detection of the microcirculation.

The liver has a dual blood supply, both from the hepatic artery and the portal vein, that gives rise to three vascular phases on CEUS study - namely arterial, portal, and late phases. Sustained enhancement in the portal venous and late phases is typically observed in almost all solid benign FLLs, and they can be further characterized by

the enhancement pattern in the arterial phase. Malignant FFLs show hypo-enhancement in the late phase, corresponding to the washout. Almost all metastases show this feature, independently from their enhancement pattern in the arterial phase. Hepatocellular carcinoma (HCC) is usually hyper-enhancing in the arterial phase, and hypo-enhancing in the portal venous and late phases, apart from well-differentiated HCC that may be iso-enhancing. With respect to liver metastasis, the washout of HCC usually starts later.

Multicenter trials have shown that the performance of CEUS for the characterization of FLLs is similar to that of contrast enhanced computed tomography (CE-CT) or contrast enhanced magnetic resonance (CE-MR). CEUS is a real-time dynamic imaging technique that can be used when CE-MR or CE-CT are inconclusive or contraindicated. In fact, the continuous real-time imaging may allow to detect the transient enhancement of a lesion that could be missed by other imaging modalities

SFS 1 ABD-2

CEUS: Hepatic & Extrahepatic Application

09:00-09:30

GBR 103

Chairpersons: **Won Jae Lee** *Samsung Medical Center, Korea*
Chang Hee Lee *Korea University Guro Hospital, Korea*

CEUS for the Liver using Sonazoid

Mi-Suk Park

Department of Radiology, Severance Hospital, Korea

Sonazoid (GE Healthcare, Oslo, Norway) is a second generation ultrasound contrast agent that consists of a lipid-stabilized suspension of perflurobutane gas micro bubbles within a hard shell of phosphatidyl-serine (2-3 μm in diameter). These microbubbles provide stable nonlinear oscillations in low-power acoustic fields and produce echoes at the second harmonic frequency of the transmitted pulse, which are used for contrast-enhanced harmonic imaging. Along with the ability of real-time vascular-phase imaging, Sonazoid microbubbles are taken up by Kupffer cells in the reticuloendothelial system of the liver, which enables parenchyma-specific liver imaging. This Kupffer-phase imaging is generally performed 10 minutes after intravenous contrast media administration, at which time the normal hepatic parenchyma is enhanced. Therefore, malignant lesions containing few or no Kupffer cells are clearly shown as contrast defects in this phase. In addition, since Sonazoid microbubbles continue to resonate with moderate ultrasound pressure without collapse, Kupffer-phase imaging is stable for more than several hours, which facilitates whole-liver scanning.

Many previous studies have reported the utility of contrast enhanced sonography using Sonazoid for detection of hepatic metastasis, detection and diagnosis of hepatocellular carcinoma, for intraoperative contrast-enhanced sonography in patients with hepatocellular carcinoma or metastasis from colorectal cancer, and real-time guidance of percutaneous biopsy or RF ablation of focal liver

lesions.

In this talk, I would like to briefly review CEUS using Sonazoid on the characteristic properties and various application for liver imaging.

References

1. Hatanaka K, Kudo M, Minami Y, Maekawa K. Sonazoid-enhanced ultrasonography for diagnosis of hepatic malignancies: comparison with contrast-enhanced CT. *Oncology* 2008; 75(suppl 1):42-47.
2. Sugimoto K, Moriyasu F, Saito K, et al. Comparison of Kupffer-phase Sonazoid-enhanced sonography and hepatobiliary-phase gadoxetic acid? enhanced magnetic resonance imaging of hepatocellular carcinoma and correlation with histologic grading. *J Ultrasound Med* 2012; 31:529-538.
3. Moriyasu F, Itoh K. Efficacy of perflubutane microbubble-enhanced ultrasound in the characterization and detection of focal liver lesions: phase 3 multicenter clinical trial. *AJR Am J Roentgenol* 2009; 193:86-95.
4. Hee Sun Park, MD, et al. Real-time contrast-enhanced sonographically guided biopsy or radiofrequency ablation of focal liver lesions using perflurobutane microbubbles (sonazoid): value of Kupffer-phase imaging. *J Ultrasound Med* 2015; 34: 411-21.
5. Park JH, Park MS, Lee SJ, et al. Contrast-enhanced US with Perfluorobutane(Sonazoid) used as a surveillance test for Hepatocellular Carcinoma (HCC) in Cirrhosis (SCAN): an exploratory cross-sectional study for a diagnostic trial. *BMC Cancer*. 2017 Apr 18;17(1):279. doi: 10.1186/s12885-017-3267-8.

Chairpersons: **Won Jae Lee** *Samsung Medical Center, Korea*
Chang Hee Lee *Korea University Guro Hospital, Korea*

Contrast Enhanced EUS for Extrahepatic Application

Dong Wan Seo

Department of Gastroenterology, Asan Medical Center, Korea

Contrast-enhanced endoscopic ultrasonography (CE-EUS) using the 2nd generation contrast agent is introduced as a new modality which can improve diagnostic yield of pancreatic and peripancreatic tumors. Compared to conventional B-mode imaging, CE-EUS can show dynamic enhancement pattern similar to dynamic CT. However, contrast agent for ultrasound is purely intravascular agent and theoretically does not diffuse out to interstitial space. Nowadays, 2nd generation contrast agent such as Sonovue or Sonazoid are commonly used for CE-EUS. Since these agents can clearly show microvessel enhancement inside tumor, CE-EUS is actively investigated for the differential diagnosis of pancreatic tumors, gallbladder lesions and vascular lesions.

CE-EUS for pancreatic tumors

Pancreatic lesions are frequently difficult to delineate clearly by trans-abdominal ultrasonography because of abdominal fat, intervening organs and gas or food material in the bowel. EUS scope can go into the stomach or duodenum and visualize the details of pancreas without difficulty. EUS can use higher frequency ultrasound than trans-abdominal ultrasonography and give us higher resolution image.

Pancreatic tumors can be categorized into two distinct entities; solid tumor and cystic tumor. Solid tumors are composed of pancreatic ductal adenocarcinoma, neuroendocrine tumor, metastatic tumor, and inflammatory tumors such as tuberculosis or autoimmune pancreatitis. Cystic tumors are composed of serous cystic tumor (SCT), mucinous cystic tumor (MCT), intraductal papillary mucinous

neoplasm (IPMN), lymphoepithelial cyst, cystic degeneration of solid tumor, etc.

CE-EUS is nowadays actively used for the differential diagnosis of pancreatic solid tumors since typical enhancement patterns are different according to the histology. Pancreatic cancer shows hypovascular or avascular pattern inside the tumor. Neuroendocrine tumor generally shows very strong early arterial enhancement pattern. Inflammatory tumors such as tuberculosis also shows relatively well-enhancing pattern but geographic avascular areas are frequently observed due to caseation necrosis. Autoimmune pancreatitis shows diffuse progressive enhancement and this pattern is different from pancreatic cancer. Compared to neuroendocrine tumor, the enhancement pattern of autoimmune pancreatitis is relatively weak and slow progressive.

CE-EUS can also be used for cystic pancreatic tumors. Compared to mucinous lesions, serous cystic tumor shows relatively well enhancing septum. CE-EUS is quite useful for the differential diagnosis of mural nodule and mucus plug inside cystic tumor.

CE-EUS for gallbladder lesions

There have been a few trials to use CE-EUS for the differential diagnosis of gallbladder mass. Our group studied the usefulness of CE-EUS and gallbladder polyp, adenoma and carcinoma were included. Benign polyps and adenomas generally showed homogeneous enhancement pattern and no perfusion defect was observed. On the other hand, gallbladder cancer showed relatively inhomogeneous enhancement pattern and several perfusion defects

were observed probably because of irregularly arrayed tumor vessel. These differential points were helpful, however, some cases showed overlapping findings. We think CE-EUS can be used as one of adjunctive tool for the evaluation of gallbladder mass.

CE-EUS for visceral vascular dissection

Celiac artery (CA) dissection or superior mesenteric artery (SMA) dissection is occasionally observed and the diagnosis is usually suggested by CT scan. Visceral artery angiography is used for definitive diagnosis and interventional therapy such as stenting can be combined when necessary. However, angiography is quite invasive. Our group tried to use CE-EUS for the diagnosis and assessment of visceral artery dissection for the first time. Color Doppler

image as well as CE-EUS are quite useful for the diagnosis of CA or SMA dissection. This technique can delineate true lumen and false lumen, intimal tearing site, and the extent of dissection. Another advantage is that we can calculate the stenosis area and percentage. These data can give critical information in deciding therapeutic strategy.

Conclusion

CE-EUS is relatively new technique and several studies suggested the usefulness of this technique for the differential diagnosis of pancreatic solid mass, cystic mass, gallbladder mass and the assessment of visceral vascular dissection. However, more data are required before generalized use of CE-EUS for pancreato-biliary disease.

CC 2 PHY-1

Physics in Emerging Ultrasound Imaging Technologies

08:30-09:00

Room 201

Chairpersons: **Dong-Guk Paeng** *Jeju National University, Korea*
Yangmo Yoo *Sogang University, Korea*

Photoacoustic Imaging: Toward Clinical Translation

Changhan Yoon

Department of Biomedical Engineering, Inje University, Korea

Photoacoustic imaging is an emerging imaging modality that combines optical contrast and high acoustic spatial resolution. Photoacoustic imaging with inherently co-registered ultrasound imaging can provide anatomical, functional and molecular information simultaneously, which allow noninvasive tissue characterization. Photoacoustic imaging has been proven to be an important imaging modality in

many pre-clinical studies, and a number of research group are now moving toward clinical translation of photoacoustic imaging. In this presentation, an array-based photoacoustic imaging system will be introduced for detection of cancer and sentinel lymph node or metastasis. In addition, clinically-relevant contrast agents for molecular imaging will be also presented.

CC 2 PHY-2

Physics in Emerging Ultrasound Imaging Technologies

09:00-09:30

Room 201

Chairpersons: **Dong-Guk Paeng** *Jeju National University, Korea*
Yangmo Yoo *Sogang University, Korea*

Categorical Course
May 26, Friday (Room 201)

Present and Future Technology for Intravascular Ultrasound Imaging

Jinhyung Park

Department of Biomedical Engineering, Sungkyunkwan University, Korea

Coronary arteriosclerosis is a blood vessel disease which has narrowed lumen blocked by enlarged plaques including thrombus, lipid and calcified structures. Conventionally, fluoroscopy has been used for diagnosing the vessel disease by projecting X-ray to the coronary artery in one direction. Since the specificity of the fluoroscopy is dependent on the projection angle, intravascular ultrasound (IVUS) imaging which can visualize the cross sectional structures of blood vessels with high resolution becomes one of the important workflows in percutaneous coronary Intervention(PCI) for expanding the narrowed blood vessels rightly with stents. Under those workflows, the roles of

IVUS Imaging are measuring the diseased blood vessels for choosing an adequate size of stent and the expansion pressures and evaluating the PCI outcomes by checking the condition of the deployed stent. Recently, the use of bio-resorbable stents (BRS) becomes an emerging trend in PCI since the stent relieves the burden of having the permanent implant. However, the vessel measurement needs to be more accurate in using BRS than the one for the conventional stent otherwise the stents may be demolished resulting in death. For visualizing the BRS properly with IVUS, higher resolution imaging seems to be pre-requisite, and those needs may lead the new trends In IVUS imaging technologies.

Chairpersons: Dong-Guk Paeng *Jeju National University, Korea*
Yangmo Yoo *Sogang University, Korea*

High Frequency Ultrasound Transducers for High Definition Imaging

Hyung Ham Kim

Department of Creative IT Engineering, Pohang University of Science and Technology, Korea

High-frequency (15 - 50 MHz) ultrasound is widely used in preclinical imaging. Mice, mouse embryos, rats or zebrafish are tested to model a variety of human diseases and high frequency ultrasound imaging provides an excellent visualization of the progress and effects of the designed experiments. Due to the complexity and difficulty in the fabrication of array transducers, single element based imaging systems were used in the earlier stage. However, the mechanical translation of the single element, required to obtain images works as a limiting factor for temporal resolution, depth of field and operating modes. Array transducer translates acoustic beams electronically and therefore may achieve higher

frame rates up to 100 frames per second. Transmit beamforming and receive dynamic focusing provide the extended depth of field. Doppler and color flow modes are offered, which were very difficult to implement with the single element. High frequency ultrasound imaging with linear, convex, and phased arrays is now expanding its applications from preclinical imaging to clinical imaging. A 20 MHz convex array, a 30 MHz phased array, and a 30 MHz linear array for preclinical and clinical imaging are presented. High frequency arrays can obtain highresolution images of any small parts adjacent to the skin or accessible through the cavity.

SC 1 THY-1

10:20-10:40

GBR 101

Chairpersons: Eun-Kyung Kim *Severance Hospital, Korea*
Younghen Lee *Korea University Ansan Hospital, Korea*

US for Thyroid Nodules: Technical Advances and Future Horizons

Kunwar Bhatia

Department of Radiology, Imperial College Healthcare NHS Trust, UK

This talk will outline recent technical advances in US in hardware technology and software post processing that allow improved visualisation and characterisation of thyroid nodules. It will also present future horizons of technologies that are either relatively new or are not universally adopted at

present but for preliminary evidence shows promise. These include commercially available modes that optimise detection of microcalcifications and low flow vascularity, 3D ultrasound, contrast enhanced ultrasound, USE elastography and computer aided diagnosis (CAD).

Chairpersons: **Jae-Joon Chung** *Gangnam Severance Hospital, Korea*
Jong Young Oh *Dong-A University Hospital, Korea*

US-CT/MRI Correlation of Liver Disease

Yangshin Park

Department of Radiology, Korea University Guro Hospital, Korea

Ultrasound is a well-recognized first imaging technique for the evaluation of liver disease, as it is an easily available, non-invasive and very cost-effective imaging modality with a lack of radiation exposure. Due to the continuously improving ultrasound techniques and the high number of abdominal ultrasound examinations, incidentally detected focal liver lesions are commonly encountered in daily clinical practice. These incidentally detected focal liver lesions have been reported with a frequency of 2.3-6.2% on screening ultrasound. In autopsy series it has been established that 20-50% of the population exhibit benign focal liver lesions, mostly cysts and hemangiomas, and that incidence rises with age.

In the cirrhotic liver the major concern is detection and characterization of hepatocellular carcinomas (HCCs). Although characteristic features of HCC are peripheral halo sign, posterior acoustic enhancement, lateral shadow, and mosaic pattern, the sonographic feature is variable and it is difficult to differentiate HCC from dysplastic or regenerative nodules in US. In the non-cirrhotic liver the situation is quite different: the most frequently encountered focal liver lesions are cysts, hemangiomas, focal nodular hyperplasia and metastases. In asymptomatic and healthy persons without any previous history of malignant or chronic liver disease the majority of incidentally detected focal liver lesions are benign, with an estimated probability of >95%. The situation is different in patients with a known extrahepatic malignancy. In these patients, the probability that a newly discovered focal liver lesion is a liver metastasis is significantly higher compared to the probability in healthy persons.

On the other hand, there is overlap between sonographic features of benign and malignant lesions. However, there are some characteristic appearances that, combined with clinical information, lead to the correct diagnosis: small echogenic lesions in a patient with no known malignancy are usually hemangiomas; an echo-poor halo ("target" sign) pattern is usually suggestive of malignancy; an anechoic area in an echogenic lesion generally equates with necrosis in the center of a malignant lesions and a focal lesion in the context of cirrhosis must be regarded as suspicious of hepatocellular carcinoma. Some liver lesions like cysts, characteristically hyperechoic hemangiomas < 3 cm in non-steatotic liver, characteristically located focal fat accumulations or focal sparing in a fatty liver can be easily diagnosed with ultrasound, without the need for further investigations. On occasion, some FNHs can be identified using Doppler techniques due to the typical 'wheel spoke' vascularization pattern.

Ultrasound is widely used and modality of choice of liver disease evaluation. However, most researches and educations have focused on CT and MRI. Therefore, in this lecture, sonographic features and differential diagnosis of focal liver lesions as well as correlation with imaging findings on CT and MRI will be described.

References

1. Kaltenbach TE, Engler P, Kratzer W, Oeztuerk S, Seufferlein T, Haenle MM, et al. Prevalence of benign focal liver lesions: ultrasound investigation of 45,319 hospital patients. *Abdom Radiol (NY)*. 2016;41(1):25-32.
2. Chiorean L, Cantisani V, Jenssen C, Sidhu PS, Baum U,

- Dietrich CF. Focal masses in a non-cirrhotic liver: The additional benefit of CEUS over baseline imaging. Eur J Radiol. 2015;84(9):1636-43.
3. Harvey CJ, Albrecht T. Ultrasound of focal liver lesions. Eur Radiol. 2001;11(9):1578-93.
4. Tchelepi H1, Ralls PW. Ultrasound of focal liver masses. Ultrasound Q. 2004;20(4):155-69.

Chairpersons: **Jae-Joon Chung** *Gangnam Severance Hospital, Korea*
Jong Young Oh *Dong-A University Hospital, Korea*

US-CT/MRI Correlation of Gallbladder Disease

Soo Jin Kim

Department of Radiology, National Cancer Center, Korea

In this lecture, we would review and correlate US and CT/MRI findings of most common and clinically significant gallbladder disease.

1. Acute Cholecystitis

- **US-CT-MR finding**

- **DDx. Gallbladder edema, GVHD**

2. Chronic Cholecystitis

: **US-CT-MR finding**

- **Adenomyomatosis**

- **Xanthogranulomatous Cholecystitis**

3. Gallbladder cancer

: **US-CT-MR finding**

4. Differential Diagnosis between adenomyomatosis/XGC and GBC

- **emphasis on wall enhancement pattern on CT,
MRI & DWI on MRI**

- **differential points on USG**

Chairpersons: **Jae-Joon Chung** *Gangnam Severance Hospital, Korea*
Jong Young Oh *Dong-A University Hospital, Korea*

US-CT/MRI Correlation of Pancreas Disease

Yedaun Lee

Department of Radiology, Haeundae Paik Hospital, Korea

Pancreas is the challenge for the beginners in abdominal ultrasonography. It is difficult to see normal pancreas. To visualize the pancreas, fasting patients for at least 7-8 hours and getting acoustic window is very important.

I. Normal anatomy: uncinated process, head, body, tail

II. Congenital lesion

1. Annular pancreas : pancreas encircles 2nd portion of duodenum.
2. Ectopic pancreas : m/c in stomach antrum
3. Intrapancreatic accessory spleen
 - a. US: round or oval mass with homogeneous texture
 - b. CT/MR: show similar attenuation/signal intensity with spleen on all the phase of CT/MR.

III. Pancreatitis

1. Acute pancreatitis

- a. US: pancreas swelling, decrease in echogenicity of pancreas, heterogeneous parenchymal echogenicity, peripancreatic fluid collection
- b. CT/MR: focal or diffuse swelling of pancreas, peripancreatic infiltration and fluid collection, pancreatic or peripancreatic necrosis

2. Chronic pancreatitis

- a. US: atrophy of pancreas, P duct dilatation, calcification with posterior acoustic shadow
- b. CT/MR: atrophy of pancreas, P duct dilatation, pancreaticolith, pancreatic calcification

3. Autoimmune pancreatitis

- a. US: similar with acute pancreatitis, enlarged and hypoechoic parenchyma
- b. CT/MR: sausage-shaped pancreas with smooth border, capsule-like peripheral rim, irregular narrowing of P duct

IV. Solid mass

1. Ductal adenocarcinoma

- a. US: hypoechoic mass with P duct dilatation
- b. CT/MR: irregular poorly enhancing mass with upstream P duct dilatation

2. Neuroendocrine tumor

- a. US: hypoechoic mass
- b. CT/MR: hypervascular mass, large and nonfunctioning tumor may show cystic and necrotic change.

3. Solid and pseudopapillary neoplasm

- a. US: Heterogenous mass with fluid-debris level
- b. CT/MR: encapsulated heterogeneous mass with hemorrhage

V. Cystic mass

1. Intraductal mucinous neoplasm

- a. US: lobulated cystic lesion, main P duct dilatation
- b. CT/MR: lobulated cystic lesion, tubular or grape-like appearance, main P duct dilatation

2. Serous cystadenoma

- a. US: hyperechoic mass (microcystic type), lobu-

lated cystic mass

- b. CT/MR: Honeycomb appearance, central calcification, high signal intensity on T2 weighted image.

3. Mucinous cystic neoplasm

- a. US: Unilocular or multiloculated cystic mass
- b. CT/MR: Enhancing septa and cystic wall, peripheral calcification, variable signal intensity on T1 weighted image

Chairpersons: **Jae-Joon Chung** *Gangnam Severance Hospital, Korea*
Jong Young Oh *Dong-A University Hospital, Korea*

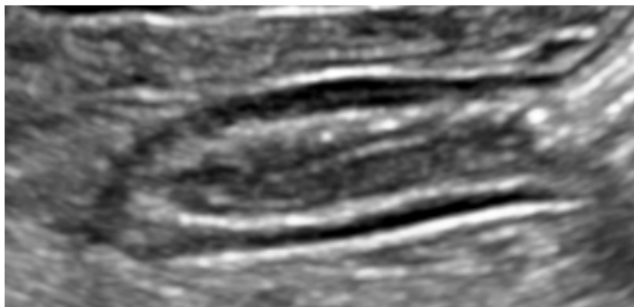
US-CT/MRI Correlation of Bowel Disease

Yoon Jin Lee

Department of Radiology, Seoul National University Bundang Hospital, Korea

1. Normal US findings of the bowel

- Mural thickness: 3-5 mm
- Gut signature: alternating hyperechoic and hypoechoic layers corresponding to histology
 - ① Innermost hyperechoic line: interface between bowel lumen and mucosa \approx mucosal layer
 - ② Thin hypoechoic layer: muscularis mucosa
 - ③ Hyperechoic layer: submucosa
 - ④ Hypoechoic layer: muscularis propria
 - ⑤ Outermost hyperechoic surface: serosa



- Vascularity in color or power Doppler imaging: low velocity flow rarely identifiable, increased in inflammatory disease, decreased in ischemia
- Motility, peristalsis: usually decreased in diseased bowel
- Compressibility: graded compression displacing bowel gas and overlying bowel loops \rightarrow improve visibility, assess compressibility and rigidity
- Mesentery: increased echogenicity of mesenteric fat, lymphadenopathy around the diseased bowel loop

2. US imaging technique

- 6-hours fasting to reduce bowel gas
- Conventional transabdominal ultrasonography with convex probe
- Targeted bowel examination with high-frequency linear probe
- Systematic scanning
 - ① RUQ hepatic flexure down to cecum \rightarrow terminal ileum \rightarrow appendix \rightarrow other quadrants
 - ② Overlapping vertical sweeps
 - ③ Retrocecal area: left decubitus position
 - ④ Attention to focal areas of tenderness or pain
- Hydrososonography, CEUS

3. Summary of ultrasonographic features of common bowel disease

Disease	Bowel wall thickness	Gut signature	Color Doppler flow
Crohn disease	\uparrow	Usually preserved	\uparrow in active inflammation
Ulcerative colitis	normal or \uparrow	Preserved	\uparrow in active inflammation
Bowel obstruction	Usually normal	Usually preserved	Usually preserved
Diverticulosis	May be mildly increased due to hypertrophy of proper muscle	Preserved	Normal
Diverticulitis	\uparrow	Usually preserved	\uparrow in active inflammation

Bowel ischemia	Usually ↑	Preserved or disrupted	Usually ↓
Bowel neoplasm	↑ focally or circumferentially	Disrupted	Variable

4. Benign diseases

1) Acute appendicitis

- Sonographic criteria: combination of findings
- ① Noncompressible blind-ending tube
- ② Maximum outside diameter > 6 mm
- ③ Wall thickness > 3mm
- ④ Loss of gut signature
- ⑤ Hyperemia on Doppler scanning
- ⑥ Hyperechoic periappendiceal fat thickening
- ⑦ Local sonographic tenderness

2) Acute diverticulitis

- outpouching lesion from colon wall, echogenic noncompressible pericolic fat, segmental hypoechoic wall thickening with hyperemia, pericolic fluid collection

3) Inflammatory bowel disease

- Crohn disease: bowel wall thickening (noncompressible, rigid), skip lesions, creeping fat, fat wrapping, variably decreased peristalsis, stricture, fistula, abscess, phlegmon
- Ulcerative colitis: wall thickening, hyperemia, loss of haustra coli

4) Infectious enterocolitis

- CDAD (previously PMC): markedly thickened colonic wall with prominent gyral pattern, blurred gut signature, linear echogenic pseudomembrane in lumen
- Intestinal tuberculosis: ileocecal wall thickening, mesenteric LAP

5) Intussusception

- lead point usually neoplastic in adult, target sign

6) Bowel obstruction

- Hyperperistalsis in acute stage, aperistalsis in high-grade obstruction

7) Bowel ischemia

- Circumferential wall thickening of long segment, decreased vascularity, abrupt transition

8) Celiac disease

- Gluten-sensitive enteropathy, prominent small bowel folds, hypomotility, excess fluid in bowel lumen, transient nonobstructive intussusception

9) Pneumoperitoneum

- Enhancement of peritoneal stripe with posterior shadowing or reverberation artifacts

10) Pneumatosis intestinalis

- Multiple intramural echogenic foci
- False positive finding: intramural foreign body such as surgical staples, air trapped between folds, beam thickness artifact

5. Neoplastic diseases

1) Lymphoma

- Hypoechoic~anechoic, disrupted gut signature, usually circumferential wall thickening, aneurysmal dilatation, lymphadenopathy

2) Adenocarcinoma, carcinoid tumor (NET), GIST

References

1. Rodgers PM. Ultrasound of the Hollow Viscera. In: Gore RM, Levine MS, ed. Textbook of Gastrointestinal Radiology. 4th ed. Philadelphia: Elsevier Saunders, 2015;56-66.
2. Muradali D, Goldberg DR. US of gastrointestinal tract disease. RadioGraphics 2015;35:50-70.
3. O'Malley ME, Wilson SR. US of gastrointestinal tract abnormalities with CT correlation. RadioGraphics 2003;23:59-72.
4. Maturen KE, Wasnik AP, Kamaya A, Dillman JR, Kaza RK, Pandya A, et al. Ultrasound imaging of bowel pathology: technique and keys to diagnosis in the acute abdomen. AJR 2011;197:W1067-W1075.
5. Wale A, Pilcher J. Current role of ultrasound in small bowel imaging. Semin Ultrasound CT MRI 2016;37:301-312.

Chairpersons: Joon Hyung Lee *Dong-A University Hospital, Korea*
Jung Hwan Baek *Asan Medical Center, Korea*

K-TIRADS - Lexicon & Risk Stratification

Jung Hee Shin

Department of Radiology, Samsung Medical Center, Korea

The Korean Society of Thyroid Radiology has recently revised consensus recommendations for ultrasonography diagnosis and imaging-based management of thyroid nodules. Korean-Thyroid Imaging Reporting and Data System (K-TIRADS) was proposed including the terminology and ultrasonography (US) features in thyroid nodule, and malignancy risk stratification system for thyroid nodules.

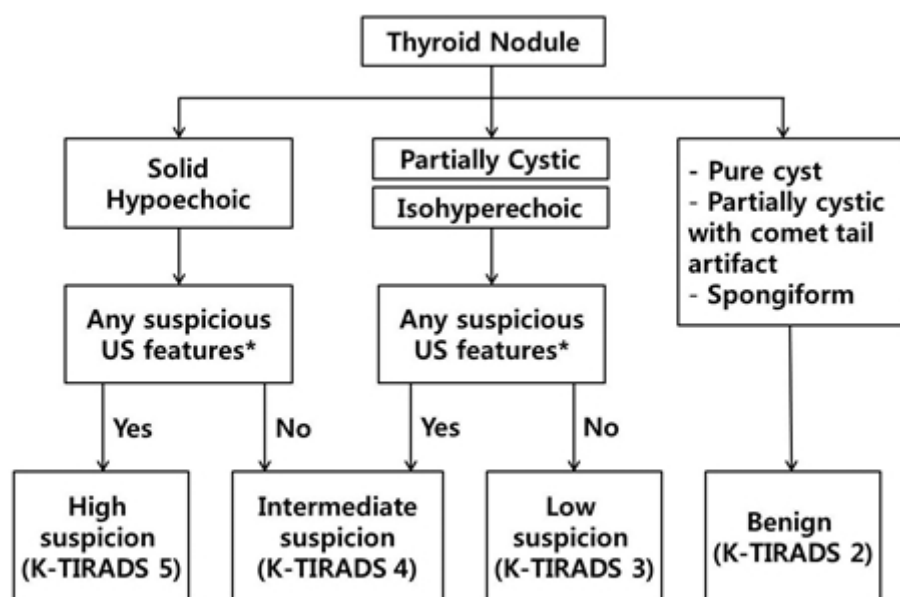
In K-TIRADS, the definition of US terminology for thyroid nodules was described. The contents are as follows. Some confusing terms will be explained in this lecture.

1. Nodule size
2. Internal content

3. Echogenicity
4. Nodule shape and orientation
5. Nodule margin
6. Calcification, echogenic foci
7. Nodule vascularity

In K-TIRADS, thyroid nodules are classified as high suspicion (category 5), intermediate suspicion (category 4), low suspicion (category 3), and benign (category 2) nodules based on their malignancy risk stratification by the US patterns, which consist of solidity, echogenicity and suspicious US features (Figure 1 and Table 1).

The indications for FNA of thyroid nodules are determined by the US features and tumor size.



* Microcalcification, Nonparallel orientation, Spiculated/microlobulated margin

Figure 1. US-RISK STRATIFICATION AND THE K-TIRADS. Adapted from Shin et al (1).

Korean radiologists recommend FNA for category 5 nodules when the size is ≥ 1.0 cm; however, the size criteria is lowered to >0.5 cm in the presence of extrathyroidal extension, cervical lymph node or distant metastasis, trachea or recurrent laryngeal nerve invasion, and tumor progression.

Table 1. Malignancy risk stratification according to K-TIRADS and FNA indications

Category	US feature	Malignancy risk (%)	FNA
5 High suspicion	Solid hypoechoic nodule with any of 3 suspicious US features	> 60	≥ 1 cm (> 0.5 cm, selective)
4 Intermediate suspicion	1) Solid hypoechoic nodule without any of 3 suspicious US features or 2) Partially cystic or isohyperechoic nodule with any of 3 suspicious US features	15-50	≥ 1 cm
3 Low suspicion	Partially cystic or isohyperechoic nodule without any of 3 suspicious US features	3-15	≥ 1.5 cm
2 Benign	Spongiform Pure cyst Partially cystic nodule with comet tail artifact	< 3 < 1	≥ 2 cm NA
1 No nodule			NA

Reference

1. Shin JH, Baek JH, Chung J, Ha EJ, Kim JH, Lee YH, Lim HK, Moon WJ, Na DG, Park JS, Choi YJ, Hahn SY, Jeon SJ, Jung SL, Kim DW, Kim EK, Kwak JY, Lee CY, Lee HJ, Lee JH, Lee JH, Lee KH, Park SW, Sung JY, Korean Society of Thyroid R, Korean Society of R 2016 Ultrasonography Diagnosis and Imaging-Based Management of Thyroid Nodules: Revised Korean Society of Thyroid Radiology Consensus Statement and Recommendations. Korean J Radiol 17:370-395.

Chairpersons: Joon Hyung Lee *Dong-A University Hospital, Korea*
Jung Hwan Baek *Asan Medical Center, Korea*

K-TIRADS - Comparison with Guidelines of Other Societies

Dong Gyu Na

Department of Radiology, GangNeung Asan Hospital, Korea

Korean Thyroid Imaging Reporting and Data System (K-TIRADS) has been recently proposed for the US malignancy risk stratification of thyroid nodules by Korean Society of Thyroid Radiology (KSThR) and KTA (Korean Thyroid Association) (1). At present, many international thyroid societies have proposed different US malignancy risk stratification systems and FNA criteria for thyroid nodules (1-7).

The US risk stratification systems can be categorized as pattern-based system (ATA, BTA, NCCN, AACE/ACE/AME, SFE, KTA/KSThR) or point-based system (ACR). The pattern-based systems categorize thyroid nodules by various combination of individual US features and the point-based system add up weighted point of each individual US feature present in a nodule. The pattern-based systems differ in the complexity of the system according to the way of combination, and has an advantage that a system can be intuitive and feasible for clinical application if the pattern system is simplified. However, the simplified system has a disadvantage that it may provide less accurate estimation of malignancy risk for each individual nodule. Point-based system has an advantage that it may more accurately estimate the malignancy risk of thyroid nodules. However, it requires rather complex calculation and less intuitive and less feasible for clinical application. The complex point-based system needs a computer-based calculation system for clinical application (8).

In our recent comparative study of international society guidelines (9) by using the retrospective cohort data (2000 nodules ≥ 1 cm) demonstrated that the KTA/KSThR (94.5%), NCCN (92.5%), and ATA (87.6%) guidelines showed the higher

sensitivity than those of AACE/AME/ETA (80.4%), ACR (74.7%), and FSE (72.7%) ($P < 0.001$); while the latter guidelines showed the higher specificity than the former ones ($P < 0.001$). The unnecessary FNA rate was the lowest in ACR (25.3%) followed by FSE (29.1%), AACE/AME/ETA (32.5%), ATA (51.7%), NCCN (54.0%), and KTA/KSThR guidelines (56.9%).

Since the diagnostic performance of US-based FNA criteria are variable according to the international society guidelines, we have to be aware of its strength and weakness in the management of thyroid nodules.

ATA = American Thyroid Association Management Guidelines for Adult Patients with Thyroid Nodules and Differentiated Thyroid Cancer, BTA = British Thyroid Association, AACE/ACE/AME = American Association of Clinical Endocrinologist/American College of Endocrinology/Associazione Medici Endocrinologi, FSE = Guidelines of the French Society of Endocrinology for the Management of Thyroid Nodules, NCCN = National Comprehensive Cancer Network guidelines, ACR = American College of Radiology

References

1. Shin JH, Baek JH, Chung J, Ha EJ, Kim JH, Lee YH, Lim HK, Moon WJ, Na DG, Park JS, Choi YJ, Hahn SY, Jeon SJ, Jung SL, Kim DW, Kim EK, Kwak JY, Lee CY, Lee HJ, Lee JH, Lee JH, Lee KH, Park SW, Sung JY; Korean Society of Thyroid Radiology (KSThR) and Korean Society of Radiology. Ultrasonography Diagnosis and Imaging-Based Management of Thyroid Nodules: Revised Korean Society of Thyroid Radiology Consensus Statement and Recommendations. *Korean J Radiol.* 2016;17(3):370-95.
2. Haugen BR, Alexander EK, Bible KC, Doherty G, Mandel

- SJ, Nikiforov YE, Pacini F, Randolph G, Sawka A, Schlumberger M, Schuff KG, Sherman SI, Sosa JA, Steward D, Tuttle RM, Wartofsky L. 2015 American Thyroid Association Management Guidelines for Adult Patients with Thyroid Nodules and Differentiated Thyroid Cancer. *Thyroid* 2016; 26:1-133.
3. Gharib H, Papini E, Garber JR, Duick DS, Harrell RM, Hegedüs L, Paschke R, Valcavi R, Vitti P; AACE/ACE/AME Task Force on Thyroid Nodules.. AMERICAN ASSOCIATION OF CLINICAL ENDOCRINOLOGISTS, AMERICAN COLLEGE OF ENDOCRINOLOGY, AND ASSOCIAZIONE MEDICI ENDOCRINOLOGI MEDICAL GUIDELINES FOR CLINICAL PRACTICE FOR THE DIAGNOSIS AND MANAGEMENT OF THYROID NODULES--2016 UPDATE. *Endocr Pract.* 2016;22(5):622-39.
4. National Comprehensive Cancer Network, Inc. 2014 Practice Guidelines in Oncology-Thyroid Carcinoma v.2. Available at: www.nccn.org/professionals/physician_gls/f_guidelines.asp.
5. Perros P, Boelaert K, Colley S, Evans C, Evans RM, Gerrard Ba G, Gilbert J, Harrison B, Johnson SJ, Giles TE, Moss L, Lewington V, Newbold K, Taylor J, Thakker RV, Watkinson J, Williams GR. Guidelines for the management of thyroid cancer. *Clin Endocrinol (Oxf)* 2014; 81:1-122.
6. We´meau JL, Sadoul JL, d'Herbomez M, Monpeysen H, Tramalloni J, Leteurtre E, Borson-Chazot F, Caron P, Carnaille B, Le´ger J, Do C, Klein M, Raingeard I, Desaillood R, Leenhardt L. Guidelines of the French Society of Endocrinology for the management of thyroid nodules. *Ann Endocrinol (Paris)* 2011;72:251-281.
7. Tessler FN, Middleton WD, Grant EG, Hoang JK, Berland LL, Teefey SA, Cronan JJ, Beland MD, Desser TS, Frates MC, Hammers LW, Hamper UM, Langer JE, Reading CC, Scoutt LM, Stavros AT. ACR Thyroid Imaging, Reporting and Data System (TI-RADS): White Paper of the ACR TI-RADS Committee. *J Am Coll Radiol.* 2017 Mar 31.
8. Choi YJ, Baek JH, Baek SH, Shim WH, Lee KD, Lee HS, Shong YK, Ha EJ, Lee JH. Web-Based Malignancy Risk Estimation for Thyroid Nodules Using Ultrasonography Characteristics: Development and Validation of a Predictive Model. *Thyroid.* 2015;25(12):1306-12
9. Ha EJ, Na DG, et al. Diagnostic Performance of Ultrasound-based Fine Needle Aspiration Biopsy Criteria for Thyroid Malignancy: A Comparative Study based on Six International Society Guidelines (unpublished).

Chairpersons: **Joon Hyung Lee** *Dong-A University Hospital, Korea*
Jung Hwan Baek *Asan Medical Center, Korea*

K-TIRADS - Current Issues and Future Directions

Eun Ju Ha

Department of Radiology, Ajou University Hospital, Korea

TI-RADS is currently evolving from the initial proposal by Horvath et al. in 2009 to the recent K-TIRADS by KSThR in 2016. However, despite these efforts, none of TI-RADS classifications have been widely adopted worldwide and there are still conflicting recommendations from several societies. Therefore, there have been still many attempts to develop a practical, standardized classification for the risk stratification of thyroid nodules and to provide consistent management in practice. Standardization of the US lexicon, along with efforts to provide an evidence-based risk stratification system, is necessary for the proper management of thyroid nodules.

Recent trends in the management paradigm of thyroid nodules tend to have moved toward a conservative approach, as an alternative to FNA. TI-RADS tend also to be geared towards more personalized management, along with minimizing unnecessary FNAs. In this respect, it may be necessary that the current risk stratification systems using 5 categories should be more segmented according to the combination of US characteristics. However, as more of the risk scoring system is segmented, it may not be clinically feasible, due to its complexity. Thyroid computer-aided diagnosis (CAD) using artificial intelligence might be one option to solve this problem. Chang et al. in 2016 reported that the use of thyroid CAD to differentiate malignant lesions from benign ones showed accuracy similar to that obtained via visual inspection performed by radiologists. In the same year, Choi et al. implemented thyroid CAD system into the US machine and demonstrated that the sensitivity for thyroid cancer was similar to that of experienced

radiologist; however specificity was higher in radiologist. The combination of thyroid CAD with a risk scoring system, implemented on a commercial US machine, could decrease operator dependency in image interpretation and assist with real-time interpretation for assessing the risk of malignancy and FNA decisions in patients with thyroid nodules.

Combined categorical reporting systems between clinical and US features or between cytology and US features should be evaluated to gain a proper indication for FNA. Ianni et al. recently reported a new cancer risk score, the so-called “CUT” score, derived from clinical and US features along with the five-tiered TI-RADS score for the preoperative assessment of thyroid nodules. In this study, the combined score represented the cytologic result of the FNA. Lee et al. demonstrated that the relative risk ratios of the initial FNA category of “atypia of undetermined significance” and thyroid US categories of US 3, US 4, and US 5 revealed a high malignancy rate. Although there are still only a limited number of studies in the literature, these findings might be useful for suggesting indications for initial and repeat US-guided FNA, which may ultimately lead to the effective management of thyroid nodules. In the future, development of CAD system and, combination of US feature, clinical and cytopathologic information could enhance diagnostic performance and minimize unnecessary biopsy and/or surgery.

In summary, the proper use of K-TIRADS, provides numerous advantages including facilitating the standardized assessment of thyroid nodules that clearly indicate a need for consistent management recommendations, as well as effective

communication between referring physicians and cytopathologists. An understanding of the current status and future developmental direction of

K-TIRADS will be of great help to physicians in the management of thyroid nodules.

SFS 2 MSK-1

Advanced Musculoskeletal US

13:10-13:40

GBR 102

Chairperson: Kil-Ho Cho Yeungnam University Medical Center, Korea

Ankle Ultrasound around the Lateral Malleolus

Carlo Martinoli

Department of Radiology, DISSAL University of Genova, Italy

The role of ultrasound (US) has become increasingly important in the assessment of tendons, joints, ligaments and other soft-tissue injuries about the foot and ankle. Being many structures to be examined, the US examination should be focused on clinical findings in an attempt to save time and increase the efficacy of the study. The area around the lateral malleolus is very commonly involved in sports injuries, accounting for 77% of all ankle traumas. The pathomechanism includes inversion and plantar flexion of the foot when landing off balance or clipping another player's foot. In inversion ankle injuries, the status of the anterior tibiotalar, anterior inferior tibiofibular (incl. the Basset fascicle)

and calcaneofibular ligaments can be assessed with effective results by means of static and dynamic scans. Some midtarsal ligaments (e.g., dorsal calcaneocuboid, superior talonavicular, bifurcate) and the frondiform retinaculum may be occasionally involved and should be evaluated systematically. US can diagnose peroneal tendon instability based on tendon displacement relative to the malleolar groove and recognize retinacular/periosteal tears. Dynamic scanning can help to detect cases of intermittent subluxation. Longitudinal splits of the peroneus brevis are well recognized with this technique. Occult fractures and ankle neuropathies (i.e., superficial peroneal) may be detected occasionally.

Chairperson: Kil-Ho Cho Yeungnam University Medical Center, Korea

Ultrasound of the Anterolateral Hip

Carlo Martinoli

Department of Radiology, DISSAL University of Genova, Italy

The anterolateral hip and the groin are challenging areas due to the complexity of anatomy and because patient's symptoms may be multifactorial and history may be ambiguous or misleading. Despite some limitations, ultrasound (US) plays an important role in the assessment of a variety of pathologic conditions affecting the regional soft-tissues, can provide dynamic evaluation and guide interventional procedures. In the anterior hip, the joint space can be effectively screened for effusion and synovitis by examining the anterior recess. Iliopsoas bursal distension, acetabular labrum tears and associated paralabral ganglia can be detected with US. Adenopathies, femoral vessel diseases and regional neuropathies (incl. femoral, obturator and lateral femoral cutaneous) can be reliably identified. US is accurate to diagnose degenerative changes and

tears of anterior hip tendons, including a variety of pathologic conditions such as tensor fascia lata tendinopathy, tears of the rectus femoris origin affecting its direct and indirect tendons, snapping and tear of the psoas tendon as well as abnormalities of the common aponeurosis at the symphysis pubis. Inguinal hernias, including indirect, direct and femoral types, can be assessed at rest and during Valsalva based on specific anatomical landmarks. In the lateral hip, US can recognize degenerative tendinopathy of the gluteus medius and gluteus minimus tendons in the context of the greater trochanteric pain syndrome providing an effective guide for trochanteric bursa injections. Then, dynamic scanning can identify iliotibial band instability as the cause of lateral snapping hip.

SFS 3 KSTU-1

Therapeutic Ultrasound

13:10-13:40

Room 201

Chairpersons: **Tai-Kyong Song** *Sogang University, Korea*
Jinwoo Chang *Yonsei University, Korea*

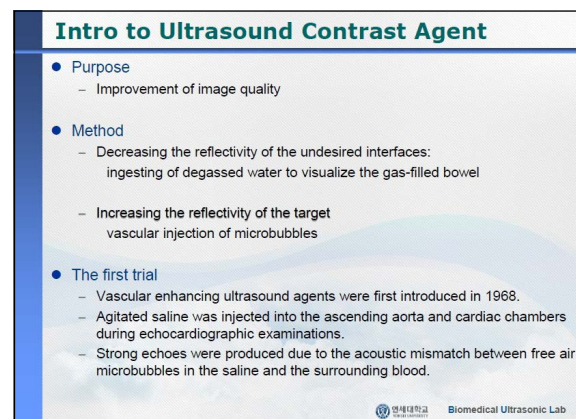
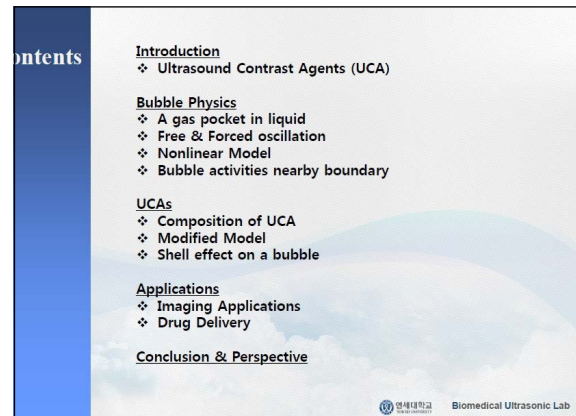
Fundamentals of Ultrasonic Contrast Agent

Jongbum Seo

Department of Biomedical Engineering, Yonsei University, Korea

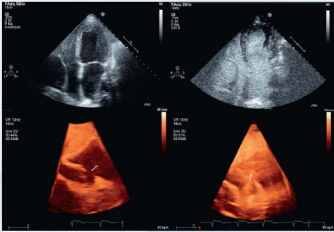
In this session, I will present the basic physics of microbubbles and their applications.

Special Focus Session
May 26, Friday (Room 201)



Ultrasound Image with UCA

- Image example



Oteo et Al. Rev Exp Cardiol. 2013

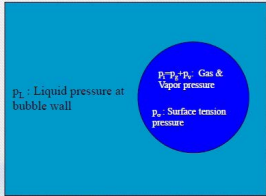
연세대학교 Yonsei University Biomedical Ultrasonic Lab

PHYSICS OF BUBBLE : CAVITATION

연세대학교 Yonsei University Biomedical Ultrasonic Lab

A bubble in liquid

- Laplace Pressure due to Surface Tension (spherical bubble)



$$p_i = p_L + p_{\sigma}$$

$$p_{\sigma} = \frac{2\sigma}{R}$$

- p_g (inside bubble) > p_g (surrounding body) due to p_{σ}
 - Gas dissolve more >> radius reduction >> p_g increase

연세대학교 Yonsei University Biomedical Ultrasonic Lab

Blake threshold pressure

- Blake Pressure
 - static pressure lower limit for a bubble before collapse

$$p_B = p_0 - p_v + \frac{4\sigma}{3} \sqrt{\frac{2\sigma}{3(p_0 + \frac{2\sigma}{R_0} - p_v)}}$$

- If p_v is neglected & surface tension is dominant,

$$p_B \approx p_0 + 0.77 \frac{\sigma}{R_0}$$

연세대학교 Yonsei University Biomedical Ultrasonic Lab

Cavitation

- Definition
 - Any kind of gas pocket activities in liquid media
 - In general (biomedical regime), bubble activities in liquid medium (water) induced by ultrasound
- Examples
 - Oscillation of bubbles by relatively low amplitude ultrasound
 - A violent bubble collapse by relatively high amplitude ultrasound
 - Bubble migration due to acoustic field

연세대학교 Yonsei University Biomedical Ultrasonic Lab

Free oscillating bubble

- Minnaert Frequency (Resonance Frequency)
 - Spherical bubble without any shell
 - Resonance frequency according to the size of bubble

$$\omega_m = \frac{1}{R_0} \sqrt{\frac{3\gamma p_0}{\rho}}$$

$$f_0 R_0 \approx 3 \left[\frac{m}{s} \right]$$

- 1 MHz ↔ 3 μm

연세대학교 Yonsei University Biomedical Ultrasonic Lab

Free oscillating bubble

- 2nd order model

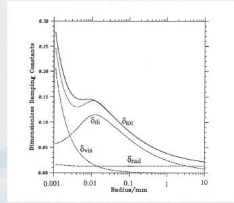
$$m\ddot{r} + b\dot{r} + kr = 0$$

$$m \approx 4\pi R_0^2 \rho$$

$$k \approx 12\pi R_0 \rho_0$$

$$b \approx \frac{m}{\omega_0} \delta$$

$$\delta = \delta_{th} + \delta_{rad} + \delta_{vis}$$



Damping Constant
Leighton, The Acoustic Bubble, 1997

연세대학교 Yonsei University Biomedical Ultrasonic Lab

Forced Oscillation (linear model)

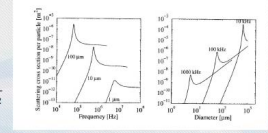
- Scattering Cross section

- Rayleigh Scatter

$$\Omega_s = 4\pi r^2 (kr)^2 \left[\left(\frac{K - K_0}{3K} \right)^2 + \frac{1}{3} \left(\frac{\rho - \rho_0}{2\rho + \rho_0} \right)^2 \right]$$

- Bubble Scatter

$$\Omega_s = 4\pi r^2 \frac{\left(\frac{\omega}{\omega_0} \right)^4}{\left(1 - \left(\frac{\omega}{\omega_0} \right)^2 \right)^2 + \left(\frac{\omega}{\omega_0} \delta \right)^2}$$



Scattering Cross Section

Hoff, Acoustic Characterization of Contrast Agents for Medical Ultrasound Imaging, Kluwer Academic Publishers, 2001

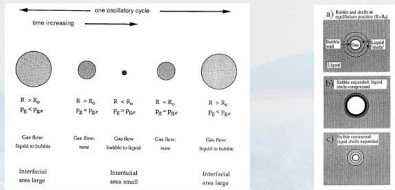
연세대학교 Yonsei University Biomedical Ultrasonic Lab

Stable Cavitation

- Oscillation of bubbles at low amplitude sound field

- Rectified Diffusion

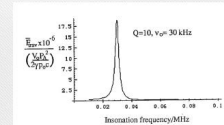
- Gas pressure gradient vs. Area of surface
- Shell thickness vs. Pressure difference (Pressure gradient)



연세대학교 Yonsei University Biomedical Ultrasonic Lab

Stable Cavitation

- Radiation force



Radiation force at resonance frequency
(damping constant = 0.1)
Leighton, The Acoustic Bubble, 1997

- Primary Bjerknes force

- Radiation force under standing wave
 - Bubble radius ≤ resonance size (oscillating in phase) → moving toward antinode
 - Bubble radius > resonance size (oscillating π out of phase) → moving toward node
- At the focus (in the pressure gradient case)
 - Bubble radius ≤ resonance size → moving toward focus
 - Bubble radius > resonance size (oscillating π out of phase) → moving away from focus

- Secondary Bjerknes force

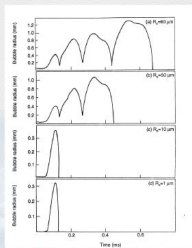
- Bubble - Bubble interaction

연세대학교 Yonsei University Biomedical Ultrasonic Lab

Nonlinear Model

- Rayleigh-Plesset Equation (including viscosity factor)

$$R\ddot{R} + \frac{3\dot{R}^2}{2} = \frac{1}{\rho} \left\{ \left(p_0 + \frac{2\sigma}{R_0} - p_v \right) \left(\frac{R_0}{R} \right)^{3\kappa} + p_v - \frac{2\sigma}{R} - \frac{4\eta\dot{R}}{R} - p_0 - P(t) \right\}$$



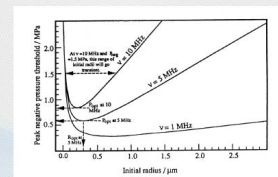
Radius of bubbles in 10 kHz field at the amplitude of $P_0 \approx 240$ kPa (Simulation Result)
Leighton, The Acoustic Bubble, 1997

연세대학교 Yonsei University Biomedical Ultrasonic Lab

Transient Cavitation

- Transient Cavitation Threshold

- Extensive growth and bubble collapse
- Apfel and Holland plot threshold for insonation by a single-cycle



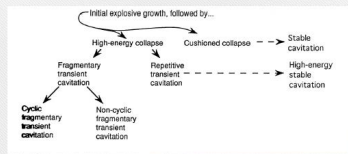
Transient Cavitation Threshold
Leighton, The Acoustic Bubble, 1997

- Mechanical Index: indication of the likelihood of transient cavitation

$$MI = \frac{P_{neg}/MPa}{\sqrt{f/MHz}}$$

연세대학교 Yonsei University Biomedical Ultrasonic Lab

Transient Cavitation



Classes of transient cavitation

Leighton, *The Acoustic Bubble*, 1997

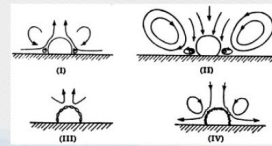


Biomedical Ultrasonic Lab

Bubble Activities near boundary

• Microstreaming

- Asymmetric boundary condition around a bubble
- Compressible gas vs. incompressible fluid media



Elder, *J. Acoust. Soc. Am.* 1959



Biomedical Ultrasonic Lab

Bubble Activities near boundary

• Asymmetric bubble collapse



Movie & Photograph courtesy of Professor LA Cnum, University of Washington



Biomedical Ultrasonic Lab

SHELLED BUBBLE : UCA

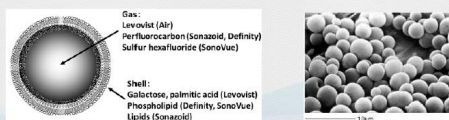


Biomedical Ultrasonic Lab

UCA Composition

• Engineered microbubbles

- Shell (stability ↔ Laplace Pressure)
- Internal gas (insoluble gas)



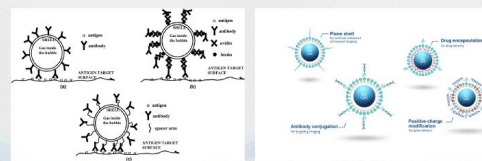
Kitano et al. *Digestive Endoscopy*, 2013



Biomedical Ultrasonic Lab

UCA Composition

• Targeted & Drug loaded



Klibanov, *Advanced Drug Delivery Reviews*, 1999

from "http://www.trust-biosonics.com/technology"



Biomedical Ultrasonic Lab

General bubble Model

- Rayleigh-Plesset Equation (reminder)

$$R\ddot{R} + \frac{3\dot{R}^2}{2} = \frac{1}{\rho} \left\{ \left(p_0 + \frac{2\sigma}{R_0} - p_v \right) \left(\frac{R_0}{R} \right)^{3\kappa} + p_v - \frac{2\sigma}{R} - p_0 - P(t) \right\}$$

$$f_0 = \frac{1}{2\pi R_0} \sqrt{\frac{3\gamma p_0}{\rho}}$$

$$f_0 R_0 \approx 3 \text{ m/s}$$

연세대학교
YONSEI UNIVERSITY

Biomedical Ultrasonic Lab

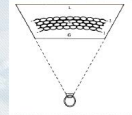
Shelled bubble Model

- Church Model (Hard protein shell)

$$R\dot{U}_1 \left[1 + \left(\frac{\rho_s - \rho_l}{\rho_s} \right) \frac{R_1}{R_2} \right] + U_1^2 \left[\frac{3}{2} + \left(\frac{\rho_s - \rho_l}{\rho_s} \right) \left(\frac{4R_2^3 - R_1^3}{2R_2^3} \right) \frac{R_1}{R_2} \right]$$

$$= \frac{1}{\rho} \left\{ P_{G,01} \left(\frac{R_{01}}{R_1} \right)^{3\kappa} - p_{v,s}(t) - \frac{2\sigma_1}{R_1} - \frac{2\sigma_2}{R_2} - 4 \frac{U_1}{R_1} \left(\frac{V_s \mu_s + R_1^3 \mu_l}{R_2^3} \right) - 4 \frac{V_s G_s}{R_2^3} \left(1 - \frac{R_{01}}{R_1} \right) \right\}$$

$$\omega_0^2 = \frac{1}{\rho_s R_{01}^2 \alpha} \left\{ 3\kappa P_{G,01} - \frac{2\sigma_1}{R_{01}} - \frac{2\sigma_2 R_{01}^3}{R_{02}^4} + 4 \frac{2V_s G_s}{R_{02}^3} \left[1 + Z \left(1 + \frac{3R_{01}^3}{R_{02}^3} \right) \right] \right\}$$



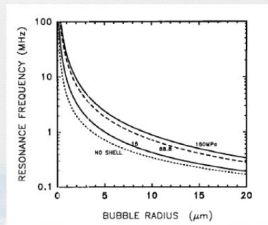
Church, J. Acoust. Soc. Am., 1995

연세대학교
YONSEI UNIVERSITY

Biomedical Ultrasonic Lab

Resonance Frequency Shifting

- Resonance frequency increase due to shell



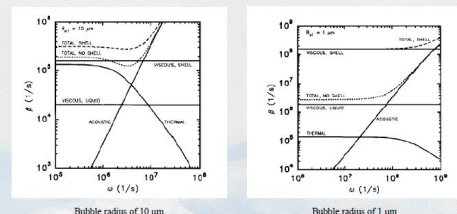
Church, J. Acoust. Soc. Am., 1995

연세대학교
YONSEI UNIVERSITY

Biomedical Ultrasonic Lab

Damping constant shift

- Shell thermal damping effect



Bubble radius of 10 μm

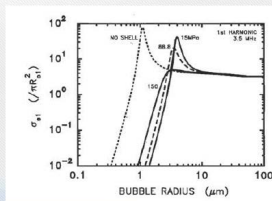
Bubble radius of 1 μm

Church, J. Acoust. Soc. Am., 1995

연세대학교
YONSEI UNIVERSITY

Biomedical Ultrasonic Lab

Scattering cross section shift



Church, J. Acoust. Soc. Am., 1995

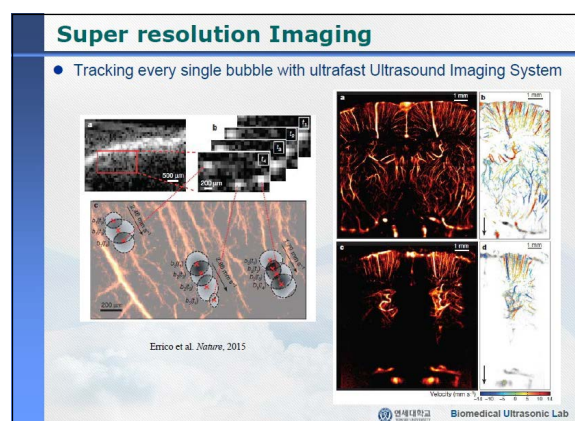
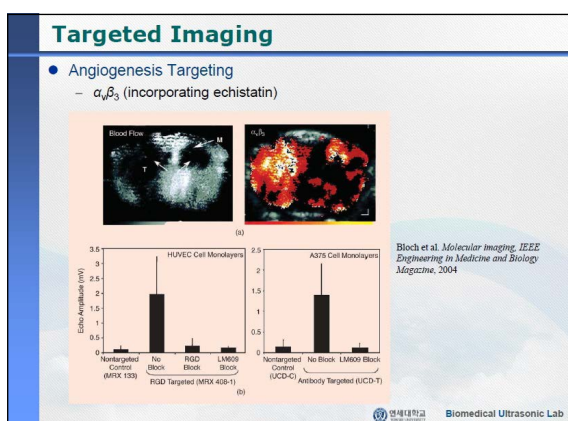
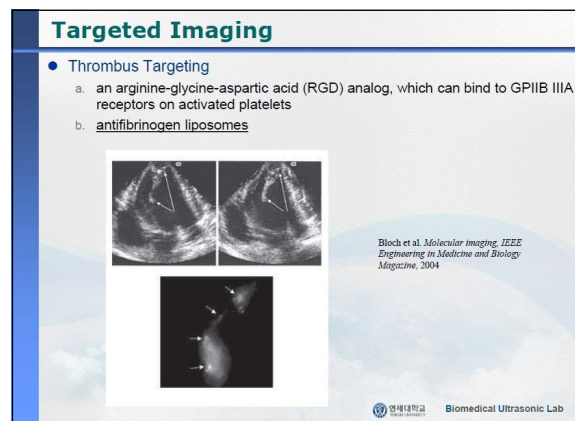
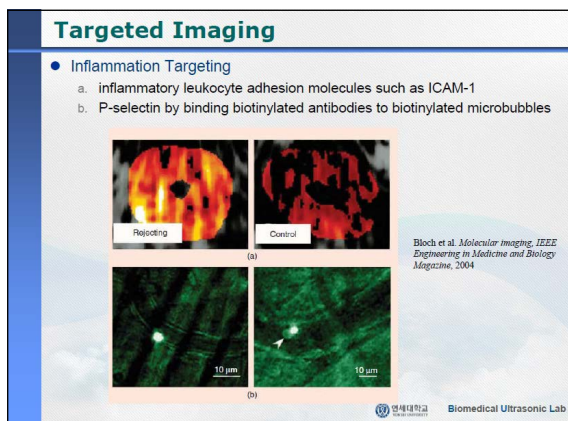
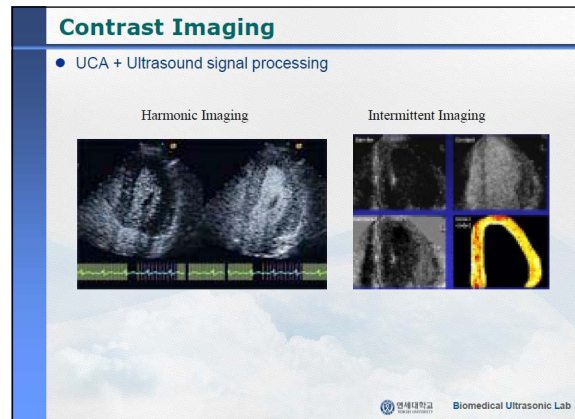
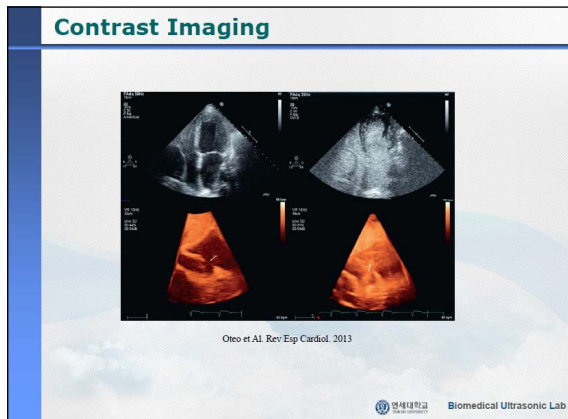
연세대학교
YONSEI UNIVERSITY

Biomedical Ultrasonic Lab

APPLICATIONS OF UCA

연세대학교
YONSEI UNIVERSITY

Biomedical Ultrasonic Lab



Drug Delivery: Sonoporation

- Drug Delivery by Cavitation
 - Bubble oscillation by stable cavitation
- Microstreaming

Zhong W et al. *Ultrasound in Med & Biol.* 2011

Wrenn SP et al. *J Theranostics.* 2012

Biomedical Ultrasonic Lab

Blood Brain Barrier

- Temporal Disturbance of Local Barriers for Drug Delivery
 - Drug Delivery thru BBB

Choi et al. *Ultrasound in Med. & Biol.* 2007

Biomedical Ultrasonic Lab

Oncology

Biomedical Ultrasonic Lab

Cancer Treatment

- RES-PNP release

Ly et al. *Scientific Report.* 2016

Biomedical Ultrasonic Lab

Gene Delivery for cancer treatment

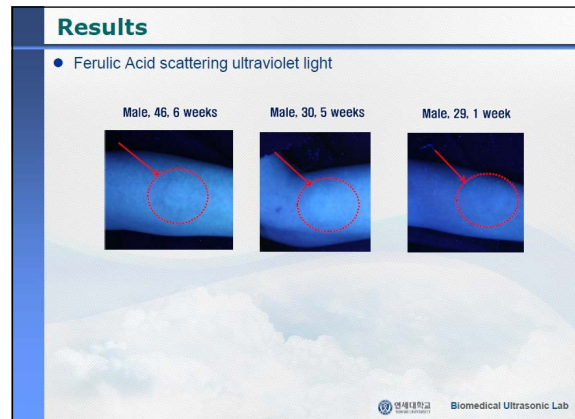
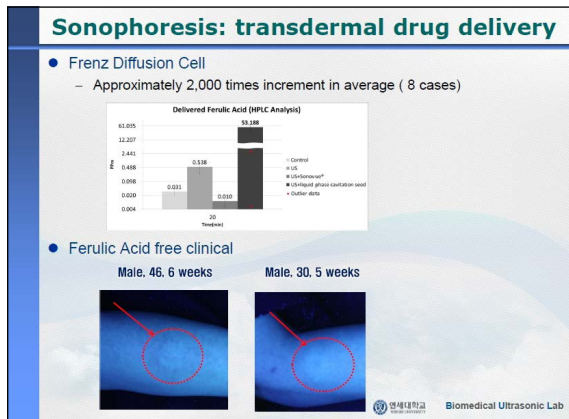
- RNAi
 - ANT2 shRNA : hormone-related cancer

Biomedical Ultrasonic Lab

Sonophoresis: transdermal drug delivery

- Using gravitation to secure location of cavitation seed on the surface of skin

Biomedical Ultrasonic Lab



CONCLUSION

Biomedical Ultrasonic Lab

- ### On going researches of UCA
- Shell
 - Nano particles
 - Proteins
 - Liposomes
 - Encapsulation
 - Multilayered
 - Water filled
 - Liquid phase internal core
- Biomedical Ultrasonic Lab

- ### On going researches of UCA Applications
- Drug Delivery
 - Blood Brain Barrier
 - Spatially targeted drug delivery
 - Gene Delivery
 - Stem cell delivery
 - Transdermal drug delivery
 - Delivery of other contrast agents
- Biomedical Ultrasonic Lab

- ### Acknowledgement
- Students
 - Unchul Shin, Ph. D. candidate, Yonsei University
 - Collaborators from other institutes
 - Hyunjin Park, Ph. D., Sungkyunkwan University
 - Chul-Woo Kim., M.D., Ph. D., Seoul National University Hospital
 - Donghee Park, Ph.D., Seoul National University Hospital
 - Funding Source
 - NRF-2014M3A6A3063636, M1AXA003-2011-0032035
 - MEST (2010-00757)
- Biomedical Ultrasonic Lab

SFS 3 KSTU-2

Therapeutic Ultrasound

13:40-14:00

Room 201

Chairpersons: **Tai-Kyong Song** *Sogang University, Korea*
Jinwoo Chang *Yonsei University, Korea*

Clinical Applications Using Therapeutic Ultrasound

Jae Young Lee

Department of Radiology, Seoul National University Hospital, Korea

The concept for treatment using high intensity focused ultrasound (HIFU) was provided about 50 years ago. However, HIFU was not used in clinical field until the 1990's. It was first used to ablate brain tissue considered as a lesion for the treatment of Parkinson's disease and then the field to be able to be treated has expanded over time. At present, diverse treatment or diverse trial using thermal and mechanical property has been being performed. Non-invasiveness and diverse interaction with tissues

that HIFU has make many academic researchers interested in HIFU. In many countries, HIFU is using for the treatment of solid tumors or for the removal of focal tissue of the uterus, prostate, brain, breasts, musculoskeletal systems, liver and prostate. Recently, drug delivery using HIFU and histotripsy is being paid attention to. I will review the application and updated knowledge on this issue during my presentation.

Chairpersons: **Tai-Kyong Song** *Sogang University, Korea*
Jinwoo Chang *Yonsei University, Korea*

Histotripsy (Mechanical Tissue Fractionation) Using Therapeutic Ultrasound

Ki Joo Pakh

Department of Biomedical Research Institute, Korea Institute of Science and Technology, Korea

High Intensity Focused Ultrasound (HIFU) is a non-invasive ultrasound technique which has been used to thermally necrose solid tumours without disruption to surrounding tissue. In recent years, an alternative HIFU technique to thermal ablation has been developed. This is known as mechanical tissue fractionation or histotripsy. Acoustic peak positive and negative pressures at the HIFU focus used in histotripsy are comparable to those in the shockwaves used in lithotripsy for kidney stone fragmentation.

In histotripsy, there are two different methods of creating pure mechanical damage of soft tissue by (a) pulsed ultrasound cavitation (i.e., Cavitation cloud histotripsy) or (b) shock wave heating and

millisecond boiling (i.e., Boiling histotripsy). In both methods, acoustic cavitation is believed to be one of the main mechanisms for inducing mechanical tissue fractionation. A well-defined lesion in the form of a cavity can be produced by histotripsy without any significant thermal damage at the periphery of the cavity.

Recent in vivo studies on kidney, prostate, heart and liver have shown that a lesion produced by histotripsy contains complete fragmentation of tissue and is sharply demarcated between treated and untreated regions. Subcellular debris remaining inside a mechanically fractionated lesion can be absorbed as part of the physiologic healing mechanism, whereas a thermally ablated lesion

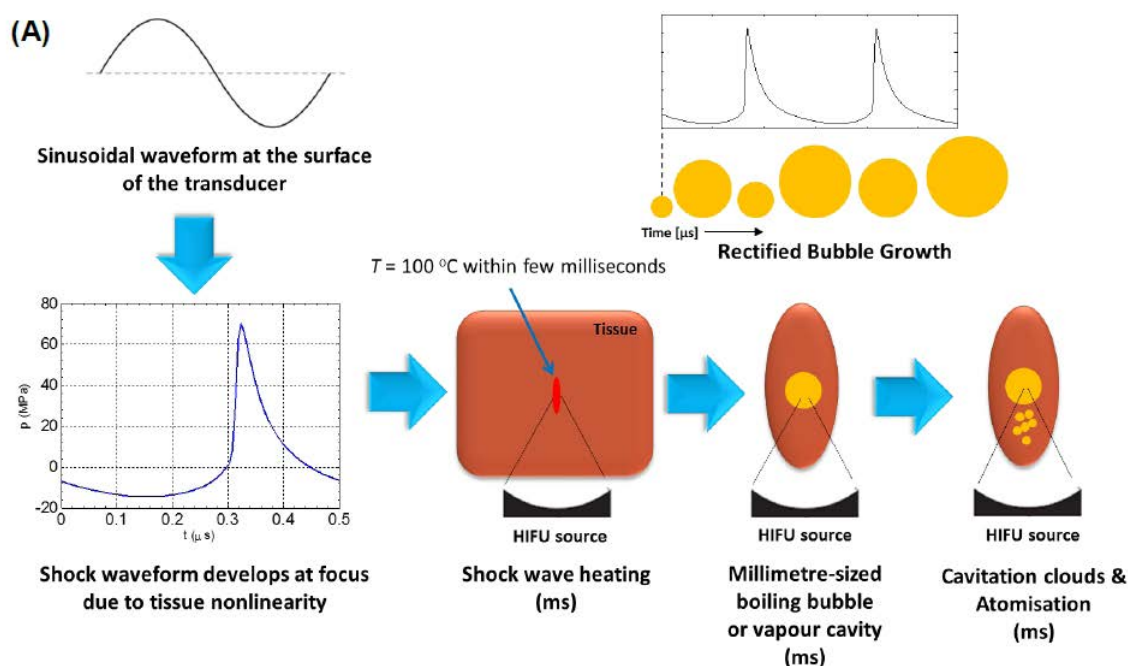


Fig. 1. (A) Possible mechanisms underpinning the formation of a mechanically fractionated lesion resulting from boiling histotripsy.

(B)

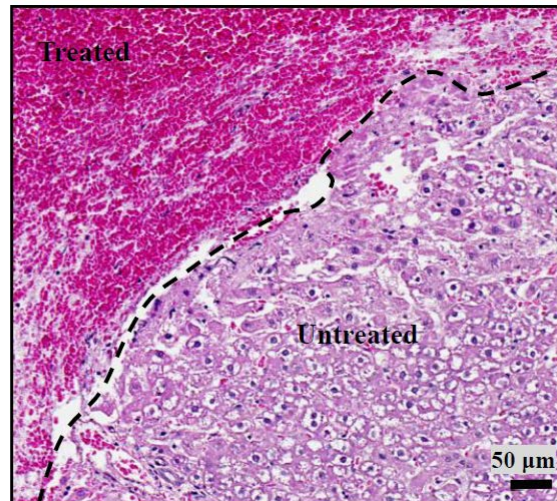


Fig. 1. (B) Histological examination (H&E) of a freshly created histotripsy lesion in the liver *in vivo*.

becomes fibrous scar tissue.

In this session, possible mechanisms behind and potential clinical applications of histotripsy will be discussed.

Contents of Lecture:

1. Introduction

- What is histotripsy?
- Ultrasound exposure conditions
- Cavitation cloud histotripsy

- Boiling histotripsy

2. Basic Theory

- Mechanisms of histotripsy

3. Potential clinical applications

- Mechanical ablation of solid tumours?
- Thrombolysis
- Cell therapy

4. Conclusion

Chairpersons: **Tai-Kyong Song** *Sogang University, Korea*
Jinwoo Chang *Yonsei University, Korea*

Emerging Technologies in Therapeutic Ultrasound

Dong-Guk Paeng

Department of Biomedical Engineering, Jeju National University, Korea

Over the last decade, the therapeutic ultrasound was rapidly developed not only to show therapeutic potentials but also to treat various diseases with imaging-guided techniques. Some diseases such as prostate, liver and breast cancers, uterine fibroids, bone metastases, and essential tremor, have already been commercially treated. However, therapeutic ultrasound is still an early stage of development and adoption. In this lecture, emerging technologies in therapeutic ultrasound will be discussed. There will be a brief summary of current commercialized

magnetic resonance-guided focused ultrasound (MRgFUS) systems and ultrasound-guided FUS (USgFUS) systems. Then several newly developed FUS systems will be briefly introduced such as ArcBlade MRgFUS system for uterine fibroid treatment, and neuronavigation-guided FUS system and CarThera system for blood brain barrier opening and drug delivery. The current MRgFUS brain system will be discussed with its limitations and future directions of the development of the brain system will be suggested with the related challenges.

JS 1

15:15-16:00

GBR 103

Chairperson: Hae Jeong Jeon *Konkuk University Medical Center, Korea*

Microbubble Pumps: Ultrasound Theragnostic Agents

Christy Holland

Department of Internal Medicine-Cardiology, University of Cincinnati, USA

Cardiovascular disease is the number one cause of death worldwide and thrombo-occlusive disease is a leading cause of morbidity and mortality. Ultrasound has been developed as both a diagnostic tool and a potent promoter of beneficial bioeffects for the treatment of cardiovascular disease. Ultrasound exposure can induce the release, delivery and enhanced efficacy of a thrombolytic drug (rt-PA), antibiotics, or bioactive gases from echogenic liposomes. By encapsulating drugs into micron-sized and nano-sized liposomes, the therapeutic can be shielded from degradation within the vasculature until delivery is triggered by ultrasound exposure. Insonification accelerates clot breakdown in combination with rt-PA and ultrasound contrast

agents, which nucleate sustained bubble activity, or stable cavitation. Mechanisms for ultrasound enhancement of thrombolysis and sonobactericide, with a special emphasis on acoustic cavitation and radiation force, will be reviewed.

Lecture Learning Objectives

At the end of this course, participants should be able to:

1. Describe the potential for ultrasound-mediated, image-guided, drug delivery
2. Discuss the mechanisms of ultrasound accelerated rt-PA thrombolysis
3. Describe the pathology of bacterial loaded biofilm responsible for vegetative endocarditis.

MP 4 PED

07:50-08:20

GBR 101

Chairperson: Gye Yeon Lim *The Catholic University of Korea, Yeouido St. Mary's Hospital, Korea*

Contrast Enhanced Ultrasound in Pediatrics

M Beth McCarville

Department of Radiology, St. Jude Children's Research Hospital, USA

With the recent Federal Drug Administration approval of an ultrasound contrast agent for both intravenous and intra-vesicle use in children in the United States, there is a burgeoning interest in this modality. Children are the ideal population for contrast ultrasonography (CEUS) because it avoids exposing this vulnerable population to the harmful effects of ionizing radiation. Contrast ultrasound has

the additional benefits of being portable, provides real-time imaging, does not require sedation and is less expensive than computed tomography and magnetic resonance imaging. In this lecture I will review safety issues related to CEUS and present the most common uses of CEUS in children including trauma, to assess focal liver lesions and contrast enhanced voiding urosonography.

MP 5 GU

07:50-08:20

GBR 102

Chairpersons: **Byung Chul Kang** *Ewha Womans University Mokdong Hospital, Korea*
Hak Jong Lee *Seoul National University Bundang Hospital, Korea*

PI-RADS Based Transrectal US Biopsy of the Prostate

Byung Kwan Park

Department of Radiology, Samsung Medical Center, Korea

Transrectal US (TRUS)-guided biopsy is still a mainstay for diagnosing prostate cancer. However, a substantial number of prostate cancers are not detected with TRUS-guided biopsy alone. Recent studies show that cancer detection rate is increased with MRI-TRUS fusion images. Frequently, TRUS cannot clearly depict a lesion, even though it is clearly seen on MR images alone. If pre-biopsy MR images are fused with TRUS images, the MRI-TRUS registration helps to localize a prostate lesion that is unclear on TRUS in a real time. First, abnormal prostate lesions should be graded with prostate imaging reporting and data system (PI-RADS) and next, the fusion biopsy is recommended if they are PI-RADS 4 or 5. However, MRI-TRUS fusion may not be complete region-by-region because of the following reasons. The shape of prostate, which is usually seen as a triangle in transverse axial images,

is frequently deformed like a banana when a TRUS probe is introduced. Axial MR images are obtained at the perpendicular to the urethra. However, these axial images are anatomically impossible to make with TRUS. The axial images, which are scanned with TRUS, are definitely oblique, but not perpendicular to urethra. Accordingly, axial TRUS images cannot be true axial, but oblique axial or coronal. PI-RADS 4 or 5 lesions are frequently seen on TRUS images. Therefore, when a PI-RADS 4 or 5 lesion is detected on pre-biopsy MRI, TRUS should be performed first to determine whether or not the lesion is visible. If it is visible on TRUS, MRI-TRUS fusion biopsy is not necessary.

The purpose of this presentation is to describe TRUS features of PI-RADS 4 or 5 cancers and to show how to perform TRUS biopsy for these lesions.

Chairperson: Hak Hee Kim Asan Medical Center, Korea

Screening with Automated Breast (ABUS) Coronal Imaging: How to Reduce Call Backs

Beverly Hashimoto

Department of Radiology, Virginia Mason Medical Center, USA

Teaching Points

1. Learn about the ABUS screening callback frequency of various breast lesions.
2. Understand the ABUS methods to avoid calling back lesions due to shadowing artifact.
3. Appreciate the difference in thought process between analyzing screening mammographic versus ABUS lesions.

B. ABUS: Previous ABUS commonly not available. Need to review previous hand-held ultrasound (HHUS) and cross correlate with mammography.

III. Shadowing Artifact: methods to avoid calling back

- A. Analyze initial appearance
- B. Evaluate other ABUS transverse and coronal views: compare appearance
- C. Produce alternate reconstruction angles to evaluate change in appearance

Table of Contents

I. Analysis of Breast Lesions Called Back from Screening ABUS

II. ABUS Mass Evaluation Approach Differs from Screening Mammography

- A. Mammography: after evaluating the mass, one immediately compare to old mammograms

CC 5 CV-1

Carotid US

08:30-08:50

GBR 101

Chairperson: **Bae Young Lee** *The Catholic University of Korea, St. Paul's Hospital, Korea*

US Evaluation of Carotid Artery: How to Do and How to Report

Eun-Ah Park

Department of Radiology, Seoul National University Hospital, Korea



Carotid Doppler ultrasonography is a popular and effective tool for diagnosis of carotid artery disease. The operator should be familiar with the physics and other parameters of Doppler ultrasonography to perform optimal Doppler ultrasonography studies. This lecture will consist of five parts; anatomy, technique, morphological evaluation, functional evaluation and pitfalls. The anatomical knowledge about differentiating between internal and external carotid arteries is the requisite for the evaluation of carotid Doppler Ultrasound. There are several anatomical traits for the differentiation of ICA from ECA; bigger size, posterior and lateral location, the presence of carotid bulb and no branches. Detecting Doppler spectrum for low resistive pattern is helpful to detect ICA. In diseased cases, the temporal tapping technique is useful to

detect ECA by spotting serration-like artifact in the ECA Doppler spectrum. Secondly, useful tips and techniques for performing effective US examination for carotid arteries include determination of Doppler angle, sample volume size and location, color scale and gain control, and heel-toe technique. Thirdly, the two-dimensional gray scale can be used for measuring the intima-media thickness, which is very good biomarker for atherosclerosis and can aid in plaque characterization. The plaque morphology is related to the risk of stroke. The ulceration of plaque is also known as one of the strong predictors of future embolic event risk. Fourthly, color Doppler ultrasonography and pulsed wave Doppler ultrasonography have been used for detecting carotid artery stenosis. Lastly, the pitfalls of carotid Doppler ultrasonography will be briefly introduced.

US Evaluation of Lower Extremity Artery: How to Do and How to Report

Jeonghyun Jo

Department of Radiology, Dong-A University Hospital, Korea

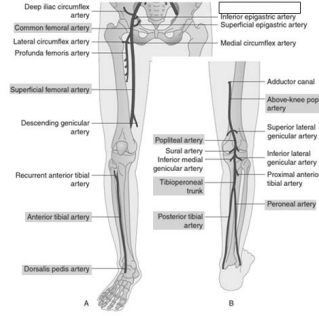
US Evaluation
of Lower Extremity Artery
: How to Do and How to Report

Colledge of Medicine Dong-A University

Jo Jeonghyun

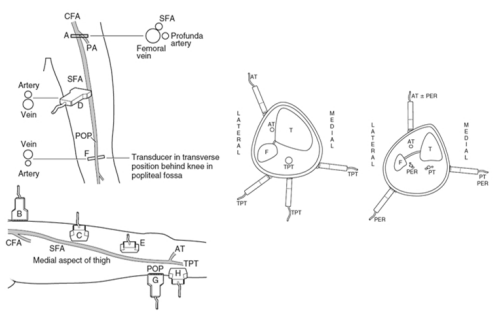
© No disclosures

L/E Arterial Anatomy

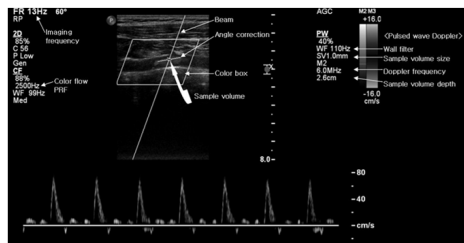


- CFA
- SFA
- PoA
- ATA
- TP trunk
- PTA
- PeA

Transducer Position



Doppler Parameter

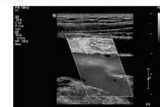
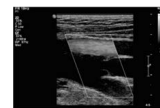


Doppler Parameter

1. Color doppler parameter

1) Color velocity scale

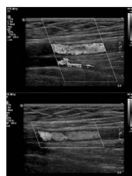
- on the color bar in the image
- changing the scale alters the pulse repetition frequency (PRF).
 - : for slow flows, scale is set low to detect the small movement between pulses
 - : for high flows, set high



Doppler Parameter

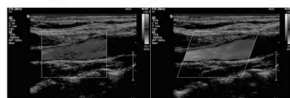
2) Color box size

- ROI
- size $\uparrow \Rightarrow$ frame rate $\uparrow \Rightarrow$ image quality \downarrow



3) Angle of color box (steering)

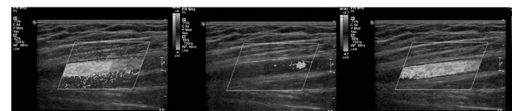
- to optimize the color box angle to the flow direction to obtain the highest Doppler shift frequencies.



Doppler Parameter

4) Color gain

- amplitude regulation of color display
- too high : noise \uparrow , color overwriting
- too low : loss of flow information



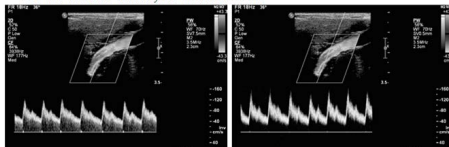
Doppler Parameter

2. Spectral doppler parameter

1) Sample volume (gate size)

- specific location in which the frequency spectrum shows blood flow

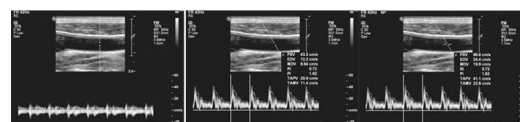
- 2/3 of vessel width, in central area



Doppler Parameter

2) Angle correction

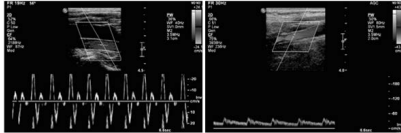
- Doppler angle : $30 \sim 60^\circ$
- lining angle cursor parallel to the vessel walls (flow direction)



Doppler Parameter

3) Velocity scale

- similar function to the scale control for colour flow imaging
- changing the scale alters the pulse repetition frequency (PRF).
- : too low, aliasing may occur
- : too high, the shape of the flow waveform is unclear and measurements are difficult.



Normal US Appearance

A. Color flow image

- interrogated rapidly using color flow imaging
- be color filling to the vessel walls
- pulsatile flow pattern, with the color alternating between red and blue due to flow reversal during the diastolic phase.

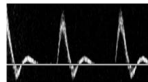


Normal US Appearance

B. Spectral doppler

1. Typical triphasic waveform (high peripheral resistance)

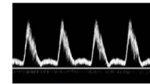
- systole : initial high-velocity, forward flow
- early diastole : short reversal flow (d/t high peripheral vascular resistance in normal peripheral circulation)
- late diastole : low velocity, forward flow (d/t proximal arterial compliance)
- with clear spectral window : laminar flow



Normal US Appearance

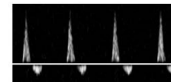
2. Monophasic waveform

- reactive hyperemia (exercise, warming), old age, infection
- the reverse flow component is also absent distal to severe occlusive lesion



3. Biphasic waveform

- old age, DM, atherosclerosis

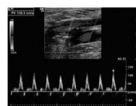


Normal US Appearance

4. Standard values

for arterial diameter and PSV in L/E

Mean Peak Systolic flow Velocities and Arterial Diameters		
Artery	Velocity \pm SD (cm/sec)	Diameter \pm SD (cm)
EIA	119.3 \pm 21.7	0.79 \pm 0.13
CFA	114.1 \pm 24.9	0.82 \pm 0.14
SFA proximal	90.8 \pm 13.6	0.60 \pm 0.12
SFA distal	93.6 \pm 14.1	0.54 \pm 0.11
PoA	68.8 \pm 13.5	0.52 \pm 0.11



Abnormal US appearance

A. Color flow image

1. Stenosis

- A localized increase in velocity occurs at the site of a stenosis \Rightarrow causes a shift in the Doppler frequency
 - an increase in color saturation or aliasing on the color image
 - an increase in the PSV on the Doppler spectral display
- The pattern of blood flow distal to the stenosis
 - : nonlaminar
 - : a large variation in both direction and amplitude

Abnormal US Appearance

- This zone of disturbed blood flow
 - increased variance of the color signals on color doppler image
 - a broadening of the spectral window on spectral waveform in the vessel.

Abnormal US appearance

2. Occlusion
 - a total absence of color flow in the vessel
 - possible to misdiagnose a long stricture as an occlusion because of very slow flow through the stricture
 - the PRF should be lowered

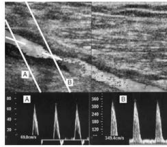
Abnormal US Appearance

B. Spectral doppler

1. Stenotic area

1) abnormal recordings

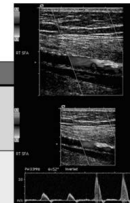
- PSV increase
- early diastolic velocity reversal disappear
- spectral broadening



Abnormal US Appearance

2) Grading of stenoses

Diameter reduction	PSV ratio	Spectrum waveform
0~49%	< 2	Triphasic, Mild spectral broadening, End-diastolic velocity ↑
50~74%	≥ 2	Biphasic or Monophasic End-diastolic velocity↑ Severe spectral broadening Flow disturbance and some damped flow on distal segment
75~99%	≥ 4	Monophasic End-diastolic velocity ↑↑ Marked spectral broadening, Damped flow on distal segment
100% (occlusion)	No flow	Often, High resistance flow pattern on proximal segment



Chairperson: Bae Young Lee *The Catholic University of Korea, St. Paul's Hospital, Korea*

US Evaluation of Lower Extremity Vein: How to Do and How to Report

You Seon Song

Department of Radiology, Pusan National University Hospital, Korea

Common Indications in practice

Thromboembolic disease
Assessment of venous insufficiency, reflux, and varicose veins

Follow-up for known venous thrombosis
Follow-up for monitoring of known distal deep vein thrombosis progression

Thromboembolic disease

Technique

- Compression ultrasound
 - Should be applied every 2cm or less in short axis scan
 - Should check common femoral, femoral, proximal deep femoral, proximal greater saphenous, popliteal vein at minimum
 - Compression test is inadequate at adductor canal
 - Δ Examiner additionally press the vein against the probe
- Spectral Doppler waveforms
 - Should be recorded to evaluate for asymmetry or loss of normal respiratory phasicity
 - at both sides of common femoral or external iliac vein
 - Should be obtained in long axis scan
- Patient position
 - Femoral v., ATV (anterior tibial vein) : supine
 - Popliteal v., PTV (posterior tibial vein), peroneal v., soleus v
 - Δ Hip abduction, slightly knee flexion
 - Δ Prone position with ankle on contralateral ankle

- Calf-popliteal DVT (>90%)
 - Pain, swelling, redness in calf of one leg
- Iliofemoral DVT (<10%)
 - Pain in buttock and/or groin region, extend to medial thigh

Report

- Gray scale images(or cine loops) should be recorded without and with compression at each anatomical levels
- Color and spectral Doppler waveforms should be recorded at both common femoral and popliteal veins
- Abnormal findings generally require additional images
 - Additional image can elucidate the symptoms
 - Extent and location of site should be clearly recorded
 - Long axis views without compression may be helpful to characterize the abnormal veins
- More detailed evaluation of the superficial venous system or deep calf vein may be necessary according to the clinical indication and patient presentation
- Other vascular and nonvascular abnormalities should be recorded, if found
- Anatomical variations
- Diagnostic criteria of thromboembolic disease
 - Direct signs
 - Δ Intramural thrombus
 - Δ Incompressibility
 - Δ Nonocclusive thrombosed vein: partially collapse
 - Δ Increase in vein diameter
 - Δ No flow on color and spectral Doppler

- Indirect signs
 - Δ Loss of phasicity : proximal thrombosis
 - Δ Loss of augmentation : distal thrombosis

Venous insufficiency

Technique

- Location and duration of reversed flow should be determined
- Duplex interrogation should be performed at as many levels as necessary
- Veins in the superficial and deep systems should be evaluated
- Augmentation with squeezing of the calf musculature should generally be used
- Increased flow during augmentation of distal part
- Valsalva maneuver may be used at the groin
- Transient absence of flow during Valsalva maneuver
- The patient should be in the erect position for the detection or exclusion of reflux
- The reverse Trendelenburg position can be used if erect scanning is not possible
- The examined leg should be in a non-weight-bearing position
- All spectral Doppler waveforms should be obtained from the long axis

Report

- Site for evaluation
 - Saphenofemoral junction
 - Saphenopopliteal junction
 - Perforator
 - Deep vein
 - Superficial vein

- Presence or absence and location of reflux
 - reflux time should be measured
 - Δ > 1 sec : femoral, popliteal vein
 - Δ > 0.5 sec : GSV, LSV, calf deep vein
 - Δ > 0.35 sec : perforators
- Varicose vein and abnormal perforating vein
- size of vessel
 - Δ Perforator vein diameter
 - > 4 mm : most of them with reflux
 - 2-3 mm : can have reflux --> check reflux on Doppler
- Anatomic variations
 - Hypoplastic or aplastic segments, significant accessory veins or duplications
 - m/c: LSV to popliteal vein at popliteal fossa
- Protocol adjustment such as more detailed evaluation may be required according to the patient presentation and clinical indication
- Other vascular and nonvascular abnormalities, if found, should be recorded

References

1. American Institute of Ultrasound in Medicine, AIUM Practice Guideline for the Performance of Peripheral Venous Ultrasound Examinations, revised 2015
2. 박재형. 심장, 혈관 영상의학 제2판: 일조각, 2013
3. Dupuy DE. 1999 plenary session: Friday imaging symposium: venous US of lower-extremity deep venous thrombosis: when is US insufficient? Radiographics 2000;20:1195-1200
4. Gillespie D, Glass C. Importance of ultrasound evaluation in the diagnosis of venous insufficiency: guidelines and techniques. Semin Vasc Surg 2010;23:85-89
5. Min RJ, Khilnani NM, Golia P. Duplex ultrasound evaluation of lower extremity venous insufficiency. J Vasc Interv Radiol 2003;14:1233-1241.

Chairperson: Bae Young Lee *The Catholic University of Korea, St. Paul's Hospital, Korea*

US Evaluation of Procedure Related Complication

Eun Ju Chun

Department of Radiology, Seoul National University Bundang Hospital, Korea

The transfemoral arterial approach is utilized to gain access for angiography, percutaneous coronary interventions or various endovascular therapy such as transcatheter aortic valve or mitral valve replacement. Puncture of the common femoral artery in its middle segment is recommended to decrease the risk of procedure-related vascular complications. However, due to inadequate access or anatomical variance, various complications including hematoma, pseudoaneurysm, arteriovenous fistula, thrombosis or dissection have occurred after transfemoral arterial interventions.

In this regard, duplex and color Doppler sonography have proved to be excellent noninvasive modalities for evaluating these transfemoral accessed procedure-related complications.

Hematomas present clinically with nonpulsatile swelling or ecchymoses at the puncture site. When localized, gray-scale imaging typically demonstrates a soft tissue mass with various echogenicity according to the time course since the bleeding occurred. Color Doppler US typically demonstrates no evidence of internal blood flow.

A pseudoaneurysm occurs when there is disruption of at least 1 layer of the arterial wall with persistent communication of blood flow into the perivascular space or an outpouching of the residual vessel wall. On color Doppler imaging, a bidirectional, turbulent swirling blood flow pattern known as the

“yin-yang” sign may be observed within a patent pseudoaneurysm. A pathognomonic to-and-fro waveform pattern also observed in the neck as a result of blood entering the pseudoaneurysm during systole and heading away from the pseudoaneurysm during diastole.

Arteriovenous fistulae may present with a palpable thrill over the access site and a bruit on auscultation. Arteriovenous fistula may present with a palpable thrill or bruit over the access site. On color Doppler imaging, a color mosaic pattern will be observed within the fistula when pulsatile, high-velocity flow within the connecting vascular channel between artery and vein. A low-resistance flow pattern with loss of the normal high-resistance triphasic waveform is characterized, whereas increased velocity with a pulsatile waveform should be observed within the draining vein.

Iatrogenic arterial dissection occurs when a wire or catheter enters the subintimal space and creates a false lumen. Gray-scale US demonstrates flap within the lumen. If the false lumen may be thrombosed, it can not distinguish from the intramural hematoma.

Other abscess formation or venous thrombosis also can evaluate by careful sonographic examinations.

Radiologists should be familiar with these interventional procedures through transfemoral approach and possible complications to facilitate prompt diagnosis and treatment.

SFS 4 BR-1

Automated Breast (ABUS)

08:30-09:00

GBR 103

Chairpersons: Beverly Hashimoto *Virginia Mason Medical Center, USA*
 Woo Kyung Moon *Seoul National University Hospital, Korea*

Introduction to Automated Breast Ultrasound (ABUS) Coronal Imaging: Normal and Abnormal Findings

Beverly Hashimoto

Department of Radiology, Virginia Mason Medical Center, USA

Teaching Points

1. Learn about the ABUS screening callback frequency of various breast lesions.
2. Understand the ABUS methods to avoid calling back lesions due to shadowing artifact.
3. Appreciate the difference in thought process between analyzing screening mammographic versus ABUS lesions.

Table of Contents

I. Analysis of Breast Lesions Called Back from Screening ABUS

II. ABUS Mass Evaluation Approach Differs from Screening Mammography

- A. Mammography: after evaluating the mass, one immediately compare to old mammograms
- B. ABUS: Previous ABUS commonly not available. Need to review previous hand-held ultrasound (HHUS) and cross correlate with mammography.

III. Shadowing Artifact: methods to avoid calling back

- A. Analyze initial appearance
- B. Evaluate other ABUS transverse and coronal views: compare appearance
- C. Produce alternate reconstruction angles to evaluate change in appearance

Chairpersons: **Beverly Hashimoto** *Virginia Mason Medical Center, USA*
Woo Kyung Moon *Seoul National University Hospital, Korea*

ABUS: Image Quality and Artifact

Sung Hun Kim

Department of Radiology, The Catholic University of Korea, Seoul St. Mary's Hospital, Korea

1. Image Quality

- Should be guaranteed for the use in clinical practice of ABUS
- 1) Prospective study (HHUS vs. ABUS) (reference 1)
 - ✓ Most cases of ABUS (97%) - identical or superior to HHUS
 - ✓ 3% - inferior to HHUS
 - Main causes - marginal blurring and acoustic shadowing by Cooper's ligament or improper compression pressure of transducer
- 2) Gel Pad Application (reference 2)
 - ✓ Coverage of breast was expanded after gel pad application
 - ✓ No significant change of image quality with/without gel pad application

2. Artifacts

- 1) Definition - variations in ultrasonographic echogenicity not caused by true attenuation differences / may create pseudo-lesions or mask true abnormalities
- 2) Types of artifacts

3. CAD Application in ABUS

- To reduce the review time and misdetection from ABUS images
- Clinical application

References

1. The image quality and lesion characterization of breast using automated whole-breast ultrasound: A comparison with handheld ultrasound. An YY, Kim SH, Kang BJ. *Eur J Radiol.* 2015 Jul;84(7):1232-5.
2. Gel pad application for automated breast sonography. Kim YJ, Kim SH, Jeh SK, Choi JJ, Kang BJ, Song BJ. *J Ultrasound Med.* 2015 Apr;34(4):713-9.

SFS 4 BR-3

Automated Breast (ABUS)

09:30-10:00

GBR 103

Chairpersons: Beverly Hashimoto *Virginia Mason Medical Center, USA*
 Woo Kyung Moon *Seoul National University Hospital, Korea*

Clinical Experience and Future of Automated Breast Ultrasound

Joo Hee Cha

Department of Radiology, Asan Medical Center, Korea

Breast ultrasound (US) is an important supplement to mammography because it is widely available, relatively inexpensive, and well-tolerated by patients. However, conventional hand-held US requires time and skill for the detection of small and non-palpable tumors and lacks in the standards.

The automated whole breast ultrasound gathers standardized uniform image sets by lesser trained personnel, allowing shorter, more efficient time use by physicians interpreting the studies. Also, the system is less dependent on the operator than hand-held US because it allows assessment of the entire breast objectively always. Since the FDA approved automated breast US for the use in screening for breast cancer as an adjunct to mammography in 2005, there are many reports about the role of automated breast US as a screening tool especially in dense breast and the performance comparing with conventional hand-held US.

However, there are several limitations in automated breast US. Many patients have pain and have difficulty of examining the axillary region. Neither Doppler nor elastography is available for automated US, which may need additional second-look US. Also, artifacts can cause false-positive results or obscure actual findings.

In this lecture, I will present our experience and

current state of automated breast US in Korea and discuss the expected role in the clinical practice.

References

1. Kim H, Cha JH, Oh HY, et al. Comparison of conventional and automated breast volume ultrasound in the description and characterization of solid breast masses based on BI-RADS features. *Breast Cancer*. 2014;21:423-8.
2. Choi WJ, Cha JH, Kim HH, et al. Comparison of automated breast volume scanning and hand-held ultrasound in the detection of breast cancer: an analysis of 5,566 patient evaluations. *Asian Pac J Cancer Prev*. 2014;15:9101-5.
3. Chae EY, Cha JH, Kim HH, et al. Comparison of lesion detection in the transverse and coronal views on automated breast sonography. *J Ultrasound Med*. 2015;34:125-35.
4. Shin HJ, Kim HH, Cha JH. Current status of automated breast ultrasonography. *Ultrasonography*. 2015;34:165-72.
5. Brem RF, Tab?r L, Duffy SW, et al. Assessing improvement in detection of breast cancer with three-dimensional automated breast US in women with dense breast tissue: the SomoInsight Study. *Radiology*. 2015;274:663-73.
6. Meng Z, Chen C, Zhu Y, et al. Diagnostic performance of the automated breast volume scanner: a systematic review of inter-rater reliability/agreement and meta-analysis of diagnostic accuracy for differentiating benign and malignant breast lesions. *Eur Radiol*. 2015;25:3638-47.

Chairperson: Kwan Seop Lee Hallym University Sacred Heart Hospital, Korea

US for Pediatric Liver Tumors

Mi-Jung Lee

Department of Radiology, Severance Hospital, Korea

Introduction

Sonography is the method of choice for evaluating both focal and diffuse liver disease. With the addition of Doppler flow imaging, sonography is effective for hepatic vasculature evaluation.

Hepatic tumors in children

- 3rd m/c abdominal neoplasm in children (after Wilms tumor and neuroblastoma)

- 2/3 malignant: hepatoblastoma (m/c), HCC, undifferentiated sarcoma, angiosarcoma

- 1/3 benign: hemangioma, hemangioendothelioma, mesenchymal hamartoma, FNH, adenoma

- Distinct distribution by age

US for hepatic tumors

- Easy to perform, confirming the presence and character of mass
- Need further CT or MRI to determine extent and respectability

RadioGraphics

Clinical, Pathologic, and Imaging Features of the More Common Malignant and Benign Hepatic Primary Tumors in Children			
Tumor Type and Name, Patient Age Group	Clinical Features	Pathologic Features	Imaging Features
Malignant epithelial			
Hepatoblastoma, <5 y	Elevated AFP level; possible associated conditions (eg, BWS); no history of liver disease	Nodular, septated; hemorrhage and necrosis are common	Solid, nodular, septated; may show hemorrhage or necrosis, calcifications at CT, lung metastases, invasion of veins
HCC, 10–14 y	Elevated AFP level (70%); history of liver disease (50%)	Varied, can be multifocal; hemorrhage, necrosis, and venous invasion are common	Varied, can be multifocal; hemorrhage and necrosis are common; possible invasion of veins or local spread
FLC, adolescents	Normal AFP level; no history of liver disease	Well-circumscribed, lobulated; central collagenous fibrous scar with or without calcifications; relative lack of Kupffer cells	Well-circumscribed, lobulated; scar is dark on T2WI and does not enhance; photopenic defect at ^{99m} Tc-sulfur colloid study
Malignant mesenchymal			
UES, 6–10 y	Normal AFP level	Circumscribed with large cystic and myxoid areas, hemorrhage, and necrosis	Myxoid component appears cystic at CT and MR imaging but solid at US; only septa and solid portions enhance
EHE, adolescents	Normal AFP level	Confluent peripheral nodules with capsular retraction	Confluent peripheral nodules with capsular retraction; targetlike enhancement
Embryonal rhabdomyosarcoma, <5 y	Normal AFP level	Grapelike projections into duct lumen	Often located near porta hepatis with intraductal growth pattern
Benign mesenchymal			
IHE, <1 y	AFP level normal for age; may have hemangiomas of skin or other organs; may have high-output heart failure, thrombocytopenia, or hypothyroidism	Solitary large mass or multiple small masses; vascular tumor; large masses have central areas of hemorrhage, necrosis, fibrosis, and calcification	Characteristic intense (similar to that of the aorta), peripheral nodular enhancement with centripetal fill-in; may have evidence of an AV shunt
MHL, <5 y	Normal AFP level	Most contain cysts, often predominantly cystic	Contains cysts or is predominantly cystic; only septa and solid portions enhance
Benign epithelial			
FNH, young children and adolescents	Normal AFP level; strong predilection for girls	Circumscribed, lobulated; central myxomatous scar; hemorrhage and necrosis are rare; contains Kupffer cells	Circumscribed, lobulated, homogeneous; scar is bright on T2WI and does enhance on delayed images; normal or increased uptake at ^{99m} Tc-sulfur colloid study
Hepatic adenoma, >10 y	Normal AFP level; oral contraceptive or androgenic steroid use; glycogen storage disease	Usually solitary but may be multiple; hemorrhage and heterogeneity are frequent; intracellular fat and glycogen	Heterogeneous appearance; intratumoral hemorrhage is common; signal loss on opposed-phase or fat-suppressed images

Note.—AV = arteriovenous, BWS = Beckwith-Wiedemann syndrome, T2WI = T2-weighted images.

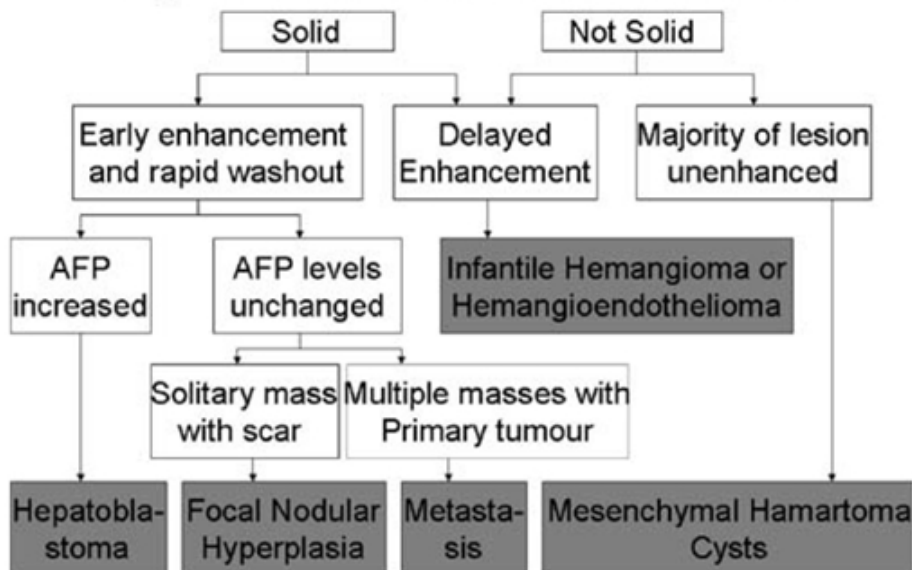
504 March-April 2011

radiographics.rsn.org

<RadioGraphics 2011; 31:483-507>

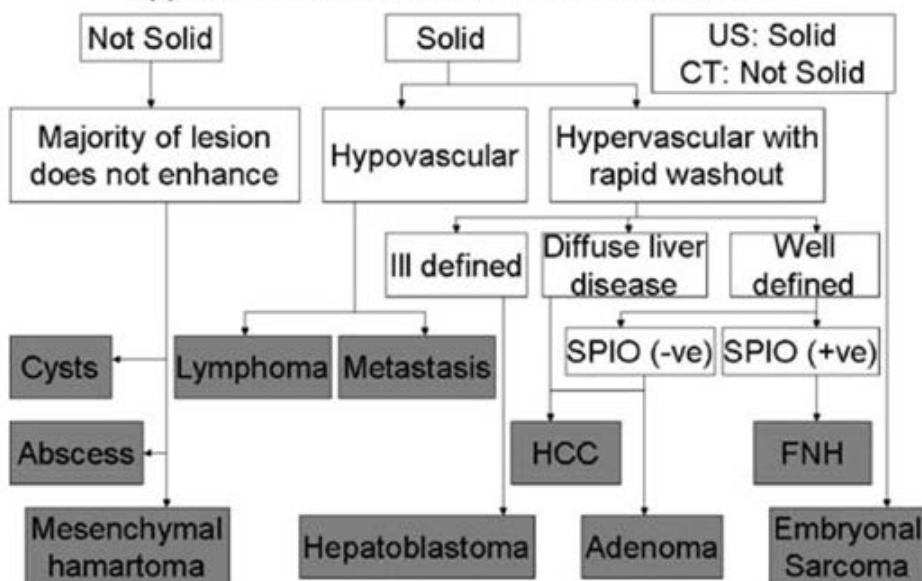
Infant and Young Child

Appearance on unenhanced and enhanced CT



Older Child (more than 10 years)

Appearance on unenhanced and enhanced CT



<Eur Radiol (2009) 19: 209-219>

Chairperson: Kwan Seop Lee Hallym University Sacred Heart Hospital, Korea

US for Pediatric Retroperitoneal Tumors

Tae Yeon Jeon

Department of Radiology, Samsung Medical Center, Korea

Learning objectives

To review imaging characteristics of common and uncommon retroperitoneal tumors in children

To discuss how an integrated imaging approach could be helpful to define the nature, origin, extent and staging of retroperitoneal tumors

Background

Retroperitoneal tumors are precisely defined with cross-sectional imaging, being ultrasound the best initial approach in children. MRI and CT are not screening methods but are very useful in detailing osseous and soft tissue changes. Selection of the optimal technique in each individual patient with a retroperitoneal mass is essential, and factors such as cost, radiation dose, and need for sedation should all be considered.

1. Renal neoplasm

1) Wilms tumor

Wilms tumor (nephroblastoma) accounts for about 80% of pediatric renal masses and its peak incidence is at 3-4 years of age, and 80% of patients present before 5 years of age. Wilms tumor is bilateral in 4%-13% of children. Although most cases are sporadic and only 2% of cases are familial, a number of associations including overgrowth syndromes (Beckwith-Wiedemann syndrome and hemihypertrophy), non-overgrowth syndromes (WAGR syndrome and Drash syndrome), and isolated anomalies (cryptorchidism,

hemihypertrophy, hypospadias, and sporadic aniridia) are recognized. It manifests as a solid intrarenal mass with a pseudocapsule and distortion of the renal parenchyma and collecting system. There may be vascular invasion of the renal vein and inferior vena cava with occasional extension into the right atrium. Metastases are most commonly found in the lungs (85% of cases), liver, and regional lymph nodes. At US, the mass has heterogeneous echogenicity, which represents hemorrhage, fat, necrosis, or calcification. CT demonstrates the heterogeneous mass and nodal metastases, as well as areas of calcification and fat. At MR imaging, Wilms tumor demonstrates low signal intensity on T1-weighted images and high signal intensity on T2-weighted images.

2) Clear cell sarcoma

Clear cell sarcoma of the kidney (bone metastasizing renal tumor of childhood) accounts for 4%-5% of primary renal tumors in children. The imaging findings and an age group of clear cell sarcoma are similar to those of Wilms tumor. The tumor is characterized by its aggressive behavior and is associated with a higher rate of relapse and mortality than Wilms tumor. It may metastasize to the bones, lymph nodes, brain, liver, and lungs.

3) Rhabdoid tumor

Rhabdoid tumor is a rare, highly aggressive malignancy of early childhood. About 80% occur in patients less than 2 years of age. The association of rhabdoid tumor with synchronous or metachronous primary intracranial masses or brain metastases has been established as a distinctive feature. Although

the appearance may closely resemble that of Wilms tumor, several features can suggest the diagnosis: subcapsular fluid collections, tumor lobules separated by dark areas of necrosis or hemorrhage, and linear calcifications outlining tumor lobules.

4) Lymphoma/leukemia

Lymphoma involves the kidney by hematogeneous metastases or direct extension from retroperitoneum. Non-Hodgkin lymphoma (especially Burkitt lymphoma) is most common in children. The most common imaging pattern is multiple renal masses or nodules distorting the collecting system, and less common findings are a solitary renal mass, diffuse infiltration, and isolated perinephric disease. Leukemic infiltration of the kidneys may often cause diffuse renal enlargement with smooth renal contour.

5) Nephroblastomatosis

Nephroblastomatosis is defined as the presence of foci of persistent embryological metanephric blastema (nephrogenic rests), which have the potential to develop into nephroblastomas (Wilms tumor). Nephroblastomatosis presents as multinodular, peripheral, cortical lesions or as a subcapsular rind-like renal mass. On imaging, they are homogeneous and of low echogenicity on US, low density on CT, and low signal intensity on both T1 and T2 weighted MR imaging. The best diagnostic clue is its homogeneity.

6) Mesoblastic nephroma

It is the most common solid renal tumor in the neonate. It is usually identified within the first 3 months of life, with 90% of cases discovered within the first year of life. Imaging findings of mesoblastic nephroma are similar to those of Wilms tumor. The mass replaces a large portion of renal parenchyma and may contain cystic, hemorrhagic, and necrotic regions. It generally exhibits benign behavior and is successfully treated with nephrectomy alone.

7) Multilocular cystic renal tumor

Multilocular cystic renal tumor tends to manifest at two age peaks: in children aged 3 months to 4 years (predominantly boys with cystic partially differentiated nephroblastoma) and in adults

(predominantly women with cystic nephroma). Imaging studies demonstrate a well-circumscribed, encapsulated mass consisting of multiple cysts with solid or nodular components.

2. Non-renal retroperitoneal neoplasm

1) Neuroblastoma

Neuroblastoma may occur in the adrenal glands (50%) or anywhere along the sympathetic nerve chain. It is the third most common pediatric tumor after leukemia and primary brain tumor. It is mostly identified between 1 and 5 years of age, and associated with neurofibromatosis type 1, Beckwith-Wiedemann syndrome, and Hirschsprung's disease. Local invasion can occur into the liver, kidneys, and through the neural foramina into the spinal canal. Metastatic disease is seen in up to 70% of patients and common sites include lymph node, bone, bone marrow, liver, and skin. The prognosis of neuroblastoma depends on stage, patient's age, histologic category, grade of tumor differentiation, status of the MYCN oncogene, chromosome 11q status, and deoxyribonucleic acid ploidy. Neuroblastoma, ganglioneuroblastoma, and ganglioneuroma represent a histologic spectrum of maturation and differentiation. The tumors are easily detected with US, CT, or MRI because the mass is generally quite large at presentation. On US, the masses have a variety of appearances with the most characteristic being that of a solid, heterogeneous, hyperechoic mass, often with small calcification. When the mass is very small, CT and MRI play a more important role than US. And the new International Neuroblastoma Risk Group Staging System requires the use of CT, MRI, or both for staging. MRI is the best imaging technique to show intraspinal extension and to assess the bone marrow involvement.

2) Adrenocortical carcinoma

Adrenocortical carcinoma is uncommon in children. A higher incidence is seen in children under the age of 4 years. Most of these tumors are functioning tumor, which causes overproduction of androgens. Girls present with virilization and boys present with pseudoprecocious puberty. Predisposing

conditions are Li-Fraumeni syndrome and Beckwith-Wiedemann syndrome. The tumors are usually large at presentation and areas of hemorrhage, necrosis, and calcification are commonly seen.

3) Adrenal hemorrhage

Adrenal hemorrhage often occurs within the first few days of life but can occur prenatally and be seen on antenatal US. It is more commonly right sided (70%) but may also be bilateral (10%). It usually occurs in situations of perinatal stress, hypoxia, sepsis, and coagulopathy. US is the modality of choice for documentation of the presence of an adrenal hemorrhage and for follow-up. US shows a suprarenal mass of variable echogenicity without flow. It later develops a hypoechoic center, followed by shrinkage of the lesion with involution of the cystic component with or without the appearance of dystrophic calcifications.

4) Pheochromocytoma

Pheochromocytoma is uncommon neoplasm in children. About 70% of tumors occur in the adrenal gland. Malignancy is present in 12% of lesions in children. It is often sporadic but may be part of MEN II or von Hippel-Lindau disease. It occurs with hypertension and elevated urinary catecholamine level. On US, the tumors may have a solid homogeneous or heterogeneous appearance due to hemorrhage, necrosis, or calcifications. On CT and MRI, the lesions show avid enhancement except for areas of necrosis or hemorrhage. Functional imaging with MIBG scan is more specific in detecting multifocal disease.

SFS 5 PED-3

US for Pediatric Oncology

11:10-11:35

GBR 101

Chairperson: Kwan Seop Lee *Hallym University Sacred Heart Hospital, Korea*

Problem Solving Abdomen US for Pediatric Oncology Patients

M Beth McCarville*Department of Radiology, St. Jude Children's Research Hospital, USA*

In this lecture I will present a case based review of a variety of conditions in pediatric oncology for which ultrasound can be used as a problem solving tool. This will include ultrasound assessment of the bowel, bladder, the liver for hepatic veno-occlusive

disease, and contrast enhanced ultrasound of focal liver lesions and primary liver tumors and contrast ultrasound for distinguishing post-operative change from recurrent tumor.

Chairpersons: **Sung Il Jung** Konkuk University Medical Center, Korea
Seong Kuk Yoon Dong-A Medical Center, Korea

US for Acute Pelvic Pain

Moon Hyung Choi

Department of Radiology, The Catholic University of Korea, Seoul St. Mary's Hospital, Korea

Acute pelvic pain

Seoul St. Mary's hospital,
The Catholic University of Korea

Moon Hyung Choi

Acute pelvic pain

- Noncyclic pain for less than 3 months
- Common symptom of women who visit emergency or outpatient department
- Variable causes
 - Gynecologic (including pregnant-related disease)
 - Non-gynecologic

Causes

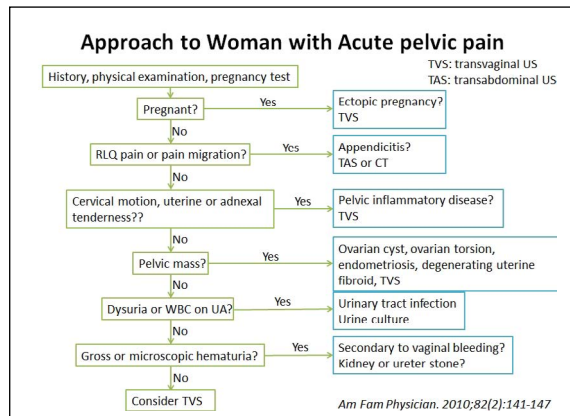
- Gynecologic
 - Simple ovarian cysts
 - Rupture or hemorrhagic ovarian cysts
 - Pelvic inflammatory disease & tubo-ovarian abscess
 - Ovarian torsion
 - Degenerating uterine fibroid
 - Pregnancy-related causes
 - Threatened abortion
 - Ectopic pregnancy
 - Ovarian hyperstimulation syndrome
- Non-gynecologic
 - Appendicitis
 - Diverticulitis
 - Inguinal hernia
 - Colitis
 - Epiploic appendagitis
 - Irritable bowel syndrome
 - Mesenteric lymphadenitis
 - Perirectal abscess

Proper imaging modality?

Gynecologic etiology suspected, Serum β -hCG negative				Relative radiation level
Radiologic Procedure	Rating	Comments	RRL*	
US pelvis transvaginal	9	Both transvaginal and transabdominal US should be performed if possible.	O	
US pelvis transabdominal	9	Both transvaginal and transabdominal US should be performed if possible.	O	
US duplex Doppler pelvis	5		O	
MRI pelvis without and with contrast	6	This procedure can be performed if US is inconclusive or nondiagnostic. See the Summary of Literature Review and ACR Manual on Contrast Media for the use of contrast media.	O	
MRI abdomen and pelvis without and with contrast	6	This procedure can be performed if US is inconclusive or nondiagnostic. See the Summary of Literature Review and ACR Manual on Contrast Media for the use of contrast media.	O	

Non-gynecologic etiology suspected, Serum β -hCG negative				Relative radiation level
Radiologic Procedure	Rating	Comments	RRL*	
CT abdomen and pelvis with contrast	9		****	
US abdomen and pelvis transabdominal	7	This procedure can be appropriate for suspected appendicitis and urinary tract pathology and to minimize radiation exposure.	O	
US duplex Doppler pelvis	7	Doppler can be used as an adjunct to assess for appendicitis or to evaluate ureteral jets for obstructive versus nonobstructive pathology.	O	
CT abdomen and pelvis without contrast	6		****	
MRI abdomen and pelvis without and with contrast	6	This procedure can be used to avoid the radiation exposure of CT in a young patient or if US is inconclusive or nondiagnostic. See the Summary of Literature Review for the use of contrast media.	O	

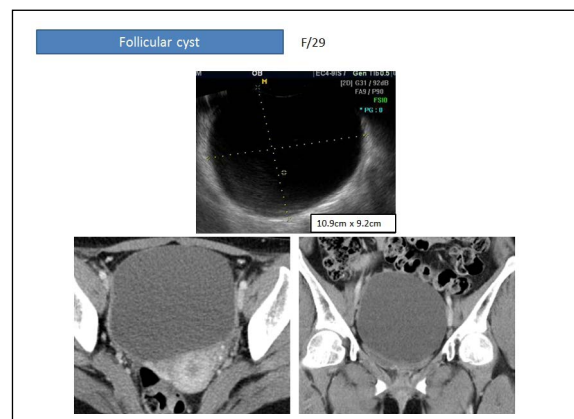
ACR appropriateness criteria® Acute pelvic pain in the reproductive age group
 Ultrasound Quarterly 2016;32:108-115



Gynecologic causes

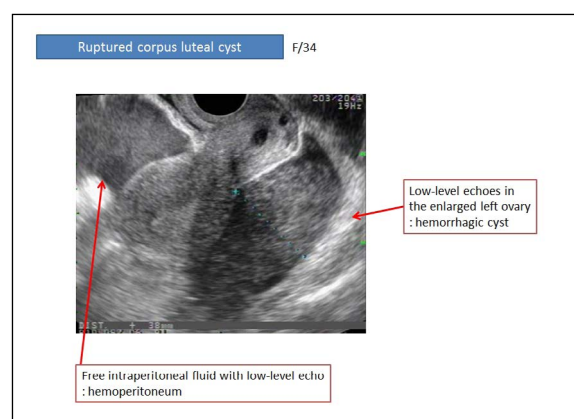
Simple ovarian cysts

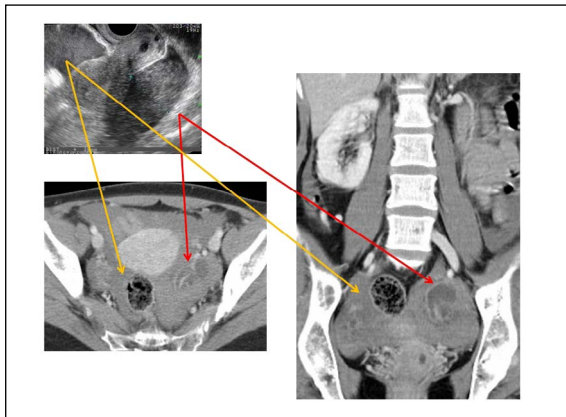
- Follicular cyst
 - Majority of simple cysts
 - Failure of the follicle to rupture or regress
 - Cyst greater than 3 cm
 - Small ovarian cysts: usually asymptomatic
 - Large or enlarging ovarian cysts can be a source of pelvic pain
 - Cysts larger than 5 cm predisposes to ovarian torsion
- US:
 - Unilocular anechoic intraovarian or exophytic ovarian mass
 - Thin, imperceptible walls
 - Posterior acoustic enhancement



Ruptured ovarian cysts

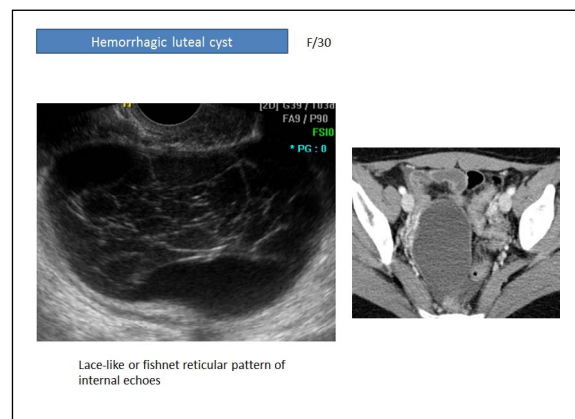
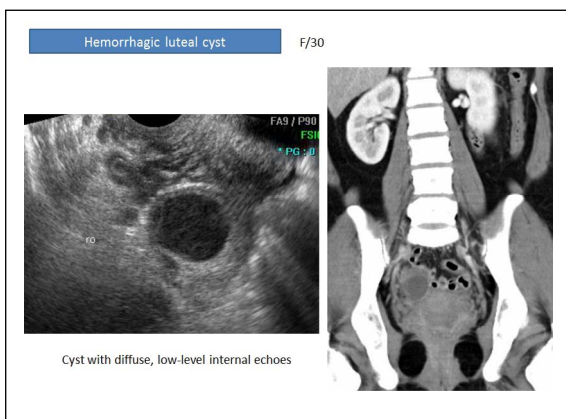
- Ruptured or hemorrhagic cyst
 - the most common gynecologic cause of acute pelvic pain in nonpregnant, afebrile women
- US
 - Hemoperitoneum
 - Cul-de-sac
 - Free intraperitoneal fluid with low-level echo
 - A completely ruptured ovarian cyst
 - Normal ovary ← fluid resorbed or dispersed throughout the peritoneal cavity
 - Leaking cyst
 - Low-level echoes or clot
 - Crenated appearance





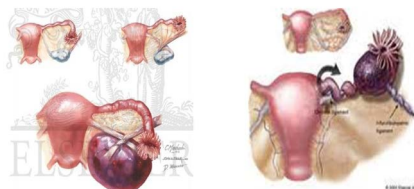
Hemorrhagic ovarian cyst

- Hemorrhage within an corpus luteum
- Variable depending on the evolution of the hemorrhage
- US
 - Cyst with diffuse, low-level internal echoes
 - Fluid-fluid level
 - No internal vascularity
 - Thin wall
 - Lace-like or fishnet reticular pattern of internal echoes

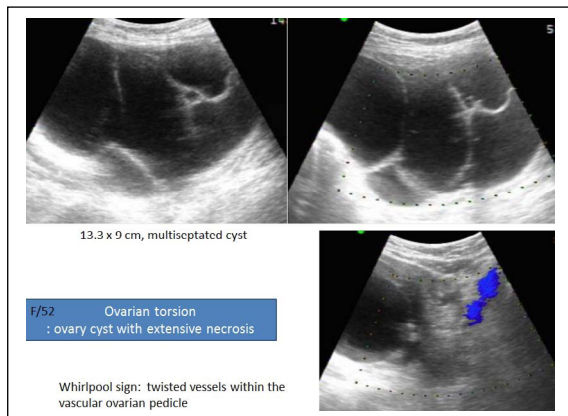


Ovarian torsion

- Gynecologic emergency
 - **Ovarian torsion:** the twisting of an ovary on its ligamentous supports and can result in a compromised blood supply.
 - **Adnexal torsion:** term that is inclusive of either the ovary, fallopian tube, or both.

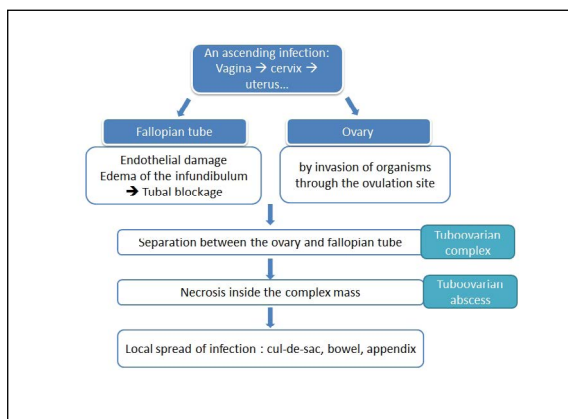


- Risk factor: cyst greater than 5 cm in size
- US finding
 - Enlarged midline ovary with peripherally displaced small follicles and heterogeneous central stroma due to hemorrhage and edema
 - Long standing torsion → complex appearance of the cyst
 - Thickened, twisted, edematous tubular vascular pedicle: specific
 - Whirlpool sign: twisted vessels within the vascular ovarian pedicle on color Doppler US
 - Spectral Doppler finding: absence of arterial flow (high specific)



Pelvic inflammatory disease

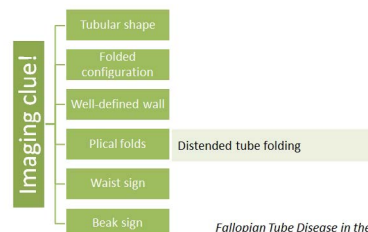
- Symptom:
 - Abdominal or pelvic pain
 - Vaginal discharge
 - Uterine bleeding
 - Dyspareunia
 - Dysuria
 - Adnexal or cervical tenderness
 - Nausea, Vomiting



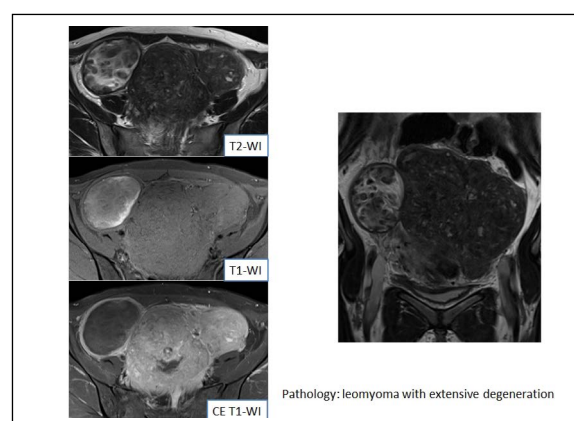
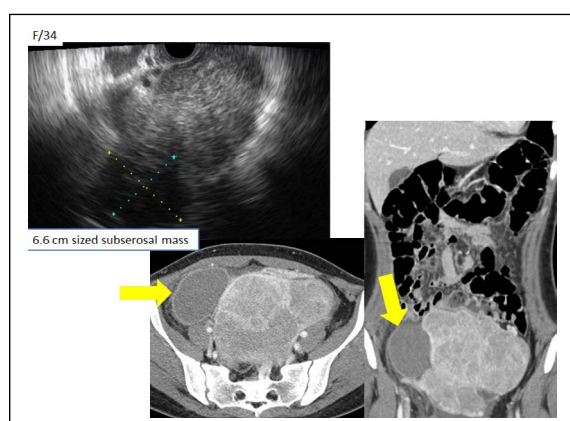
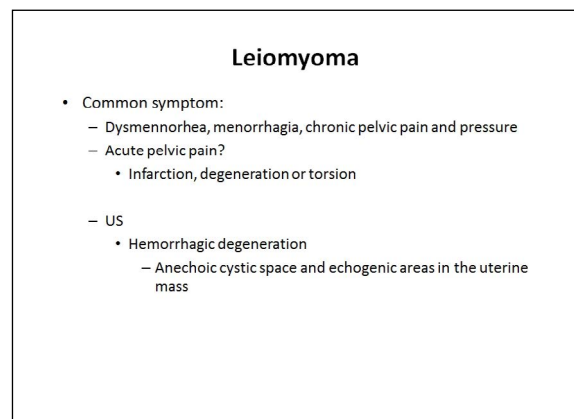
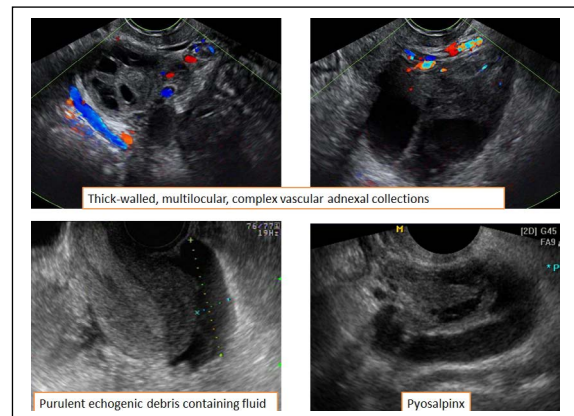
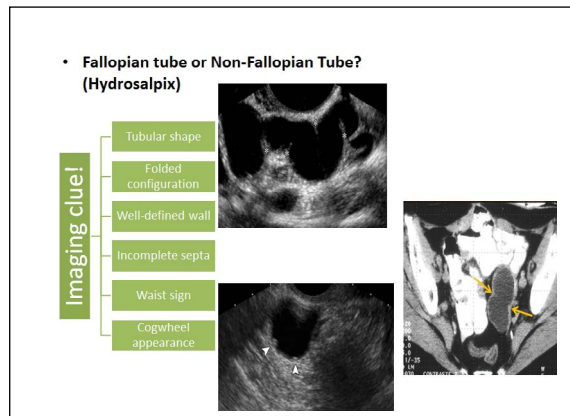
- US findings
 - Cervicitis: usually normal, marked pain during TVS
 - Endometritis:
 - presence of fluid or gas within the endometrial canal
 - Heterogeneous thickening, increased vascularity, indistinct endometrial stripes
 - Fallopian tube
 - Wall thickening, distension with fluid, incomplete septa
 - Pyosalpinx: low-level echoes or multiple fluid-fluid levels with echogenic debris
 - Cogwheel sign
 - Echogenic edematous walls and associated echogenic mucosal folds

- Tuboovarian abscess
 - Ovary and tube are confluent and cannot be identified as separate structures
 - Thick-walled, multilocular, complex vascular adnexal collections
 - Increased echogenicity of pelvic fat
 - Purulent echogenic debris containing fluid within the cul-de-sac

- Hydrosalpinx
 - Fallopian tube or Non-Fallopian Tube?
 - US: thin- or thick-walled C- or S-shaped anechoic tubular structure separate and distinct from the uterus and ovary



Fallopian Tube Disease in the Nonpregnant Patient
Radiographics. 2011;31:527-48

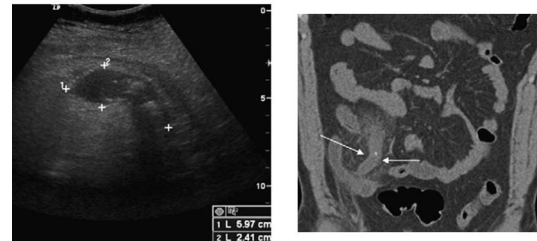


Pregnant-related disease → in 4th lecture

Non-gynecologic causes

Appendicitis

- The most common non-gynecologic causes of acute pelvic and right lower quadrant pain
- US finding
 - Distended, noncompressible tubular blind-ending structure
 - Wall-to-wall diameter > 7 mm or individual wall > 3 mm in thickness
 - Transverse section: double concentric ring like target sign
 - Appendicolith
 - Periappendiceal abscess: hypoechoic fluid collection



Ultrasound for pelvic pain II: nongynecologic causes
Obstet Gynecol Clin North Am. 2011;38:69-83

Diverticulitis

- Diverticulitis
 - Inflammation of an outpouching of the colon
 - Left lower quadrant > right lower quadrant (in western country)
- US finding
 - Segmental area of thickened bowel wall
 - Inflamed diverticulum: hypo or hyperechoic outpouching of the bowel wall
 - Inflamed pericolic fat
- CT: mainstay imaging modality in the diagnosis of diverticulitis and its complication



TVS: thickening and edema of the rectum and sigmoid colon



Diverticulum with wall thickening, hyperechoic content

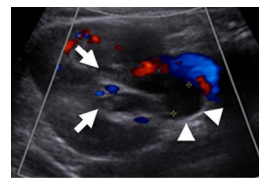


Diffuse wall edema in sigmoid colon and pericolic fat stranding

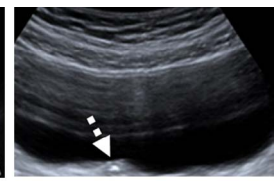
Diverticulitis: a comprehensive review with usual and unusual complications
Insights Imaging. 2017;8:19-27.

Ureter stone

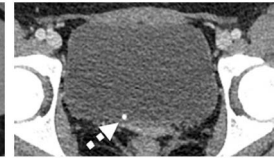
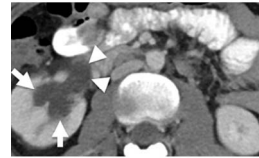
- Urolithiasis → obstructive uropathy → acute pelvic pain
- Most common sites
 - Ureteropelvic junction
 - Ureters crossing over iliac vessels
 - Ureterovesical junction
- US
 - Hyperechoic calculi + posterior acoustic shadowing
 - \pm hydronephrosis, hydroureter, perinephric or periureteral fat stranding



TAS: Right hydronephrosis



TAS: a 3mm calculus at right ureterovesical junction



CC 6 GU-2

Genitourinary Emergency US

10:40-11:00

GBR 102

Chairpersons: **Sung Il Jung** *Konkuk University Medical Center, Korea*
Seong Kuk Yoon *Dong-A Medical Center, Korea*

US of Acute Flank Pain

Ki Choon Sim

Department of Radiology, Korea University Anam Hospital, Korea

Sonography has a well established modality in evaluating the abdominal pain, especially flank pain. Acute flank pain in adults is most commonly due to renal stone disease and acute pyelonephritis (APN). The classic presentation of renal colic is the acute onset of unilateral flank pain with radiation to the groin, dysuria, and hematuria. Sonography can diagnose stones in the renal collecting system (pelvicalyceal system and ureter) when a focal area of echogenicity with acoustic shadowing is identified. There may be associated dilatation of the renal collecting system depending on the size and location of the stone, the length of time the obstruction has been present, and whether the obstruction is partial or complete. However, in daily practice, cross-sectional imaging is essential and widely used for

confirmation of renal or ureteral stones and for differentiation from other diseases causing flank pain. In acute pyelonephritis, the sonographic appearance of the kidney is usually normal (the CT finding of the kidney is also normal), but it may be enlarged and have a hypoechoic parenchyma with loss of the normal corticomedullary junction. Furthermore, clinical and laboratory correlations are essential for diagnosis of APN with imaging study.

Lastly the possibility of non-renal etiologies of flank pain should keep in mind in daily practice. Common causes include the following: Musculoskeletal strain, Musculoskeletal contusion, Dermatologic conditions, Neurologic conditions, Compression from local growth of a mass, Referred pain from thoracic pathologies.

Chairpersons: **Sung Il Jung** *Konkuk University Medical Center, Korea*
Seong Kuk Yoon *Dong-A Medical Center, Korea*

US of Acute Scrotal Pain

Young Sup Shim

Department of Radiology, Gachon Univeristy Gil Medical Center, Korea

Acute scrotal pain is a common urological problem that can be easily diagnosed by ultrasound. In most cases, ultrasound is used as a confirmatory test, without additional studies such as CT or MRI. Therefore, it is important to understand the method of performing scrotal ultrasonography and to understand the ultrasound image of diseases that may cause acute scrotal pain.

Common causes of acute scrotal pain are testicular torsion, appendicitis, and epididymitis. Testicular torsion is rare, but is the most important disease requiring urgent ultrasonography in acute scrotal pain patient. In testicular torsion, grayscale of ultrasonography showed heterogeneous echogenicity in testis due to hemorrhage and infarction after 24 hours of symptom onset. However, in the early 4-6 hours, the testis swelled up slightly and the echogenicity of testis was slightly changed to a normal or slight decrease. Detection of twisted spermatic cord is also useful to diagnose testicular torsion. Grayscale alone is insufficient for diagnosis of testicular torsion, so Doppler USG should be used in parallel. Power Doppler can be used to diagnose torsion by observing blood flow more sensitively. The most common cause of acute scrotum pain is

epididymitis. It is rare in children before puberty, and it is important to distinguish them from testicular torsion in young adults (35 years or younger). The most common site of epididymitis is the epididymal tail portion. In ultrasound, the epididymis is enlarged with increased or decreased echogenicity. There is typically increased vascularity on Doppler ultrasound. It can be accompanied by orchitis, hydrocele, and varicocele. Torsion of the testicular appendage is common in pre-adolescent children and usually occurs in 2 to 12 years of age. It must be distinguished from testicular torsion in young male presenting with acute scrotum pain. On ultrasound, testicular appendage is enlarged without vascularity. However, in fact, testicular appendage is not easy to observe from ultrasound. So it is important to find out testicular appendage in advance. And increased perfusion in the head of the epididymis may be helpful in diagnosis.

In addition to the above-mentioned diseases, there are additional cases of scrotal trauma, testicular or epididymal tumors, and extratesticular & extraepididymal scrotal diseases (hydrocele, varicocele, abscess, etc.). It should be to distinguish, too.

CC 6 GU-4

Genitourinary Emergency US

11:20-11:40

GBR 102

Chairpersons: **Sung Il Jung** *Konkuk University Medical Center, Korea*
Seong Kuk Yoon *Dong-A Medical Center, Korea*

US of Acute Abdominal Pain in Pregnancy

Sung Kyoung Moon

Department of Radiology, Kyung Hee University Hospital, Korea

Abdominal pain during pregnancy can be caused by a wide variety of diseases including disorders of the obstetric, gynecologic, gastrointestinal, hepatobiliary, genitourinary, and vascular systems. Some causes are unique to pregnancy, exacerbated by pregnancy, or require an altered imaging algorithm for diagnosis during pregnancy. The educational objectives of this lecture are to improve understanding of the imaging evaluation of abdominal pain during pregnancy.

The clinical diagnosis of an intraabdominal disease in pregnant women can be obscure by concurrent maternal physiologic and anatomic changes. Ureteral compression and displacement of intraabdominal organs, including the appendix, by the enlarged uterus may also confound the clinical presentation. Imaging can clarify a confusing clinical picture and expedite diagnosis. Ultrasound is widely used as the initial diagnostic imaging technique during pregnancy because of its availability, portability, and lack of ionizing radiation. Ultrasound often can elucidate the cause of abdominal pain, particularly if pain is due to an obstetric and gynecologic abnormality.

During the pregnancy, common causes of abdominal and pelvic pain include early pregnancy failure, ectopic pregnancy, preterm labor and the less common, but more severe, complications of placental abruption and uterine rupture. Common gynecologic causes of pain during pregnancy include complications related to adnexal masses, ovarian torsion, and leiomyomas. Adnexal masses are often first detected at the time of a routine first trimester dating or second trimester anatomic

survey ultrasound examination. Ovarian torsion and leiomyoma degeneration both have a higher incidence during pregnancy.

Gastrointestinal causes of pain during pregnancy include appendicitis and other inflammatory, infectious, and obstructive processes of the bowel. These diseases are neither unique to nor more common in pregnancy but can be more difficult to diagnose during pregnancy. The approach to imaging the bowel of a pregnant patient also differs from that of a nonpregnant patient because ultrasound and MRI are typically preferred over techniques that impart ionizing radiation such as radiography and CT.

Two hepatic complications unique to pregnancy that can present with acute abdominal pain are HELLP (hemolysis, elevated liver enzymes, low platelet count) syndrome and acute fatty liver of pregnancy (AFLP). Although pancreatitis is not unique to pregnancy, the approach to imaging pregnant patients with pancreatitis differs from that of the nonpregnant patient.

Urinary tract causes of pain during pregnancy include physiologic and obstructive hydronephrosis and infectious causes such as cystitis and pyelonephritis, which do not usually require imaging for diagnosis and treatment. The incidence of urolithiasis does not increase during pregnancy. However, the approach to imaging urolithiasis and the need to differentiate between physiologic and obstructive hydronephrosis differs between pregnant and nonpregnant patients.

SC 2 BR-1

10:20-10:40

GBR 103

Chairpersons: **Boo-Kyung Han** *Samsung Medical Center, Korea*
Eun-Kyung Kim *Severance Hospital, Korea*

Artificial Intelligence in Breast US

Bong Joo Kang

Department of Radiology, The Catholic University of Korea, Seoul St. Mary's Hospital, Korea

Contents

- What is deep learning (artificial intelligence)?
(And how is it different from “old school”
computer-aided diagnosis?)
- Where are we now? (recent results)
- From detection of specified abnormalities (a nice
helper of radiologist) to general reporting (a
replacement of radiologist)
- Do patients accept diagnosis made by software
instead of radiologists?
- Computer-assisted diagnosis and deep learning:
what are the limits?

Chairperson: Hee Jung Lee Keimyung University Dongsan Medical Center, Korea

US for Precocious Puberty

Jung-Eun Cheon

Department of Radiology, Seoul National University Hospital, Korea

Introduction

Precocious puberty represents a unique diagnostic problem in which imaging plays an important role. Precocious puberty is defined as development of secondary sex characteristics before the age of 8 years in girls and 9 years in boys. Precocious puberty can be classified into two types: central precocious puberty (CPP, inappropriate activation of the hypothalamic-pituitary axis with release of gonadotropin) and peripheral precocious puberty (PPP, gonadotropin-independent secretion of sex steroids by the adrenal glands or gonads). A variety of lesions can manifest with precocious puberty, including various central nervous system (CNS) lesions, adrenal lesions, and sex cord-stromal tumors of the testis or ovary. CPP may be idiopathic or related to a CNS lesion such as a neoplasm, cyst, or hydrocephalus. CPP in girls is usually idiopathic, whereas the vast majority of cases in boys are due to an intracranial lesion. Whereas CPP is characteristically isosexual, the PPP may be either isosexual or heterosexual (virilization in girls / gynecomastia or other signs of feminization in boys). Isosexual PPP in girls is most commonly caused by an autonomously functioning ovarian cyst but may also be caused by a juvenile granulosa cell tumor (GCT) of the ovary or, rarely, a feminizing adrenal cortical neoplasm (ACN). Heterosexual PPP in girls is most often related to androgen production by the adrenal glands due to a functioning ACN or congenital adrenal hyperplasia (CAH). In boys, PPP is usually due to CAH or sex steroid hormone secretion by a sex cord-stromal tumor of the testis. We review the approach to imaging evaluation of precocious puberty

with emphasis on role of ultrasonography (US), which is the primary imaging modality for evaluating the reproductive organs and may also be useful to evaluate for adrenal abnormalities.

US Examination for Precocious Puberty in Girls

1. Normal anatomy and developmental changes of female pelvis

Transabdominal US is performed through a filled bladder with a 3.5-6 MHz sector probe. Uterine and ovarian anatomy changes during pediatric life. The neonatal uterus is prominent, under the influence of maternal hormones. The newborn uterine configuration is spade shaped. The cervix is larger than the fundus and the fundus: cervix ratio based on anterior/posterior (AP) dimensions is 1:2. The endometrial lining often echogenic, and endoluminal fluid can be demonstrated in some female newborns. At 2 to 3 months of age, the uterus regresses to a prepubertal size and develops a somewhat tubular configuration. The uterine length of the prepubertal uterus is 2.5 to 3.0 cm, with the fundus:cervix ratio 1:1. The endometrial stripe when it is seen appears as thin as a pencil line. The uterine length increases gradually between 3 and 8 years of age, measuring up to 4.3 cm at the end of this phase of development. The tubular uterine configuration during this time is maintained until puberty, at which time the uterine length gradually increases to 5 to 7 cm. The uterus then assumes a pear-shaped configuration at puberty with the fundus:cervix AP ratio 3:1. The echogenicity and thickness of the endometrial lining then varies according to the phase of the menstrual cycle.

Ovarian size is most reproducible and best described by measurement of the ovarian volume, which can be calculated mechanically on the US unit or by a simplified modified equation for determination of the volume of an ellipse: length \times width \times depth \times 0.523 5 volume (in mL). The mean ovarian volumes in girls younger than 6 years old is usually less than or equal to 1 mL. Neonatal ovarian volumes, however, may be quite large as a result of maternal hormonal stimulation during intrauterine life, which may take several months to regress. Ovarian volume gradually begins to increase again at approximately 6 years with the mean ovarian volume measurement in premenarchal girls between 6 and 11 years of age ranging between 1.2 mL and 2.5 mL.

2. Central precocious puberty in girls

A pelvic US in female patients will identify whether the uterus and ovaries maintain their prepubertal size and configuration, or whether there has been estrogen stimulation of these organs. The ovaries are symmetrically increased in volume and show numerous follicles. The uterine features are more accurate than ovarian characteristics, namely increased uterine size, thicker fundus, endometrial echo complex. MRI of the brain is the preferred imaging modality to confirm or exclude a CNS abnormality in patients with precocious puberty.

3. Peripheral precocious puberty in girls

1) Isosexual precocious puberty in girls

Excess estrogen production causes endometrial stimulation and vaginal bleeding. Breast development may or may not be present. It is important in this group of patients to exclude a functioning ovarian and adrenal tumor. The most common ovarian source is an autonomous estrogen-secreting follicular (granulosa-thecal) cyst. Other causes are estrogen-producing ovarian neoplasms, such as granulosa cell tumors and rare estrogen-secreting adrenal neoplasms.

McCune-Albright syndrome has been classically described as a triad: gonadotropin-independent precocious puberty, café au lait spots, and polyostotic fibrous dysplasia of bone. The sexual precocity in girls with McCune-Albright syndrome is caused by

autonomously functioning luteinizing follicular cyst(s) of the ovaries. In most patients, the follicular cyst is unilateral, with internal smaller follicles (daughter cyst sign). Ovarian asymmetry is a classic US hallmark of peripheral precocious puberty linked to autonomous follicular cysts.

2) Heterosexual precocious puberty in girls

These children present with virilization, i.e. the development of male secondary sexual characteristics. Non-salt-losing CAH is the most common cause of female virilization in the older child. Adrenal adenomas or adrenal carcinomas may produce increased levels of androgens and virilization. Ovarian neoplasms such as Sertoli-Leydig cell tumors or thecomas may secrete androgens and cause virilization.

US Examination for Precocious Puberty in Boys

Isosexual precocious puberty in boys is associated with an increase in circulating androgens or androgen-like substances. CAH is the most common cause for excessive androgen production by the adrenal gland of either sex. Isosexual precocious puberty in boys can occur because of androgen secreting neoplasms of the adrenal cortex and it can rarely be caused by an androgen secreting Leydig cell tumor of the testis. Tumors that secrete beta-HCG may stimulate the Leydig cells to produce testosterone. Hormonally active central and peripheral germ cell tumors, hepatoblastoma, and hepatocellular carcinomas may all secrete beta-HCG.

US for Adrenal Gland

1. Normal anatomy

The adrenal gland is made up of two distinct endocrine glands: the medulla, which produces catecholamines, and the cortex, which produces steroid hormones. The cortex is made up of three zones: the zona glomerulosa, which produces mineralocorticoids (aldosterone); the zona fasciculata, which, along with the zona reticularis, produces glucocorticoids (cortisol); and the zona reticularis, which synthesizes sex steroids (mostly

androgens) in addition to glucocorticoids. Adrenal androgens are responsible for masculinization of external genitalia in the fetus and for pubertal pubic and axillary hair growth. The neonatal adrenal gland is large due to the presence of persistent fetal cortex, which rapidly involutes in the first few months of life. The normal large glands are easily visualized at US in young infants. A central echogenic stripe that represents the medulla and prominent central veins is noted. This is surrounded by a thicker hypoechoic region with a smooth or slightly undulating surface representing the fetal and definitive adrenal cortex. Once involution of the fetal cortex has occurred, the normal adrenal gland is seen only at CT or MRI.

2. Congenital adrenal hyperplasia

CAH is a form of adrenal insufficiency in which one of the enzymes of the adrenal steroid synthetic pathway is deficient. The 21-Hydroxylase deficiency and 11-beta-Hydroxylase deficiency account for over 90% of the CAH. This deficiency leads to excessive pituitary adrenocorticotrophic hormone (ACTH) production which leads to chronic stimulation of the adrenal glands, hyperplasia of the adrenal cortex and overproduction of androgens. It affects both females and males. Girls with CAH are born with an enlarged clitoris and normal internal genitalia. Boys have normal external genitals at birth and may go undetected in early infancy. The diagnosis of CAH is confirmed by the presence of elevated serum 17-hydroxyprogesterone (17-OHP). In certain cases there is also an absence of aldosterone production, leading to salt loss syndrome. US of the adrenal glands may show nodular and cerebriform contours of the adrenal gland.

3. Adrenal Neoplasm

Most frequent adrenal neoplasm is neuroblastoma, arising in the adrenal medulla or neural crest. ACNs are rare in childhood. Adrenal cortical carcinoma

is about 3-times more common than an adrenal adenoma. Clinical presentation is usually with signs of endocrine malfunction and precocious puberty.

Summary

Sexual precocity has a wide range of causes involving multiple endocrine organs, and imaging plays an important role in the evaluation and diagnosis of children with symptoms of early sexual maturation. CPP is usually idiopathic in girls but is most commonly related to a CNS lesion in boys. PPP may be caused by gonadal lesions or adrenal abnormalities, which are best initially evaluated with US. Early diagnosis and treatment reverse the endocrine disorder with its physical changes, preserve adult height potential, and may be potentially life saving.

References

1. Delman BN. Imaging of pediatric pituitary abnormalities. *Endocrinol Metab Clin North Am* 2009;38(4):673-98.
2. Chang YW, Hong HS, Choi DL. Sonography of the pediatric thyroid: a pictorial essay. *J Clin Ultrasound* 2009;37(3):149-57.
3. Na DG, Baek JH, Sung JY, et al. Thyroid Imaging Reporting and Data System Risk Stratification of Thyroid Nodules: Categorization Based on Solidity and Echogenicity. *Thyroid* 2016;26(4):562-72.
4. Rosenberg HK. Sonography of the pelvis in patients with primary amenorrhea. *Endocrinol Metab Clin North Am* 2009;38(4):739-60.
5. Carty H, Brunelle F, Stringer DA, Kao S, eds. *Imaging children*, 2nd ed. Elsevier, 2005: 955-1020.
6. Avni FE, ed. *Imaging endocrine disease in children*. Springer, 2012.
7. Chung EM, Biko DM, Schroeder JW, Cube R, Conran RM. From the radiologic pathology archives: precocious puberty: radiologic-pathologic correlation. *Radiographics*. 2012;32(7):2071-99.

Thyroid US in Children and Adolescents

Hyun Sook Hong

Department of Radiology, Soonchunhyang University Bucheon Hospital, Korea

Introduction

Thyroid imaging in pediatric patients is indicated in the evaluation of congenital hypothyroidism (CH) during newborn screening or for a palpable thyroid mass. The primary imaging modalities for newborn screening are ultrasonography (US) and radionuclide scintigraphy.

Embryology

The thyroid gland develops from the median and paired lateral anlagen during the first trimester of pregnancy. It consists of two distinct cell types: thyroid follicular cells and parafollicular cells. Thyroid follicular cells originate as the median thyroid anlage, an endodermal thickening in the floor of the primordial pharynx, between the first and second pharyngeal arches during the fourth to fifth gestational age. The thickening rapidly forms a small outpouch, referred to as the thyroid primordium. The thyroid primordium then elongates into a bilobed diverticulum and descends caudally. The thyroglossal duct, which disappears by the 7th week of gestation, is a connection between the tongue and the caudal migration of the thyroid primordium. By the 7th week, the gland attains its normal final position anterior to the second and third tracheal rings. Lateral anlagen arise from ultimobranchial bodies that are derived from the fourth and fifth pharyngeal pouches and give rise to parafollicular C cells that secrete calcitonin.

Congenital disorders

CH is a relatively common endocrine disorder, with a prevalence in Korea of 1 in every 3,981 live births. CH is classified according to the site, associated types, and duration of disease. Most cases of CH are due to a developmental defect known as dysgenesis (aplasia, ectopy, hypoplasia), or to defective thyroxine synthesis within a structurally normal thyroid gland - dyshormonogenesis - which is caused by various autosomal recessive mutations. Most cases of CH are permanent and arise from dysgenesis. There appears to be wide molecular heterogeneity involving several causative genes. Among them, the TSH receptor (TSHR) gene and thyroid peroxidase (TPO) genes account for the majority of mutation-positive cases of dysgenesis and dyshormonogenesis, respectively. Dyshormonogenesis causes goitrous CH. Diagnosis of the transient form is important to avoid unnecessary, lifelong therapy. The prevalence of transient CH is reported to be around 9.8% in Korea. It is caused by maternal antibodies, perinatal illness, or congenital abnormalities. Rarely, a central type, such as panhypopituitarism, causes CH.

Aplasia is defined as the failure to detect thyroid tissue on US and scintigraphy. US reveals a hyperechoic structure, reflecting remnants of the ultimobranchial body. A Tc^{99m} scan can confirm the absence of detectable thyroid activity and only visible background soft tissue and the salivary gland. Ectopic thyroid tissue can be found anywhere along the migration course of the thyroid primordium. A complete failure of descent of the thyroid results in a lingual thyroid at the base of the tongue, the most

common type of functioning ectopic thyroid tissue. An ectopic gland typically appears as a round or oval area of uptake in the midline of the upper neck on scintigraphy. Scintigraphy is more sensitive than US for detecting an ectopic thyroid. Overdescent may result in an ectopic thyroid in the lower neck or mediastinum. In patients with hypoplasia, the thyroid gland appears normal or slightly smaller in size on US. However, scintigraphy reveals decreased isotope uptake. Transient CH is diagnosed by the presence of normal thyroid function, a thyrotropin-releasing hormone study, and a scintigraphy performed during trial-off therapy. Hemiplasia is generally discovered incidentally, and thyroid function may be decreased during puberty when the need for thyroid hormone is high. Dyshormonogenesis involves an inborn error in thyroxine synthesis. Iodide becomes trapped in the gland and cannot be organified. US shows an enlarged gland. Scintigraphy also shows increased uptake. The most common pitfall in isotope scanning is a lack of uptake despite the presence of thyroid tissue, leading to the spurious diagnosis of aplasia. This condition may occur for several reasons: a scan delayed beyond 4-5 days of T4 treatment; iodine exposure; blocking TSHR antibodies causing transient hypothyroidism; and, rarely, defects affecting iodide uptake. Concurrent US is helpful in avoiding this misdiagnosis.

Incomplete degeneration of the thyroglossal duct may result in a persistent fistulous tract, or in a TGDC, which accounts for approximately 70% of congenital abnormalities in the neck along the path of migration from the foramen cecum at the tongue base to the anterior lower neck. On US, a classic TGDC has a cystic lesion with a well-defined margin and thin walls. A ruptured cyst may result in a thyroglossal duct sinus that opens through the skin. TGDC can be associated with malignancy. Papillary thyroid cancer (PTC) is the most common type of malignancy. If the cyst has calcifications, a soft tissue component, or invasion of the surrounding tissue without a history of infection, associated malignancy should be suspected. Although a TGDC can often be diagnosed clinically, preoperative imaging can determine the anatomical extent of the cyst, detect ectopic thyroid tissue, and evaluate the potential for malignancy within the cyst.

Diffuse thyroid disease

Diffuse thyroid disease (DTD) encompasses several relatively common thyroid disorders. Diffusely enlarged thyroid glands with a heterogeneous echotexture, diffuse hypoechogenicity, and inhomogeneity or an irregular echo pattern have been described as common US findings. Hashimoto's thyroiditis and Graves' disease are the most common autoimmune diseases.

Acute suppurative thyroiditis is rare and results from microbial infection. Patients present with a palpable mass with erythema and tenderness. US shows an enlarged and ill-defined hypoechoic lesion in the left lobe of the thyroid gland, as well as surrounding inflammation. An esophagogram shows a pyriform sinus fistula, reflecting the third pharyngeal pouch remnant.

Hyperthyroidism is rare in children and is most commonly caused by Graves' disease. It affects 1 in 5,000 children. The peak incidence occurs from 11-15 years of age, with a female predominance. A positive family history is common. It is characterized by hyperplasia and hyperfunction of the thyroid gland. Lymphocytes and plasmacytes infiltrate the thyroid gland and retro-orbital tissue. The patient presents with an enlarged thyroid gland, exophthalmos, and thyrotoxicosis. US shows a markedly enlarged and inhomogeneous decrease in echogenicity. Color Doppler imaging reveals a hypervascular pattern, referred to as a "thyroid inferno". During remission, the gland shows normal echogenicity, and during relapse, hypoechogenicity and high-flow vessels are seen. On scintigraphy, the gland shows a markedly increased uptake. Hashimoto's thyroiditis (HT) is the most common DTD and is characterized by diffuse lymphocytic infiltration on histopathology. Patients present with painless enlargement of the thyroid gland, resulting from diffuse lymphocytic infiltration, and growth retardation. Diagnosis is made by detecting antithyroid antibodies. It affects 1.3% of children and has a female predominance. US shows an enlarged gland with a diffusely heterogeneous coarse echotexture. There may be discrete hypoechoic micronodules or coarse septation. In the chronic stage, the gland shows atrophy. HT can be

associated with benign and malignant nodules.

According to the American Thyroid Association (ATA) management guidelines for children, US should be performed in any patient with a suspicious thyroid examination, such as a suspected nodule or significant gland asymmetry, particularly palpable cervical lymphadenopathy.

Thyroid nodules

Thyroid nodules are less common among children compared to adults but are more likely to be malignant in children referred for the evaluation of nodular thyroid disease (22-26% in children versus approximately 5% in adults). Estimates from US and post-mortem examinations suggest that 1-1.5% of children, and up to 13% of older adolescents or young adults, have thyroid nodules. With a 1-year increase in age, the rate of incidental of thyroid abnormality is increased to 9% in children.

A solid hypoechoic nodule with any suspicious US features is now categorized as 5, high suspicion, according to the Korean Thyroid Imaging Reporting and Data System (K-TIRADS), based on the solidity and echogenicity of the thyroid nodule. A non-parallel shape, ill-defined, spiculated margin, and microcalcifications are considered suspicious US features. Solid hypoechoic nodules have revealed a high malignancy rate of about 79%, and that in partially cystic or isohyperechoic nodules has revealed an intermediate risk (25%). A partially cystic or isohyperechoic nodule without any suspicious US features is categorized as 3, low suspicion. A solid hypoechoic nodule without any suspicious US features, or a partially cystic, isohyperechoic nodule with any suspicious US feature, is categorized as 4, intermediate suspicion. The presence of intranodular vascularity might increase the risk of malignancy; there are no consistent results regarding the association of an intranodular vascularity pattern with risk of malignancy.

The majority of incidentally-detected thyroid lesions in children are cysts, other benign nodules such as nodular hyperplasia, and intrathyroidal thymus. US shows similar results to a normal thymus and linear echogenic lines and dots. The lesions are more common in males than females, in contrast

to the higher incidence of incidental thyroid lesions in adult females. Thyroid nodules are uncommon in children. However, nodules in children carry a greater risk of malignancy compared to those in adults (22-26% vs. 5-10% in most series).

PTC accounts for 90% or more of all childhood thyroid malignancies. Follicular thyroid cancer is uncommon, while medullary thyroid cancer, poorly differentiated tumors, and anaplastic thyroid carcinomas are rare in young patients. Children with PTC are more likely to have regional lymph node involvement, extrathyroidal extension, and pulmonary metastasis. Despite extensive disease at clinical presentation, children are much less likely to die from disease ($\leq 2\%$ of long-term cases lead to specific mortality) than adults. Thyroid cancer is the 11th-most frequently diagnosed cancer in Korean boys under the age of 14 years and the 5th-most common cancer in girls. In the USA, among 15-19-year-old adolescents, thyroid cancer is the 8th-most frequently diagnosed cancer and the 2nd-most common cancer among girls. Compared with adult PTC, childhood PTC is characterized by a higher prevalence of gene rearrangement and a low frequency of point mutations in the proto-oncogenes. The BRAF mutation is rare in children. This may be important because point mutations of RAS and BRAF lead to genomic instability and dedifferentiation. In contrast, RET/PTC rearrangements are more common in PTC in children and do not lead to genomic instability. These molecular differences might be one of the reasons for the better response to radioactive iodine treatment in children and could partially explain their low mortality and rare progression to less differentiated tumors.

According to the ATA management guideline for adults, fine needle aspiration (FNA) is not warranted for the evaluation of nodules less than 1-cm in size unless the patient is considered high risk. Because the thyroid volume changes with age, the size of the nodule alone does not predict malignant histology. Therefore, US characteristics and the clinical context should be used more preferentially to identify nodules that warrant FNA. Due to the apparent increased probability of malignancy among these indeterminate categories in children, definite surgery (lobectomy plus isthmusectomy) is

recommended for indeterminate FNA. The limited data available suggest these indeterminate FNA categories account for ~35% of pediatric FNA and that, in children, 28% of AUS/FLUS lesions and 58% of suggestive of follicular or Hurtle cell neoplasms are malignant. For hyperfunctioning nodules, surgical resection, most commonly lobectomy, is recommended. The mutagenic effect of low-activity radioiodine on normal thyroid tissue and up to one third of patients may harbor an incidentally discovered differentiated thyroid cancer associated with an autonomous nodule. The diffuse infiltrative form of PTC may occur in children and should be considered in a clinically suspicious gland. For the majority of patients with PTC, total thyroidectomy is recommended as an initial surgical approach because of the increased incidence of bilaterality and multifocality (30% and 65%, respectively). Central neck dissection is recommended for children with gross extrathyroidal invasion and/or locoregional metastasis on preoperative staging or intraoperative findings. Treatment is individualized based on staging and continuous risk stratification.

Conclusion

In summary, dual imaging with US and scintigraphy increases the diagnostic yield for CH. Thyroid malignancy presents with a suspicious malignant nodule or a diffusely-infiltrating carcinoma that can mimic thyroiditis. Additional genetic studies have a limited role in children. In terms of the apparent increased probability of malignancy among indeterminate categories and hyperfunctioning nodules in children, definite surgery is recommended for indeterminate cytology on FNA. US is the most sensitive diagnostic modality for evaluating thyroid nodules, and for diagnosis of thyroid cancer. Moreover, US enables FNA and can be used in lymph node evaluation.

References

1. Som PM, Smoker WR, Reidenberg JS, Bergemann AD, Hudgins PA, Laitman J. Embryology and anatomy of the neck. In: Som PM, Curtin HD, eds. *Head and neck imaging*, 5th ed. St. Louis, MO: Mosby, 2011:2117-2163
2. Yoon HC, Kim NC, Lee DH. A cost-benefit analysis on neonatal screening of phenylketonuria and congenital hypothyroidism in Korea. *Korean J Pediatr* 2005;48:369-375
3. Donaldson M, Jones J. Optimising outcome in congenital hypothyroidism; current opinions on best practice in initial assessment and subsequent management. *J Clin Res Pediatr Endocrinol* 2013;5 Suppl 1:13-22
4. Lee J, Lee DH. Incidence and clinical findings of transient congenital hypothyroidism. 2014. Annual meeting of Korean Society of Pediatrics. abstract
5. Hong HS, Lee EH, Jeong SH, Park J, Lee H. Ultrasonography of various thyroid diseases in children and adolescents: a pictorial essay. *Korean J Radiol* 2015; 16: 419-429
6. Som PM, Smoker WR, Curtin HD, Reidenberg JS, Laitman J. Congenital lesions of the neck. In: Som PM, Curtin HD, eds. *Head and neck imaging*, 5th ed. St. Louis, MO: Mosby, 2011:2235-2285
7. Pearce EN, Farwell AP, Braverman LE. Current concepts. Thyroiditis. *N Engl J Med* 2003;348:2646-2655.
8. Hoang JK, Lee WK, Lee M, Johnson D, Farrell S. US features of thyroid malignancy: pearls and pitfalls. *Radiographics* 2007; 27:847-865
9. Francis GL, Waguespack SG, Bauer AJ, Angelos P, Benvenga S, Cerutti JM, et. al. Management guidelines for children with thyroid nodules and differentiated thyroid cancer. The American Thyroid Association Guidelines Task Force on Pediatric Thyroid Cancer. *Thyroid* 2015; 25:716-759
10. Avula S, Daneman A, Navarro OM, Moineddin R, Urbach S, Daneman D. Incidental thyroid abnormalities identified on neck US for non-thyroid disorders. *Pediatr Radiol* 2010;40:1774-1780
11. Shin JH, Baek JH, Chung J, Ha EJ, Kim J, Lee YH et al. Ultrasonography diagnosis and imaging-based management of thyroid nodules: revised Korean Society of Thyroid Radiology consensus statement and recommendations. *Korean J Radiol* 2016;17(3):370-395

Chairperson: Hee Jung Lee Keimyung University Dongsan Medical Center, Korea

Breast US in Children and Adolescents

Yun-Woo Chang

Department of Radiology, Soonchunhyang University Seoul Hospital, Korea

- > Breast imaging modality for pediatric patient
- > Normal breast development
- > Pitfalls of sonography
- > Pediatric Breast disease

Breast Imaging Modality

- Mammography
 - Detection of microcalcifications
 - Radiation
 - Decreased sensitivity in fibroglandular tissue
 - Rarely used in children
- Ultrasonography
 - Appropriate initial imaging modality in children
- CT
 - No role in workup of breast mass
 - Incidentally detected breast lesions
- MRI
 - Surgical planning
 - Lesions for multiple anatomical compartments

US evaluation

- Attention to patient comfort, especially school age girls and adolescents
- 15-17MHz linear transducer
- Landmark for posterior boundary of the breast: Pectoralis muscle

Pitfalls of US exam

- Rib
- Nipple

- Cooper's suspensory ligament

Normal breast development

1. First phase

- 5-6th weeks of fetal development
- Epidermal cells invaginate
- Form the primary mammary ridges
- Extending bilaterally from the axilla to the groin
- Peripheral milk lines involute
- Leaves at 4th intercostal space to develop into the breast

Normal breast development in Neonates

- Breast hypertrophy due to stimulation from maternal hormones
- Occurs in both males and females
- Sometimes associated with milky discharge
- Subareolar palpable nodules
- Resolves within 6-12 months of age

2. Second phase

- known as thelarche
 - Girls as the breast bud develops during puberty
 - Estrogen: ductal elongation and differentiation
 - Progesterone: terminal lobular development
 - Mean age of thelarche, 9.8 years
 - Premature, < 8 years
 - Delayed, >13 years

Premature thelarche

- 1) Isolated premature thelarche
 - Girl aged 1-3 years
 - Nonprogressive
 - Reassurance is all that
- 2) Part of precocious puberty
 - Other form of sexual maturation
 - Bone age, abdominal and pelvic USG

adolescence

- Imbalance of estrogen and testosterone; Enzyme of leptin
- Anabolic steroid, tricyclic antidepressants, cimetidine, etc
- Resolve within 2 years, reassurance
- Extreme or prepubertal: Sertoli-Leydig testicular tumor, adrenal tumor, liver disease, Klinefelter syndrome
- Pseudogynecomastia

Congenital and Developmental abnormalities**1. Accessory nipple (Polythelia)**

- 1-2% of population
- Clinically mistaken for a nevus

2. Accessory breast gland (Polymastia)

- Clinically mound
- Cyclic breast pain or masses

3. Hypoplasia or amastia

- Poland syndrome
- Iatrogenic from biopsy or excision of breast bud, radiation therapy

Difference of breast mass in children

- The majority of the breast masses are benign or normal breast gland
- Primary breast cancer is rare
- Most malignant masses are metastases from non-breast neoplasms
- Conservative approach of clinical and sonographic follow up
- Biopsy is thoughtfully recommended

Non-neoplastic lesions**1. Cyst**

- Near nipple, obstructed glands of Montgomery located at the edge of areolar

Gynecomastia

- Excessive development of male breast, normal

Sonographic characteristics of normal breast development

Breast stage	Clinical findings	US findings
Stage 1 (pre-thelarche)	TS 1: elevation of papilla only	Small focus of subareolar echogenic tissue Absence of the breast bud
Stage 2 (Breast bud stage)	TS 2: elevation of both breast and papilla, with a small mound and enlargement of areolar diameter.	Subareolar hypoechoic nodules appears (the breast bud), within echogenic adipose and loose connective breast tissue
Stage 3	Clinical palpable subareolar nodule TS 3: Further enlargement of breast and areolar without separation of their contours	Enlargement of the hypoechoic breast bud that: Overall maintains a rounded morphology Displays linear projections and a spider shape as ducts elongate
Stage 4	TS 4: projection of areolar and papilla to form a secondary mound above the level of the breast	Echogenic tissue fans out Hypoechoic breast bud becomes more widely elongated, losing the rounded appearance Subcutaneous fat may be present
Stage 5	TS 5: projection of papilla only, due to recession of areolar to the general contour of the breast	Loss of the hypoechoic breast bud Mature breast tissue composed of hypoechoic fat lobules intermixed with echogenic glandular and stromal tissue Superficial subcutaneous fat

TS Tanner stage

- Common, middle age women
- Unilocular, well-circumscribed, anechoic, posterior acoustic enhancement
→ NO treatment or follow up is necessary
If symptomatic, aspiration for short term relief

2. Duct ectasia

- Rare, unknown etiology
- Infancy and early childhood
- Maternal hormones
- Retroareolar dilated, anechoic tubular structures
→ Conservative with antibiotics, cessation of breast feeding

3. Mastitis and abscess

- Older pediatric group
- Staphylococci, streptococci species
- Warmth, erythema, tenderness, fluctuant mass
- Sonography guided needle aspiration for abscess
→ Oral antibiotics, aspiration, incision and drainage for large abscess
→ Follow up to ensure resolution

Benign solid masses

1. Fibroadenoma

- M/C, breast mass in adolescence
- Benign proliferation of fibroepithelial tissue, 10-15% multiple
- Round or oval, well circumscribed margin, hypoechoic, parallel orientation, no vascularity, posterior enhancement

Classification of fibroadenoma:

Histology and size

- 1) Conventional FA: M/C, usually 2-3 cm
- 2) Giant fibroadenoma
 - 5-10 cm
 - Cellular subtype
- 3) Juvenile fibroadenoma
 - Rare 7-8% of cases
 - Larger stromal component
 - Sonographic features are overlapped from other fibroadenoma or phyllodes tumor

Treatment of Fibroadenoma

Depending on size and symptom

- Asymptomatic, typical sonographic features, <5 cm
- Sonographic follow up at 6 months for 2 years
- Stability in size
- Symptomatic, large >5 cm, rapid growing masses
- Surgical excision

2. Juvenile papillomatosis

- Rare benign disease, older adolescents
- Fibrotic mass with small cysts & dilated ducts; Swiss cheese disease
- Family history of breast cancer (33-58%)
- Concurrent breast carcinoma (5-15%)
- Risk for breast cancer: bilateral, recurrent, family history of breast ca
→ Complete surgical excision Closely monitored

3. PASH (Pseudoangiomatous stromal hyperplasia)

- Rare benign disease, older adolescents
- Fibrotic mass with small cysts & dilated ducts; Swiss cheese disease
- Family history of breast cancer (33-58%)
- Concurrent breast carcinoma (5-15%)
- Risk for breast cancer: bilateral, recurrent, family history of breast ca
→ Imaging follow up

4. Phyllodes Tumor

- Rare type of fibroepithelial neoplasm
- Histologic categorize: Benign, intermediate or malignant
- Fluid-filled peripheral cyst or cleft: not pathognomonic
- Main differential consideration for fibroadenoma
- US guided core needle biopsy in advance of surgery
 - Intra-lesional cystic component
 - Rapid growing of mass
- Surgical excision
 - solid mass larger than 6 cm
- Prognosis is favorable

- 20% benign phyllodes tumors recur following complete excision

Malignant breast mass

1. Metastatic disease

- M/C, malignant pediatric breast mass
- Hematological malignancy or metastasis
 - lymphoma/ leukemia, rhabdomyosarcoma or neuroblastoma
- Multiple or bilateral masses
- Variable sonographic findings
- Leukemia and lymphoma: well-defined or ill-defined hypoechoic solid masses
- Any breast lesion in the presence of a known cancer should be considered suspicious
- Further evaluation with biopsy

2. Low grade malignant Phyllodes Tumor

- Malignant variety of phyllodes tumor is rare
- M/C primary breast malignancy in pediatric population
- Features of a low-grade spindle cell sarcoma
- 3% mortality rate
- Imaging findings of benign and malignant tumors overlap

3. Primary breast carcinoma

- 0.03 cases/ 100,000 younger than 20 years
- Radiation for Hodgkin disease, treated between 10-16 years
- Familial cancer syndrome such as BRCA1 and BRCA 2

Imaging management

- Atypical features
 - Non-circumscribed margin
 - complex solid and cystic components
 - posterior acoustic shadowing
- Clinical history
 - History of growth

- Prior chest radiation
- Known concurrent non-breast cancer
- Familial breast cancer
 - Core needle biopsy

Summary

- > The approach to pediatric breast mass differs from that in adults.
- > The most lesions are benign and management is conservative.
- > The role of the radiologist is to provide reassurance or require further evaluation.
- > Knowledge of the normal anatomy, common pitfalls and benign entities are needed.
- > US is the essential imaging and short term US follow-up is commonly required.
- > Any breast lesions of known cancer history should be considered biopsy.

References

1. Valeur NS, Rahbar H, Chapman T. Ultrasound of pediatric breast masses: what to do with lumps and bumps. *Pediatric radiology*. 2015;45(11):1584-99; quiz 1-3.
2. Chung EM, Cube R, Hall GJ, Gonzalez C, Stocker JT, Glassman LM. From the archives of the AFIP: breast masses in children and adolescents: radiologic-pathologic correlation. *Radiographics : a review publication of the Radiological Society of North America, Inc*. 2009;29(3):907-31.
3. Gutierrez JC, Housri N, Koniaris LG, Fischer AC, Sola JE. Malignant breast cancer in children: a review of 75 patients. *The Journal of surgical research*. 2008;147(2):182-8.
4. Kaneda HJ, Mack J, Kasales CJ, Schetter S. Pediatric and adolescent breast masses: a review of pathophysiology, imaging, diagnosis, and treatment. *AJR American journal of roentgenology*. 2013;200(2):W204-12.
5. Gao Y, Saksena MA, Brachtel EF, terMeulen DC, Rafferty EA. How to approach breast lesions in children and adolescents. *European journal of radiology*. 2015;84(7):1350-64.

Chairpersons: Min Hoan Moon SMG-SNU Boramae Medical Center, Korea
Young Taik Oh Severance Hospital, Korea

An Update on the Value of Elastography in the Diagnosis of Prostate Cancer

Trong Nguyen Quang

Department of Radiologist at Imaging, Franco-Vietnamese Hospital, Vietnam

ABSTRACT. Digital rectal examination combines with PSA are widely applied in the world. Systematic biopsy (beginning with 6 cores and modifying 12 cores) help to detect early prostate cancer. This update is concerned with a new modality in ultrasound help to improve the result of core biopsy beside the systematic biopsy. Many researches have been putted forward the role of tissue elastography ultrasound: An SE targeted core was 2.9 to 4.7 fold more likely to be cancer positive than a systemic core. So, the combination B-mode with Elastography and Power Doppler ultrasound with improve the rate of prostate cancer.

I. Introduction

New developments in diagnostic and treatment modalities that help improving prognosis of prostate cancer (PC), especially in European-American countries where the incidence is high.

Vietnam does not belong to the epidemiological area of PC with a low incidence comparing to other countries but this ratio is increasing due to the urbanization.

Many studies state that approximately 75% of PC was found in the peripheral zone (PZ) of the gland, 20% in the transitional zone (TZ) and 5% in the central zone (CZ).

The *American Society of Clinical Oncology* has recommended using the prostate specific antigen (PSA) combined with digital rectal examination (DRE) for early detection of PC and this method is widely applied in the world for high risk patients. This helped increase significantly the 5-year survival rate with early diagnosed cases of PC.

Digital rectal examination for detection of PC is based on the stiffness of the cancerous tissue. But PC is usually at late clinical stage when detected during DRE. Moreover, small tumors or tumors located far from the rectal wall will be missed in DRE.

PSA is a biological marker for prostate tissue but not specific for any pathology of the prostate. PSA increases in *not only* on PC *but also on* other benign diseases of the prostate (BPH, prostatitis or even after an invasive procedure in the prostate).

The normal threshold for PSA is 4 ng/ml.

- When the PSA level is 4 - 10 ng/ml, PC in about 30% cases [Bunting, P.S].
- When the PSA level is above 10 ng/ml, PC in 50% of cases [Gretzer MB].
- Besides, up to 15% of PC does not have PSA level above 4 ng/ml.

To increase the specificity of PSA level test, we can use PSA density (PSA density = PSA concentration/prostate volume), the elevation rate of PSA in year, the percentage of free PSA/total PSA (Djavan B) .

- The PSA density over 20%.
- The elevation rate of PSA over 0,75 ng/ml/year.
- The percentage of free PSA/total PSA below 20%.

High PSA level and/or the DRE is suspicious, transrectal ultrasound (TRUS) will be to do.

TRUS provides information about the anatomic structure of the prostate and surrounding structures such as seminal vesicles, bladder, rectum. Additionally TRUS can also provide the hemodynamic information of lesions by Doppler ultrasound or contrast-enhanced ultrasound. The typical US characteristics of prostate cancer is hypoechoic and hypervascular lesions and often located at the peripheral zone. But the sensitivity

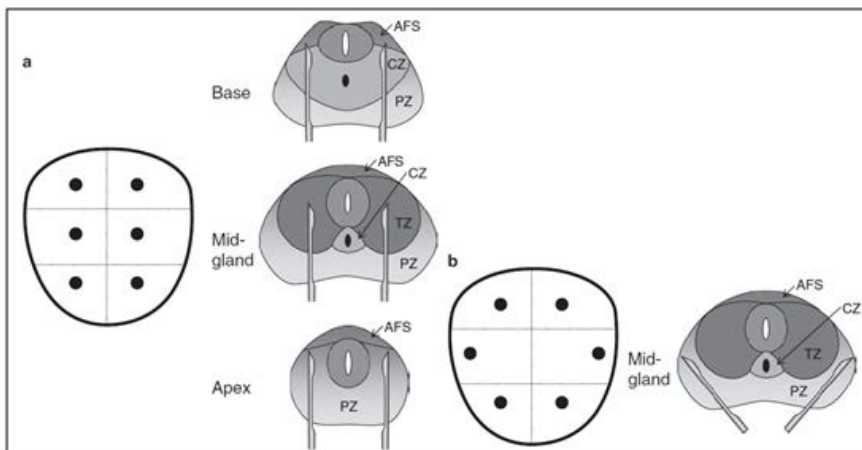


Fig. 1. (a) This is the original sextant biopsy as described by Hodge et al. b) These coronal and axial figures represent the modified sextant technique (2).

of ultrasound in detecting PC is low, about 50% [Halpern, Blake.].

II. Systematic biopsy

PC often is multifocal, and different Gleason grades may be present in different foci. The Gleason score is widely used to demonstrate the malignancy of PC and as guidance for treatment decision. The total score of Gleason is above 6, the tissue is classified as significantly malignant and referred to treatment.

Ultrasound is used as a tool to identify anatomic regions: base, middle and apex of the prostate in the 12 cores biopsy protocol modified from the sextant biopsy suggested by Hodge et al. The biopsy protocol with 6-12 cores is called systemic biopsy.

Although ultrasound guided systemic biopsy is widely used, it also presented disadvantages:

- The high rate of false negative that required repeat biopsy (about 25% of PC are missed in the 1st biopsy).
- Miss the PC located in the anterior area.

III. Targeted biopsy

To increase the detection rate of prostate cancer and also a guiding technique for targeted biopsy. These techniques include: Doppler US, contrast-enhanced US, multiparametric MRI and elastography US...

For PC detection, B-mode has sensitivity of 48%, specificity of 81% and accuracy of 64%, whereas strain elastography (SE) had a sensitivity of 66%, specificity of 78% and accuracy of 72%. (Ferrari et al.

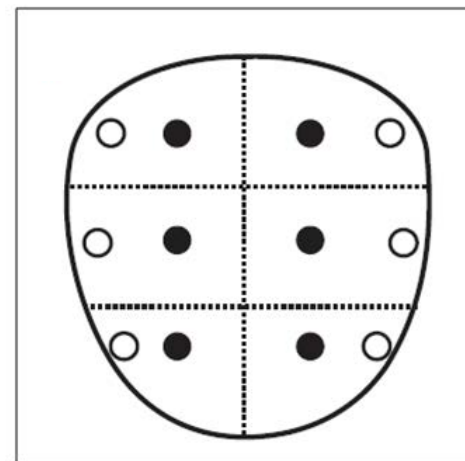


Fig. 2. These coronal representations show the ideal targets for 12 PZ biopsies: increases the cancer detection rate by 15% (2).

2009).

An SE targeted core was 2.9 to 4.7 fold more likely to be cancer positive than a systemic core (Aigner et al. 2010).

The rate of detection: Targeted biopsies from suspicious areas with either SE or power Doppler US was about 30% (29% or 31% respectively). If SE combines power Doppler US targeted biopsy cores (50%) was significantly higher than that of the systematic biopsy (SB) cores (15%) (1).

IV. Role of Strain Elastography

The main principles of Strain elastography (SE) is based on the fact that the stiffer the tissue is, the harder for it to be deformed and vice versa, the softer the tissue is, the easier for it to be deformed.

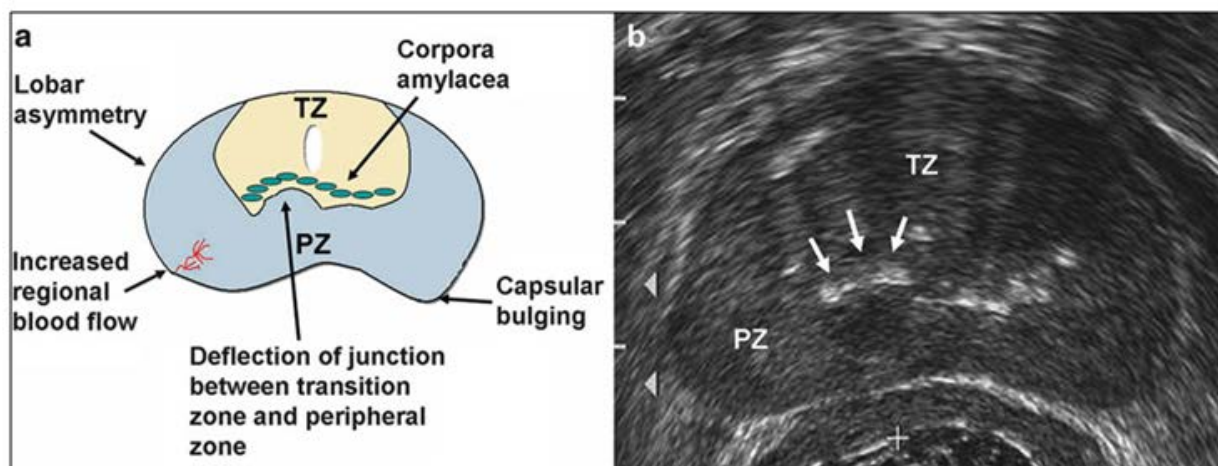


Fig. 3. TRUS findings suspicious for prostate cancer. (a) Lobar asymmetry, capsular bulging, increased blood flow, and deflection of the junction between the TZ and PZ can all be indicators of prostate cancer on TRUS. (b) Transverse image of the prostate demonstrating upward deflection of the junction between the TZ and PZ. The corpora amylacea (arrows) indicate this junction (3).

The strain imaging technique is performed by using the probe continuously compress and release on different sections of the prostate from the apex to the base.

- Focus zone should be placed in the far field of the ROI.
- The ROI should cover the entire prostate gland and the surrounding tissues, but avoid the bladder.

The normal peripheral zone (PZ) of the prostate is of intermediate stiffness, whereas the lateral and basal portions appear slightly stiffer. The elastographic pattern of the transition zone varies with the volume of the gland.

In young healthy patients, the stiffness of the prostate is usually homogeneous.

With advancing age and increasing volume, increasing stiffness is often observed, especially in the inner (transitional zone and central zone) gland. A pericapsular “soft rim artifact” is often seen, corresponding to the capsule of the prostate; its absence may indicate extracapsular extension (ECE) (Pallwein et al.).

The peripheral zone at any age always demonstrates soft tissue color code.

Kamoi's Classification (1)

- Score 1: Normal appearance (homogeneous strain, the entire gland is green).

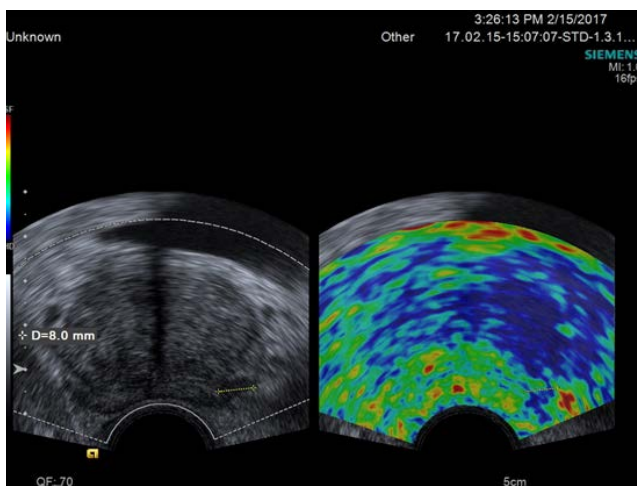
- Score 2: Probably normal (symmetric heterogeneous strain, the gland is a symmetric mosaic pattern of green and blue).
- Score 3: Indeterminate (no focal lesion suspected on 2D, but on elastography, the focal asymmetric lesion in blue [stiff]).
- Score 4: Probably carcinoma (the peripheral part of lesion in green and the central part of lesion in blue [stiff]).
- Score 5: Definitely carcinoma (the entire lesion with or without the surrounding area in blue [stiff]).

Kamoi et al. A **cut-off point is grade 3**, SE had 68% sensitivity, 81% specificity and 76% accuracy. SE was comparable to Doppler ultrasound (70% sensitivity, 75% specificity and 73% accuracy) and had significantly higher than B-mode ultrasound (68% vs. 50%).

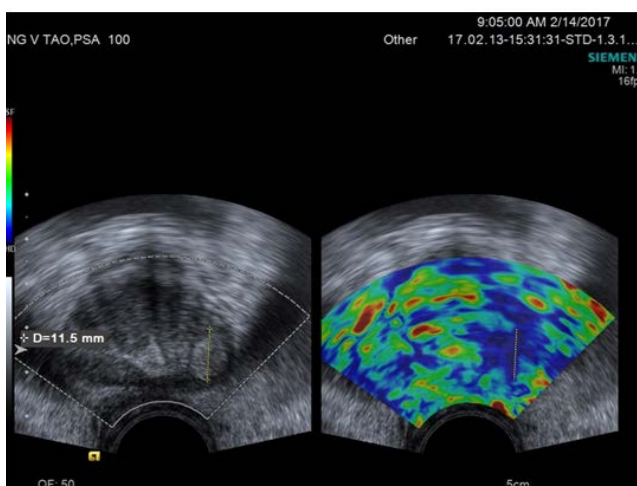
The combination of SE with power Doppler US further increased the sensitivity to 78%.

SE is a method that dependent operator. To reduce false-positive findings, we can calculate **strain ratio (Semi-quantification)**. Zhang et al. with the **cut-off point of 17.4** demonstrate that the strain ratio (SR) has a high value in the differential diagnosis of cancerous tissue and normal tissue with the sensitivity and specificity of 74.5% and 83.3% respectively.

Limitation for all Elastography techniques-that is, not all cancers are stiff, and all stiff lesions are not cancerous (calcifications, fibrosis, etc.) (Correas et al. 2013a, 2013b). Lack of uniform compression over the entire gland, intra- and inter-operator dependency (Correas et al. 2013a, 2013b). Penetration issues in large prostate glands leads to poor SE image quality. Limited value in the detection of small cancers and may miss carcinomas with a lower Gleason score.



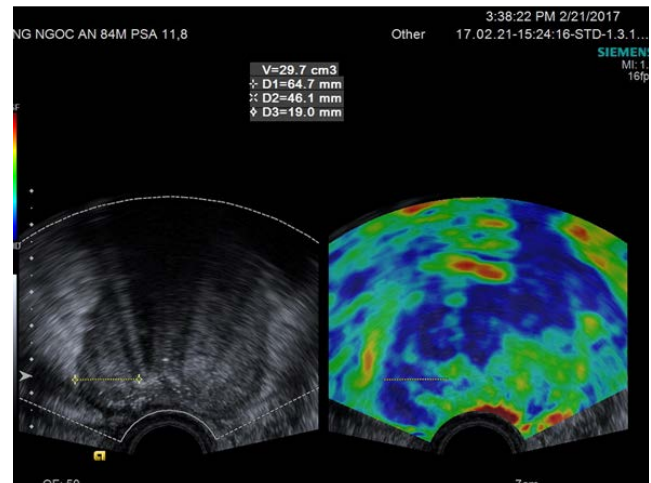
Vietnamese patient: hypoechoic nodule at the left peripheral zone.
Core biopsy: Adenocarcinoma.



Vietnamese patient: hyperechoic nodule at the left peripheral zone.
Core biopsy: Adenocarcinoma.

V. Role of Shear Wave Elastography

Shear wave elastography (SWE) does not require



Vietnamese patient: No lesion suspected on B mode ultrasound, Elastography shows a hard lesion at the right peripheral zone. Core biopsy: Adenocarcinoma.

compression/release of the probe. This technique is based on measurement of shear wave speed propagating through the tissues (Bercoff et al. 2004).

The shear wave speed can be displayed either in m/s or in kPa. The color-coded for each pixel and displayed as an overlay on the image in B-mode. All vendors color-code stiff tissues as red, whereas soft tissues are coded in blue (note: reverse with color-coded SE!).

Optimized setting: elasticity scale (70-90 kPa). The SWE box is enlarged to the maximum to cover as much of the gland as possible. For each plane, the transducer is maintained in a steady position for 3 to 4s until the signals stabilize. Hypo-echoic lesions coded stiff (red) are highly suspicious for malignancy.

The ROI should encompass only the area of the stiff lesion. The SI (stability index) of above 90% confirms satisfactory shear waves for analysis. The elasticity values (mean, standard deviation, min and max) are automatically calculated for each ROI. The ratio between the mean values of two ROIs placed in a suspicious region and in the adjacent normal peripheral zone (stiffness ratio) can also be calculated.

In young patients without prostatic disorders, the peripheral and central zones are coded in blue with a very homogeneous pattern (with stiffness value ranging from 15 to 25 kPa), whereas the transitional zone exhibits stiffness below 30 kPa.

Conversion of shear wave velocity to the Young modulus (kPa)	
kPa	m/s
180	7.7
150	7.1
125	6.5
100	5.8
90	5.5
80	5.2
70	4.8
60	4.5
50	4.1
40	3.7
30	3.2
25	2.9
20	2.6
15	2.2
10	1.8

Table 1. Table for conversion between kPa and m/s (4).

With the development of BPH, the peripheral zone remains soft with very homogeneous color encoding in blue (soft tissue), whereas the transition zone becomes heterogeneous and hard (red color), with a heterogeneous color pattern and elasticity values ranging from 30 to 180 kPa.

In the largest study (Correas et al. 2015), including 184 patients, sensitivity, specificity and positive and negative predictive values were 97%, 70%, 70% and 97%, respectively, for a **35-kPa cutoff for diagnosing PC** with Gleason scores ≥ 6 . This threshold is very similar to that reported by Barr et al. (2012) (37 kPa); however, it is lower than those found by others (Ahmad et al. 2013; Boehm et al. 2015a, 2015b; Woo et al. 2014) (70, 43 and 50 kPa, respectively) (1).

Limitation for all Elastography techniques-that is, not all cancers are stiff, and all stiff lesions are not cancerous (calcifications, fibrosis, etc.) (Correas et al. 2013a, 2013b). The shear wave pulse penetrates only 3 to 4 cm. In a large prostate, this may not be deep enough to measure the anterior zone. The transitional zone and central zone are more difficult to evaluate than the peripheral zone with SWE. Slow frame rate, small SWE box, image stabilization.

VI. Conclusion

Several studies access the value of both SE and SWE.

Studies of prostate cancer grading with stiffness values revealed a correlation between Gleason and stiffness values.

Prostate SE or SWE should be an additional US modality for routine prostate examination and biopsy procedures to improve cancer detection and identify additional lesions, resulting in an increase in the rate of diagnosis of prostate cancer.

Declaration of interest: The authors have no conflict of interest.

References

1. Richard Barr et al. WFUMB GUIDELINES AND RECOMMENDATIONS ON THE CLINICAL USE OF ULTRASOUND ELASTOGRAPHY: PART 5. PROSTATE. Ultrasound in Med. & Biol., Vol. 43, No. 1, pp. 27-48, 2017.
2. Osamu Ukimura et al. Contemporary Interventional Ultrasonography in Urology. Springer-Verlag London Limited 2009.
3. Pat F. Fulgham et al. Practical Urological Ultrasound. Springer Science+Business Media New York 2013.
4. Richard G. Barr. Breast Elastography. 2015 by Thieme Medical Publishers, Inc.
5. J.M. Correa et al. Ultrasound elastography of the prostate. State of art. Diagnostic and Interventional Imaging (2013) 94, 551-560.
6. Stijn W. T. P. J. Heijmink et al. State-of-the-art uroradiologic imaging in the diagnosis of prostate cancer. Acta Oncologica, 2011. 50:sup1, 25-38, DOI: 10.3109/0284186X.2010.578369.
7. Tomoaki Miyagawa et al. Real-time Elastography for the Diagnosis of Prostate Cancer: Evaluation of Elastographic Moving Images. Jpn J Clin Oncol 2009;39(6)394-398.
8. Călin R. Giurgiu et al. Real-time sonoelastography in the diagnosis of prostate cancer. Medical Ultrasonography 2011, Vol. 13, no. 1, 5-9.
9. Leo Pallwein et al. Ultrasound of prostate cancer: recent advances. Eur Radiol (2008) 18: 707-715.
10. J.M. Correas et al. Update on ultrasound elastography: Miscellanea. Prostate, testicle, musculo-skeletal. European Journal of Radiology 82 (2013) 1904-1912.
11. F.S. Ferrari et al. Real-time elastography in the diagnosis of prostate tumor. Journal of Ultrasound (2009) 12, 22-31.

12. G. Zacharopoulos et al. Real-time compression elastography of the peripheral zone prostatic cancer: the impact in improving the diagnostic approach. ECR 2012.
13. Ren Wang et al. Transrectal real-time elastography-guided transperineal prostate biopsy as an improved tool for prostate cancer diagnosis. *Int J Clin Exp Med* 2015;8(4):6522-6529.
14. State-of-the-art urologic imaging in the diagnosis of prostate cancer. *Acta oncologica* (Stockholm, Sweden) · June 2011
15. Jean-Michel Correas et al. Prostate Cancer: Diagnostic Performance of Real-time Shear-Wave Elastography. *Radiology*; Volume 275: Number 1-April 2015.
16. Markus Porsch et al. New aspects in shear-wave elastography of prostate cancer. *J Ultrason* 2015; 15: 5-14.
17. Sungmin Woo et al. Shear Wave Elastography for Detection of Prostate Cancer: A Preliminary Study. *Korean J Radiol* 2014;15(3):346-355.

Chairpersons: Min Hoan Moon *SMG-SNU Boramae Medical Center, Korea*
 Young Taik Oh *Severance Hospital, Korea*

MR US Fusion Imaging

Sung Il Hwang

Department of Radiology, Seoul National University Bundang Hospital, Korea

Prostate cancer is most common male cancer in US and 2nd cause of death. One in 6 men will be clinically diagnosed with prostate cancer. For the detection of prostate cancer, digital rectal exam, prostate specific antigen and transrectal ultrasound are used. Magnetic resonance imaging has been used as main imaging modality for the evaluation of the prostate for its superiority to other imaging modality in detection, localization and assessing disease extent of prostate. Recent advances in multiparametric MRI can help increase diagnostic accuracy of prostate cancer. In addition to the evaluation of prostate cancer, MR can show detailed information for planning prostatectomy and prediction of postoperative complication.

Although, prostate MR is known to be most accurate imaging method for the detection of prostate cancer, it is usually performed after confirmation of prostate cancer for the staging. Transrectal biopsy of prostate is usually guided by transrectal ultrasound. Because the sensitivity/specificity of prostate cancer by ultrasound is not so high, randomized systematic biopsy of prostate over twelve cores still remains gold standard method for the definite diagnosis. However, outnumbered core biopsy jeopardizes patients by increased complication rates. Moreover, systematic randomized biopsy yields misleading information. Tumor with high Gleason score which needs active treatment can be missed by sampling error, while patients with small clinically insignificant cancer undergo overtreatment including radical prostatectomy despite of its high probability of complications; thus, early detection of clinically significant cancer is essential for the proper treatment of prostate cancer patients. And

the concept of MR guidance rises to compensate low detection yield of ultrasound for prostate cancer. . Because of this superior detectability of cancer with highest Gleason score with MRI, MRI guided prostate biopsy is introduced. Although, it has great advantage of reducing the number of biopsy core, the increased procedure time and costs make the approach less practical.

MR-US fusion technique is regarded as a powerful alternative option for guidance of prostate biopsy. Reduction of time and cost of direct MRI guidance without sacrificing diagnostic accuracy can be achievable. Fusion of MR imaging with US can solve a few of these problems compared with in bore MR biopsy. Operator can perform biopsy with realtime guidance of both MR and US, target precisely and lesion with high suspicion. T2WI can offer high resolution images of prostate and periprostatic tissue. Tumors with high Gleason score have tendency of low ADC value in diffusion image. Therefore targeted biopsy of tumor with highest Gleason score can be achievable by fusion of ADC map and ultrasound image. It can be done within minutes at local clinic base under local anesthesia.

A few fusion devices have been developed. For tracking mechanism, external magnetic field generator or mechanical arm with encoders are frequently used. Using these fusion image techniques, the detection rate of prostate cancer is increased from 7% to 21% by Sonn et al. And 38% with Gleason score over 7 cancers detected only on targeted biopsy, which means that targeted biopsy can guide for highest grade or representative lesion. In our experience, cancer with Gleason 7 can be detected under fusion guidance in patients with

repeated prior biopsy negative history. From 2012 to 2016, 507 patients underwent fusion biopsy in our hospital. Among them, 211 (41.6%) patients were diagnosed as prostate cancer patients. Target biopsy can detect index lesion (highest GS lesion) in 81.3 % of the patients. Higher PIRADS score from MRI led to higher gleason score of cancer as well as increased cancer detection. Gleason 7 cancer localized in anterior fibromuscular zone, which area usually is not sampled during routine biopsy, can be also detected using fusion guidance.

There lies some technical limitations. Current

fusion method mainly uses rigid registration. However after insertion of probe into rectum, prostate is deformed elastically and nonrigid registration including warping technique will be more beneficial and can reduce registration errors.

In conclusion, MR/Ultrasound fusion technology may be routinely used for targeting of prostate cancer. It can help in the determination of treatment between active surveillance and definite treatment, and can offer another treatment option such as focal therapy

Chairpersons: **Min Hoan Moon** SMG-SNU Boramae Medical Center, Korea
Young Taik Oh Severance Hospital, Korea

Multiparametric US for Focal Testicular Lesions

Trong Nguyen Quang

Department of Radiologist at Imaging, Franco-Vietnamese Hospital, Vietnam

ABSTRACT. The aim of this review presents ultrasound techniques beyond B-mode ultrasound, including colour Doppler ultrasound, contrast-enhanced ultrasound (CEUS) and tissue elastography, in the characterisation of both benign and malignant focal testicular lesions. Testicular malignancies are usually appear an increase in colour Doppler signal, but neither speciality nor sensitivity. CEUS confirms lack of vascularity in benign lesions and Elastography allows evaluation of the tissue elasticity, the "hard" lesions are more likely to be malignant, and a "soft" area may suggest benignity. Combination the all ultrasound modalities with improve the differential diagnosis of focal testicular lesions.

I. Overview

Germ cell tumors account for 95% of testicular malignancies and can be divided into seminomatous and non-seminomatous germ cell tumors. The most common germ cell tumor is seminoma, which comprises up to 50% of all germ cell tumors. Non-germ cell tumours of the testis derive from the sex cords (Sertoli cells) and stroma (Leydig cells). They are usually benign but have malignant potential (90% of non-germ cell tumours are benign). Both Leydig cell and Sertoli cell tumors may be amenable to testis-sparing resection. Primary testicular lymphoma is the most common testicular malignancy in old men (> 60 yo). Metastasis to the testis is rare and usually occurs with advanced disease. The most common cancers to metastasize to the testis are melanoma, prostate, and lung (3). Almost tumours are focal lesions, but many focal lesions are benign

(epidermoid cyst, focal orchitis, hematoma...). How to differential diagnosis?

Radical orchidectomy is currently considered the standard treatment for testicular masses of malignant or unknown origin. But, many lesions may be benign at final histologic examination (unnecessary loss testicles). Testis-sparing surgery (TSS) has been proposed as an alternative treatment for small testicular lesion, in order to spare as much healthy parenchyma as possible (avoiding over treatment; preservation of endocrine and exocrine function; with no risk of local recurrence; and the further psychological and cosmetic benefits) (1).

Conventional US is sensitive for detecting focal testicular lesions but almost focal lesions are the same appearance (hypoechoic). Colour Doppler US (CDUS), contrast-enhanced US (CEUS) and elastography, have recently been proposed to increase diagnostic confidence and accuracy when characterising testicular lesions.

II. Role of multiparametric ultrasound

1. B-mode ultrasound

Seminoma: typically appear as a solid round homogeneous hypoechoic nodule without calcification inside.

Non-seminomatous germ cell tumours: tumours may be heterogeneous, with areas of increased echogenicity, calcification and cyst formation.

Non-germ cell tumours: usually small in size, and most are discovered incidentally, appear as well-circumscribed homogeneous hypoechoic lesions.

Lymphoma: focal or multifocal hypoechoic lesions.

Metastasis: usually multifocal hypoechoic lesions.

Focal benign lesions: homogenous or heterogenous hypoechoic.

Conventional US is highly sensitive for identifying small intra-testicular lesions (96.6%), topographic position, as well as assessing size and shape of lesions. However, the specificity for a specific tissue diagnosis is low (44%) because the technique cannot differentiate benign from malignant lesions.

2. Colour Doppler ultrasound

Seminoma: demonstrable vascularity within the lesion.

Non-seminomatous germ cell tumours: Increased vascularity may or may not be demonstrated, and therefore may be mistaken for a benign avascular abnormality.

Non-germ cell tumours: usually internal vascularity.

Lymphoma: internal vascularity.

Metastasis: no or few internal vascularity.

Focal benign lesions: usually no internal vascularity.

Testicular tumours are generally well vascularized, with the exception of any cystic component and regions of necrosis. With rare exceptions, any solid intratesticular lesion with an increase in colour Doppler flow should be considered suspicious for malignancy. The histologic findings of the tumour did not correlate with the vascularity of the lesion as seen at color Doppler US. There was a general correlation of tumor size and vascularity.

William G. Horstman et al (1991). Small tumours (< 1.5 cm) are hypovascular, large tumours are hypervascular (> 1.5 cm). Abdullah Hamdan et al (2014). Tumours > 1.8 cm were usually hypervascular, tumours < 1.8 cm were usually hypovascular.

The main limitation of Doppler technology: low sensitivity of detecting signals from small vessels and from low intravascular blood flow, less sensitivity with small nodule. Optimized technique for Color Doppler: low PRF (≤ 1000 Hz), use Power Doppler. Color Doppler US cannot differentiate benign from malignant lesions.

3. Contrast enhanced ultrasound

Seminoma: rapid enhancement in the nodule

(higher than the surrounding normal testicular parenchyma) and loss of the normal linear vascular pattern. Washout of the contrast within the lesion may be rapid, but with persistence of the abnormal “crossing” vessels within the lesion.

Non-seminomatous germ cell tumours: movement of individual microbubbles may be seen within the lesion in a chaotic pattern, which suggests that the abnormal vascularity favours a malignant diagnosis to the differential of a benign lesion.

Non-germ cell tumours: early enhancement on CEUS, which seems to persist longer than the normal testicular parenchymal enhancement.

Lymphoma: increased enhancement.

Metastasis: few internal vascularity with peripheral contrast enhancement.

Focal benign lesions: no contrast enhancement.

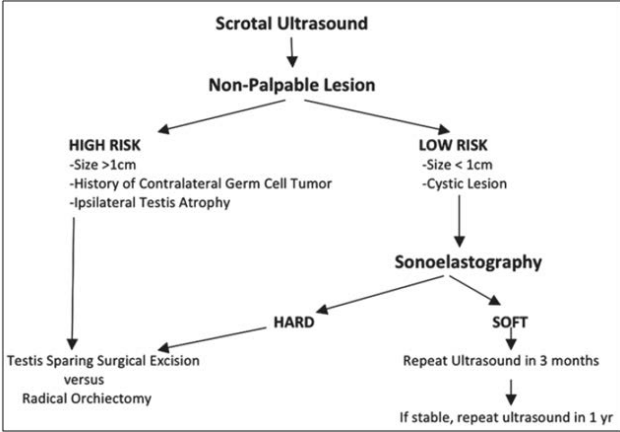
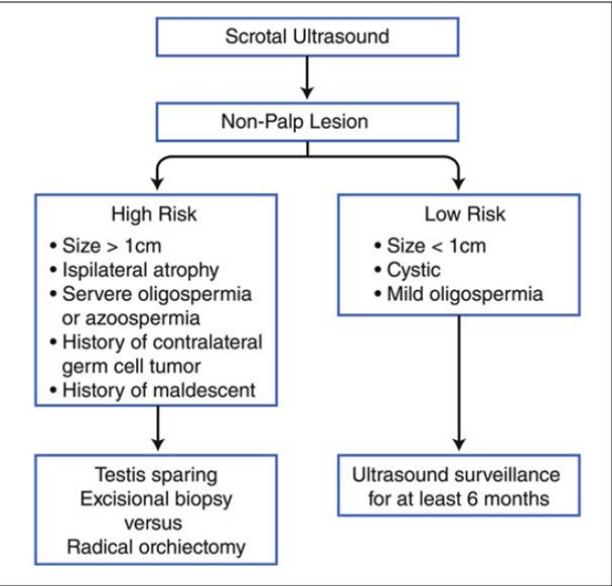
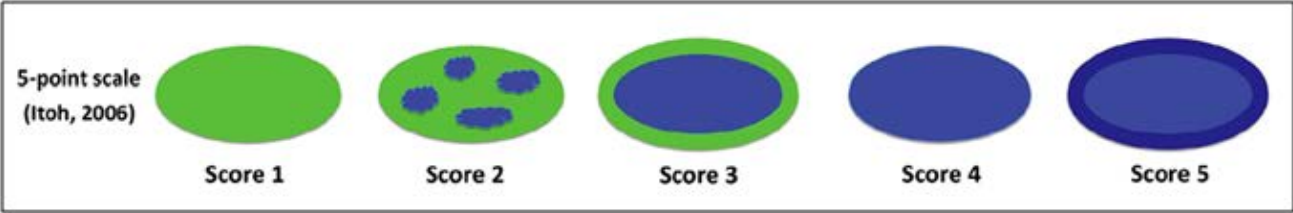
Guntram Lock et al (2011). Hyper-enhancement of a testicular lesion had a PPV of 97.4% (95% CI 84.9-99.9%) for neoplasia. It may be particularly valuable in the assessment of small intratesticular masses where color-coded ultrasound comes to its limits.

CEUS enables visualisation of the microcirculation to provide an improved assessment of tumour vascularity over CDUS; even intra- testicular lesions < 1 cm in diameter and those with low- volume blood flow can be characterized. CEUS allows a conclusive demonstration of an avascular abnormality, which is likely to be benign in nature and may resolve, would allow the option of “watch and wait” with ultrasound, without an unnecessary surgery (2). The presence of disordered vascularity on contrast-enhanced ultrasonography implies a malignant lesion, whereas absence of vascularity usually implies a benign lesion (15).

4. Elastography ultrasound

Base on 5-point scale of Itoh, 2006: Scores 1 and 2 are generally considered suggestive of benignity, score 3 as an indeterminate/ambiguous lesion, and score 4 and 5 suggestive of malignancy (7).

RTE measures the mechanical stiffness of tissue, which enables the improved differentiation between benign and malignant testicular lesions. Tissue compression and decompression generates strain within the tissue, enabling the identification of tissue elasticity. Incidentally found solid testicular



Incidentally found solid testicular masses that are not palpable, without role of elastography (3).

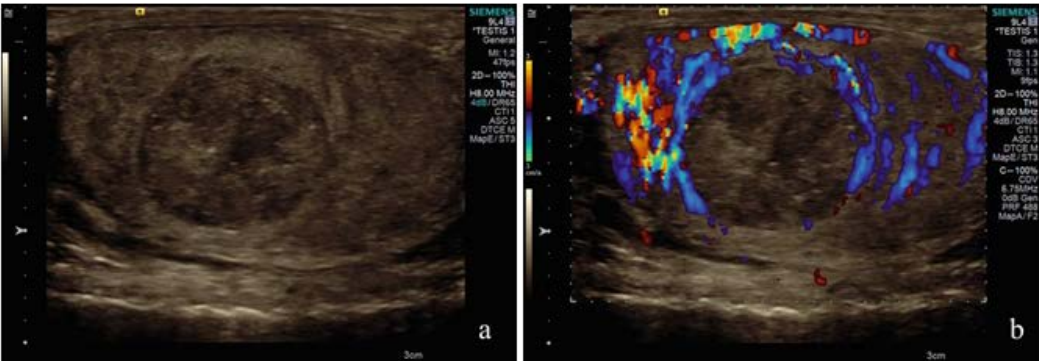
Incidentally found solid testicular masses that are not palpable, without role of elastography (5).

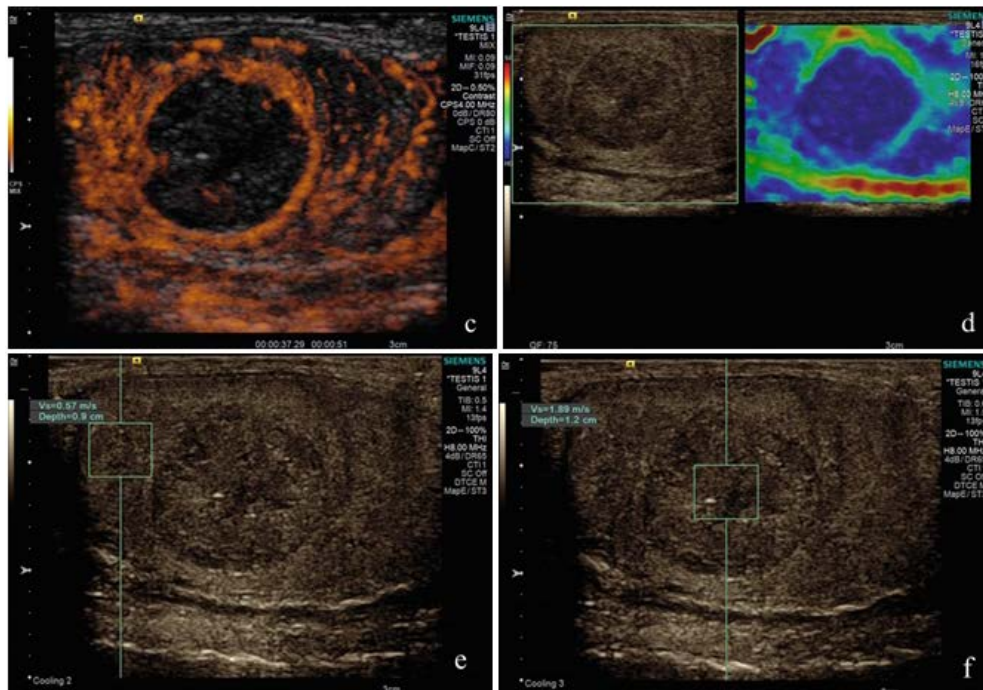
masses that are not palpable are usually benign. With sonoelastography, non-palpable lesions can be differentiated into “hard” or “soft”. The “hard” lesions are more likely to be malignant, and a “soft” area may suggest benignity as the density of cells and in malignancy than in normal tissue (2). Almost focal benign lesions are soft, except epidermoid cyst, but this lesion has a high sensitivity and high specificity to diagnosis with B-mode (pathognomonic appearance: “onion-skin” rims of calcification).

Friedrich Aigner et al (2012). RTE showed a sensitivity of 100%, a specificity of 81%, a NPV of 100%, a PPV of 92%, and an accuracy of 94% in the diagnosis of testicular tumors (12). Alfredo Goddi et al (2012). RTE gave 87.5% sensitivity, 98.2% specificity, 93.3% PPV, 96.4% NPV and 95.8% accuracy in differentiating malignant from benign lesions (13). D. Y. Huang et al (2014). RTE has a very high NPV of 96.4% so a negative finding justifies a more conservative management of these patients (2).

III. Demonstration

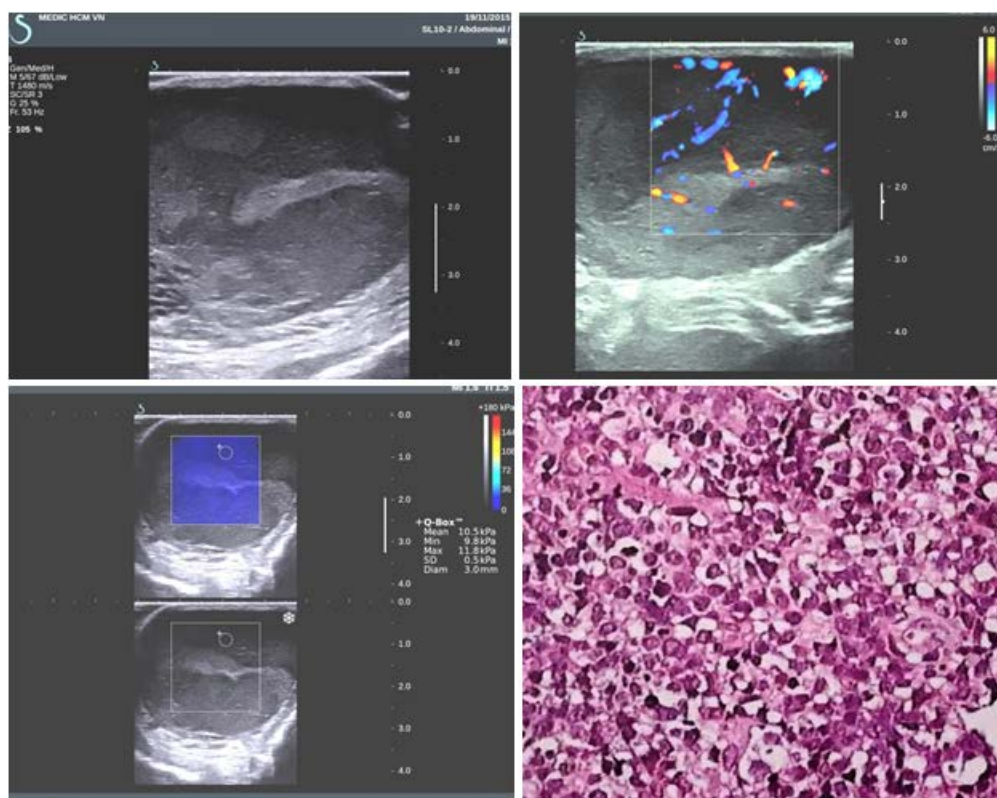
Cas 01: Seminoma (14).





Stable focal testicular lesion in 3 year with B mode (a) and Color Doppler (no internal vascularity)(b) suggesting an haemorrhagic cyst. But, CEUS (c) confirmed a marginal contrast uptake in the tumour, which is not consistent with a haemorrhagic cyst. RTE(d) shows hard lesion. In VTQ mode, the shear wave velocity was measured in the normal tissue with a velocity of $v = 0.57$ m/s (e). The shear wave velocity was measured in the tumour tissue with a velocity of $v = 1.89$ m/s (f). Result of biopsy is seminoma.

Cas 02:



VN male patient, 42 yo with past history of diffuse large B cell lymphoma in palatine. The patient presents a swelling of the left scrotum. The images shows diffuse hypo-heterogeneous mass on B mode, internal vascularity on color Doppler and soft on elastography. Anapathology shows diffuse large B cell lymphoma.

IV. Conclusion

The implementation of CEUS and RTE in the routine examination of the scrotal pathology can be very helpful in confirming the benign or malignant nature of the lesion. Lesional stiffness may confirm benignity or malignancy and CEUS serve as a powerful tool to confirm the presence or absence of internal vascularity where CDUS fails to give a definitive answer. Multiparametric US for Focal Testicular Lesions help us have a good choice for management:

- Follow up by US.
- or Testis-sparing surgery (TSS).
- or Radical orchidectomy.

Declaration of interest: The authors have no conflict of interest.

References

1. D.Y. Huang et al. Focal testicular lesions: colour Doppler ultrasound, contrast enhanced ultrasound and tissue elastography as adjuvants to the diagnosis. *The British Journal of Radiology*, 85 (2012), S41-S53.
2. D. Y. Huang et al. The Use of Colour Doppler Ultrasound, Contrast - Enhanced Ultrasound and Tissue Elastography as Adjuvants for Patient Selection for Testis Sparing Surgery for Focal Testicular Lesions. *ECR* 2014.
3. Bruce R. Gilbert et al. *Ultrasound of the Male Genitalia*. Springer Science+Business Media New York 2015.
4. Carolina Kachramanoglou et al. Multiparametric Sonography of Hematologic Malignancies of the Testis: Grayscale, Color Doppler, and Contrast-Enhanced Ultrasound and Strain Elastographic Appearances With Histologic Correlation. Volume 36, Issue 2 *J Ultrasound Med*. February 2017.
5. Pat F. Fulgham et al. *Practical Urological Ultrasound*. Springer Science+Business Media New York 2013.
6. Courtney Coursey Moreno et al. Testicular Tumors: What Radiologists Need to Know-Differential Diagnosis, Staging, and Management. *RadioGraphics* 2015; 35:400-415.
7. C. Pozza et al. Diagnostic value of qualitative and strain ratio elastography in the differential diagnosis of non-palpable testicular lesions. *Andrology*, 2016, 4, 1193-1203.
8. Gibran Yusuf et al. Multiparametric Sonography of Testicular Hematomas. *J Ultrasound Med* 2015; 34:1319-1328.
9. Eric M. Ghiraldi et al. Impalpable Testicular Seminoma Identified on Sonoelastography. *Journal of Medical Ultrasound* (2015) 23, 150e153.
10. Barbara Eibenberger et al. Multiparametric Ultrasonography of the acute scrotum. *D I E U R O P E* SEPTEMBER 2013
11. Ketul Patel et al. Features of Testicular Epidermoid Cysts on Contrast-Enhanced Sonography and Real-time Tissue Elastography. *J Ultrasound Med* 2012; 31:115-122.
12. Friedrich Aigner et al. Real-time Sonoelastography for the Evaluation of Testicular Lesions. *Radiology*: Volume 263: Number 2-May 2012.
13. Alfredo Goddi et al. Real-time tissue elastography for testicular lesion assessment. *Eur Radiol* (2012) 22:721-730.
14. Dirk-André Clevert et al. *Atlas of Elastasonography*. Springer International Publishing Switzerland 2017.
15. Ounali S. Jaffer et al. Contrast-Enhanced Ultrasonography of the Testes. *Ultrasound Clin* 8 (2013) 509-523.

CC 8 BR-1

Advanced Techniques and Interventions in Breast US

13:10-13:40

GBR 103

Chairpersons: Eun Suk Cha *Ewha Womans University Mokdong Hospital, Korea*
 Sun Mi Kim *Seoul National University Bundang Hospital, Korea*

Advanced Techniques in Breast Ultrasound

Ah Young Park

Department of Radiology, Bundang CHA Medical Center, Korea

Introduction

Color Doppler imaging (CDI) or power Doppler imaging (PDI) is a widely available technique to evaluate tumor vascularity indirectly. Doppler imaging can be adjunctive to B-mode US in differentiating between malignant and benign breast tumors by detecting malignant Doppler signs such as hypervascularity, central vascularity, penetrating or branching vessels. However, conventional Doppler imaging has a limitation in evaluating microvessels, and thus there is a significant overlap of Doppler features between benign and malignant tumors.

Recently, more sophisticated Doppler technique and US contrast agents are being developed to assess tumor vascularity more effectively. 'Superb Micro-vascular Imaging (SMI)' (equipped in Aplio™ 500 and later models, Toshiba Medical Systems Corporation, Japan) is an advanced Doppler technique to improve sensitivity to microvessels with high resolution and less motion artifact. And contrast-enhanced ultrasound (CEUS) with the 2nd generation contrast agents is another sensitive Doppler technique enabling to evaluate tumor microcirculation and perfusion. This lecture will introduce imaging principles and preceding researches about two vascular techniques and demonstrate clinical applications.

Superb Micro-Vascular Imaging (SMI)

♦ Imaging principles of SMI

The strong clutter signals overlap the low velocity flow components. SMI uses multi-dimensional filter

to separate flow signals from clutter, remove only the clutter and preserve low velocity flow signals.

♦ Clinical application of SMI for breast masses

SMI provides vascular imaging in two modes, 'color' and 'monochrome'. The color mode demonstrates gray-scale and color information simultaneously and the monochrome mode focuses only on the vasculature by subtracting the background information.

The quantitative analysis of tumor vascularity became possible recently using dedicated software ("VI test app" or built-in software) by calculating "Vascular index". Vascular index (%) indicates the ratio between the pixels for Doppler signal and those for the total lesion. Our early experiences in evaluation of 40 solid breast tumors showed that mean vascular index of malignancy was higher than that of benign tumors ($17.1 \pm 6.8\%$ vs. $7.6 \pm 8.1\%$, $P < 0.001$).

There are several tips for obtaining optimal SMI image as followed: Adjust color gain and ROI size to lower scale (< 1.5) to increase for sensitivity; change SMI frequency for better resolution or penetrating; make the patients hold their breath to reduce motion artifact; press the target lesion gently with the probe not to collapse microvessels.

♦ Investigations about the utility of SMI in breast tumor evaluation

Recent several investigators revealed the superiority of SMI in evaluating breast tumor vascularity and improving diagnostic performance of US, compared to CDI or PDI. Ma et al. reported that the degree of blood flow was significantly higher

on SMI compared to CDI and emphasized larger difference value of vessel numbers between SMI and CDI as a feature of malignancy. Yonfeng et al. reported that SMI detected more flow signals and improved the sensitivity of PDI (86% vs. 71%). Zhan et al. reported that SMI improved the diagnostic performance (AUC, from 0.914 to 0.947) by detecting more penetrating vessels of category 3 or 4 avascular masses. In a recent investigation with the enrollment of 191 breast masses in Korea University Ansan Hospital, SMI detected more number of vessels, branching or penetrating vessels, and both centrally and peripherally distributed vessels in comparison to CDI and PDI, and the diagnostic performance of gray-scale US plus SMI was higher than those of gray-scale US alone, and gray-scale and CDI or PDI (AUC, 0.815 vs. 0.774, 0.789, 0.791).

◆ Potentials and limits of SMI

SMI is superior in sensitivity to microvessels and thus allows us to evaluate vessel complexity and distribution in more details. Furthermore, the quantitative analysis of vascular index provides more objective information about the degree of vascularity. However, imaging acquisition can be operator-dependent and the certain amount of learning curve is needed to get good-quality image. Further large-scale investigation is needed to find out the optimal criteria in discriminating breast cancer from benign tumors.

Contrast-enhanced Ultrasound (CEUS) with the 2nd generation contrast agents

◆ Imaging principles of CEUS

Microbubble US contrast agent in the vasculature enhances the backscatter of US waves, results in a marked amplification of the flow signals and provides microvascular information. With the development of 2nd-generation US contrast agents and the advances of the contrast-specific mode with a low-mechanical index techniques (<0.3), hemodynamic evaluation is also available.

◆ Clinical application of CEUS for breast masses

With CEUS and the 2nd generation contrast

agents, both qualitative and quantitative analyses are available. Qualitative analysis indicates the evaluation of enhancement pattern of lesion, including enhancement degree, order, margin, internal homogeneity, penetrating vessel or perfusion defect. Quantitative analysis indicates time-intensity curve analysis.

In Korea University Ansan Hospital, CEUS was performed with Aplio 500 system and SonoVue contrast agent. The contrast agent was injected via a peripheral vein in a bolus fashion. CEUS examinations were performed in two steps: first, 3.6 mL injection of the contrast agent and continuous scanning for 2 minutes for subsequent time-intensity curve analysis; second, 1.2 mL injection for microflow imaging. For time-intensity curve analysis, the built-in software was used. When a ROI was placed selectively in the area of the strongest enhancement and the following quantitative parameters were automatically calculated: peak intensity, time to peak, mean transit time, slope, and area under the time-intensity curve.

◆ Investigations about the utility of CEUS in breast tumor evaluation

Many studies have investigated the utility of CEUS in discriminating breast cancer from benign tumors. In recent studies, malignancy tends to show heterogeneous enhancement, centripetal enhancement order, penetrating vessel and perfusion defect qualitatively and fast and strong enhancement quantitatively. And most of studies suggested that the additional use of CEUS on B-mode US improves diagnostic performance of B-mode US alone (sensitivity 64-100%, specificity 38-97%). In a recent investigation with the enrollment of 98 solid breast masses in Korea University Ansan Hospital, malignant masses showed more frequent hyperenhancement, centripetal enhancement, penetrating vessel, and perfusion defect, higher peak intensity, higher slope, and higher area under the time-intensity curve.

◆ Potentials and limits of CEUS

The diagnostic performance of CEUS has greatly improved due to the development of high-end US system and the introduction of the 2nd generation

US contrast agents. The development of dedicated software also allows us to more objective quantitative analysis for lesion vascularity. However, there are no standardized criteria for differentiating between malignant and benign tumors, because of the variety of imaging equipment, acquisition, and interpretation. In addition, intravenous contrast injection and time-consuming post-imaging analysis can be reasons why CEUS is not routinely used in clinical practice.

Comparison of SMI and CEUS in Breast Cancer Diagnosis

There has been just one study that compared the clinical utility of SMI and CEUS. Xiao et al. evaluated 132 breast tumors with SMI and CEUS, and assessed the microvascular architecture of breast lesions into five patterns. They concluded that the crab claw-like pattern was associated with breast cancer and the diagnostic performance of SMI was not different with CEUS when using this pattern as diagnostic criteria (sensitivity 77.6% vs. 89.6%, specificity 90.5% vs. 87.8%, accuracy 84.8% vs. 88.6%, AUC 0.865 vs. 0.791).

Recently, 98 suspicious solid breast masses were evaluated with SMI and CEUS in Korea University Ansan Hospital. Malignant SMI features were higher vascular index, complex vessel morphology, central vascularity, penetrating vessel on SMI and malignant CEUS features were higher peak intensity, slope, area, hyperenhancement, centripetal enhancement, penetrating vessel, perfusion defect. When using these malignant features as diagnostic criteria, the diagnostic performance of SMI was equivalent to that of CEUS (sensitivity 78.1% vs. 65.9%, specificity 75.4% vs. 86.0%, accuracy 76.5% vs. 77.6%, AUC 0.823 vs. 0.848).

Conclusion

SMI and CEUS can be used as adjunctive US techniques in evaluation of breast tumor vascularity. Wide application and further large-scale investigations are needed for standardization of image acquisition and interpretation of both US techniques.

References

1. Schroeder RJ, Bostanjoglo M, Rademaker J, Maeurer J, Felix R. Role of power Doppler techniques and ultrasound contrast enhancement in the differential diagnosis of focal breast lesions. *European radiology*. 2003;13(1):68-79.
2. Ma Y, Li G, Li J, Ren WD. The Diagnostic Value of Superb Microvascular Imaging (SMI) in Detecting Blood Flow Signals of Breast Lesions: A Preliminary Study Comparing SMI to Color Doppler Flow Imaging. *Medicine*. 2015;94(36):e1502.
3. Yongfeng Z, Ping Z, Wengang L, Yang S, Shuangming T. Application of a Novel Microvascular Imaging Technique in Breast Lesion Evaluation. *Ultrasound in medicine & biology*. 2016;42(9):2097-105.
4. Zhan J, Diao X-H, Jin J-M, Chen L, Chen Y. Superb Microvascular Imaging-A new vascular detecting ultrasonographic technique for avascular breast masses: A preliminary study. *European journal of radiology*. 2016;85(5):915-21.
5. Chung YE, Kim KW. Contrast-enhanced ultrasonography: advance and current status in abdominal imaging. *Ultrasonography*. 2015;34(1):3-18.
6. Drudi FM, Cantisani V, Gnechi M, Malpassini F, Di Leo N, de Felice C. Contrast-enhanced ultrasound examination of the breast: a literature review. *Ultraschall in der Medizin*. 2012;33(7):E1-7.
7. Du J, Wang L, Wan CF, et al. Differentiating benign from malignant solid breast lesions: combined utility of conventional ultrasound and contrast-enhanced ultrasound in comparison with magnetic resonance imaging. *European journal of radiology*. 2012;81(12):3890-9.
8. Zhao H, Xu R, Ouyang Q, Chen L, Dong B, Huihua Y. Contrast-enhanced ultrasound is helpful in the differentiation of malignant and benign breast lesions. *European journal of radiology*. 2010;73(2):288-93.
9. Wan C, Du J, Fang H, Li F, Wang L. Evaluation of breast lesions by contrast enhanced ultrasound: qualitative and quantitative analysis. *European journal of radiology*. 2012;81(4):e444-50.
10. Xiao X-y, Chen X, Guan X-f, Wu H, Qin W, Luo B-m. Superb microvascular imaging in diagnosis of breast lesions: a comparative study with contrast-enhanced ultrasonographic microvascular imaging. *The British Journal of Radiology*. 2016;89(1066):20160546.

CC 8 BR-2

Advanced Techniques and Interventions in Breast US

13:40-14:10

GBR 103

Chairpersons: **Eun Suk Cha** *Ewha Womans University Mokdong Hospital, Korea*
Sun Mi Kim *Seoul National University Bundang Hospital, Korea*

Intervention in Breast US

Eun Young Ko

Department of Radiology, Samsung Medical Center, Korea

Intervention in Breast US

Eun Young Ko, MD. PhD.
Department of Radiology,
Samsung Medical Center,
Sungkyunkwan University School of Medicine
Seoul, Korea.

Breast Interventional Procedures

Diagnostic
Therapeutic
Both diagnostic and therapeutic

- FNA (Fine Needle Aspiration)
- Gun Biopsy (true-cut needle)
- Vacuum-assisted biopsy
- Pre-surgical localization (wire localization, tattooing)

General Considerations

- Substituting procedures for surgery
 - Less or similar morbidity
 - Similar accuracy
 - Reduced cost
- Based on high-quality breast imaging

US-guided intervention

- Operator experience
- Patient comfort
- Efficiency
- Economy
- Sample accuracy (Real-time imaging)

FNA

- 21 – 25G fine needle
- Simple, safe
- Cytology
- Insufficient sample rate: 34%
- Overall accuracy: 77%
- False negative rate: 3.1-8%
- False positive (+)
- Highly dependent on the experience of radiologist & pathologist

FNA▪ **Indications****Cysts & cystic masses (C2 or cystic C3 lesions)**

- do not fulfill the US criteria for simple cysts
- Symptomatic
- Documentation of evacuation is desirable
- Avoid complications
- Suspected abscess or infected cysts

Gun Biopsy

- Most commonly used method for the biopsy of breast lesion
- Overall accuracy: around 97%
- False positive : almost 0%
- False negative : 0.9-2.9%
- Better lesion characteristics than FNA (ex. DCIS from invasive ca., specific benign diagnosis)
- Histologic underestimation (+)

Gun Biopsy**Indications**

- ✓ Category 3: probably benign finding
→ symptomatic C₃,
in the cases that we can not follow up,
high risk patient, etc.
- ✓ Category 4: suspicious abnormality
→ diagnosis
- ✓ Category 5: highly suggestive of malignancy
→ to confirm malignancy

- No. of sampling
→ 3 ~ 5 cores including center of the lesion (97~100%)
- Complications
→ hematoma, pseudo aneurysm, abscess, fistula

 BARD MEDICAL
Vacuum-assisted Biopsy

Vacuum-assisted breast biopsy (VAB) is an alternative technique for core needle biopsy.

It provides consistent quality tissue samples and subsequent reduced possibility of false negative results or histologic underestimate.

Vacuum-assisted Biopsy

- Vacuum-assisted handheld device
- Large volume of sample
- Single insertion, continuous sampling
- Removal of benign lesion

Size of Specimen



Vacuum-assisted Biopsy

Advantage

- Sampling error ↓
- Suction function (vacuum): decrease bleeding, lesion shifting due to dense tissue
- Re-biopsy rate ↓
- Histologic underestimation ↓
- Can be used as a tool for Removal of Benign mass

Vacuum-assisted Biopsy

Indications

- Biopsy for non-mass forming lesions or microcalcifications
- Biopsy for mass forming lesions: decrease underestimation (ex. small nodules)
- Re-biopsy after benign results of image-pathology discordant cases
- Removal of benign lesions

Limitation of VAB (removal)

Complete removal of the lesion on US

- removal of the evidence on images, not histological complete removal
- histologic residual lesion: 60%

(March DE, et al. Radiology 2003;227:549-55)

Residual or recurrent tumor

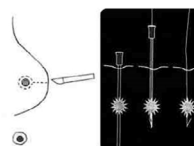
- 8 - 18.5% of all imaginary complete removal on F/U US after more than 6 months (SMC, etc.)

Management after US-guided biopsy

1. Image – pathology correlation
 - concordant malignant/ benign lesions
 - discordant malignant/ benign lesions
2. Re-biopsy for discordant benign results
3. Follow up for concordant benign results
4. High risk lesions

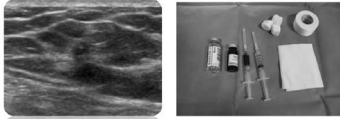
US-guided Localization

- US-guided wire localization



US-guided Localization

- US-guided tattooing localization



The aqueous suspension of carbon was injected through a percutaneous needle joined to a syringe. A trail of carbon was left in the breast parenchyma from the lesion out to the skin.

Charcoal is histologically inert and inexpensive. There is no risk of displacement, and it allows the most appropriate surgical route to be followed when excision of a residual lesion is necessary.

Complications

- Displacement
- Skin pigmentation
- Foreign body granuloma and fibrosis

CC 8 BR-3

Advanced Techniques and Interventions in Breast US

14:10-14:40

GBR 103

Chairpersons: Eun Suk Cha *Ewha Womans University Mokdong Hospital, Korea*
Sun Mi Kim *Seoul National University Bundang Hospital, Korea*

Image-Pathology Concordance/Discordance Evaluation after US Guided Intervention

Youngjean Park

Department of Radiology, Severance Hospital, Korea

Image-guided percutaneous breast biopsies have become more prevalent and have replaced excisional biopsy as the preferred diagnostic tool. As histologic diagnoses are made with less breast tissue, imaging-pathology correlation is crucial in ensuring that accurate sampling has been achieved and to guide appropriate clinical management. This

session reviews the need and how to determine imaging-pathology concordance after US-guided interventions, also by showing relevant cases. In addition, recent topics will be briefly reviewed, including management after benign concordant core needle biopsies and several high-risk lesions.

SS 1 HN**Head & Neck****08:30 - 10:00****GBR 101****Chairpersons:****So Lyung Jung** *The Catholic University of Korea, Seoul St. Mary's Hospital, Korea***Jeong Hyun Lee** *Asan Medical Center, Korea***SS 1 HN-1 08:30 - 08:40****Ultrasonographic Determination of the Location of Parotid Gland Tumor Relative to the Facial Nerve**Jeong Kyu Kim, Ho-Jin Son*Department of Otorhinolaryngology, Daegu Catholic University Medical Center, Korea*

PURPOSE: To assess the value of ultrasonography in the preoperative determination of the location of parotid gland tumors relative to the facial nerve.

MATERIALS AND METHODS: The medical records of 118 patients who underwent preoperative ultrasonography and parotidectomy were reviewed. Stensen's duct which can be identified as echogenic lines on the ultrasonography was used as the criterion to determine the location of parotid gland tumors. The ultrasonographic and operative findings were compared to assess the accuracy of the criterion.

RESULTS: Ultrasonography determined the tumor as superficial to facial nerve in 50 (42.4.0%) patients and as deep to facial nerve in 30 (25.4%) patients, could not determine the location in 38 (32.24%) patients. According to the operative records, the tumors were located superficial to facial nerve in 70 (59.3%) patients, deep to facial nerve in 28 (23.7%) patients, superficial and deep to facial nerve in 4 (3.4%) patients and inferior to the cervical branch of facial nerve in 16 (13.6%) patients. To calculate the accuracy of ultrasonographic criterion, 16 patients with tumor inferior to the cervical branch of facial nerve were excluded and the tumors located both superficial and deep to facial nerve were defined as located deep to facial nerve. The indeterminate tumors on ultrasonography were defined as located superficial to facial nerve. Finally,

the ultrasonographic criterion showed 89.2% of accuracy, 78.1% of sensitivity, 94.3% of specificity, 86.2% of positive predictive value, and 90.4% of negative predictive value.

CONCLUSION: Stensen's duct on ultrasonography can be a useful criterion to determine the location of parotid gland tumor relative to the facial nerve.

SS 1 THY**Thyroid****08:30 - 10:00****GBR 101****Chairpersons:****So Lyung Jung** *The Catholic University of Korea, Seoul St. Mary's Hospital, Korea***Jeong Hyun Lee** *Asan Medical Center, Korea***SS 1 THY-1 08:40 - 08:50****Comparison Between Benign & Malignant Mass**Kalpana Tayade*Department of Otorhinolaryngology, MCI, India*

PURPOSE: To compare and correlate between diagnostic accuracy of US Doppler in benign and malignant masses with FNAC. Thyroid scanning now a day is cheapest and safe modality. The characteristics appearance like echogenicity, margins, microcalcification, lobulations and lastly flow gives you clues for differentiation between benign and malignant masses. After evaluation in modalities now again it is very easy when scanned by and use of Ultrasound contrast. Partially cystic malignant thyroid nodules are eccentric, see for acute angle and flow is centripetal.

MATERIALS AND METHODS: We scanned 102 patients from January 2009 to December 2009. We performed Doppler study and then after FNAC. As the patients flow is less and different types cases are not coming we categories them into three 1) Malignant Mass 2) Benign Mass and 3) Mixed opinion.

RESULTS: In 102 patients we found 23 malignant, 54 benign and 25 mixed opinion.

CONCLUSION: Real time scanning with Doppler has got high accuracy and sensitivity in thyroid scanning.

In this study with kept only three categories as flow of patients in our region is less hence the diagnostic accuracy become little less. The aim of this study to compare the US findings and correlation between FNAC to differentiate benign and malignant masses.

SS 1 THY-2 08:50 - 09:00

The Implication of Doppler Ultrasonography in Thyroid Nodules Showing Intermediate Features on Gray-Scale US

Ilah Shin

Department of Radiology, Severance Hospital, Korea

PURPOSE: To evaluate the utility of Doppler ultrasonography (US) in characterizing thyroid nodules with indeterminate US pattern based on the 2015 ATA guidelines.

MATERIALS AND METHODS: This retrospective study included 418 nodules from 406 patients, which showed indeterminate US pattern based on the 2015 ATA guidelines. All nodules were cytopathologically confirmed as benign or malignant. Vascularity pattern on Doppler US was qualitatively categorized in one of none, perinodular, intranodular and both for each nodule. Age, sex, size of nodule, macrocalcification on US and Doppler US vascularity pattern were obtained for each nodule. Multivariable logistic regression analysis was done to identify variables that can predict the histopathologic characteristics (malignant or benign) of an indeterminate thyroid nodule.

RESULTS: Among the 418 indeterminate nodules, 360 nodules (86.1%) were confirmed as benign and 58 nodules (13.9%) were confirmed as malignant. Among age, sex, size of nodule, presence of macrocalcification and vascularity pattern, only the subgroup of intranodular vascularity pattern showed significant difference between malignant and benign group ($p=0.001$). Similarly, in univariable and multivariable logistic regression analysis, only the intranodular vascularity pattern on Doppler US showed significant correlation with the malignant group ($p=0.004$).

CONCLUSION: Indeterminate thyroid nodules showing intranodular vascularity pattern on Doppler US have a higher probability of being malignant.

SS 1 THY-3 09:00 - 09:10

Different Impact of Nodule Size on Malignancy Risk According to Ultrasonography Pattern of Thyroid Nodule

Min Ji Hong¹, Dong Gyu Na², Jung Hwan Baek³, Jin Yong Sung⁴, Ji-Hoon Kim⁵

¹Department of Radiology, Gachon University Gil Medical Center, Korea

²Department of Radiology, GangNeung Asan Hospital, Korea

³Department of Radiology, Asan Medical Center, Korea

⁴Department of Radiology, Daerim St. Marys Hospital, Korea

⁵Department of Radiology, Seoul National University Hospital, Korea

PURPOSE: The association of nodule size with malignancy risk is controversial in thyroid nodules. The objective was to determine the association of nodule size with malignancy risk according to ultrasonography (US) patterns of thyroid nodules.

MATERIALS AND METHODS: This study is a post hoc analysis using data from the Thyroid Imaging Reporting and Data System (TIRADS) multicenter retrospective study, in which a total of consecutive 2000 thyroid nodules (≥ 1 cm) with final diagnoses were included. The malignancy rate of nodules was assessed according to the nodule size and US patterns (Korean-TIRADS) by using the χ^2 or Fisher exact test.

RESULTS: In overall nodules, the malignancy rate did not increase as nodules enlarged. In high suspicion nodules, the malignancy rate has no relationship with nodule size ($p = 0.59$). In intermediate or low suspicion nodules, there was a trend of increasing malignancy risk as nodule size increases ($p = 0.004$, respectively). The malignancy rate of large nodules (≥ 3 cm) was higher than that of nodules (< 3 cm) in intermediate suspicion nodules (40.3% vs. 22.6%, $p = 0.001$) and in low suspicion nodules (11.3% vs. 7%, $p = 0.035$). There was a trend of decreasing proportion of papillary carcinoma and increasing proportion of follicular carcinoma among malignant tumors as nodule size increases ($p < 0.001$, respectively).

CONCLUSION: The impact of nodule size on the

malignancy risk was different according to US patterns. The nodule size should be considered for the estimation of malignancy risk in the intermediate or low suspicion nodules.

SS 1 THY-4 09:10 - 09:20

Role of Ultrasound in Predicting Tumor Invasiveness in Follicular Variant of Papillary Thyroid Carcinoma

Soo Yeon Hahn¹, Jung Hee Shin¹, Young Lyun Oh², Tae Hyuk Kim³

¹Department of Radiology, Samsung Medical Center, Korea

²Department of Pathology, Samsung Medical Center, Korea

³Department of Internal Medicine-Endocrine, Samsung Medical Center, Korea

PURPOSE: Noninvasive follicular thyroid neoplasm with papillary like nuclear features (NIFTP) was recently reported as a new type of follicular variant of papillary thyroid carcinoma (FVPTC). The purpose of this study was to assess the role of ultrasound (US) in predicting tumor invasiveness in FVPTC.

MATERIALS AND METHODS: From January 2014 to May 2016, preoperative US examinations were performed on 151 patients with 152 FVPTCs who underwent surgery. Based on a pathologic analysis, we categorized the FVPTCs into 3 groups (NIFTP, invasive encapsulated FVPTC [iE-FVPTC], or infiltrative FVPTC [I-FVPTC]). Each nodule was categorized based on the US pattern according to the Korean Thyroid Imaging Reporting and Data System (K-TIRADS) and the American Thyroid Association (ATA) guidelines. The correlation between tumor invasiveness and the K-TIRADS or ATA category was investigated using the Spearman

RESULTS: Among the 152 FVPTCs, there were 48 NIFTPs (31.6%), 60 iE-FVPTCs (39.5%), and 44 I-FVPTCs (28.9%). All US characteristics of the FVPTCs differed significantly according to tumor invasiveness (all p values ≤ 0.030). Tumor invasiveness showed a significant positive correlation with K-TIRADS ($r = 0.591$; $p < 0.001$) and ATA categories ($r = 0.532$; $p < 0.001$). According to both K-TIRADS and ATA guidelines, the most common

subtype was NIFTP in low suspicion nodules (52.6% and 51.6%), iE-FVPTC in intermediate suspicion nodules (52.7% and 54.2%), and I-FVPTC in high suspicion nodules (82.5% and 69.4%). After surgery, lymph node metastases were confirmed in 2 NIFTP cases (4.2%), 3 iE-FVPTC cases (5.0%), and 8 I-FVPTC cases (18.2%) ($p = 0.001$). The results of the BRAF mutation analysis were not significantly different among the groups ($p = 0.507$).

CONCLUSION: Increasing tumor invasiveness from NIFTP to iE-FVPTC to I-FVPTC is positively correlated with the level of suspicion on US using both K-TIRADS and ATA guidelines.

SS 1 THY-5 09:20 - 09:30

Thyroid Incidentalomas Detected on 18F-FDG PET/CT: Malignant Risk Stratification Using US Features According to the Guidelines

Saerom Chung, Young Jun Choi, Jeong Hyun Lee, Jung Hwan Baek

Department of Radiology, Asan Medical Center, Korea

PURPOSE: To stratify malignancy risk of thyroid incidentalomas detected by 18F-FDG PET/CT using US features according to guidelines for thyroid nodules and thereby suggest management plans.

MATERIALS AND METHODS: Between October 2008 and September 2015, a historical cohort of 96,942 consecutive patients underwent 18F-FDG PET/CT, among them 1,342 patients with 1,364 nodules underwent US evaluation for focal uptake in thyroid gland, and final diagnosis was made for 913 patients with 949 nodules. We retrospectively reviewed US images and stratified malignancy risk according to the previously published guidelines (American and Korean Thyroid Association) for thyroid nodules. Malignancy risk was calculated as the denominators ranged from the number of nodules that received US to the number of nodules that received a final diagnosis and the numerator was the number of final malignancies.

RESULTS: The overall malignancy risk of thyroid incidentalomas detected by 18F-FDG PET/CT ranged from 38.6% (527 of 1364) to 55.5% (527 of 949). The malignancy risk of thyroid incidentalomas with high

and intermediate suspicion had trends toward higher (87.8~93.9% and 29.2~51.8%, respectively) than that of guidelines. The malignancy risk of thyroid incidentalomas with low suspicion and very low suspicion or benign was within the range (4.4~10.3% and 0%, respectively) of that of guidelines.

CONCLUSION: US examination can be used to stratify malignancy risk of thyroid incidentalomas detected by 18F-FDG PET/CT. Thyroid incidentalomas with low suspicion and very low suspicion or benign did not increase risk of malignancy, therefore conservative diagnostic approach may be needed to thyroid incidentalomas with those categories.

SS 1 THY-6 09:30 - 09:40

Indeterminate Lymph Nodes in Thyroid Cancer Patients: Rate of Lymph Node Metastasis and US Findings Predictive of the Metastasis

Roh-Eul Yoo, Ji-Hoon Kim

Department of Radiology, Seoul National University Hospital, Korea

PURPOSE: To evaluate the rate of lymph node (LN) metastasis and US findings predictive of the metastasis for indeterminate LNs in thyroid cancer patients.

MATERIALS AND METHODS: A total of 361 LNs in 269 consecutive thyroid cancer patients, who underwent fine-needle aspiration (FNA) with washout thyroglobulin or core-needle biopsy (CNB) between December 2006 and June 2015, were included in this study. LNs were analyzed for: laterality with respect to index nodules, level, size and size ratio, fatty hilum, echogenicity, presence or absence of cystic change, calcifications, and vascular pattern. Unpaired t-test was used to compare the LN sizes and size ratios between metastatic and nonmetastatic LNs and diagnostic performance of the size and size ratios for predicting the metastasis was assessed. The incidences of eccentric fatty hilums, loss of fatty hilums, and laterality were compared between two groups with Fisher exact test.

RESULTS: Metastasis was found in 32% (26 of 81) of indeterminate LNs. LNs with no fatty hilums tended to have a higher rate of metastasis than those

with eccentric fatty hilums (36% vs. 9%, $P = .095$). The short-long diameter ratio was significantly higher in metastatic than in nonmetastatic LNs (0.59 ± 0.16 vs. 0.52 ± 0.14 , $P = .047$). Sensitivity and specificity for predicting the metastasis were 73% and 53%, respectively, using the cutoff ratio of 0.49. Eccentric fatty hilums and loss of fatty hilum were more common in nonmetastatic and metastatic LNs, respectively ($P = .095$). The incidence of ipsilaterality did not differ significantly between nonmetastatic and metastatic LNs ($P = .360$).

CONCLUSION: The rate of LN metastasis was not negligible in indeterminate LNs on US and tended to be higher in cases with no fatty hilums than in those with eccentric fatty hilums. The short-long diameter ratio and loss of fatty hilum were US findings that could help predict the LN metastasis.

SS 1 THY-7 09:40 - 09:50

Computer-Aided Diagnosis System for Thyroid Nodules on Ultrasound: Initial Experience

Young Jin Yoo, Eun Ju Ha, Yoon Joo Cho, Miran Han
Department of Radiology, Ajou University Hospital, Korea

PURPOSE: To prospectively evaluate the diagnostic performance of a computer-aided diagnosis (CAD) system for thyroid US in the differential diagnosis of thyroid nodules and to determine interobserver agreement between the CAD system and experienced radiologist.

MATERIALS AND METHODS: We consecutively enrolled patients with thyroid nodules with final diagnoses whether benign or malignant between June 2016 and July 2016. An experienced radiologist reviewed US characteristics of thyroid nodules, and a CAD system provided nodule diagnosis whether benign or malignant in a prospective design. We compared the diagnostic performance of experienced radiologist, CAD system, and CAD system assisted radiologist for detecting thyroid cancer and determined interobserver agreement between the CAD system and experienced radiologist.

RESULTS: A total of 117 thyroid nodules from 50 consecutive patients were included. The mean size of nodules was 1.5 ± 1.1 cm (range: 0.5-10.0 cm)

and final diagnoses were 67 (57.3%) benign nodules and 50 (42.7%) malignant nodules. The CAD system showed similar sensitivity and specificity compared with the experienced radiologist (sensitivity: 80.0% versus 87.0%, $P = 0.754$; specificity: 88.1% versus 95.5%, $P = 0.180$). The diagnostic accuracy was not significantly different between the CAD and experienced radiologist (84.6% versus 90.6%, $P = 0.646$). The CAD system assisted radiologist reached the higher diagnostic sensitivity when compared to the radiologist without the CAD system (91.8% versus 87.0%, $P = 0.031$). The interobserver agreement between radiologist and CAD system were substantial agreement for a final diagnosis ($\kappa = 0.661$).

CONCLUSION: The diagnostic performance of CAD system for differentiating thyroid nodule was as good as that of the experienced radiologist with a substantial agreement. The CAD system assisted radiologist could achieve the highest diagnostic sensitivity for thyroid cancer.

SS 1 THY-8 09:50 - 10:00

Growth Rate and Size of Large Thyroid Nodules of 2 cm or Larger: Be Useful to Differentiate Malignancy from Benignity?

Song Lee, So Lyung Jung, Jinhee Jang, Hyunsuk Choi, Kookjin Ahn, Bum-Soo Kim
Department of Radiology, The Catholic University of Korea, Seoul St. Mary's Hospital, Korea

PURPOSE: To clarify whether or not the growth rate and size are the useful measures for distinguishing malignancy from benignity in large thyroid nodules.

MATERIALS AND METHODS: From 2012 to 2015, fine needle aspiration (FNA) or core needle biopsy (CNB) was done for 1856 nodules with longest diameter over the 2 cm in our institute. Sensitivity, specificity, accuracy, positive predictive value, and negative predictive value of the FNA and CNB were evaluated in benign and malign tumor confirmed by surgical pathology. Among them, nodules with previous ultrasonography with at least 12 months of time interval and accurate 3 dimension measurement available were identified for calculation of growth rate of nodule. The rate of tumor growth was defined

as increase of the longest diameter and volume per follow up period.

RESULTS: From 2012 to 2015, fine needle aspiration (FNA) or core needle biopsy (CNB) was done for 1856 nodules with longest diameter over the 2 cm in our institute. Sensitivity, specificity, accuracy, positive predictive value, and negative predictive value of the FNA and CNB were evaluated in benign and malign tumor confirmed by surgical pathology. Among them, nodules with previous ultrasonography with at least 12 months of time interval and accurate 3 dimension measurement available were identified for calculation of growth rate of nodule. The rate of tumor growth was defined as increase of the longest diameter and volume per follow up period.

CONCLUSION: The growth rate and size of thyroid nodule may not be the useful measures for distinguishing malignancy from benignity in large thyroid nodules.

SC 1 THY

Thyroid

10:20 - 11:50

GBR 101

Chairpersons:

Eun-Kyung Kim Severance Hospital, Korea
Younghen Lee Korea University Ansan Hospital, Korea

SC 1 THY-2 10:40 - 10:50

Application of the 2015 ATA Guidelines on Thyroid Nodules with Atypia of Undetermined Significance / Follicular Lesion of Undetermined Significance (AUS/FLUS) Cytology

Ji Hye Lee, Kyunghwa Han, Eun-Kyung Kim, Hee Jung Moon, Jung Hyun Yoon, Youngjean Park, Jin Young Kwak
Department of Radiology, Severance Hospital, Korea

PURPOSE: The purpose of this study was to evaluate the predictive value of ultrasonography (US) patterns based on the 2015 American Thyroid Association (ATA) guidelines for malignancy in Atypia of Undetermined Significance or Follicular Lesion of Undetermined Significance (AUS/FLUS) nodules.

MATERIALS AND METHODS: From January 2014 to August 2015, 133 thyroid nodules measured ≥ 1 cm that were initially diagnosed as AUS/FLUS on US-guided fine needle aspiration (FNA) were included in this study. Each nodule was assigned a category with US patterns defined by the 2015 ATA guidelines. Clinical characteristics and US patterns were compared between the benign and malignant nodules using the chi-square test, Fisher's exact test, independent t test, or Mann-Whitney U test, and malignancy rates were calculated according to the 2015 ATA guidelines.

RESULTS: Of the 133 AUS/FLUS lesions, 94 (70.7%) were AUS, and 39 (29.3%) were FLUS. The malignancy rates in the very low suspicion group was 0.0 % in AUS/FLUS nodules. When applying the 2015 ATA guidelines, significant differences existed for US patterns between the benign and malignant nodules in the AUS group ($P = 0.032$), but not in the FLUS group ($P = 0.168$).

CONCLUSION: For nodules with AUS/FLUS cytology with the very low suspicion pattern by the 2015 ATA guidelines, follow-up US can be recommended instead of repeat FNA. US patterns defined by the 2015 ATA guidelines can provide risk stratifications for thyroid nodules with AUS cytology, but not for ones with FLUS cytology.

tested for the incremental ratios of the malignancy rates between applying and not applying each size criterion (2 cm or larger, 3 cm or larger, and 4 cm or larger, respectively) for each US pattern of the 2015 ATA guidelines.

RESULTS: Twenty-five (2.0%) of the 1,230 nodules were malignant. The malignancy rate was 4.5% in nodules 2 cm or larger with the intermediate suspicion pattern, 3.6% in nodules 3 cm or larger with the low suspicion pattern, and 3.4% in nodules 4 cm or larger with the very low suspicion pattern. Applying the size criteria of 2 cm or larger for nodules with the intermediate suspicion pattern, 2 cm or larger for nodules with the low suspicion pattern, and 3 cm or larger for nodules with the very low suspicion pattern significantly increased the malignant diagnosis rate (4.5% vs. 2.2%, $P < 0.001$, 2.8% vs. 1.6%, $P = 0.014$, and 2.7% vs. 1.2%, $P < 0.001$, respectively).

CONCLUSION: Malignancy rates differ according to nodule size and US pattern. Repeat FNA considering nodule size and US pattern may decrease the rate of false-negative diagnosis in nodules with initially benign cytologic results.

SC 1 THY-3 10:50 - 11:00

Validation of the 2015 American Thyroid Association Management Guidelines for Repeat Fine-Needle Aspiration Biopsy in Thyroid Nodules with Benign Cytology

Yeun-Yoon Kim, Kyunghwa Han, Eun-Kyung Kim, Hee Jung Moon, Jung Hyun Yoon, Youngjean Park, Jin Young Kwak

Department of Radiology, Severance Hospital, Korea

PURPOSE: To validate the 2015 American Thyroid Association (ATA) guidelines for repeat fine-needle aspiration (FNA) in cytologically benign thyroid nodules.

MATERIALS AND METHODS: This retrospective study included 1,208 patients with 1,230 cytologically benign nodules at initial FNA performed from June 2012 to December 2014. Statistical significance was

SC 1 THY-4 11:00 - 11:10**Diagnostic Performance of Ultrasound-Based Fine Needle Aspiration Biopsy Criteria for Thyroid Malignancy: A Comparative Study Based on Six International Society Guidelines**

Eun Ju Ha¹, Dong Gyu Na², Jung Hwan Baek³,
Jin Yong Sung⁴, Ji-Hoon Kim⁵

¹Department of Radiology, Ajou University Hospital, Korea

²Department of Radiology, Human Medical Imaging and Intervention Center, Korea

³Department of Radiology, Asan Medical Center, Korea

⁴Department of Radiology, Thyroid Center, Daerim St. Marys Hospital, Korea

⁵Department of Radiology, Seoul National University Hospital, Korea

PURPOSE: To investigate the diagnostic performances of ultrasound (US)-based fine needle aspiration (FNA) criteria for detecting thyroid cancer and to compare the unnecessary FNA rates based on the six international society guidelines (ATA, AACE/AME/ETA, FSE, KTA/ KSThR, NCCN, and SRU).

MATERIALS AND METHODS: From January 2010 to May 2011, a total of consecutive 2000 thyroid nodules (≥ 1 cm) with final diagnoses in 1802 patients were included in this study. US features of the thyroid nodules were retrospectively reviewed and classified according to the categories defined by the six international society guidelines. The diagnostic performance of US-based FNA criteria for detecting thyroid cancer and unnecessary FNA rates were calculated and compared by using the generalized estimating equation method.

RESULTS: Of the 2000 thyroid nodules, 1546 (78.3%) were benign and 454 (22.7%) were malignant. The KTA/KSThR (94.5%), NCCN (92.5%), and ATA (87.6%) guidelines showed the higher sensitivity than those of AACE/AME/ETA (80.4%), FSE (72.7%), and SRU guidelines (70.9%) ($p < 0.001$); while the latter guidelines showed the higher specificity than the former ones ($p < 0.001$). The unnecessary FNA rate was the lowest in FSE (29.1%) followed by AACE/AME/ETA (32.5%), SRU (45.2%), ATA (51.7%), NCCN (54.0%), and KTA/KSThR guidelines (56.9%).

CONCLUSION: Since the diagnostic performance of US-based FNA criteria are variable based on the international society guidelines, we have to be aware of its strength and weakness in the management of thyroid nodules.

SC 1 THY-5 11:10 - 11:20**Ultrasound Guided Core Needle Biopsy for Intermediate or Low Suspicion Thyroid Nodules: Which Method is Effective for Diagnosis?**

Soo Yeon Hahn, Jung Hee Shin

Department of Radiology, Samsung Medical Center, Korea

PURPOSE: To retrospectively compare the diagnostic performances between two different techniques of ultrasound (US) guided core needle biopsy (CNB) for intermediate or low suspicion thyroid nodules.

MATERIALS AND METHODS: One hundred and forty consecutive biopsies for the 140 intermediate or low suspicion thyroid nodules were randomly performed using two different biopsy techniques between August 2015 and December 2016. In the first technique, two specimens were targeted to include nodular tissue, nodular margin, and surrounding normal parenchyma (i.e., margin target). In the second technique, two specimens were obtained from two different target areas, one for margin target and another for intranodular target. Diagnostic performances of two different biopsy techniques to predict thyroid neoplasm and malignancy were compared.

RESULTS: During the study period, CNB was performed for 80 intermediate or low suspicion thyroid nodules (57.1%) with the first technique and 60 (42.9%) with the second technique. The accuracy of the first biopsy technique significantly higher than that of the second biopsy technique (100% vs. 93.3%, $P = 0.032$ for predicting thyroid neoplasm; 88.8% vs. 75.0%, 0.033 for predicting thyroid malignancy). The negative predictive value of the first biopsy technique for predicting thyroid malignancy was significantly higher than that of the second biopsy technique (87.5% vs. 72.2%, $P = 0.035$). The sensitivity, specificity, and positive predictive value were comparable between two different biopsy

techniques.

CONCLUSION: For intermediate or low suspicion thyroid nodules, US-guided core biopsy to obtain two specimens with marginal targets only is more effective in diagnosing thyroid neoplasm or malignancy than with marginal and intranodular target.

SC 1 THY-6 11:20 - 11:30

Web-Based Thyroid Imaging Reporting and Data System: Malignant Risk Calculated by a Combination of Ultrasonography Features and Biopsy Results

Young Jun Choi¹, Jung Hwan Baek¹, Jung Hee Shin², Jeong Hyun Lee¹

¹Department of Radiology, Asan Medical Center, Korea

²Department of Radiology, Samsung Medical Center, Korea

PURPOSE: Atypia of undetermined significance/follicular lesion of undetermined significance (AUS/FLUS) showed a variable risk of malignancy according to subcategorization and ultrasonography (US) features. This study aimed to construct a web-based predictive model using the combined information of US characteristics and subcategorized biopsy results for thyroid nodules of AUS/FLUS to stratify the risk of malignancy.

MATERIALS AND METHODS: Consecutive patients' data included 672 thyroid nodules from 656 patients from two university hospitals. We analyzed US images of thyroid nodules according to internal content, echogenicity of the solid portion, shape, margin, and calcifications and analyzed biopsy results according to nuclear atypia and architectural atypia. Multivariate logistic regression analysis was performed to predict whether nodules were diagnosed as malignant or benign.

RESULTS: US features, including solid composition, spiculated margin, ill-defined margin, marked hypoechogenicity, microcalcification, macrocalcification, and rim calcification, and biopsy results, including nuclear atypia, showed significant differences between groups. A 13-point risk scoring system was developed, and the risk of malignancy

ranged from 11.2% to 98.1%, which was positively associated with increases in risk scores. The areas under the receiver operating characteristic curve of the development and validation sets were 0.837 and 0.830, respectively. Our model is available online (http://www.gap.kr/thyroidnodule_b3.php).

CONCLUSION: We have devised a simple web-based predictive model using the combined information of US characteristics and biopsy results for thyroid nodules of AUS/FLUS to stratify the risk of malignancy.

SC 1 THY-7 11:30 - 11:40

Radiofrequency Ablation of Small Follicular Neoplasms: Initial Clinical Outcomes

Su Min Ha¹, Jin Yong Sung², Jung Hwan Baek³, Dong Gyu Na⁴, Ji-Hoon Kim⁵, Hyunju Yoo², Ducky Lee², Dong Whan Choi²

¹Department of Radiology, Chung-Ang University Hospital, Korea

²Department of Radiology, Daerim St. Mary's Hospital, Korea

³Department of Radiology, Asan Medical Center, Korea

⁴Department of Radiology, GangNeung Asan Hospital, Korea

⁵Department of Radiology, Seoul National University Hospital, Korea

PURPOSE: In thyroid gland, radiofrequency ablation (RFA) has been applied to both recurrent cancers and benign nodules, although, according to the American Thyroid Association (ATA) and the Korean Society of Thyroid Radiology (KSThR) guidelines, surgery is the first-line treatment for follicular neoplasm. However, it has been argued that follicular neoplasm with lower risk of malignancy can be managed by close follow-up. In this study, we evaluated the effectiveness of RFA of small follicular neoplasms, examining reductions in volume and related clinical problems, and making observations over long term follow-up.

MATERIALS AND METHODS: We evaluated 10 follicular neoplasms in 10 patients who were treated with RF ablation between 2009 and 2011. A RF generator and an 18-gauge internally cooled

electrode were used to perform complete ablation of the whole nodules. Changes in nodules or ablated zones on follow-up ultrasound, and complications during and after RF ablation, were evaluated.

RESULTS: The mean follow-up period was 66.4 ± 5.1 months (range, 60-76 months). In eight patients, single session of RF ablation was sufficient, while two patients required two sessions. There was a significant reduction in the mean volume ($99.5 \pm 1.0\%$) of lesions, with eight ablated zones (8/10, 80%) disappearing completely. No recurrences were found in any ablated zones at last follow-up. Transient mild neck pain ($n=6$) during the procedure subsided spontaneously within 1 day.

CONCLUSION: In addition to active surveillance, RF ablation may be an effective and safe alternative for management of patients with small (2 cm) follicular neoplasm suspected on thyroid biopsy and who strongly refuse surgery.

SC 1 THY-8 11:40 - 11:50

US-Guided Radiofrequency Ablation for Primary Thyroid Cancer: Efficacy and Safety of Long-Term Follow-Up in a Large Population

Hyun Kyung Lim¹, Seon Mi Baek², Jung Hwan Baek³

¹Department of Radiology, Soonchunhyang University Seoul Hospital, Korea

²Department of Radiology, Haeundae Sharing and Happiness Hospital, Korea

³Department of Radiology, Asan Medical Center, Korea

PURPOSE: To assess the long-term follow-up efficacy and safety of US-guided radiofrequency ablation (RFA) for primary thyroid cancer in a large population single center study.

MATERIALS AND METHODS: Between May 2008 and January 2017, we included the patients who underwent RFA for primary thyroid cancers in patients at high surgical risk (old age, severe comorbidity) and in patients who refuse to undergo surgery, with follow-up more than 6 month. RFA was performed using Cool-Tip RF system, modified straight-type internally cooled electrode and moving-shot technique.

RESULTS: Finally, 188 primary papillary thyroid

cancers of 151 patients were included. The mean follow-up duration was 40 ± 24 months. The number of RF session was one (167 cancers) or two (21 cancers). Mean maximum diameter of tumors was 4 ± 2.1 mm (range, 1 - 19 mm). 173 tumors (92.0%) were completely disappeared. There was no local tumor recurrence at treatment site. No distant or neck lymph nodes metastasis were detected during follow-up period. In four patients, new papillary thyroid carcinoma was detected during follow-up period, and complete disappeared after additional RFA. There was no procedure-related death or major complication. Minor complications such as minor bleeding (2), skin burn (1), transient hoarseness (1) and transient hypothyroidism (5) were reported.

CONCLUSION: This large population and long-term follow-up study demonstrated that RFA is effective and safe treatment for primary papillary thyroid cancer in patients at high surgical risk and in patients who refuse to undergo surgery.

SS 2 MSK

Musculoskeletal

10:20 - 11:10

GBR 102

Chairpersons:

Won-Hee Jee The Catholic University of Korea, Seoul St. Mary's Hospital, Korea

Ik Yang Hallym University Kangnam Sacred Heart Hospital, Korea

SS 2 MSK-1 10:20 - 10:30

Acoustic Radiation Force Impulse in Peripheral Lymph Nodes Assessment

Chau Tran, Quyen Vo, Hai Phan

Department of Radiology, Medic Medical Center, Vietnam

PURPOSE: The purpose of this study is to determine the role of acoustic radiation force impulse in evaluation of peripheral lymph nodes (PLNs) to select which indicated an excisional biopsy.

MATERIALS AND METHODS: This is a retrospective study. We applied virtual touch tissue quantification on Siemens Acuson S2000 with 4-9 MHz linear

probe by measuring solid part of 39 lymph nodes (LNs) (20 inflammatory LNs, 19 nodes that are necessary for biopsy including 8 tuberculosis and 11 malignancy) in 39 patients (mean age, 35.82, range 8-61). Medcalc statistical software was used to analyze and compare the ARFI values.

RESULTS: The mean ARFI value of inflammatory LNs was 1.84 ± 0.53 (m/s), of forced biopsy LNs was 2.85 ± 0.51 (m/s) ($P < 0.001$) including tuberculosis was 2.72 ± 0.39 and malignancy was 2.95 ± 0.59 . The ARFI cutoff level for forced biopsy LNs was estimated to be 2.44 m/s. With the use of a receiver operating characteristic curve with this cutoff value, the mean predicted necessary for biopsy with sensitivity of 89.5%, specificity of 95%, and an area under the curve of 0.903. With t-test, there was significant statistically difference between 2 groups of inflammatory LN nad forced biopsy LN ($P < 0.0001$), but no significant statistically difference between 2 groups of tuberculosis and malignancy.

CONCLUSION: This is an initial perspective of ARFI role in PLN assessment. These elastic velocities increase significant statistically in tuberculosis and malignancy. We suggest the cutoff value for selecting excisional biopsy LNs.

SS 2 MSK-2 10:30 - 10:40

Ultrasonographic Measurement of the Axillary Recess Thickness in Unilateral Shoulder Pain

Gi-Young Park, Dong Rak Kwon, Dae-Gil Kwon, Won-Bin Jung

Department of Rehabilitation Medicine, Daegu Catholic University Medical Center, Korea

PURPOSE: To evaluate the axillary recess thickness (ART) using ultrasound (US) in patients with frozen shoulder (FS) or other shoulder pain, and correlation between ART and clinical impairment in FS.

MATERIALS AND METHODS: We recruited 322 patients (119 male, 203 female, Age 57.0 ± 9.7) with unilateral shoulder pain. The stage of frozen shoulder was determined utilizing clinical criteria described by Hannafin. Patients were divided into three groups, pre-adhesive stage (group 1p, 77 patients), freezing or frozen stage (group 1f, 110 patients), and other shoulder pain (group 2, 135 patients). Clinical

parameters including visual analogue scale (VAS), Cyriax FS stage, and shoulderpassive range of motion (PROM), were assessed in group 1f. All patients were examined in upright sitting position with shoulder abduction at 90 degrees, and the ultrasound transducer was placed on the mid-axillary line. We calculated AR ratio (affected/unaffected ART).

RESULTS: ART in the affected shoulder was significantly greater than that in the unaffected shoulder in group 1 (4.4 ± 1.1 vs. 2.7 ± 0.6 mm, $p < .01$) and group 2 (3.0 ± 0.8 vs. 2.8 ± 0.6 mm, $p < .01$). There was significant difference in AR ratio among three groups (group 1p; 1.46 ± 0.34 , group 1f; 1.83 ± 0.42 , group 2; 1.08 ± 0.21 , $p < .01$) (Figs 1, 2). AR ratio in group 1f was negatively correlated with all PROM including forward flexion ($r = -0.343$), abduction ($r = -0.338$), external ($r = -0.390$), and internal rotation ($r = -0.221$), and positively correlated with VAS during motion ($r = 0.242$, $p < .01$) and not with Cyriax FS stage.

CONCLUSION: We highly recommend ultrasound measurement of ART and calculation of AR ratio for the diagnosis of unilateral FS. Additionally, AR ratio may be a useful value to discriminate the stage of FS.

SS 2 MSK-3 10:40 - 10:50

Sonoelastography in Evaluation of Various Benign Soft Tissue Lesions

Eunjin Hwang, Eun-Kyung Khil, Seun-Ah Lee, Jung-Ah Choi

Department of Radiology, Dongtan Sacred Heart Hospital, Korea

PURPOSE: To evaluate usefulness of sonoelastography for characterizing various benign soft tissue lesions.

MATERIALS AND METHODS: We evaluated conventional B-mode US and compression type sonoelastography (SE) for 31 soft tissue lesions of 31 patients, from January to October 2016. Both quantitative and qualitative grading were done for each examination using the color-code grading system and the tissue-elasticity ratio by semi-automatic range of interest (ROI) at least 3 times by one experienced radiologist. The color pattern was graded into three major patterns: blue-hard, green-soft and red-softer.

RESULTS: The range of tissue-elasticity ratio was from 0.35 to 6.13. There were 18 masses of blue, 1 green, 4 reds, 2 blue/green, 2 green/red and 3 blue/red. Fourteen lesions were assessed on US as epidermal inclusion cysts, six of which were pathologically confirmed. Twelve of epidermal inclusion cysts showed relatively lower tissue-elasticity (mean value: 1.66, from 0.35 to 6.13) and half of epidermal inclusion cysts showed blue color. We assessed 2 neurogenic tumors, 3 nodular fasciitis, 2 hemangioma, 2 fibromatosis coli of pediatrics, 2 benign fibrous histiocytoma, 1 lipoma and 1 lymph node. They all showed blue and the mean value of tissue-elasticity ratio was 3.39, ranging from 1.23 to 5.73. We assessed 2 ganglions, 1 abscess and 1 TGDC. They showed mostly red and the tissue-elasticity ratio was 0.89, ranging from 0.59 to 1.14.

CONCLUSION: The results of our study showed relatively good correlation between SE value, color grading and diagnosis on B-mode US. SE may be a useful diagnostic tool for characterization of benign soft tissue lesions.

SS 2 MSK-4 10:50 - 11:00

Feasibility of Shear Wave Ultrasound Elastography in Diagnosis of Superficial Benign Soft Tissue Tumor

Hyun Jung Yeoh, Tae-Yoon Kim, Jeong Ah Ryu
Department of Radiology, Hanyang University Guri Hospital, Korea

PURPOSE: To investigate the feasibility of shear wave ultrasound elastography in differentiation of superficial benign soft tissue masses by comparison of the elasticities of the each kind of the masses

MATERIALS AND METHODS: The institutional IRB permitted this study. We retrospectively analysed the 48 shear wave ultrasound elastographies of the 48 masses in the 44 patients from 2014 February to 2016 May. All of the 48 masses were confirmed by excision, biopsy, needle aspiration or MRI, respectively. Shear wave ultrasound elastography had performed by 16 year-experienced musculoskeletal radiologist with 5 year-experience of shear wave ultrasound elastography. One musculoskeletal radiologist and one radiology resident retrospectively

reviewed these 48 exams and analysed in consensus. The conventional ultrasonography findings and shear wave elasticities of the masses were investigated. The elasticities of each kind of masses were compared by Kruskal-Wallis test and the SPSS 20.0 was used.

RESULTS: There were statistically significant differences among the superficial soft tissue masses. We compared the elasticities of the epidermal cysts, ganglion cysts, lipomatous tumors, and miscellaneous lesions (38.7, 5.8, 9.2, 25.4 kPa respectively. Kruskal-Wallis test, $p=0.003$) Miscellaneous lesions included schwannoma, neurofibroma, vascular leiomyoma, granuloma, granulation tissue, panniculitis, arteriovenous malformation, cavernous hemangioma, thrombosed pseudoaneurysm, and lymph node. Epidermal inclusion cysts showed higher elasticity than ganglion cysts, and lipomatous tumors. The ganglion cysts showed similar elasticity to the lipomatous tumors.

CONCLUSION: There were significant differences among the epidermal cysts, ganglion cysts, and lipomatous tumors. Shear wave elastography may be helpful for the differentiation of these superficial benign soft tissue masses.

SS 2 MSK-5 11:00 - 11:10

Ultrasonographic Findings of Scleroderma Adultorum

Dong-Ho Ha¹, Sujin Kim²

¹Department of Radiology, Dong-A University Hospital, Korea

²Department of Pathology, Dong-A University Hospital, Korea

PURPOSE: Scleroderma (adultorum) Buschke is a rare connective tissue disease and characterized by the diffuse and non-pitting induration of the skin. Ultrasonographic (US) findings have been rarely published, as far as we know. The purpose of our study was to evaluate the US features of scleroderma.

MATERIALS AND METHODS: This study was approved by our IRB, and informed written consent was waived. We retrospectively reviewed 8 patients with scleroderma who performed US studies. Demographic data, including location of

lesion, period of symptoms, diabetes history, level of Hemoglobin (Hb) A1c, and etc. were reviewed. US images were assessed for the thickness of dermis, echogenicity, presence of multiple echogenic spots, posterior shadowing, and vascularity of the lesion.

RESULTS: In all patients, the thickening and erythematous discoloration of the skin were at the posterior neck. Six of the 8 patients had a history of diabetes. Two patients denied the diabetes history. However, all patients show the increased hemoglobin A1c level. The dermis was thickened in all cases. The mean dermal thickness on US was 7.0 ± 1.95 mm, similar to a previous study. US imaging revealed the increased echogenicity, multiple echogenic spots in the dermis, posterior shadowing at the lower dermis, and no vascularity.

CONCLUSION: When echogenic spots in the thickened, echogenic dermis and posterior shadowing of the lower dermis on US are observed at the posterior neck, scleredema should be considered in the differential diagnosis.

CR

Musculoskeletal

11:10 - 11:50

GBR 102

Chairperson:

Sun Joo Lee *Inje University Busan Paik Hospital, Korea*

CR-1

11:10 - 11:20

Musculoskeletal Case Based Reviews

Hee-Dong Chae

Department of Radiology, Seoul National University Hospital, Korea

Case 1

Of the accessory hypothenar muscles, the accessory abductor digiti minimi (ADM) muscle is the most common, with a prevalence of 24%. It originates from the antebrachial fascia, coursing anterior to the ulnar neurovascular structures in the Guyon's canal and inserting into the ADM or separately onto the ulnar aspect of the base of the proximal phalanx. At axial cross-sectional imaging, an accessory ADM is evident as a muscular structure anterior to the ulnar neurovascular bundle, on the radial aspect of the pisiform bone. We present a case of a 65-year-old-woman who presented with the tingling sensation in the hypothenar regions of both hands for three years. Ultrasonography of the left wrist showed an accessory muscle superficial to the ulnar neurovascular bundle. She underwent Guyon's canal release and accessory ADM was confirmed in the surgical field.

Case 2

Kimura's disease or eosinophilic hyperplastic lymphogranuloma is a chronic inflammatory disorder of unknown etiology that occurs predominantly in young Asian male patients. Kimura's disease is most commonly manifested as painless unilateral cervical lymphadenopathy or subcutaneous masses in the head and neck area, but other less common sites of involvement include the axilla, popliteal region, and upper extremity. Here, we report a 22-year-old man who presented with palpable masses of seven years in the bilateral elbows. Ultrasonography revealed irregular low echoic masses with prominent

vascularity at the medial side subcutaneous layer of both upper arms. Ultrasound-guided gun-biopsy showed changes consistent with Kimura's disease.

CR-2

11:20 - 11:30

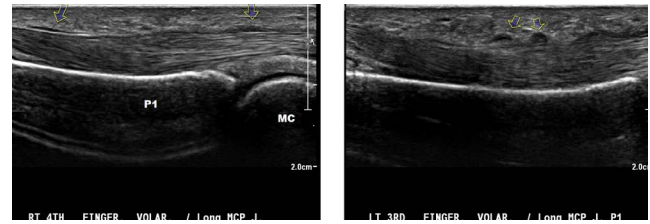
Hand Disease

Sekyoung Park

Department of Radiology, Kosin University Gospel Hospital, Korea

1. We present a case of calcific tendinitis of the extensor carpi ulnaris tendon in a 40-year-old woman.

2. 33-year-old woman presented with a synovial chondromatosis arising from the interphalangeal joint of the thumb.



Case 2. Venous malformation (hemangioma)

- Definition
 - Benign lesions closely resembling normal blood vessels, classified by predominant vessel type and location
- Most common tumor in infancy and childhood
- US findings
 - Complex ill-defined mass characterized by a mixture of hypoanechoic and hyperechoic (reactive fat overgrowth) components
 - Prominent vascular channels can be identified on gray-scale and Doppler imaging as well
 - One-to-one correlation between US and MR images shows good correspondence between intratumor hyperechoic areas and fat (high T1 signal), and hypoechoic components and blood-filled cavities (high T2 signal)
 - Phleboliths within the mass are present in approximately 50% of cases and are best identified on plain films

CR-3

11:30 - 11:40

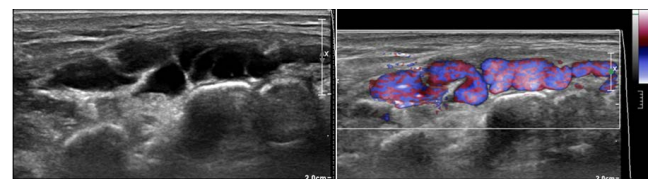
Trigger Finger (pulley thickening) / What You See is Not Everything; Venous Malformation

Esther Koh

Department of Radiology, Chonbuk National University Hospital, Korea

Case 1. Trigger finger

- Definition
 - Type of stenosing tenosynovitis
- Cause
 - Pulley thickening, RA, De Quervain's disease, gout, diabetes
- US findings
 - Diffuse hypoechoic thickening of the A1 pulley and abnormalities of the underlying flexor tendons
 - The affected tendons are typically swollen and, as a whole, they have a more rounded cross-section under the pulley than that observed in the contralateral or adjacent finger
 - During tendon gliding, passive movements of the surrounding soft tissues can be observed due to fibrosis and adhesions



CR-4 **11:40 - 11:50**
Elastography of Fat Necrosis / Sonography of Atypical Pulled Elbow

Yura Kim

Department of Radiology, Korea University Anam Hospital, Korea

Case 1

Atypical pulled elbow is a condition caused by the failure of manual reduction in radial head subluxation. Since it is clinically diagnosed and reductions are usually performed immediately, it is rare to have sonographic images of the pulled elbow. In our case, 5 years old male patient with atypical pulled elbow went through pre-operative MRI followed by sonography and serial follow up sonography after intra-operative reduction. The ultrasound images showed swollen supinator muscle and dynamic relation of the adjacent structures.

Case 2

Sonographic images of the fat necrosis vary and only a few literatures were describing the characteristic of the fat necrosis of the trunk or extremities. Sixty three years old male patient visited our hospital having palpable and painful soft tissue mass at right buttock area. Sonography was performed for the mass evaluation and ill-defined, heterogeneously hypoechoic mass was revealed. By the palpation, the mass was very hard in its texture and elastography was helpful in analyzing the hardness of the mass.

YIA Young Investigator Award Session

14:10 - 14:40

GBR 102

Chairperson:

Joon Koo Han Seoul National University Hospital, Korea

YIA-1 **14:10 - 14:20**

Difference in Applicability, and Reproducibility, and Elasticity Value Between Transient Elastography, Point Shear Wave Elastography, and Two-Dimensional Shear Wave Elastography: A Phantom Study

Sang Min Lee¹, Jeong Min Lee², Won Chang Chang³, Hyo-Jin Kang², Su Joa An², Jeong-Hoon Lee⁴

¹Department of Radiology, Hallym University Sacred Heart Hospital, Korea

²Department of Radiology, Seoul National University Hospital, Korea

³Department of Radiology, Seoul National University Bundang Hospital, Korea

⁴Department of Internal Medicine-G-I/Hepatology, Seoul National University Hospital, Korea

PURPOSE: To compare applicability, reproducibility, and elasticity values of transient elastography (TE), point shear wave elastography (pSWE), and two kinds of two dimensional (2D) SWE techniques using 15 different tissue-mimicking phantoms.

MATERIALS AND METHODS: In this *in vitro* study, we evaluated four different ultrasound shear wave elastography (USE) platforms using 15 different elastography phantoms. To evaluate influence of abdominal wall thickness on applicability and reproducibility of elasticity measurements, we created 15 phantoms by covering the five phantoms with pork belly subcutaneous fat and muscle in two different thickness. All measurements were performed by 3 observers. The applicability rate of the four USE platforms in the 15 phantoms were compared by Chi square. The absolute repeatability of each measurement was evaluated by coefficient of variation (CV). Intra-and interobserver reproducibility of the platforms were determined by intraclass correlation coefficient (ICC). The elasticity

values measured using the four techniques were compared via Kruskal-Wallis test test.

RESULTS: The applicability rates were significantly different among four USE platforms ($p < 0.001$). Supersonic SWE showed lower applicability rate (68.9%) compared with the other three platforms due to higher technical failure rates in phantoms with thick fake wall ($p < 0.01$). The CVs were significantly different according to platforms ($p < 0.001$) and fake abdominal wall thickness ($p < 0.001$). The four platforms showed good reproducibility with ICCs (0.97-0.99). There was a considerable difference in the mean elasticity values obtained by the four USE systems ($P = 0.001$). However, the values were not significantly different depending on fake abdominal wall in all platforms ($p = 0.622$).

CONCLUSION: Despite its excellent reproducibility, each platform showed significantly different applicability, repeatability, and elasticity measurements. Furthermore, the applicability and repeatability of USE might be affected by abdominal wall thickness.

YIA-2

14:20 - 14:30

Comparison of Diagnostic Performance Between 3 Modes of CAD System and an Expert Radiologist for Diagnosis of Breast Mass Detected with US

Seung Mi Ha, Boo-Kyung Han, Ji Soo Choi, Eun Young Ko, Eun Sook Ko

Department of Radiology, Samsung Medical Center, Korea

PURPOSE: The aim of this study was to compare the diagnostic performance of three different modes of ultrasound-computer aided diagnosis (US-CAD) system and an expert breast radiologist for differentiating between benign and malignant masses.

MATERIALS AND METHODS: US images of a total of 253 breast masses (173 benign, 80 malignant) in 226 consecutive women were prospectively obtained in 2 or 3 planes using 3-16 MHz linear probe. By the retrospective review of stored US images, the lesions were categorized as benign or malignant by one radiologist with 20-years experience in breast US and CAD system (S-Detect™) with three

different modes: accuracy (AC), sensitivity (SN), and specificity (SP) modes with blind to final pathology. Diagnostic performance was compared using the receiver operating characteristic (ROC) curve and sensitivity, specificity, accuracy, positive predictive value (PPV) and negative predictive value (NPV) were calculated.

RESULTS: The area under the ROC curves (AUC) of the expert radiologist, AC, SN and SP modes were 0.902, 0.902, 0.871 and 0.685, respectively. The AUC values of the expert and AC mode were similar each other ($P = 0.9975$) and the value of AC mode showed significantly higher than that of SP modes ($P < 0.0001$). Among the three CAD modes, the AC mode showed significantly higher accuracy (92.1%), specificity (95.4%), PPV (89.5%) than the SN modes ($P < 0.05$) and similar NPV (93.2%) to the SN mode ($P = 0.06$). The SP mode showed significantly lower values ($P = 0.001$) in sensitivity (38.8%), accuracy (79.4%), and NPV (77.6%) than the AC mode.

CONCLUSION: The AC mode of US-CAD system showed the best performance to differentiate between benign and malignant masses on breast US. The performance of US-CAD system is comparable to that of an expert radiologist.

YIA-3

14:30 - 14:40

Differentiation of Thyroid Malignant Lymph Node from Benign Lymph Node Using Artificial Intelligence

Jeonghoon Lee¹, Sueyoung Oh², Eunsol Lee³, Jung Hwan Baik⁴

¹Department of Computer Science and Information Engineering, Seoul National University, Korea

²Department of Computer Science and Information Engineering, Pohang University of Science and Technology, Korea

³Department of Radiology, Gapyeong-goon Public Health Care Center, Korea

⁴Department of Radiology, Asan Medical Center, Korea

PURPOSE: To differentiate and localize metastatic lymph nodes from thyroid cancer with normal lymph node on ultrasound.

MATERIALS AND METHODS: We enrolled 400

cases of metastatic lymph node from thyroid cancer and 400 cases of normal lymph node. We applied convolutional neural network to differentiate malignant lymph node from benign lymph node. In addition, we also used class activation map method to find location of lymph node from neck structure on ultrasound. We used 537 cases for training and 63 cases for test with 200 validation set. We evaluate diagnostic performance of classification and localization.

RESULTS: The heatmap image derived from the CAM well reflected the location of the lymph nodes. From the test set, accuracy, sensitivity and specificity are 96.8%, 93.94% and 100% respectively. From the validation set, accuracy, sensitivity and specificity are 83.0%, 79.5% and 87.5% respectively.

CONCLUSION: Detection and differentiation of malignant lymph node from benign lymph node are feasible using artificial intelligence.

SS 3 ABD

Abdomen

13:10 - 14:40

GBR 103

Chairpersons:

Seung Yon Baek *Ewha Women's University Hospital, Korea*

Joon-II Choi *The Catholic University of Korea, Seoul St. Mary's Hospital, Korea*

SS 3 ABD-1 13:10 - 13:20

Ultrasound Guided Percutaneous Microwave Ablation Liver Partition and Portal Vein Embolization for Planned Hepatectomy: A Promising Tool to Replace the First Step of ALPPS

Zeng Zeng, Xiaoming Fan

Department of Ultrasound, Zhejiang Provincial People's Hospital, China

PURPOSE: Our aim of the study was to retrospectively evaluate whether percutaneous microwave ablation (PMA) liver partition can replace the first step of associating liver partition with portal vein ligation for staged hepatectomy (ALPPS) or not.

MATERIALS AND METHODS: This study was approved by the ethical and scientific review board of Zhejiang Provincial People's Hospital. From January 2015 to December in 2016, we retrospectively reviewed 21 patients with multiple right liver tumors and their future liver remnant (FLR) were not enough for surgery. Ultrasound-guided PMA was performed by using PMCT cold circulation microwave treatment apparatus. Portal vein embolization (PVE) was performed 1 day after PMA. The response of the increase of FLR was evaluated by computed tomography 1 week after PVE. Procedure-related complications, perioperative morbidity and mortality, progression-free survival and overall survival rates were analyzed.

RESULTS: 21 patients with primary liver tumors were included in the study. Preoperative CT volumetry of the left lateral lobe showed 352.0 mL in median (range, 296.9-407.1 mL). After a median waiting period of 7 days (range, 4-21 days), the volume of the left lateral lobe had increased to 527.2 mL in median (range, 476.3-656.1 mL). Five patients (23.8%) had perioperative complications. No perioperative mortality was recorded. The median follow-up time was 21.5 months (range, 13.3-24.0 months). The 6-month and 12-month survival rates were 95.2% and 76.2%, respectively.

CONCLUSION: Compared with laparotomy associating liver partition, PMA obeys the operation rule of no touch in malignant tumors with less procedure-related complications, increases the overall survival rates and is a promising tool to replace laparotomy associating liver partition for planned hepatectomy.

SS 3 ABD-2 13:20 - 13:30

Manual Versus Full-Automatic Image Fusion of Real-Time Ultrasound and MR/CT Images for Radiofrequency Ablation of Hepatic Tumors: An Interim Report of a Randomized Prospective Trial

Moon Hyung Choi, Joon-II Choi, Young Jonn Lee, Jae Young Byun, Sung Eun Rha

Department of Radiology, The Catholic University of Korea, Seoul St. Mary's Hospital, Korea

PURPOSE: To compare the registration error,

time required for the image fusion and clinical outcomes of manual and full-automatic image fusion of ultrasound (US) and MR/CT images for radiofrequency ablation (RFA) of HCC and colorectal cancer liver metastasis (CRLM).

MATERIALS AND METHODS: 67 patients with HCC or CRLM were prospectively enrolled. Patients are randomly assigned to a) manual fusion group, or b) automatic fusion group. Two interventional radiologists performed RFA for HCCs or CRLM with manual or full-automatic image fusion of real-time US and MR/CT. Time for image registration (sec), number of point locks, registration error (mm) and technical success rate were compared between the manual group and the automatic group.

RESULTS: 32 HCCs and one CRLM were treated using the manual image fusion and 34 HCCs were treated using the automatic image fusion. Mean sizes of HCCs were 1.60 cm for the manual fusion and 1.63 cm for the automatic fusion ($p=0.903$). Averages of time for image registration, number of point locks and the registration error were 149 sec, 3.6 and 6.0 mm for the manual group, and 147 sec, 3.4 and 5.6 mm for the automatic group, respectively, and there were no significant difference. Technical success rate was 97.0% (32/33) for the manual group and 97.1% (33/34) for the automatic group and there was no significant difference between each other ($p=1.000$).

CONCLUSION: The technical performance of the full-automatic fusion technique is comparable to that of manual fusion technique.

SS 3 ABD-3 13:30 - 13:40

Liver Stiffness Evaluation by ARFI Imaging in Type 2 Diabetes Mellitus Patients

Anh Nguyen, Hung Nguyen, Hai Phan

Department of Radiology, Medic Medical Center, Vietnam

PURPOSE: Using ARFI SIEMENS S2000 for measuring liver stiffness to grade liver fibrosis regardless liver steatosis.

MATERIALS AND METHODS: *OPD diabetic patients > 18 yrs and euthyroid; No consumption beer / alcohol >20g/day HBV (-), HCV (-), drug induced hepatitis (-), autoimmune hepatitis (-),

Pregnancy (-), breast-feeding period (-).

*Descriptive cross-section statistics.

*Assess liver steatosis (semi-quantitative scale / B mode: S0, S1, S2, S3) and liver fibrosis (ARFI imaging: F0, F1, F2, F3, F4) (5 times/patient)

RESULTS: Nov 2016-Feb 2017. 80 type 2 DM patients 28-79y. Duration of acquired DM= first onset -20years. Significant fibrosis (F2-F3): 28.75% with or without steatosis. Severe fibrosis (F4): 15% with steatosis. 100% severe steatosis (S3) are significant /severe fibrosis. 5.0% significant fibrosis (F2-F3) without steatosis: long time DM (7-15 y) Liver steatosis diagnosed by ultrasound is very frequently found in type 2 DM patients (67/80 #83.75%), a significance of them having moderate/severe steatosis (S2, S3: 31/80 #38.75%).

A significant liver stiffness increase was found in more than 40% of DM patients and was not correspondence with steatosis severity. Fibrosis seemed to depend on acquired DM duration. But severe steatosis (S3) was concerned with significant /severe fibrosis. ARFI technique is a fast, useful valuable tool as comparable as transient elastography in diabetic liver stiffness assessment, but more convenient in cases of obese, ascites and narrow intercostal space.

*The best accuracy for ARFI in NAFLD patients occurred when distinguishing between patients with no or moderate fibrosis (F0 to F2) and those with severe fibrosis or cirrhosis (F3-F4).

CONCLUSION: A significant liver stiffness increase was found in more than 40% of DM patients. Liver stiffness assessment in type 2 diabetic patients should be performed systematically to identify those with significant liver fibrosis. ARFI technique is comparable with TE and more convenient in liver stiffness assessment.

SS 3 ABD-4 13:40 - 13:50**Additional Value of Contrast Enhanced Ultrasonography on Fusion Guided Percutaneous Biopsies of Focal Liver Lesions: Prospective Feasibility Study**

Hyo-Jin Kang¹, Jung Hoon Kim¹, Sang Min Lee²,
Hyun Kyung Yang¹, Joon Koo Han¹

¹Department of Radiology, Seoul National University Hospital, Korea

²Department of Radiology, Hallym University Sacred Heart Hospital, Korea

PURPOSE: To determine the incremental value of contrast enhanced ultrasonography (CEUS) on real-time fusion guided percutaneous biopsies of focal liver lesions.

MATERIALS AND METHODS: Forty patients with focal liver lesions identified CT or MRI were prospectively enrolled. For biopsy planning, real-time imaging fusion of CT or MR images with USG (hereafter USG-Fusion) was performed and subsequently real-time SonoVue contrast enhanced USG was fused with CT or MR images (hereafter CEUS-Fusion) in all patients. Necrotic degree of target lesion was assessed on CT or MR image and biopsy operator was evaluating lesion visibility, confidence level of technical success before procedure (4 point scale), and safety route accessibility on conventional USG (step 1), USG-Fusion (step 2), and CEUS-Fusion (step 3). Occurrence of change in biopsy target also assessed.

RESULTS: Among 40 target lesions in 40 patients, 9 (22.5%) lesions were invisible on Step 1 and 2. After applying the CEUS fusion, 7 of 8 (77.8 %) focal hepatic lesions were visualized. Confidence level of technical success before procedure is significantly increased on CEUS-Fusion compared Step 1 ($p=0.051$) or 2 ($p=0.02$) and presumed target lesion were changed in 16 of 40 (40%) patients after CEUS-Fusion. As the lesion is more necrotic, the presumed target lesions were more frequently changed after CEUS-Fusion (50%, 12 of 24 necrotic mass; 25.0%, 4 of 16 non-necrotic mass). Confirmative diagnostic results were reported in 39 patients (97.5%, 37 malignant and 3 benign). Accessibility of safety route to target lesion did not reach statistical differences.

CONCLUSION: Applying a new real-time CEUS

fusion with CT/MRI improved tumor visibility and viable portion assessment, and leading to higher operator confidence and diagnostic yield, comparing conventional USG and real-time CT/MRI fusion with USG.

SS 3 ABD-5 13:50 - 14:00**What I See on Ultrasound, I Treat it with Ultrasound: Feasibility and Efficacy of Ultrasound Guided Percutaneous Glue Embolization in the Management of Iatrogenic Bleed in Cirrhotics**

Sudheer Pargewar¹, Saloni Desai²,
Somsharan Betgeri³, S Rajesh⁴, Amar Mukund⁵

¹Department of Radiology, Gleneagles Global Hospitals, Mumbai, India

²Department of Radiology, SIR H.N. Reliance Foundation Hospital and Research Centre, Mumbai, India

³Department of Radiology, Caritas Hospital, Kottayam, Kerala, India

⁴Department of Radiology, Renai Medicity, Kochin, India

⁵Department of Radiology, Institute of Liver and Biliary Sciences (ILBS), New Delhi, India

PURPOSE: To evaluate the feasibility, safety and efficacy of ultrasound guided percutaneous glue (N-butyl-2-cyanoacrylate) embolization for the management of iatrogenic bleeding complications in cirrhotics.

MATERIALS AND METHODS: During a period of six years (January 2011- December 2016), retrospective evaluation of 29 haemodynamically unstable cirrhotic patients due to abdominal or thoracic wall bleeding following percutaneous interventions (Paracentesis/ Thoracocentesis) was performed. A meticulous Doppler ultrasound and/or CT angiography were used to localize the site of bleeding and patients were either taken up for percutaneous glue embolization (group-1) or endovascular closure of bleeding vessel (group-2). Complete cessation of the active bleeding and stabilization of hemodynamic factors with favorable patient outcome were considered as factors for technical success and clinical success respectively. In these groups, time from onset of bleed (percutaneous

procedure) to diagnosis, time from diagnosis to embolization, time for embolization procedure and their outcomes were analyzed.

RESULTS: Out of 29 patients, 18 patients (Group-1) were subjected to ultrasound guided percutaneous glue embolization and remaining 11 patients (Group-2) underwent endovascular trans-arterial embolization. Diagnosis to embolization mean time period and procedure time in group-1 were 5.3 and 7.3 minutes respectively while in group-2 were 35 and 39 minutes respectively (statistically significant, $p < 0.001$). Thirty-day survival was better in group-1 (67% versus 57%) with the odds of mortality in group-2 being 1.2 (95% CI, 0.55-2.48) times higher as compared to group-1, but it did not translate into a statistically significant value.

CONCLUSION: Our initial experience suggests that ultrasound guided percutaneous glue embolization is a quick and effective treatment for iatrogenic active bleed/pseudoaneurysm following paracentesis/thoracocentesis in cirrhotics with comparable results to endovascular therapy. Thus, a meticulously performed Doppler ultrasound not only helps in diagnosing an abdominal/ thoracic wall bleeder, but also guides in safe, quick and effective management with probable improved outcomes.

SS 3 ABD-6 14:00 - 14:10

A Deep Convolutional Neural Network for Prediction of METAVIR Score Using B-Mode Ultrasonography Images

Tae Wook Kang¹, Jung Hyun Lee¹, Dong Hyun Sinn², Sang Yun Ha³, Chung Hwan Choi⁴, Gun Woo Lee⁴, Jong Hyon Lee⁴

¹Department of Radiology, Samsung Medical Center, Korea

²Department of Internal Medicine-G-I/Hepatology, Samsung Medical Center, Korea

³Department of Pathology, Samsung Medical Center, Korea

⁴Department of Medical Imaging Group, Samsung Electronics, Korea

PURPOSE: Liver fibrosis is one of the important prognostic factors in patients with chronic liver disease. We developed a deep convolutional neural network (CNN) for prediction of METAVIR score using B-mode ultrasonography (US) images.

MATERIALS AND METHODS: The approval of the Institutional Review Board was obtained and the requirements for informed consent were waived. Among 7,273 patients with 140, 605 B-mode US images, who had a chronic liver disease and performed surgical resection or transient elastography, 2,798 patients with 5,517 B-mode US images were used for training a CNN. METAVIR score of surgical specimen as a reference standard was determined by specialized pathologists. In addition, estimated METAVIR score derived from transient elastography was used. Our training model was trained by S-detect for liver quantification which was based on the Visual Geometry Group-16 neural network with image appearance normalization technique. Two class (F0, F1, F2, F3 vs. F4) and four class (F0 vs. F1 vs. F2 vs. F3 vs. F4) models were developed. After the training, 675 patients' images were tested for the concordance of METAVIR score.

RESULTS: The trained algorithm for two class showed that sensitivity 81.6%, specificity 96.4%, and accuracy 88.3%. The four class algorithm showed that sensitivity 64.5%, specificity 89.0%, and accuracy 72.7%. The expected METAVIR score was displayed in the application within 2 seconds in average.

CONCLUSION: The proposed deep CNN-based METAVIR score prediction system revealed remarkable diagnostic accuracy using B-mode US images. Along with this technique, it will assist radiologist to identify METAVIR score easily so that reduce time and labor costs, while resulting objective diagnosis.

SS 3 ABD-7 14:10 - 14:20

Prospective Comparison of Two Point Shear Wave Elastographic Techniques by Acoustic Radiation Force Impulse Quantification for Assessing Liver Stiffness in Patients with Chronic Liver Disease

Su Joa Ahn, Jeong Min Lee, Won Chang, Sang Min Lee, Hyo-Jin Kang, Hyun Kyung Yang, Jeong Hee Yoon, Sae Jin Park, Joon Koo Han
Department of Radiology, Seoul National University Hospital, Korea

PURPOSE: To assess reproducibility of a new point shear-wave elastography method (pSWE, S-shear wave) and compare accuracy in assessing liver stiffness (LS) with another pSWE technique (ARFI).

MATERIALS AND METHODS: Thirty-three patients were enrolled in this prospective study. LS values were measured by ARFI and S-shear wave in the same session, followed by two S-shear wave sessions for inter- and intra-observer variation. The technical success rate and reliable measurements of both the pSWE techniques were compared. The intra-, inter-observer reproducibility were determined by intra-class correlation coefficient (ICCs). LS values were measured with both methods of pSWE, and the diagnostic performance in severe fibrosis ($F \geq 3$) and cirrhosis ($F = 4$) was evaluated using ROC curve analysis and the Obuchowski measure, with the LS values of transient elastography (TE) as a reference standard.

RESULTS: ARFI (100%, 33/33) and S-shear wave (96.9%, 32/33) showed neither significant difference in technical success rate ($p = 0.63$) nor reliable LS measurements (96.9%, 32/33; 93.9%, 30/32, respectively, $p = 0.61$). The inter- and intra-observer agreement for LS measurements using the S-shear wave technique was excellent (ICC = 0.98 and 0.99,

respectively). The LS values of both pSWE techniques were not significantly different and showed good correlation ($r = 0.78$). For detecting $F \geq 3$ and $F = 4$, both ARFI elastography and S-shear wave showed comparable diagnostic accuracy: AUROC = 0.87 (95% CI 0.70-0.96), 0.89 for ARFI (95% CI 0.74-0.97); and AUROC = 0.84 (95% CI 0.67-0.94), 0.94 (95% CI 0.80-0.99) for S-shear wave, respectively ($p > 0.48$). Obuchowski measures were similarly high for S-shear wave and ARFI (0.94 vs. 0.95).

CONCLUSION: S-shear wave showed excellent inter-and intra-observer agreement and comparable diagnostic performance to ARFI for detecting hepatic fibrosis.

SS 3 ABD-8 14:20 - 14:30

Monitoring of Hepatic Steatosis Using Ultrasound: Usefulness of Acoustic Structure Quantification

Dong Ho Lee, Jae Young Lee
Department of Radiology, Seoul National University Hospital, Korea

PURPOSE: To evaluate prospectively whether monitoring hepatic steatosis by using ultrasound with an acoustic structure quantification (ASQ) technique is feasible when using magnetic resonance spectroscopy (MRS) as a reference standard.

MATERIALS AND METHODS: Thirty-six patients with suspected fatty liver disease underwent both ultrasound with ASQ and MRS on the same day as the initial examinations. After a mean follow-up of 11.4 ± 2.5 months, follow-up ultrasound with ASQ and MRS were performed on 27 patients on the same day to evaluate whether hepatic steatosis improved. The focal disturbance (FD) ratio, as calculated using ASQ and hepatic fat fraction (HFF) and estimated by MRS, was obtained at both initial and follow-up examinations, and changes that occurred during follow-up were assessed. Pearson's correlation coefficient was calculated to assess correlations between ordinal values.

RESULTS: The FD ratio showed a strong, negative linear correlation with HFF after logarithmic transformation of both variables on both initial examination in 36 patients ($\rho = -0.888$; $P < 0.001$)

and follow-up examination in 27 patients ($p=-0.920$; $P<0.001$). During the follow-up period, the mean change was $-3.3\pm 41.1\%$ for HFF and $49.4\pm 137.0\%$ for FD ratio. There was also a significant, negative linear correlation between the change in the logarithm of the FD ratio and the change in the logarithm of the HFF on MRS during follow-up ($p=-0.645$; $P<0.001$).

CONCLUSION: The FD ratio was significantly correlated with HFF at both initial and follow-up examinations, and there was also a significant correlation between the changes in the FD ratio and the changes in HFF during the follow-up period.

SS 3 ABD-9 14:30 - 14:40

Shear Wave Velocity Measurement Using Acoustic Radiation Force Impulse Elastography for Colorectal Cancer Liver Metastasis: Assessment of Reproducibility

Dong Ho Lee, Jae Young Lee

Department of Radiology, Seoul National University Hospital, Korea

PURPOSE: To evaluate measurement reproducibility of shear wave velocity (SWV) of colorectal cancer liver metastases (CRLMs) using acoustic radiation force impulse (ARFI) elastography.

MATERIALS AND METHODS: We prospectively enrolled 20 patients (M:F=17:3; mean age, 61.6 ± 9.8 [standard deviation] year-old) with CRLMs. Two abdominal radiologists measured shear wave velocity (SWE) for representative CRLM as well as for liver parenchyma ten times in each patient using ARFI elastography. SWV value of CRLM was compared to that of liver parenchyma using independent t-test. Reproducibility of SWV measurement for CRLM as well as liver parenchyma was assessed by using intraclass correlation coefficients (ICCs) and 95% Bland-Altman limits of agreement.

RESULTS: Measurement of SWV for CRLM was successful in all of patients. Mean size of CRLM was 4.2 ± 2.4 cm (range; 1.4-12.2 cm). Mean SWV was 2.06 ± 0.68 m/s for CRLM and 1.45 ± 0.26 m/s for liver parenchyma, respectively. The SWV of CRLM was significantly higher than that of liver parenchyma ($P<0.001$). ICCs was 0.783 (95% confidence interval [CI]: 0.536-0.907) for CRLM and

0.762 (95% CI: 0.406-0.856) for liver parenchyma, respectively. 95% limit of agreement was -46.2% to 60.4% for CRLM and -37.5% to 23.9% for liver parenchyma, respectively.

CONCLUSION: Substantial agreement could be achieved between two radiologists for SWV measurement of CRLM using ARFI elastography.

SS 4 GU

Genitourinary

08:30 - 08:50

GBR 102

Chairperson:

Eun Ju Lee Aju University Hospital, Korea

SS 4 GU-1 08:30 - 08:40

Renal Cortical Elastography: Normal Values and Variations

Harsh Singh¹, Om Biju Panta², Umesh Khanal³, Ram Kumar Ghimire³

¹Department of Radiology, King George Medical University, Lucknow, India

²Department of Radiology, Siriraj Hospital, Thailand

³Department of Radiology, Tribhuvan University Teaching Hospital, Nepal

PURPOSE: To establish a nomogram of renal cortical elasticity values and assess their variation in between right and left kidney as well as with age, gender, BMI, renal dimensions and skin to cortex distance.

MATERIALS AND METHODS: The study was a hospital based cross sectional study performed at TUTH, a tertiary care center in Kathmandu. The study population was all individuals referred for USG from General Health Check up clinic. Patient with abnormal ultrasound findings and abnormal renal function test were excluded from the study. Renal morphometry including length, cortical thickness, skin to cortex distance was measured in B mode imaging and Renal cortical elastography was measured with region of interest box of 1×0.5 cm. All analysis was done using SPSS 20.0 soft ware.

RESULTS: A total of 95 individuals who met the inclusion criteria were included in the study. The

mean values of right and left renal cortical shear wave velocity were 1.49 ± 0.19 m/sec and 1.54 ± 0.19 m/sec respectively. The renal shear wave velocity was seen to decrease with age, however the correlation was not statistically significant. No significant difference was also noted in renal shear wave velocity among various sex or BMI groups. There was statistically significant negative correlation noted between skin to cortex distance renal cortical shear wave velocities. However no statistically significant correlation was noted between renal dimensions and renal cortical shear wave velocities.

CONCLUSION: Renal elasticity is independent of the age, gender, BMI and renal dimensions.

SS 4 GU-2 08:40 - 08:50

Mimics of Renal Calculi

Prakash Tayade

Department of Radiology, MCI, India

PURPOSE: Renal calculus disease is a frequent cause of lumbar pain, but an incorrect diagnosis of renal calculus disease can have important clinical implications for the patient. The complete treatment and prognosis is depending on Radiologist report. If lumbar pain is erroneously ascribed to the presence of a renal calculus, the patient may be deprived of appropriate treatment. Proper sonographic technique usually allows visualization of most calculi larger than 5 mm. When imaging smaller renal calculi; however, recognition and diagnostic accuracy are less clear, and such stones may be missed or misdiagnosed because of the presence of many inherently bright intrarenal noncalculus echoes. This presentation on those bright echoes that represent sonographic artifacts.

MATERIALS AND METHODS: Real time scanning on 200 patients for various causes. Philips clear view scanner is used. Convex probe for scanning. All transabdominal scan.

RESULTS: At various point simple mistakes by radiologist the bright reflectors are wrongly diagnosed as calculus. By this study help to diagnosed correctly.

CONCLUSION: By simple differentiation we can make correct diagnosis and best treatment to

patients.

SS 4 PED

Pediatric

08:50 - 10:00

GBR 102

Chairpersons:

Young Seok Lee Dankook University Hospital, Korea

Hye-Kyung Yoon Kangwon National University Hospital, Korea

SS 4 PED-1 08:50 - 09:00

Accurate Measurement of Liver Stiffness Using Shear Wave Elastography in Children and the Role of Stability Index

Eun Kyoung Hong¹, Young Hun Choi¹,
Jung-Eun Cheon¹, Woo Sun Kim¹, In-One Kim¹,
Sun Young Kang²

¹Department of Radiology, Seoul National University Hospital, Korea

²Department of Clinical Ultrasound, DongSeo Medicare Co., Ltd. and SuperSonic Imagine, Korea

PURPOSE: To evaluate the usefulness of stability index (SI) in decreasing the variability of liver stiffness measurements and the number of measurements required for adequate acquisition of data during free breathing (FB) and breath holding (BH) in children.

MATERIALS AND METHODS: A total of 29 children who underwent liver stiffness measurement using shear wave elastography (SWE) during FB and BH were included in our study. Ten SWE measurements were acquired using a region of interest in each of the 4 groups: FB and BH groups with and without using SI. The rate of failure of acquisition of SI over 90% was calculated. To evaluate variability in the SWE measurement, standard deviation, coefficient of variation, and percentage of unreliable measurement were compared. Intraobserver agreement and the optimal minimal number of measurements were calculated by using intraclass correlation coefficients.

RESULTS: A failure to acquire SI values over 90% was observed in 5/29 patients (17%) in the FB group and in 2/29 patients (7%) in the BH group. In

both FB and BH groups, the groups that utilized SI showed significantly lower standard deviation and coefficient of variation compared with those that did not. When using SI, the percentage of unreliable measurements decreased from 16.7% to 8.3% in the FB group and 14.8% to 0% in the BH group. Further, with the use of SI, intraobserver agreement was increased in both the FB and BH groups, and the optimal minimal number of repeated measurements with acceptable error range was decreased from 8 to 5 in the FB group and 6 to 2 in the BH group.

CONCLUSION: Utilization of SI in the measurement of liver SWE in children reduced measurement variability during both FB and BH, and it may reduce the scan time by decreasing the number of repeated measurements in children.

SS 4 PED-2 09:00 - 09:10

Ultrasonography of Normal Filum Terminale

Myoungae Kwon, Bo-Kyung Je, Doran Hong
Department of Radiology, Korea University Ansan Hospital, Korea

PURPOSE: The filum terminale (FT) is a fibrous band-like structure that connects the conus medullaris to the posterior body of the second coccyx. Normal FT has been described as a hyperechoic cord, surrounded by the echogenic nerve roots of the cauda equina. By the advances of US technology and improvement of the image resolution, we aimed to re-establish the US features of normal FT in infants younger than 6 months of age.

MATERIALS AND METHODS: We retrospectively reviewed spinal US including the static images, as well as, video clips of normal FT. The echogenicity of FT, the detectability of the central canal, and the methods to distinguish the FT from the surrounding nerve roots of the cauda equina were assessed.

RESULTS: Among 114 spinal US scans, 30 scans for normal FT were enrolled in this study. The pia mater of the FT was more echogenic than cauda equina in 8 cases (27%) and isoechoic in 22 cases (73%). The central canal of normal FT was apparent in 18 cases (60%). The transverse scan was superior to the longitudinal scan to distinguish FT from the cauda equina in 18 cases (60%).

CONCLUSION: On US, normal FT is a hypoechoic tubular structure covered with the hyperechoic pia mater. The central canal of the FT was defined on US in over half of the patients. The hyperechoic pia mater of FT and the use of transverse scan were helpful when distinguishing normal FT from the cauda equina.

SS 4 PED-3 09:10 - 09:20

Normal Change Limit of Pediatric Testicular Volume and Elasticity on Ultrasonography Including Shear Wave Elastography

Hyun Joo Shin¹, Myung-Joon Kim¹, Haesung Yoon¹, Yong Seung Lee², Sang Won Han², Yun Ho Roh³, Mi-Jung Lee¹

¹Department of Radiology, Severance Hospital, Korea

²Department of Urology, Severance Hospital, Korea

³Department of Statistics, Yonsei University College of Medicine, Korea

PURPOSE: To evaluate the normal change limit of pediatric testicular volume and elasticity on ultrasonography (US) including shear wave elastography (SWE).

MATERIALS AND METHODS: Testicular US images including SWE evaluation of children (≤ 18 years old) were retrospectively reviewed from February 2015 to January 2017. We included grossly normal testes or testes with only small hydrocele (depth of deep pocket < the longest diameter of testis). After comparison of the volumes and elasticities between testes with and without hydrocele, all data were used for correlation analyses. The correlations between age and testicular volume or elasticity were evaluated with Spearman test and linear regression test. The normal ranges of testicular volumes and elasticities were presented with 95% confidence bands according to their age.

RESULTS: Total 62 boys (mean age of 48 ± 53 months) were included and 35 children had small hydrocele. There was no difference in testicular volume ($p=0.074$) and elasticity ($p=0.123$) between testes with and without hydrocele. There was positive correlation between age and testicular volume ($r=0.695$, $p<0.001$) and negative correlation

between age and elasticity ($r=-0.410$, $p=0.001$). Following equations were developed using linear regression test; Volume (cc) = $0.004 \times (\text{month}) + 0.440$ ($2=0.265$, $p<0.001$), $0.099 \times (\text{month}) - 8.501$ (≥ 10 years old, $R^2=0.497$, $p=0.023$), Elasticity (kPa) = $-0.008 \times (\text{month}) + 4.035$ ($R^2 = 0.218$, $p<0.001$). The 95% confidence bands of normal pediatric testicular volume and elasticity were presented.

CONCLUSION: In normal children, testicular elasticity decreased while volume increased as increasing age. We presented normal change limit of pediatric testicular volume and elasticity according to the age.

SS 4 PED-4 09:20 - 09:30

Localized Cystic Disease of the Kidney in Children: US Findings

Haesung Yoon, Myung-Joon Kim, Mi-Jung Lee,
Hyun Joo Shin

Department of Radiology, Severance Hospital, Korea

PURPOSE: To describe the spectrum of renal findings using ultrasonography (US) in patients with localized cystic disease of the kidney and how these features differentiate this disease from other renal cystic disease.

MATERIALS AND METHODS: From January 2002 to December 2016, medical records and image features of patients who were suspicious for localized cystic disease of the kidney were retrospectively reviewed. Clinical presentations including age, symptoms, and renal functions were reviewed. US features of affected and contralateral kidneys were reviewed, and compared with other image findings, if they had CT or MRI.

RESULTS: Total 18 patients (M:F=11:7, mean 7.4 years, range 0-25 years, right:left = 11:7) underwent US and suspected to have localized cystic disease of the kidney. Initial clinical presentations were incidental finding in 12 patients (66.7%), hematuria, urinary tract infection, and nausea. On US exam, 8 patients had multifocal involvement of the localized cystic lesions in affected kidney and 3 patients had tiny cysts at contralateral kidney. US appearances of all patients were characterized by multiple variable sized conglomerated round cystic lesions with

intervening normal renal parenchyma and preserved cortical rim. These lesions showed no predisposition to renal cortex or medulla. Eight patients (44.4%) out of 18 patients showed multiple hyperechoic foci with ring down artifact within the cystic lesions on US. Out of these eight patients, six patients showed focal calcifications in the cysts on CT. During the follow up (mean follow up interval: 934 days, range 0-4076 days) two patients showed increased size of cystic lesions. There was no renal function impairment at initial presentation or during follow up in all patients.

CONCLUSION: When multiple conglomerated cystic lesions with combined hyperechoic foci are discovered in one kidney on US, localized cystic disease of the kidney can be distinguished from other cystic renal disease.

SS 4 PED-5 09:30 - 09:40

A Preliminary Study of Shear Wave Elastography for the Evaluation of Varicocele in Adolescent and Young Adults

Young Jin Ryu¹, Young Hun Choi², Jung-Eun Cheon²,
Woo Sun Kim², In-One Kim², Ji Eun Park³

¹Department of Radiology, Seoul National University Bundang Hospital, Korea

²Department of Radiology, Seoul National University Hospital, Korea

³Department of Radiology, Kyungpook National University Hospital, Korea

PURPOSE: We sought to evaluate potential relationship between elasticity of bilateral testes using shear wave elastography (SWE) and clinical grade of varicocele in adolescent and young adults.

MATERIALS AND METHODS: From July 2016 to February 2017, a total of 27 patients (mean age, 15.9 years; range, 12-20 years) with varicocele were divided into two groups by pediatric urologists according to clinical grade (group A, grade II or III, n = 20; Group B, grade I or absent, n = 7). The patients underwent grayscale ultrasonography and SWE. On SWE, elasticity of bilateral testicles was measured at rest and with Valsalva maneuver. The absolute value and the percentage of differences in the elasticity between the two conditions were compared between

groups A and B.

RESULTS: Group A showed significant elevation in the elasticity of left testicles during the Valsalva maneuver from resting condition than group B (group A vs. group B; $0.75 \text{ kPa} \pm 0.70 \text{ kPa}$ vs. $0.03 \text{ kPa} \pm 0.30 \text{ kPa}$, $p = .011$; $26.1\% \pm 23.9\%$ vs. $1.6\% \pm 12.5\%$, $p = .016$). However, there was no difference between groups A and B with regard to the differences in the elasticity of right testicles between the two conditions (group A vs. group B; $0.03 \text{ kPa} \pm 0.20 \text{ kPa}$ vs. $0.00 \text{ kPa} \pm 0.24 \text{ kPa}$, $p = .935$; $1.3\% \pm 7.8\%$ vs. $1.2\% \pm 8.3\%$, $p = .978$). However, In addition, there was positive correlation between the differences in the elasticity of left testicles between the two conditions and the clinical grade ($\rho = 0.608$, $p = .001$).

CONCLUSION: SWE seems to be a useful tool to reflect the clinical grade of varicocele. In addition, SWE has the potentials to predict influence of the varicocele to spermatogenesis, which might reflect the abnormal semen analysis.

SS 4 PED-6 09:40 - 09:50

Risk Estimation for Biliary Atresia in Neonatal Cholestasis: Development and Validation of a Predictive Score

Jeong Rye Kim, Hee Mang Yoon, Young Ah Cho, Jin Seong Lee, Ah Young Jung

Department of Radiology, Asan Medical Center, Korea

PURPOSE: Early detection of biliary atresia is extremely important as early surgical intervention is required to achieve successful treatment outcomes. However, diagnosis of biliary atresia is sometimes challenging, because there is a high degree of overlap in clinical, radiological and histologic features of biliary atresia with other causes of neonatal cholestasis. This study aimed to develop and validate a simple scoring system based on clinical and imaging features to predict the risk of biliary atresia in patients with neonatal cholestasis.

MATERIALS AND METHODS: Patients with neonatal cholestasis who underwent both ultrasound and hepatobiliary scintigraphy between January 2000 and September 2016 were selected. Clinical and imaging features associated with biliary atresia

were assessed. Histopathologic findings or results of intraoperative cholangiography served as a reference standard for biliary atresia. A prediction model was developed by using backward logistic regression and transformed into a scoring system. Internal validity of this system was estimated by bootstrapping method.

RESULTS: A total of 371 patients with neonatal cholestasis were identified, of whom 97 (26.15%) had biliary atresia. Four factors were independently associated with biliary atresia: fullterm baby (odds ratio[OR]=8.88), presence of triangular cord sign on ultrasound (US, OR=1.99), abnormal gallbladder morphology on US (OR=31.62) and failure of radioisotope excretion to the small bowel on hepatobiliary scintigraphy (OR=358.12). A scoring system using these four factors was constructed with a maximum possible score of 7 points. This system showed excellent discrimination ability (area under the curve [AUC] = 0.98) and calibration ($p=0.33$ on Hosmer and Lemeshow Goodness-of-Fit test). Internal validation with 1000 bootstrap resampling showed AUC of 0.98.

CONCLUSION: A simple novel scoring system combining clinical and imaging features accurately can estimate the risk of biliary atresia in patients with neonatal cholestasis.

SS 4 PED-7 09:50 - 10:00

Diagnostic Value of the Renal Doppler Ultrasound for Detecting Renovascular Hypertension in Children

Seunghyun Lee, Young Hun Choi, Yeon Jin Cho, Ji Young Ha, Jung-Eun Cheon, Woo Sun Kim, In-One Kim

Department of Radiology, Seoul National University Hospital, Korea

PURPOSE: To evaluate renal Doppler ultrasound for detecting renal artery stenosis in children who suspected renovascular hypertension.

MATERIALS AND METHODS: We retrospectively reviewed pediatric renal Doppler US and CT angiography for 56 patients who had diagnosed as hypertension between January 2000 and April 2016 at our institution. Two pediatric radiologists reviewed

imaging studies and documented relevant findings. The tardus parvus waveform was interpreted as a positive examination of ultrasound.

RESULTS: Thirty-six boys and twenty girls underwent renal Doppler US and confirmatory CT (mean age = 11.0 years). There was three cases of truly negative, 10 cases of false negative, 32 of truly positive, and 3 of falsely positive in renal Doppler US. The renal Doppler US had a sensitivity and specificity of 76% and 50%, respectively, for detecting a renal artery stenosis. Among the false negative cases, six children (6/10, 60%) had primary renal artery stenosis: four with an accessory renal artery, one with stenosis of segmental renal artery, and one with very tiny stenotic portion in main renal artery. Three children with false negative cases (3/10, 30%) had a poor cooperation performing the renal Doppler US.

CONCLUSION: Renal Doppler US reliably detects renovascular hypertension caused by renal artery stenosis in children. However, when renovascular hypertension was suspected, renal Doppler US should be performed at multiple sites for vascular anatomical abnormality such as intrarenal and accessory renal artery stenosis.

SC 2 BR

Breast

10:20 - 11:50

GBR 103

Chairpersons:

Boo-Kyung Han *Samsung Medical Center, Korea*

Eun-Kyung Kim *Severance Hospital, Korea*

SC 2 BR-2 10:40 - 10:50

The Value of 3D Automated Breast Volume Scanner (ABVS) as a Breast Screening Tool

Yi Li (Grace) Wong, Sharifah Majedah Idrus Alhabshi
Department of Radiology, Hospital University
Kebangsaan Malaysia (HUKM), KL, Malaysia

PURPOSE: Automated Breast Volume Scanner (ABVS) is a new ultrasound technology enabling visualization of 3D breast anatomy via multi-planar

images. Our objective was to determine whether ABVS could replace the combination of mammogram and supplementary 2D hand held ultrasound (M+HHUS) as a breast cancer-screening tool.

MATERIALS AND METHODS: From 15th January 2013 to 8th November 2016, ABVS was performed on 136 patients who underwent M+HHUS. We compared the sensitivity, specificity, accuracy, positive and negative predictive value of ABVS and M+HHUS. The histopathology results of 121 breast lesions were used as gold standard. Agreement on lesion detection and findings between ABVS and M+HHUS as well as inter-rater reliability were calculated.

RESULTS: Sensitivity, specificity, PPV, NPV and accuracy values for ABVS were 88.1%, 83.5%, 74.0 %, 93.0% and 85.1% in comparison to M+HHUS were 95.3%, 76.9%, 69.5%, 96.8% and 83.5% respectively ($p < 0.0001$). There was almost perfect agreement between ABVS and M+HHUS in detecting architectural distortion ($k=0.9$), moderate agreement in detecting masses ($k=0.6$), poor agreement in detecting suspicious cluster of micro calcifications ($k=0.3$) and almost perfect agreement for final BIRADS classification ($k=0.9$). There was also strong inter-rater reliability between the two readers of different experience for interpretation of ABVS images.

CONCLUSION: ABVS was found to be less sensitive in comparison to M+HHUS. This was mainly due to poor detection of suspicious cluster of micro calcification. ABVS was also found to detect more sub-centimeter benign lesion, which were clinically not significant. Therefore, we do not recommend ABVS to be a sole screening tool for breast cancer. Nevertheless, there is promising potential for ABVS to replace conventional 2D hand held ultrasound or as an adjunct for breast imaging.

SC 2 BR-3 10:50 - 11:00**Value of Ultrasound-Guided Fine Needle Aspiration in Diagnosing Axillary Lymph Node Recurrence After Breast Cancer Surgery**

Youngjean Park, Eun-Kyung Kim, Hee Jung Moon, Jung Hyun Yoon, Min Jung Kim

Department of Radiology, Severance Hospital, Korea

PURPOSE: To assess the diagnostic performance of ultrasound-guided fine needle aspiration (US-FNA) in diagnosing axillary lymph node (ALN) recurrence in patients with a history of breast cancer and investigate the frequency and final outcome of ALNs with inadequate results.

MATERIALS AND METHODS: From January 2005 to June 2015, 269 US-FNA examinations performed for suspicious axillary lesions in 254 patients with a history of breast cancer were included. The diagnostic performance of US-FNA for ALN recurrence was evaluated. We also investigated the final outcome of 38 axillary lesions with inadequate cytological results.

RESULTS: The overall sensitivity, specificity, PPV and NPV of US-FNA for diagnosing ALN recurrence per examination were 98.3% (59/60), 100% (171/171), 100% (59/59) and 99.4% (171/172). The sensitivity, specificity, PPV and NPV of US-FNA was 97.0% (32/33), 100% (158/158), 100% (32/32), and 99.4% (157/158) in examinations for ALNs detected during routine surveillance and 100% (27/27), 100% (14/14), 100% (27/27), 100% (14/14) in those detected at diagnostic examinations. None of the 38 (14.1%) cytologically inadequate axillary lesions developed ALN recurrence during a median follow-up period of 63.3 months.

CONCLUSION: US-FNA is a reliable method for diagnosing axillary recurrence in patients with a history of breast cancer.

SC 2 BR-4 11:00 - 11:10**The Usefulness of Breast Ultrasound CAD to Diagnose Breast Cancer Based on the BIRADS Lexicon and Quantitative Characteristics**

Yumi Kim¹, Bong Joo Kang², Sung Hun Kim², Jung Min Lee²

¹Department of Radiology, The Catholic University of Korea, Bucheon St. Mary's Hospital, Korea

²Department of Radiology, The Catholic University of Korea, Seoul St. Mary's Hospital, Korea

PURPOSE: The aim of this study was to evaluate the usefulness of a computer-aided diagnosis (CAD) system by comparing the diagnostic performance among BI-RADS lexicons and quantitative variables in general ultrasound and CAD.

MATERIALS AND METHODS: Between October 2015 and December 2016, 432 women (mean age, 48.6 ± 11.7 years) with 521 breast lesions were enrolled and underwent general ultrasound with CAD (S-detect™). Among 521 breast lesions, 79 lesions had been confirmed as malignant histologically. Other 442 breast lesions had been diagnosed as benign histologically or stable for more than 2 years. We assessed diagnostic performance among the BI-RADS lexicons and quantitative variables (width, height, height/width (H/W) ratio, area, and depth). In addition, we evaluated the concordance between orientations in general ultrasound and H/W ratios in CAD. Finally, we evaluated the concordance between lexicons in general ultrasound and CAD.

RESULTS: AUC, sensitivity, specificity, PPV and NPV of general ultrasound and CAD were 0.82 vs. 0.78, 95% vs. 78%, 69% vs. 78%, 36% vs. 39%, and 99% vs. 95%, respectively. In all lexicons and quantitative variables, the height and H/W ratio (cut off=0.55) showed the highest AUC (0.76 and 0.75) and H/W ratio (cut off=0.55) showed the highest sensitivity (91%). The mean H/W ratios of parallel orientation and not-parallel orientation were significantly different (0.6 ± 0.1 vs. 0.9 ± 0.2 , <0.001). According to the concordance analysis, orientation, shape, and echogenicity showed moderate agreement. Margin, posterior feature, and final category showed fair agreement.

CONCLUSION: In the ultrasound CAD, we could obtain not only BI-RADS lexicon, but also accurate

quantitative variables. The orientation and h/w ratio could be a consistent key factor for differentiation between benign and malignancy in both of general ultrasound and CAD.

SC 2 BR-5 11:10 - 11:20

Application of Computer Aided Diagnosis (CAD) on Breast US: Evaluation of Diagnostic Performances and Agreement of Radiologists According to Different Levels of Experiences

Eun Cho¹, Eun-Kyung Kim², Min Jung Kim², Hee Jung Moon², Youngjean Park², Jung Hyun Yoon²
¹Department of Radiology, Dong-A University Hospital, Korea

²Department of Radiology, Severance Hospital, Korea

PURPOSE: To investigate the feasibility of a computer-aided diagnosis (CAD) system (S-Detect™) for breast US, according to radiologists with various degree of experiences on breast imaging.

MATERIALS AND METHODS: From December 2015 to March 2016, 119 breast masses in 116 women were included. US images of the breast masses were retrospectively reviewed and analyzed by two radiologists specializing in breast imaging (7 and 1 years, respectively), and S-Detect™, according to the individual US descriptors of the 5th edition of ACR BI-RADS and final assessment categories. Diagnostic performance and the interobserver agreement among the radiologists and S-Detect™ was calculated and compared.

RESULTS: Among the 119 breast masses, 54 (45.4%) were malignant, and 65 (54.6%) were benign. Compared to the two radiologists, S-Detect™ had absolutely higher specificity (90.8% to 49.2% and 55.4%) and positive predictive value (86.7% to 60.7% and 63.8%) (all $p < 0.001$). Both radiologists had significantly improved specificity, PPV, and accuracy when using S-Detect™ compared to US alone (all $p < 0.001$). Area under the receiving operator curve (AUC) of the both radiologists did not show significant improvement when applying S-Detect™ compared to US alone (all $p > 0.05$). Moderate agreement was seen in final assessments made by each radiologist and and S-Detect™ ($\kappa = 0.404$ and

0.457, respectively).

CONCLUSION: S-Detect™ is a clinically feasible diagnostic tool that can be used to improve the specificity, PPV, and accuracy of breast US, with moderate degree of agreement in final assessment, regardless of the experience of the radiologist.

SC 2 BR-6 11:20 - 11:30

Two-View Scanning Technique of Automated Breast Ultrasound System (ABUS) for Breast Cancer Screening: Comparison on the Diagnostic Performance with Three-View Scan Technique

Soo-Yeon Kim, Jung Min Chang, Woo Kyung Moon
 Department of Radiology, Seoul National University Hospital, Korea

PURPOSE: To evaluate and compare the detection performance of benign and malignant breast lesions using 3D volume data obtained by two or three view scans of automated breast ultrasound (ABUS).

MATERIALS AND METHODS: This study was approved by the IRB and informed consent was obtained. Between March and April 2016, bilateral whole breast ultrasound examinations were performed with ABUS for 32 consecutive women with known breast cancer (mean age, 50.5 years; range, 35-78). Two-view or three-view scans of ABUS for each breast were randomly assigned for the women who had less than 20 cm of breast width on mammography. Two breast radiologists who were unaware of results of image and clinical information reviewed the ABUS data. Sensitivity and specificity in detecting malignant lesions on ABUS were calculated.

RESULTS: Thirty-seven malignancy (mean size, 1.9 ± 1.1 cm) in 33 breasts, and 31 breasts with negative or benign findings were included. Average width on mammography and depth in ultrasound (US) were 18.3 cm and 2.3 cm in the two-view scan, and 18.2 cm and 2.2 cm in the three-view scan ($p > 0.05$). The sensitivity was 93.3% (14/15) in the two-view scan, and 90.9% (20/22) in the three-view scan ($p > 0.05$). The specificity was lower in two-view scan group (46.7%, 7/15) than three-view scan group (75%, 12/16), but did not show statistical significance ($p = 0.077$). In three cases of false-

negative, all cancers were included in the scans, but 2 DCIS was missed due to non-mass finding, and 1 invasive cancer was obscured by the heterogeneous background echotexture on ABUS.

CONCLUSION: In detection of malignant breast lesions, there was no difference in sensitivity between two-view scans and three-view scans of ABUS. Therefore 2 scans of ABUS is feasible to detect breast cancers in women with small breasts, although specificity loss is observed.

SC 2 BR-7 11:30 - 11:40

The Benefits and Harms of Breast Ultrasound CAD; Focused on the Borderline Lesions

Yumi Kim¹, Bong Joo Kang², Na Young Jung¹, Sung Hun Kim², Jung Min Lee²

¹Department of Radiology, The Catholic University of Korea, Bucheon St. Mary's Hospital, Korea

²Department of Radiology, The Catholic University of Korea, Seoul St. Mary's Hospital, Korea

PURPOSE: The aim of this study was to evaluate the benefits and harms of computer-aided diagnosis (CAD) system for breast ultrasound focused on the borderline lesions.

MATERIALS AND METHODS: Between October 2015 and December 2016, 432 women (mean age, 48.6 ± 11.7 years) with 521 breast lesions were enrolled and underwent general ultrasound with ultrasound CAD (S-detect™). Among 521 breast lesions, 79 lesions were pathologically confirmed as malignant and 35 lesions were confirmed as borderline after core-needle biopsy or surgery. Other 407 lesions had been diagnosed as benign histologically or unchanged for more than 2 years. We assessed the imaging positive rate of borderline lesions among the general ultrasound, CAD, combination, and mammography alone. We also compared the diagnostic performance of malignancy only and malignancy including borderline lesion.

RESULTS: Total 35 borderline lesions included 18 papillary lesions, 10 atypical ductal hyperplasias, 2 flat epithelial atypias, 2 radial scars, 2 phyllodes tumors, and 1 mucocoele like lesion. In general ultrasound, 27/35 lesions were classified as positive. In CAD, 11/35 lesions were classified as positive.

In combination, 26/35 lesions were classified as positive. And, 6/35 lesions were classified as positive on mammography. When malignancy only defined as positive, mammography showed the highest (0.9) AUC, followed by combination (0.83), general ultrasound (0.82), and CAD (0.78). When malignancy and borderline defined as positive, combination result showed the highest (0.82) AUC, then general ultrasound (0.81), mammography (0.8), and CAD (0.71). When malignancy and borderline lesion defined as positive, sensitivities were decreased in all modalities, especially in mammography (88% to 67%) and CAD (78% to 64%) without change in specificity.

CONCLUSION: Ultrasound CAD was designed to diagnose malignancy, not borderline lesion, fundamentally. When diagnosing malignancy including borderline lesion sensitively, combination of general ultrasound and ultrasound CAD is essential.

SC 2 BR-8 11:40 - 11:50

Significance of Microvascular Evaluation in the Dilatation of Mammary Ducts: Influence on Diagnostic Performance

Eun Sil Kim¹, Bo Kyoung Seo¹, Ah Young Park², Ok Hee Woo³, Kyoonsun Jung⁴, Kyu Ran Cho⁵, Jaehyung Cha⁶

¹Department of Radiology, Korea University Ansan Hospital, Korea

²Department of Radiology, Bundang CHA Medical Center, Korea

³Department of Radiology, Korea University Guro Hospital, Korea

⁴Department of Diagnostic Radiology, Hallym University Sacred Heart Hospital, Korea

⁵Department of Radiology, Korea University Anam Hospital, Korea

⁶Department of Medical Science Research Center, Korea University Ansan Hospital, Korea

PURPOSE: To investigate the significance of vascularity in ductal dilatations without associated masses at breast ultrasound by comparing gray-scale only with combined use of Doppler ultrasound.

MATERIALS AND METHODS: A total of 62 ductal

dilatations in consecutive 61 patients were evaluated with gray-scale and three Doppler techniques, Superb Micro-Vascular Imaging (SMI), color Doppler (CDI), and power Doppler imaging (PDI) before biopsy. Two breast radiologists assessed the presence of ductal wall thickening, calcifications, and intraluminal content at gray-scale imaging, and number, distribution (intraductal, periductal, or both), and morphology (dot, linear, or penetrating) of vessels at Doppler imaging. They assessed BI-RADS categories at gray-scale and Doppler imaging of each lesion. These features were correlated with pathological results. We obtained interobserver variability in imaging analyses and compared diagnostic performance between gray-scale only and combined use of each Doppler imaging for distinguishing benign from malignant lesions with the area under the receiver operating characteristic curve (AUC) values.

RESULTS: Pathological diagnoses revealed 12 cancers and 50 benign lesions. Interobserver

variability was substantial to almost perfect (range of intraclass correlation coefficients, 0.69-1.00). Doppler imaging showed significant differences between benign and malignant lesions ($P<0.001$) and these were prominent at SMI (in cancers, more than 8 vessels, 20.8% for CDI, 37.5% for PDI, and 75.0% for SMI; both intra- and periductal distribution, 58.3% for CDI, 66.7% for PDI, 91.7% for SMI; penetrating morphology, 20.8% for CDI, 33.3% for PDI, 95.8% for SMI). In the diagnostic performance, the AUC of combined use of Doppler imaging (0.92 for SMI, 0.85 for CDI, and 0.86 for PDI) was greater than that of gray-scale only (0.71) ($P<0.01$) and the AUC of SMI was higher than those of CDI and PDI ($P=0.01$).

CONCLUSION: Assessment of vascularity improves diagnostic performance in distinguishing benign from malignant ductal dilatations at breast ultrasound and SMI is superior to CDI or PDI in characterization of vascularity.

Abdomen

SE 001

Is Contrast-Enhanced Ultrasound with Sonazoid Helpful for Percutaneous Biopsies of Focal Hepatic Lesions?: Prospective Feasibility Study

Sang Min Lee¹, Jung Hoon Kim², Hyun Kyung Yang²,
Hyo-Jin Kang², Joon Koo Han²

¹Department of Radiology, Hallym University Sacred Heart Hospital, Korea

²Department of Radiology, Seoul National University Hospital, Korea

PURPOSE: To determine whether the Sonazoid-enhanced US (SEUS) would be helpful for percutaneous biopsies for focal hepatic lesions.

MATERIALS AND METHODS: This prospective study included 40 consecutive patients who planned for percutaneous liver biopsy for focal hepatic lesions. Before biopsy, all patients underwent B-mode US (B-US) followed by SEUS. The radiologist conducting biopsy was evaluating the number of detected lesions, the presence of necrosis, the conspicuity of the targeted lesion and the subjective technical feasibility using a 4-point scale on B-US and CEUS. The technical failure and occurrence of change in biopsy target were also assessed.

RESULTS: On SEUS, the number of detected lesions was increased in 55% (22 of 40). The mean number of detected lesions on SEUS was significantly greater than that on conventional B-US (5.1 ± 6.2 vs. 2.8 ± 3.8 , $p < 0.001$). The targeted lesion was changed in 6 of 40 (15%) on SEUS. The conspicuity of targeted lesion was improved in 67.5% (27 of 40) on SEUS. The conspicuity of the targeted lesion was significantly greater than that on B-US (3.6 ± 0.8 vs. 2.8 ± 0.9 , $p < 0.001$). The necrosis within the lesion was more visualized in 7 of 40 (17.5%) on SEUS. The subjective technical feasibility on SEUS was significantly greater than that on B-US (2.3 ± 1.0 vs. 3.3 ± 0.9 , $p < 0.001$). The technical failure was observed in 1 of 40 (2.5%).

CONCLUSION: SEUS would be helpful for percutaneous biopsy of focal hepatic lesions in terms with detection, improving conspicuity, tumor viable portion assessment, and leading to higher operator confidence comparing B-US.

SE 002

Contrast Enhanced Ultrasound for the Characterization of Hepatocellular Carcinoma

Hoang Nguyen Huy, Hanh Tuong Thi Hong,
Riep Tran Van

Department of Radiology, 108 Military Central Hospital, Vietnam

AIM: To analyze the hepatocellular carcinoma (HCC) characterizations on Contrast enhanced ultrasound and the correlation between these characterizations with tumor size and tumor differentiations.

MATERIALS AND METHODS: This study included 135 patients with 135 HCC nodules confirmed by histopathology between February 2014 and May 2016. All patients were evaluated by Contrast Enhanced Ultrasound with contrast agent SonoVue (Bracco Company, Neitherland), using US machine (Philips EPIQ 5G, US) that has contrast programe including contrast auto-tracking software ROI, following the 2012 WFUMB's Guidelines.

RESULTS: Of 135 nodules, 134 nodules (99.3%) presented full enhancement pattern, 01 nodule (0.7%) with non-enhancement pattern, 53 nodules (39.3%) with incomplete enhancement pattern, 65 nodules (48.1%) with heterogeneous enhancement, 43 nodules (31.9%) with necrosis. There were 99.3% of HCCs with enhancement pattern in the arterial phase, 61.5% of HCCs wash-out in the portal phase and 85.9% of HCCs wash-out in the late phase. There were undifferentiated between HCCs with level's size (< 20 mm, $20 - 39$ mm, ≥ 40 mm), the well-differentiated HCCs and the moderately to poorly HCCs from time to peak (TP) and enhancement slope (ES). However, there were differentiated between HCCs with level's size (< 20 mm, $20 - < 40$ mm, ≥ 40 mm), the well-differentiated HCCs and the moderately to poorly HCCs from wash-out time (WOT) and clearance slope (CS) with statistically significant ($p < 0,05$).

CONCLUSION: The HCCs nodules showed a "fast-in" and "fast-out" enhancement pattern. The wash-out time (WOT) and clearance slope (CS) correlate with HCCs's size and play an important role in predicting the differentiation of HCCs.

SE 003**The 100 Most-Cited Articles Focused on Ultrasound Imaging: A Bibliometric Analysis**

Eun Joo Yun, Ji Yoon Moon, Chul Soon Choi,
Dae Young Yoon

*Department of Radiology, Kangdong Sacred Heart
Hospital, Korea*

OBJECTIVE: The number of citations that an article received reflects its impact on a particular research area. The aim of this study was to identify the 100 most-cited articles focused on ultrasound (US) imaging and to analyze the characteristics of these articles.

METHODS: We determined the 100 most-cited articles on US imaging via the Web of Science database, using the search term. The following parameters were used to analyze the characteristics of the 100 most-cited articles: publication year, journal, journal impact factor, number of citations and annual citations, authors, department, institution, country, type of article, and topic.

RESULTS: The number of citations for the 100 most-cited articles ranged from 1,849 to 341 (median, 442.0) and the number of annual citations ranged from 108.0 to 8.1 (median, 22.1). The majority of articles were published in 1990-1999 (39%), published in radiology journals (20%), originated in the United States (45%), were clinical observation study (67%), and dealt with vascular (35%). Department of Internal Medicine at University of California and Research Institute of Public Health at University of Kuopio (n=4 each) were the leading institutions and Salonen JT and Salonen R (n=4 each) were the most prolific author.

CONCLUSION: Our study presents a detailed list and analysis of the 100-cited US articles, which provides a unique insight into the historical development in this field.

KEY WORDS: Bibliometrics; Citation analysis; Ultrasound; Publication.

SE 004**A Study of Ultrasound Signs in Acute Pancreatitis, Swelling Form**

Narantungalag Nyamkhuu¹, Badamsed Tserendorj²

*¹Department of Radiology, Mongolian National
University of Medical Sciences, Mongolia*

*²Department of Radiology, Shastin Hospital in
Ulaanbaatar, Mongolia*

OBJECTIVES: To determine main ultrasound signs of swelling form of Acute pancreatitis.

MATERIALS AND METHODS: We retrospectively revised ultrasound imaging data of 48 adults who were diagnosed with enlarged form of acute pancreatitis between 2015 and 2017 at the Shastin Central Hospital in Ulaanbaatar, Mongolia.

RESULTS: In our study, pancreas size was normal or 9 (18.75±5.6), diffusely enlarged 26 (54.17±7.2), partially enlarged 13 (70.83±6.5) with pancreas contour of well defined 34 (70.83±6.5) and ill-defined 14 (29.17±5.0), Pancreas structure was homogenous or 20 (41.67±6.8) and heterogenous 28 (58.33±7.1), Pancreas density was anechoic or hypoechoic with partial hyperechoic areas of 32 (66.67±6.8), hypoechoic with diffuse hyperechoic 11 (22.92±6.1), and combined echogenicity of increased and decreased zone with anechoic part of 5 (10.41±4.4). Local or Restricted fluid detected around pancreas in 9 (18.75±5.6) No detection of fluid in surrounding tissue of pancreas was in 39 (81.25±5.6)

CONCLUSION: Pancreas was partially enlarged with well defined contour in 70.83%. Anechoic and hypoechoic with partial hyperechoic zone in 66.67%. No detection of fluid in surrounding tissue of pancreas in 39(81.25±5.6)

SE 005**Ultrasonographic Atlas of Spleen**

Gayoung Choi, Kyeong Ah Kim, Jeong Woo Kim,
Yang Shin Park, Jongmee Lee, Jae Woong Choi,
Chang Hee Lee, Cheol Min Park

*Department of Radiology, Korea University Guro
Hospital, Korea*

PURPOSE: 1) To understand fundamentals of splenic ultrasonography. 2) To illustrate key imaging findings of splenic abnormalities in ultrasonography.

CONTENT ORGANIZATION: 1) Normal anatomy of spleen and basic technique of splenic ultrasonography. 2) Ultrasonographic findings of various benign and malignant splenic diseases.

SUMMARY: Ultrasonography (US) is widely used in abdominal imaging. Due to its nature of noninvasiveness, extensive availability, and inexpensive cost, US is a useful and valuable tool for the detection, diagnosis, and follow-up of splenic abnormalities. Even though other imaging modalities are becoming increasingly competitive, US of the spleen still plays an important role.

SE 006

Determination of Hepatic Segment in Intrahepatic Tumor Using Ultrasound Contrast Agent (Sonazoid): Can it Help the Surgeon Decide Hepatic Segmentectomy or Sectionectomy?

Sangyun Lee, Jinhan Cho, Heejin Kwon,
Jongyoung Oh, Younghoon Roh

*Department of Radiology, Dong-A University
Hospital, Korea*

BACKGROUND AND PURPOSE: In the case of intrahepatic tumors requiring surgical removal, especially malignant tumors such as HCC, many patients have chronic liver disease or cirrhosis. In these patients, hepatic resection requires minimal resection, such as segmentectomy or sectionectomy because of decreased liver function. The Couinaud classification performed by radiologic examination determines the hepatic segment based on the position of the hepatic vein and the portal vein. However, in the actual operation, portal vein ligation is performed and the liver is resected based on the

distribution of hepatic portal blood flow. These discrepancies between Couinaud classification and portal flow distribution which can lead to a number of problems. The purpose of this study is to segment the liver based on the portal flow, as in the actual operation, using sonazoid and compared with the postoperative hepatic segment of intrahepatic tumor.

MATERIALS AND METHODS: 11 patients who underwent contrast enhanced ultrasound and hepatic resection were included in this preliminary study. First, we performed sonographic evaluation of liver tumors in low MI (mechanical impulse) imaging using a sonazoid. And then, High MI imaging was used to select the portal vein to destroy the sonazoid. Finally, The hepatic segment of intrahepatic tumor was determined at the delayed images and compared with the postoperative hepatic segment of intrahepatic tumor.

RESULTS: Compared with the postoperative findings, the hepatic segment using sonazoid showed higher sensitivity, specificity and accuracy than the Couinaud classification. In Cohen's kappa, the hepatic segment using sonazoid also showed a higher agreement than the Couinaud classification. The hepatic segment using sonazoid showed significant anatomical accuracy with hepatic segment in the actual operation.

CONCLUSION: The hepatic segment using sonazoid can be helpful for the surgeon such as accurate resection, preservation of hepatic function, and lowering the post operative tumor recurrence.

SE 007

The Study and Characterization of Indefinite Spleen Lesions in Primary Ultrasound after Oncoming by Emergency as Abdominal Trauma: Capability of MRI

Undarmaa Dorjpalam, Enkhbold Sereejav
*Department of Radiology, The First Central Hospital
of Mongolia, Mongolia*

OBJECTIVES: To determine the value of MR imaging for follow-up and characterization of indeterminate spleen lesions in primary US of patients with blunt abdominal trauma.

METHODS: Twenty-five patients (10 female, mean

age 51.6 ± 22.4 years) with an indeterminate spleen lesion diagnosed at US after blunt abdominal trauma underwent MR imaging with T2- and T1-weighted images pre- and post-contrast material administration. MR images were reviewed by two radiologists. Patient history, clinical history, imaging and two-month clinical outcome including review of medical records and telephone interviews served as reference standard.

RESULTS: From the 30 indeterminate spleen lesions in US, 14 (44%) were traumatic and 16 (56%) non-traumatic. The ISS ($P < 0.001$) and length of hospital-stay ($P = 0.03$) were significantly higher in patients with traumatic spleen lesions as compared to those without. All other parameters were similar among groups (all, $P > 0.05$). The MR imaging features ill-defined lesion borders, variable signal on T1- and T2-weighted images, focal contrast enhancement indicating traumatic pseudoaneurysm, perilesional contrast enhancement and edema were indicative for traumatic spleen lesions. As compared to US (4/30), MR images (7/30) better depicted thin subcapsular hematomas as indicator of traumatic spleen injury.

CONCLUSION: MR imaging shows value for follow-up and characterization of indeterminate spleen lesions in primary US after blunt abdominal trauma and is helpful for discriminating traumatic from non-traumatic spleen lesions.

SE 008

Pictorial Review of Ultrasound and Doppler in Diagnosis and Post Endovascular Intervention Surveillance of Patients with Budd-Chiari Syndrome

Saloni Desai¹, Sudheer Pargewar², Nitesh Agrawal³, S Rajesh⁴, Amar Mukund⁵

¹Department of Radiology, SIR H.N. Reliance Foundation Hospital and Research Centre, Mumbai, India

²Department of Radiology, Gleneagles Global Hospital, Mumbai, India

³Department of Radiology, Fortis Escorts Heart Institute and Research Centre, Okhla, New Delhi, India

⁴Department of Radiology, Renai Medicity, Kochin, India

⁵Department of Radiology, Institute of Liver and Biliary Sciences (ILBS), New Delhi, India

Budd-Chiari syndrome (BCS) refers to a diverse group of conditions with hepatic venous outflow obstruction which may be at the level of the large hepatic veins and/or the supra-hepatic segment of the inferior vena cava which lead to congestive hepatopathy. Ultrasound and Doppler play an indispensable role in the diagnosis of patients suspected to have BCS. Findings specific for this condition include hepatic vein (HV) thrombosis, ostial/juxta-ostial stenosis and non-visualization/fibrous cord transformation of HV. Doppler findings of intrahepatic collateral circulation like venovenous and portocaval collaterals, subcapsular venous collaterals, alterations in phasicity of patent HV segment and dilated caudate vein raise a strong possibility of BCS. Other ancillary features which can be seen in BCS include heterogeneous hepatic echotexture, caudate lobe hypertrophy, regenerative nodules, ascites and extrahepatic venous collaterals. Endovascular interventions which play a major role in management of BCS include HV angioplasty/stenting, IVC angioplasty/stenting and direct intrahepatic portosystemic shunts (DIPS) either alone or in combination. In these post-intervention patients, Doppler surveillance at periodic intervals is a must to detect procedure related complications. Baseline Doppler findings at 24-48 hours post

intervention serves as a road map for subsequent follow-up in future. Ultrasound and Doppler in tandem help in timely diagnosis of complications like HV stent stenosis/thrombosis, DIPS stent stenosis/thrombosis, portal vein thrombosis and refractory ascites. The red alert findings include change in stent position as compared to prior USG, stent kinking, luminal narrowing, abnormal aliasing, echogenic thrombi causing filling defects, in-stent velocity changes compared to baseline values, low portal vein velocity and reversal of flow (hepatopetal flow) in intrahepatic portal veins. Thus, it is imperative to establish an ideal screening schedule with Doppler in post intervention patients of BCS for early identification and management of complications.

SE 009

Competency of Ultrasound Diagnosis of Acute Appendicitis with Histo-Pathological Findings

Soyolmaa Erdenebaatar¹, Sarnaitsetseg Munkhbat², Baigalmaa Jantsansengee³, Bilegt Altangerel³

¹Department of Radiology, National Center for Communicable Diseases, Mongolia

²Department of Radiology, Intermed Hospital of Mongolia, Mongolia

³Department of Epidemiology, Field Epidemiology Training, National Center for Communicable Diseases, Mongolia

BACKGROUND: Preoperative imaging has been demonstrated to improve diagnostic accuracy in appendicitis. Aim of this study was to demonstrate diagnostic value of abdominal ultrasonography for diagnosing acute appendicitis and correlate with histological findings of appendectomy specimens.

METHODS: We conducted cross-sectional study and collected data from patients with clinical suspicion of appendicitis and were subjected to ultrasound examination in June 2015 to 2016. Ultrasound positive cases were subjected to surgery. We used high resolution B-mode ultrasonography (model Siemens Accuson S2000) with linear and curved transducer and ultrasound frequencies between 2.5 and 7.5 MHz. Accuracy of ultrasound in the diagnosis of appendicitis was compared with surgical and histopathological examination reports.

RESULTS: Of 74 patients with acute appendicitis 47.3% (n=35) were male and 52.7% female (n=39) with median age of 33 years (range: 9-83). In ultrasound examination, outline diameter of appendix was greater than 6 mm with wall thickening and were spherical shape in all patients. In addition, hyperemia on Doppler, the presence of free fluid in right lowe quadrant and infiltration of the periappendiceal fat. Histopathologic examination were acute suppurative inflammation (25.7%, n=19), acute suppurative inflammation with perforation (21.6%, n=16), acute appendicitis with periappendicitis (16.2%, n=12), acute suppurative inflammation with periappendicitis (13.5%, n=10), acute gangrenous inflammation with perforation appendicitis (10.8%, n=8) and lymphoid hyperplasia (9.5%, n=7) and chronic appendicitis (2.7%, n=2).

CONCLUSION: All patients had appendectomy and histopathologic findings were consistent with acute appendicitis diagnosis in ultrasound examination. As ultrasound examination is sensitive and specific diagnostic method of acute appendicitis and no ionizing radiation and non-invasive diagnostic method that can be promoted widely in acute appendicitis diagnosis.

SE 010

Diagnosing Necrotic Type of Acute Pancreatitis

Saruulzaya Rentsensambuu, Badamsed Tserendorj
Department of Radiology, ACH Medical Institute of Mongolia, Mongolia

PURPOSE: The purpose of the research is to determine main and additional signs of necrotic type of acute pancreatitis in regard to ultra sound diagnosis.

MATERIALS AND METHODS: We made analysis and conclusion of ultra sound diagnosis and test results of 15 patients who were diagnosed in Ultra Sound Department of Radiological Imaging Department of the State Third Central Hospital of Mongolia named after P.N. Shastin in 2016 and 2017.

RESULTS: In case of necrotic type of acute pancreatitis, hypermegaly of pancreas is occurred in 66.7% of all cases ($P < 0.05$), unclear outline of pancreas is occurred in 86.7% ($P < 0.001$), change of

regular contrast of pancreas is occurred in 80.0% ($P < 0.001$), increase of density of pancreas in 60% ($P < 0.05$) and the restricted liquid in 60% ($P < 0.05$).

On the basis of our research, we divided signs of necrotic type of acute pancreatitis in two types as main signs and additional signs in regard to diagnostic significance. Herein: main signs: a. unclear outline of pancreas, b. irregular contrast of pancreas, c. increase and decrease of ultra sound reflection and unreflected zone of ultra sound. Additional signs: a. hypermegaly of pancreas, b. the restricted liquid around pancreas, c. the restricted liquid in body of pancreas.

CONCLUSION: We divided signs of necrotic type of acute pancreatitis in two types as main signs and additional signs in regard to diagnostic significance on the basis of diagnostic significance.

SE 011

Ultrasound Characteristics of Stomach Cancer

Amartuvshin Bor, Tuvshinjargal Tsendjav,

Tsetsegee J., Erdembileg Tsevegmid

Department of Radiology, Tsjetsjin Clinic, Mongolia

PURPOSE: To evaluate the ultrasound characteristics of stomach cancer.

MATERIALS AND METHODS: Between 2013-2016 years, the total of 68 patients with stomach cancer was evaluated by transabdominal ultrasound examination. The diagnosis was proved by endoscopy and biopsy in all cases. The gastrointestinal tract is filled with 400-500 ml, 20-300 C saline. Hitachi Eub. 6000, Sono-Ace R3 and Aloka alfa-10 ultrasound machines equipped with Convex (3.5-5 MHz) and Linear (9-13 MHz) transducers were used.

RESULTS: Among of these 68 patients, irregular internal surface of the stomach was in 49 cases, irregular wall thickening in 68 (9-22 mm), image ratio 1,9-49, infiltration of the gastric wall was depicted in 46 cases, wall injuries in 68 cases (with the length from 39 to 78 mm), the loss of elasticity in 63 cases, decrease of the stomach volume in 58 cases, the loss of stomach wall layer structure in 59 and loss of peristalsis of the stomach in 59 cases, "Color Jewel" sign of vessels malformations on color Doppler observed in 28 patients.

CONCLUSION: Irregular internal surface and irregular wall thickening, infiltration of the gastric wall, wall injuries, the loss of elasticity, peristalsis and stomach wall layer structure, decrease of the stomach volume and "Color Jewel" signs are the most common ultrasound characteristics of stomach cancer.

SE 012

Ultrasonic Characterization of Chronic Constipation

Tuvshinjargal Tsendjav¹, Amartuvshin Bor¹,

Tsetsegee J.¹, Erdembileg Tsevegmid²

¹*Department of Radiology, Tsjetsjin Clinic, Mongolia*

²*Department of Radiology, Gurvan Gal Teaching Hospital, School of Medicine, Mongolian National University of Medical Sciences, Mongolia*

PURPOSE: To identify the ultrasonic characteristics of chronic constipation.

MATERIALS AND METHODS: The total of 128 patients aged between 18-58 years with chronic constipation was examined. Ultrasound examination was carried out by a single-stage transabdominal ultrasound colonography using oral gastrointestinal contrast media, the specific "Tsetsegee Method" developed by our team. The gastrointestinal tract is filled with 3000-3500 ml saline using special exercises. Hitachi Eub. 6000, Sono-Ace R3 and Aloka alfa-10 ultrasound machines equipped with Convex (3.5-5 MHz) and Linear (9-13 MHz) transducers were used.

RESULTS: We have identified the characteristics of colon during the chronic constipation: the diameter expanded (from 45.9 ± 0.24 mm up to 52.1 ± 0.24 mm), the wall of the intestine unevenly thickened (from 3.04 ± 0.12 to 4.26 ± 0.78 mm), in the sigmoid colon the length between the haustra's is unequally different, smoothening of transverse folds, the different peristalsis of the bowels. The first emptying after drinking saline begins at 106.0 ± 0.18 minutes. All cases were compared with X-ray and CT images.

CONCLUSION: Ultrasound characteristics of chronic constipation are the expansion of the colon diameter, lengthening the distance between haustration, uniform thickening of the wall of no more than 4.2

mm, the preservation of lamination, elasticity and straightening of the bowel wall.

SE 013

From Basics to Clinical Practice of Abdominal Ultrasonography for Beginners: To be an Expert!

Jeong Woo Kim, Chang Hee Lee, Yang Shin Park, Jongmee Lee, Jae Woong Choi, Kyeong Ah Kim, Cheol Min Park

Department of Radiology, Korea University Guro Hospital, Korea

OBJECTIVES: 1. To review fundamentals of abdominal ultrasonography

2. To describe operating methods of ultrasound equipment

3. To illustrate adjustment methods for acquisition of “good image” in abdominal ultrasonography

INTRODUCTION: 1. Principle and basic physics of ultrasonography

2. Instrumentation of ultrasonography

1) Transmitter, 2) Transducer, 3) Receiver, 4) Image display

3. Image quality

1) Spatial resolution (Axial/ Lateral), 2) Contrast resolution

CONTENTS: 1. Gray scale image (2-dimensional image)

1) Operating methods

2) Adjustment methods for “good image”

2. Color Doppler image

1) Operating methods

2) Adjustment methods for “good image”

3. Spectral Doppler image

1) Operating methods

2) Adjustment methods for “good image”

SE 014

Typical and Atypical Paradoxical Hepatic Tumors

Sudheer Pargewar¹, Saloni Desai², Nitesh Agrawal³, S Rajesh⁴

¹Department of Radiology, Gleneagles Global Hospital, Mumbai, India

²Department of Radiology, SIR H.N. Reliance Foundation Hospital and Research Centre, Mumbai, India

³Department of Radiology, Fortis Escorts Heart Institute and Research Centre, Okhla, New Delhi, India

⁴Department of Radiology, Renai Medicity, Kochin, India

Undifferentiated embryonal sarcoma (UES) is a rare but third most common pediatric hepatic malignancy predominantly affecting older children with a total of about 150 cases being reported till date. It is known as “Paradoxical hepatic tumor” due to its typical appearances on different imaging modalities. We report a case of such typical paradoxical hepatic tumor in a 10 year old afebrile male child presenting with an epigastric mass. Ultrasound revealed a predominantly solid mass lesion with cystic areas within in the left hepatic lobe mimicking a partially liquefied hepatic abscess. However, hemogram and alpha fetoprotein level were normal. This prompted further evaluation with a contrast enhanced CT scan which revealed a predominantly cystic lesion with very minimal enhancing peripheral solid component in contrast to ultrasound picture of a predominant solid component. This paradox of appearance on different imaging modalities raised the possibility of UES. Histopathological examination of the specimen after left hepatectomy confirmed the diagnosis of UES.

We report another case of a 43 year old afebrile female presenting with upper abdominal pain since two weeks. Ultrasonography revealed a predominantly cystic subcapsular hepatic lesion with an avascular solid peripheral component having features consistent with an abscess. However, her hemogram was normal and further evaluation revealed elevated LDH and CEA levels. Contrast enhanced CT scan was thus performed which showed an enhancing predominantly solid hepatic lesion with

very minimal cystic component, suggesting a paradox on different imaging modalities. There was no extrahepatic organ involvement. Histopathological diagnosis suggested hepatic lymphoma. On USG, the most common appearance of hepatic lymphoma is that of a hypoechoic solid mass without posterior acoustic enhancement. This atypical rare cystic appearance of hepatic lymphoma on ultrasound and paradoxical solid appearance on CT prompted us to label it "Atypical Paradoxical hepatic tumor".

SE 015

Focal Intrasplenic Extramedullary Hematopoiesis Masquerading as Tubercular Abscess

Saloni Desai¹, Sudheer Pargewar², Nitesh Agrawal³, S Rajesh⁴, Chhagan Bihari⁵, Ankur Arora⁶

¹Department of Radiology, SIR H.N. Reliance Foundation Hospital and Research Centre, Mumbai, India

²Department of Radiology, Gleneagles Global Hospital, Mumbai, India

³Department of Radiology, Fortis Escorts Heart Institute and Research Centre, Okhla, New Delhi, India

⁴Department of Radiology, Renai Medicity, Kochin, India

⁵Department of Pathology, Institute of Liver and Biliary Sciences (ILBS), New Delhi, India

⁶Department of Radiology, Worthing Hospital, Western Sussex Hospital, Nhs Foundation Trust, United Kingdom

Extramedullary hematopoiesis (EMH) in spleen usually presents as an infiltrative process resulting in diffuse enlargement of the organ. Reports of focal involvement are extremely rare. We report the case of a middle-aged man with abdominal tuberculosis and a solitary splenic lesion which was thought to represent tubercular abscess at initial presentation finally turning out to be focal intrasplenic extramedullary hematopoiesis.

This 41 year old man presented with left hypochondriac pain associated with low-grade fever, anorexia and gradually progressive abdominal distension since one month as well as loose stools for 8-10 days. Hemogram revealed low

hemoglobin with significant leukocytosis having lymphocyte predominance. Ultrasound evaluation revealed splenomegaly with a solitary well defined hyperechoic focal lesion within associated with omental thickening. Further evaluation with contrast enhanced CT confirmed these findings of ultrasound along with retroperitoneal lymphadenopathy. Ultrasound guided omental biopsy showed coalescing epithelioid cell granulomas with Langhan's type of giant cells and focal necrosis. Ziehl-Neelsen staining showed presence of acid fast bacilli confirming the diagnosis of tuberculosis. In view of gross ascites, the splenic lesion was not biopsied for risk of bleeding and it was assumed to represent an evolving tubercular abscess. The patient was started on anti-tubercular therapy and kept on regular follow-up. However, the lesion increased in size despite clinical and radiological resolution of tuberculosis, prompting a histopathological examination of the lesion which was consistent with EMH. Further evaluation revealed that the patient had underlying hematological disorder in the form of homozygous delta-beta thalassemia.

Thus, when focal splenic lesions are incidentally identified in a patient with known hematological disorder, possibility of EMH can be considered. However, given the non-specific imaging findings, follow-up imaging is usually needed to ensure their stability. In rare cases though, biopsy may be necessary to establish the diagnosis, as was required in our case.

SE 016**Correlation between Thigh Fat Content Measured on MRI and Fatty Change of the Liver on Ultrasound**

Hee Jin Park

Department of Radiology, Kangbuk Samsung Medical Center, Korea

OBJECTIVES: We evaluated the correlations between thigh fat content, the degree of fatty liver on ultrasound (US), and other quantitative factors such as the hepatic steatosis index.

METHODS: We evaluated 44 patients (M:F = 29:15, mean age of 57 years) who visited our institution and underwent hip or thigh MRI and abdominal US. We measured the thickness and cross-sectional area of the subcutaneous fat layer of the patients' thighs on MRI. Grading of the degree of fatty liver was performed through US. We also calculated the hepatic steatosis index (HSI) of each patient. Correlations between the fat content of the thigh, fatty liver grade and HSI were evaluated.

RESULTS: Mean depth of the fat layer (Lmean) was 17.1 ± 7.8 mm and the mean fat to total area (F/T) ratio was 0.42 ± 0.12 . Lmeans showed a moderate correlation ($R_{co} = 0.551, 0.420$) with the grade of fatty liver on US and the HSI. The F/T ratios also showed moderate correlation ($R_{co} = 0.524, 0.402$) with the grade of fatty liver on US and the HSI.

CONCLUSION: The amount of thigh fat content had a positive relationship with the fatty liver degree on US and the HSI, which diverges from previous evidence suggesting a negative correlation between thigh fat and metabolic syndrome.

SE 017**Degree of Hepatic Steatosis in Chronic Hepatitis C Patient: Comparison with Healthy and Chronic Hepatitis B Patients**

Chul Soon Choi, Eun Joo Yun, Kyoung Ja Lim, Young Lan Seo, Dae Young Yoon

Department of Radiology, Kangdong Sacred Heart Hospital, Korea

PURPOSE: To determine degree of hepatic steatosis in chronic hepatitis C patients and compare it with healthy and chronic hepatitis B patients.

MATERIALS AND METHODS: From December, 1 2015 to January, 31 2016, we collected ultrasonograms of patients with hepatitis C virus (Male to Female ratio=11:24, Mean age=55.9 with standard deviation (SD) of 9.5) and patients with hepatitis B virus patients (Male to Female ratio=19:101 Mean age=47.6 years with SD 8.2) and healthy patients (M:F=10:18, Mean age=46.0 years with SD of 11). Ultrasonograms were obtained at the portion of border of liver and right kidney in supine position of the patient with 3-5 MHz convex transducer for abdomen and US equipment was iu-22 (Philips, Bothel, Washington, U.S.A.). After obtaining the images we measured histogram of liver and kidney with Image J (NIH, Bethesda, Maryland, U.S.A.) in tissue of same distance from the transducer in DICOM images. We calculated ratio of liver and kidney echogenicity under the assumption that echogenicity of liver reflects degree of fatty contents. We compared the ratio of three groups with Jonckheere-Terpstra test and p-value less than 0.05 was considered statistically significant.

RESULTS: Mean ratio of chronic hepatitis C was 1.79 with SD of 2.3. Mean ratio of normal patients was 2.65 with SD 1.7. Mean ratio of chronic hepatitis B patients was 1.94 with SD of 1.25. Compared with two groups, mean ratio of chronic hepatitis C was not different from other two groups ($p=0.127$)

CONCLUSION: Hepatic steatosis of chronic hepatitis C patients is not prevalent on the contrary to general belief that chronic hepatitis C virus induces fatty liver by virus core protein.

SE 018**Clinical Utility of Real-Time Fusion Guidance for Percutaneous Biopsy of Focal Hepatic Lesions**

Su Joa Ahn, Jeong Min Lee, Won Chang,
Sang Min Lee, Hyo-Jin Kang, Hyun Kyung Yang,
Joon Koo Han

*Department of Radiology, Seoul National University
Hospital, Korea*

PURPOSE: The purpose of this study was to prospectively evaluate the clinical utility of real-time US CT/MRI fusion imaging for the percutaneous needle biopsy of focal liver lesions (FLLs) and to compare its successes rate with that of propensity-score matched, conventional US guided biopsy group.

MATERIALS AND METHODS: Patients who were referred to Department of Radiology for percutaneous biopsy of FLLs were enrolled in the study. Tumor visibility, safety access route, technical feasibility were assessed on the conventional US first and later on the real-time fusion imaging by one of the four abdominal radiologists, and then the differences in scores between the real-time fusion imaging, and the conventional US were determined. The overall diagnostic success rate of the fusion imaging-guided biopsy was compared with that of the propensity-score matched, the conventional US guided biopsy group.

RESULTS: 90 patients were enrolled in the prospective study. On real-time fusion imaging, tumor visibility, safety biopsy access route and operator's technical feasibility were significantly improved compared with the conventional US ($P < .001$). And all invisible ($n=13$) and not feasible ($n=10$) focal hepatic lesions became visible and feasible to percutaneous US-guided biopsy after applying the fusion system. The diagnostic success rate of real-time fusion guided biopsy was 94.4% (85 of 90). As a historical control group, the propensity score-matched cohort included 100 patients who underwent conventional US-guided liver biopsy. The biopsy success rates were significantly improved in the fusion guided biopsy group than the conventional US guided using propensity score matching group (94.4% vs. 83%, $P < .03$) and reduced biopsy procedure time (7.1 ± 3.5 vs. 9.7 ± 2.8 , $P < .02$).

CONCLUSION: Realtime US-CT/MR fusion imaging guidance was able to improve the diagnostic success rate of the percutaneous US-guided biopsy by improving the visibility of FLLs and safe biopsy access route.

Breast**SE 019****Near-Infrared Photothermal Therapy of Triple Negative Breast Cancer Using Anti-EGFR Antibody-Conjugated Gold Nanorods**

Meihua Zhang, Hoe Suk Kim, Tiefeng Jin,
Woo Kyung Moon

*Department of Radiology, Seoul National University
Hospital, Korea*

This study was to evaluate the feasibility of photoacoustic imaging (PAI)-guided near-infrared photothermal therapy (NIR-PTT) for aggressive human triple negative breast cancer (TNBC) using anti-EGFR antibody-conjugated gold nanorods (anti-EGFR-GNs). NIR-PTT combined with anti-EGFR-GNs exerted synergic anti-proliferative and apoptotic actions through the upregulation of HSP70 and cleaved caspase-3, the downregulation of Ki-67 and EGFR, and the inhibition of intracellular signaling molecules (mTOR, AKT, ERK1/2, and FAK), resulting in the greatest therapeutic effectiveness. This study suggests that PAI-guided NIR-PTT using anti-EGFR-GNs is an encouraging therapeutic strategy for EGFR-targeted TNBCs.

SE 020**Differentiation of Benign and Metastatic Axillary Lymph Nodes in Breast Cancer: Additive Value of Shear Wave Elastography to B-mode Ultrasound**

Yu-Mee Sohn, Mirinae Seo

Department of Radiology, Kyung Hee University Medical Center, Korea

AIM: The purpose of this study was to evaluate the additive value of shear wave elastography (SWE) for differentiating benign from metastatic axillary lymph nodes (LNs) in breast cancer.

MATERIALS AND METHODS: A total of 54 LNs from 51 patients with breast cancer were examined by both B-mode ultrasound (US) and SWE from May 2014 to August 2016. On conventional B-mode US, long-axis and short-axis diameter, cortical thickness, and presence of hilum were documented. Regarding SWE, maximum, mean, and minimum stiffness, standard deviation (in kilopascal (kPa)), as well as, elasticity ratio between lesion and fatty tissue in the axilla area were collected. Diagnostic performance of the area under the receiver operator characteristic curve (AUC), sensitivity, and specificity were compared among three modalities (B-mode US alone, elastography alone, and combined modalities).

RESULTS: Final histopathological results showed 20 benign and 32 metastatic LNs. Cortical thickness on B-mode US was found to have the highest diagnostic performance, followed by maximum stiffness on SWE (AUC of 0.912 for cortical thickness and 0.887 for maximum stiffness). AUC for combined B-mode US and SWE (cortical thickness + maximum stiffness) was 0.946. Sensitivity was significantly higher for combined modality than for cortical thickness (94.12% vs. 82.35%, $p=0.046$). Among 34 metastatic LNs, Four were correctly diagnosed as metastasis using the combined modality, compared with B-mode US alone using a cutoff value from cortical thickness.

CONCLUSION: Combined B-mode US and SWE may improve detection of metastatic axillary LNs in breast cancer patients.

SE 021**Ultrasonography Findings of Male Breast Disease, with Pathological Correlation: A Pictorial Essay**

Youngseon Kim, Mi Soo Hwang

Department of Radiology, Yeungnam University Medical Center, Korea

PURPOSE: The two most common and clinically important diseases of the male breast are gynecomastia and breast cancer. Most other diseases of the male breast are arising from the skin and subcutaneous tissues. The majority of male breast diseases are benign, but the most critical diagnosis is a breast cancer. Generally, radiologists are less familiar with breast disease in male compared with female. Knowledge of the imaging findings suggestive of breast disease in male is helpful to provide optimal care. Therefore we would like to present ultrasonography findings of various diseases that affect the male breast to better understand and recognize of male breast disease.

CONTENTS: 1. Anatomy of the male breast
2. Benign disease of the male breast
i. Gynecomastia - nodular, dendritic, diffuse type
ii. Fat necrosis
iii. Epidermoid cyst
iv. Sparganosis
v. Myofibroblastoma
vi. Inflammatory pseudotumor
vii. Schwannoma
3. Malignant disease of the male breast
i. Breast carcinoma
ii. Metastasis

CONCLUSION: Although the most common disease arising from male breast is gynecomastia, many other benign and neoplastic diseases including primary breast carcinoma can develop in male breast. This pictorial essay has demonstrated various ultrasonography findings of benign and malignant male breast diseases. It may be helpful for radiologists to establish the correct diagnosis in male patients.

SE 022**Interobserver Agreements of Breast Ultrasound Categorization Modified by the ABCS-K for the Mammography and Ultrasonography Study for Breast Cancer Screening Effectiveness (Must Be) Trial**

Eun Jung Choi¹, Eun Hye Lee², You Me Kim³,
Sung Hun Kim⁴, Jae Kwan Jun⁵

¹Department of Radiology, Chonbuk National University Hospital, Korea

²Department of Radiology, Soonchunhyang University Bucheon Hospital, Korea

³Department of Radiology, Dankook University Hospital, Korea

⁴Department of Radiology, The Catholic University of Korea, Seoul St. Mary's Hospital, Korea

⁵Department of National Cancer Control Institute, Korea Cancer Center Hospital, Korea

PURPOSE: To evaluate interobserver agreements of breast ultrasound categorization based on the Breast Imaging Reporting and Data system (BI-RADS) and modified by the Alliance for Breast Cancer Screening in Korea (ABCS-K).

MATERIALS AND METHODS: Ten breast radiologists with 3-16 years of experience participated in a quality control workshop in March 2016 for the Mammography and Ultrasonography Study for Breast Cancer Screening Effectiveness (MUST BE) trial. Two investigators selected 125 sets of breast lesions, those were pathologically proven to be malignant or clinically proven to be benign showing stability for at least 2-years, and prepared power point slides showing 2 representative orthogonal images per each lesion. After a brief lecture about the modified categorization, 10 radiologists independently categorized the lesions blinding to mammographic images and pathologic results. The interobserver agreements were measured using kappa statistics.

RESULTS: The overall and overall weighted kappa values for the modified categorization (2, 3, 4, and 5) were 0.52 and 0.72, respectively. The overall kappa value was 0.66 when dichotomizing the interpretation into benign (BI-RADS 1, 2, and 3) or suspicious (BI-RADS 4, 5). However, those for the subdividing category 4 (a, b, and c) were 0.37

and 0.56, respectively. The overall kappa value was increased up to 0.48 when dichotomizing the interpretation into low suspicion (BI-RADS 4a) or over moderate suspicion (BI-RADS 4b and 4c).

CONCLUSION: In the modified categorization, ABCS-K radiologists showed moderate interobserver agreements for the decision of biopsy (category 2, 3 vs. 4, 5) and fair agreements for the subdividing category 4. More clear guidance for the modified categorization and further effort to improve interobserver agreements are needed for successful performance of MUST BE trial.

SE 023**Value of Combination of Shear-Wave Elastography and Color Doppler US for Preventing Unnecessary Excision of Equivocal Fibroepithelial Lesions Diagnosed by Core Needle Biopsy**

Ji Soo Choi, Eun Young Ko, Boo-Kyung Han,
Eun Sook Ko

Department of Radiology, Samsung Medical Center, Korea

PURPOSE: To evaluate the diagnostic value of shear-wave elastography (SWE) and color Doppler ultrasound (US) for preventing unnecessary surgical excision of equivocal fibroepithelial lesions (FELs) diagnosed by core needle biopsy (CNB).

METHODS: This retrospective study included 89 patients with equivocal FEL [FEL with a possibility of both fibroadenoma (FA) and phyllodes tumor (PT)] diagnosed by CNB. Of 89 patients, 78 underwent surgical or vacuum-assisted excision and 11 underwent follow-up US without excision. Mean elasticity (E_{mean}), maximum elasticity (E_{max}), and vascularity were determined by SWE and Doppler US for each lesion. For excised 78 FELs (52 FAs, 26 PTs), diagnostic performances were calculated to differentiate FAs and PTs. For non-excised 11 FELs, follow-up results were assessed.

RESULTS: In excised equivocal FEL, median E_{mean} and E_{max} were significantly lower for FAs than PTs (E_{mean}, 37.3 vs. 71.4 kPa, P=0.02; E_{max}, 46.8 vs. 78.5 kPa, P=0.03). Low vascularity (0-1 vessel flow) on color Doppler US were more frequent in FAs

than in PTs ($P < 0.01$). In differentiating between FAs and PTs, the combination of SWE and Doppler US with 'E_{mean} > 57.0 kPa or high vascularity (≥ 2 vessel flows)' showed a higher area under the curve (0.702) than SWE or Doppler US alone (0.648-0.663), and sensitivity and negative predictive value of combined modes were 100%. Of the 11 equivocal FELs without excision, two lesions with 'E_{mean} \leq 57.0 kPa and low vascularity' showed no change during follow-up. Among other nine non-excised FELs showing 'E_{mean} > 57.0 kPa or high vascularity', one (11.1%, 1/9) lesion showed interval increase in size during follow-up.

CONCLUSION: Equivocal FELs showing both low elasticity value and low vascularity were not upgraded to PTs on further excision. Our result suggests that combination of SWE and color Doppler US may help select patients with equivocal FELs diagnosed by CNB for whom further excision is not needed.

SE 024

Early Prediction of Response to Neoadjuvant Chemotherapy in Breast Cancer: Quantitative Analysis of Dynamic Contrast-Enhanced Ultrasound

Yun Ju Kim¹, Sung Hun Kim², Byung Joo Song³, Ahwon Lee², Bong Joo Kang²

¹Department of Radiology, National Cancer Center, Korea

²Department of Radiology, The Catholic University of Korea, Seoul St. Mary's Hospital, Korea

³Department of Surgery, The Catholic University of Korea, Bucheon St. Mary's Hospital, Korea

PURPOSE: To determine the diagnostic performance of dynamic contrast-enhanced ultrasound (DCE-US) parameters to predict response to neoadjuvant chemotherapy (NAC) in breast cancer patients.

MATERIALS AND METHODS: The institutional review board approved the study, and written informed consent was obtained from each patient. DCE-US was performed before and after 1 cycle of NAC in 39 patients with breast cancer. Various DCE-US perfusion parameters were obtained from single-section region of interest. After surgery, all DCE-

US parameters and their changes obtained before and after NAC were compared with histopathologic response using the Miller-Payne Grading system.

RESULTS: Twelve (30.8%) patients showed a good response (Miller-Payne grade 4 or 5) and 27 (69.2%) showed a minor response (Miller-Payne grade 1, 2, or 3). The % change in rise time was significantly higher in good responders than in minor responders. No statistically significant difference was found for the other parameters between the two groups. The statistical analysis for diagnostic performance showed that % change of rise time showed fair prediction (AUC 0.71).

CONCLUSION: Prolonged in-flow of contrast agent in the tumor was identified in good responders on DCE-US after first cycle of NAC.

SE 025

Development and Estimation of the Quality Control Program for Breast Ultrasound in Must-Be Trial: Initial Results

Hye Won Kim¹, Sun Hye Jeong², You Me Kim³, Keum Won Kim⁴, Jin Hwa Lee⁵, Eun Jung Choi⁶, Minseo Bang⁷, Yun-Woo Chang⁸, Jae Kwan Jun⁹, Eun Hye Lee²

¹Department of Radiology, Wonkwang University School of Medicine & Hospital, Korea

²Department of Radiology, Soonchunhyang University Bucheon Hospital, Korea

³Department of Radiology, Dankook University Hospital, Korea

⁴Department of Radiology, Konyang University Hospital, Korea

⁵Department of Radiology, Dong-A University Hospital, Korea

⁶Department of Radiology, Chonbuk National University Hospital, Korea

⁷Department of Radiology, Ulsan University Hospital, Korea

⁸Department of Radiology, Soonchunhyang University Seoul Hospital, Korea

⁹Department of Preventive Medicine, National Cancer Center, Korea

PURPOSE: The purpose of this study was to develop a quality control program for breast

ultrasound equipment and evaluate the effect and its management status.

MATERIALS AND METHODS: Ultrasound equipment from eight institutions participating in the Mammography and Ultrasonography Study for Breast cancer screening Effectiveness (MUST BE) trial were targeted. The breast imaging specialists of each institute were familiar with the examination methods and evaluation criteria through hands-on training using the standard phantom for breast ultrasound (ATS-550). The phantom image test consisted of items such as uniformity, accuracy, contrast resolution, spatial resolution, near field resolution and sensitivity. Safe and clean inspection consisted of the equipment factors (transducer, monitor, touch panel / keyboard, cord / cable, wheel, air filter) and environmental factors (lighting, ventilation, temperature and noise).

RESULTS: All 17 breast ultrasound equipment underwent quality control test. Uniformity was observed in 14 units (82%) while slightly non uniformity was observed in 3 (18%). The measured values in each item were compared with reference values (RV). Inaccuracy, mean axial diameter was 55.8 ± 1.6 mm (RV, 55 mm) and mean lateral diameter was 5.0 ± 0.4 mm (RV, 5 mm). Contrast resolution of anechoic sphere was $102.1 \pm 5.6\%$ (RV, 100%) and echogenic sphere was $99.5 \pm 4.3\%$ (RV, 100%). Axial and lateral spatial resolution in both proximal and distal groups was 0.6 ± 0.2 mm (RV, ≤ 1.0 mm). Near field resolution was 1.1 ± 0.2 mm (RV, 3.0 mm). Sensitivity was 6.1 ± 0.3 cm (RV, ≥ 5 cm) in filaments and 5.7 ± 0.6 cm (RV, ≥ 5 cm) in spheres. Clean and safe inspection was managed very well made in all equipment.

CONCLUSION: It is expected that it will be able to maintain efficient management and high quality image as a standardized breast ultrasound quality control test.

SE 026

Imaging Findings of Medullary Carcinoma of the Breast

Hyeon Ji Jang, Bo Bae Choi

Department of Radiology, Chungnam National University Hospital, Korea

OBJECTIVE: The objective of our study is to describe the mammographic, sonographic, and MRI findings of medullary carcinoma of the breast and compare each imaging findings.

MATERIALS AND METHODS: In recent 5 years, total 15 patients (mean age, 49.6 years; age range, 29-68 years) with pathologically confirmed medullary carcinoma or invasive ductal carcinoma with medullary features of the breast were retrospectively evaluated according to BI-RADS criteria given by the American College of Radiology. Mammography findings were reviewed for the followings : lesion type (mass, asymmetry, calcification) and mass characteristics (shape, margin, and density). Sonographic findings were reviewed for shape, margin, orientation, echogenicity, and posterior acoustic features. Breast MRI lesions were reviewed for lesion type (mass and nonmass like enhancement), enhancement pattern, and mass characteristics (shape, margin, and heterogeneity).

RESULTS: The most common mammographic features were a round or oval shape (8/13, 61.5%) and circumscribed margin (8/13). But three were indistinct margin. Two patients showed focal or global asymmetry on mammography, and the others were masses. On sonography, all masses were hypoechoic masses. Masses were irregular shaped (7/15), oval and round shaped (4/15). But microlobulating (7/15) and angulated marginated masses (3/15) also seen. All 12 tumors were seen as a mass on MRI. All patients showed rim enhancement with or without internal septation except one. Only one patient showed homogeneous internal enhancement on contrast-enhanced MRI. On histopathologic examination, 5 patients were diagnosed as medullary carcinoma and others were diagnosed as invasive ductal carcinoma with medullary features.

CONCLUSION: Medullary carcinoma of the breast appeared as an oval or lobular shaped mass with

circumscribed margin. It is difficult to differentiate medullary carcinoma with benign breast tumors using single imaging modality because of overlapping findings. As sonography and MRI provide additional useful findings, multimodality assessment is needed.

SE 027

Breast Lesions Correlation of the Ultrasound BI-RADS Classification with Pathologic Results

Sarnaitsetseg Munkhbat, Khulan Khurelsukh,
Zaya Duisyenbi, Altantsetseg Adiya,
Chantsalsuren Galbaatar
*Department of Radiology, Intermed Hospital,
Mongolia*

PURPOSE: The main goal of study is to determine correlations between the ultrasound (US) BI-RADS classification and pathology when assessing breast lesions.

MATERIALS AND METHODS: We analyzed ultrasound findings of 50 patients with breast lesion diagnosed in Radiology Department of Intermed Hospital from May 2014 to March 2016. The radiological findings are proven by core needle biopsy and excision biopsy. BIRADS category 2, 3, 4a are indicated benign lesions. BIRADS category 4b indicates suspicious lesion, 4c, 5 and 6 indicate malignant lesions. Pathologic test grouped into 4 groups as benign, suspicious, locally aggressive and malignant breast lesions. The research designed to collect data and assess by MS Excel and SPSS 21 analysis software.

RESULTS: Of total 50 patients, according to the category BI-RADS (2, 3, 4a, 4b, 4c, 5, 6) 2, 9, 24, 6, 5 and 2 patients were assessed into respectively. In pathologic results, two patients in BI-RADS 2(100%) were proved benign, 6(66.67%) patients diagnosed benign, 2(22.22%) patients were suspicious and one patient has malignant lesion from 9 patients categorized by BI-RADS 3. From 24 patients who were grouped into BIRADS 4a, 18(75%) were predicated benign lesion, 2(8.33%) were suspicious and 4(16.67%) were proved malignant lesion. Of 6 patients has BIRADS 4b, 4(66.67%) patients had benign lesions and 2(33.33%) patients were maintained malignant. 5 patients has assessed by

BIRADS 4c, 2(40%) were benign and 3(60%) were in malignant. About BIRADS 5 and 6 categories patients has confirmed malignant lesions in pathology. P value ($p=0.057$) indicates statistical significance between 2 entities.

CONCLUSION: This study showed that significant concordance exists between radiologic BIRADS classification and histologic result.

SE 028

Breast Augmentation: Pictorial Review of Ultrasonographic, Mammographic, and Magnetic Resonance Imaging Findings

Sang Soo Roh, Young Mi Park, Gi Won Shin,
Sun Joo Lee, Hye Jung Choo, Dong Wook Kim,
Yoo Jin Lee, Hae Woong Jeong
*Department of Radiology, Inje University Busan Paik
Hospital, Korea*

Recently, breast augmentation is growing in number throughout the world not only for simple cosmesis but also for breast cancer surgery. Accordingly, role of radiologists for interpreting the breast augmentation imaging becomes more important.

There are various types of surgical techniques and materials used in breast augmentation, and accordingly, there are various related complications. Therefore, radiologists should recognize the normal appearance of various types of breast augmentations at multiple imaging modalities. Also, recognition of the imaging features for breast augmentation-related complications can help exact and timely management, because these complications are often asymptomatic or have non-specific symptoms.

In this presentation, we review the normal imaging appearances of the breast augmentation to which implant materials including silicone and saline are used most commonly, using multiple imaging modalities including ultrasonography, mammography, and magnetic resonance imaging. Also, we review the imaging appearances of the unusual breast augmentation including silicone or paraffin injection, autologous fat augmentation, and polyacrylamide gel injection.

We also present some of complications that may be frequently encountered, including capsular

contracture, intracapsular rupture, extracapsular rupture, gel bleed, and mastitis.

Finally, we present an interesting case that breast cancer was detected within the augmented breast.

SE 029

Sonographic Findings of Radial Scar Detected on Screening Breast US

Jin Hwa Lee¹, Jae Hong Yoon¹, Eun Cho¹, Sujin Kim²

¹Department of Radiology, Dong-A University Hospital, Korea

²Department of Pathology, Dong-A University Hospital, Korea

PURPOSE: The purpose of this study was to investigate the sonographic features of the radial scar detected on screening breast ultrasound (US).

MATERIALS AND METHODS: Among the patients who had undergone screening breast US in this hospital from September 2004 to February 2015, we included patients who had radial scar at US-guided core needle biopsy (CNB). All cases had to have either subsequent vacuum-assisted (VAE) or surgical excision or minimum of 2 years of imaging follow-up. A total of 83 radial scars in 74 patients (mean age 44.5 years, range from 32 to 75 years) was included and its US features were analyzed.

RESULTS: Of the 83 lesions diagnosed as radial scar at US-guided CNB, 6 (7.3%) were combined with atypical ductal hyperplasia (AHD). VAE or surgical excision was performed in 14.5% (12/83) and the upgraded rates to ADH combined were 16.7% (2/12). None was upgraded to malignancy. Seventy one lesions (85.5%) were followed and all of them were stable during follow-up period (mean 35.7 months, range from 24 to 119 months). The size of lesions ranged from 3 mm to 17 mm (mean 7.5 mm) and the most common sonographic features were irregular, hypoechoic mass with indistinct margins and no posterior features.

CONCLUSION: Knowledge of the sonographic features of the radial scar which can be occasionally encountered in screening breast US may be helpful for the differential diagnosis of the various breast lesions.

SE 030

Role of Ultrasound: Hypoxia-Angiogenesis Pathway in Breast Cancer

Myoungae Kwon¹, Bo Kyoung Seo¹, Kyu Ran Cho², Ok Hee Woo³, Ju-Han Lee⁴, Jaehyung Cha⁵

¹Department of Radiology, Korea University Ansan Hospital, Korea

²Department of Radiology, Korea University Anam Hospital, Korea

³Department of Radiology, Korea University Guro Hospital, Korea

⁴Department of Pathology, Korea University Ansan Hospital, Korea

⁵Department of Medical Science Research Center, Korea University Ansan Hospital, Korea

Hypoxia-angiogenesis pathway is a main cause of tumor progression and metastasis. Hypoxia drives tumor angiogenesis; ineffectively-vascularized tumor tissue becomes hypoxic, stimulating angiogenesis to improve the influx of oxygen, thereby diminishing the angiogenic drive. Tumor hypoxia develops due to altered metabolism, uncontrollable cell proliferation and abnormal tumor blood vessels which lead to reduced transport of oxygen and nutrients. A master regulator of hypoxic response is the transcription factor, Hypoxia Inducible Factor 1 (HIF-1). HIF-1 α and HIF-2 α have been proven to be involved in all steps of blood vessel formation. Angiogenesis can be assessed with vascular endothelial growth factor (VEGF) receptor and microvessel density (MVD) on histopathology.

Recent breast ultrasound techniques allow characterizing gross morphology as well as quantitative assessment of tumor vascularity using superb microvascular imaging (SMI) and contrast-enhanced ultrasound (CEUS). The purpose of this exhibit is to demonstrate the role of breast ultrasound to understand tumor hypoxia-angiogenesis pathway and to contribute precision medicine. We will show the correlation of breast ultrasound findings with HIF-1, VEGF, and MVD in 98 breast tumors.

Acknowledgements: This research was conducted by 2016 Korea University Ansan Hospital R&D support project through the support of Vice President for Medical Affairs of Korea University special research funds (K1613741) and Toshiba Medical Systems

Korea Co.,Ltd.

SE 031

Breast Parenchymal Echogenicity and Neoadjuvant Chemotherapy in Postmenopausal Breast Cancer

Alisher Kakhkharov¹, Jamoliddin Kahhorov²,
Fatima Kakhkharova²

¹Department of Oncology and Radiology, Tashkent Medical Academy, Uzbekistan

²Department of Radiology, National Scientific Oncologic Center, Uzbekistan

OBJECTIVE: To analysis the correlation between breast parenchymal echogenicity and neoadjuvant chemotherapy features in breast cancer patients.

MATERIALS AND METHODS: 35 breast ultrasounds of postmenopausal patients with locally advanced breast cancer treated in 2014-2016 were analyzed. Breast parenchymal echogenicity were evaluated before starting neoadjuvant chemotherapy. Breast parenchymal echogenicity were divided into two groups: heterogenous and homogenous one. Radical mastectomy was performed on 14 days after completion chemotherapy cycles. Histological response was evaluated according to NSABP B-18 classification.

RESULTS: 12 (34,2%) of patients had heterogenous breast parenchymal echogenicity and 23 (63,8%) homogenous one. In group of patients with heterogenous breast parenchymal echogenicity more commonly there were no response for 1st line of chemotherapy (antracycline-based) and after 2 or 3 cycles they started receiving taxane-based chemotherapy (75% vs. 43,5% respectively $p < 0,050$) and patients of this group usually received more cycles (6-8 cycles) than in patients with homogenous breast parenchymal echogenicity. Patient with homogenous breast parenchymal echogenicity had more pCR than patients with heterogenous one (16,6% vs. 39,1% respectively $p < 0,050$).

CONCLUSION: Breast parenchymal echogenicity correlated with efficiency, quantity and pathological response of neoadjuvant chemotherapy of postmenopausal breast cancer patients.

SE 032

Ultrasound Signs of Breast Cancer as Risk Factors of Further Metastases Development

Nigora Atakhanova¹, Alisher Kakhkharov¹,
Jamoliddin Kahhorov²

¹Department of Oncology and Radiology, Tashkent Medical Academy, Uzbekistan

²Department of Radiology, National Scientific Oncologic Center, Uzbekistan

OBJECTIVE: To determine ultrasound signs of breast cancer which can serve as risk factors of further metastases development.

MATERIALS AND METHODS: Retrospective analyzes of 58 patients with breast cancer which were treated from 2010 to 2016. They were divided into 2 groups: I group-32 patients with further metastatic disease which was developed during 5 years after complex treatment, 36 patients without any signs of metastases during 5 years after treatment. Multifactorial analyzes was done.

RESULTS: T3-T4 size ($RR = -8,217$, $p < 0,050$), invasion to skin ($RR = -12,010$, $p < 0,050$), heterogenesity ($RR = -10,688$, $p < 0,050$), posterior shadowing ($RR = -6,354$, $p < 0,050$) and hyperechogenic rim ($RR = -7,389$, $p < 0,050$) are risk factors of metastatic disease development during 5 years after complex treatment completion.

CONCLUSION: Detection of risk factors can help to select patients with high risk of metastases development and differentiate the approach for breast cancer patients management.

SE 033**Imaging Features of Lobular Neoplasia in the Breast Diagnosed at Ultrasound-Guided Biopsies**

Ik Jung Hwang, Young Mi Park, Gi Won Shin,
Sun Joo Lee, Hye Jung Choo, Dong Wook Kim,
Yoo Jin Lee, Hae Woong Jeong

Department of Radiology, Inje University Busan Paik Hospital, Korea

PURPOSE: The purpose of our study was to evaluate the imaging features of lobular neoplasia (LN) in the breast diagnosed at ultrasound-guided needle biopsy and evaluate the surgical pathology outcome of these lesions.

MATERIALS AND METHODS: Of the 5196 ultrasound-guided breast biopsies performed from January 2004 through March 2017, 27 yielded a diagnosis of LN. The LN, which were incidentally detected with other benign pathology (n=5), arised from fibroadenoma (n=2) or phyllodes tumor (n=1), appeared as microcalcifications (n=4), found with breast cancer (n=3) or have not available sonographic images (n=2), were excluded. Finally, 10 LN in 9 patients were included. Imaging features were analyzed in consensus by two radiologists. Correlation of biopsy findings with surgical pathologic results was performed.

RESULTS: Ten LN lesions were all women (mean age, 48 years; age range, 33-70 years). On sonography, LN lesions (mean size, 16.3 mm) appeared as 5 masses, 4 non-masses, one intraductal lesions. Five masses had commonly irregular shape (3/5, 60%), non-spiculated margin (4/5, 80%), iso- or hypoechoic echotexture (4/5, 80%), no posterior acoustic features (4/5, 80%), and parallel orientation (3/5, 60%). All but one LN were categorized as BI-RADS category 4 (9/10, 90%). Of the two LN that were seen on mammography (2/9, 22.2%), one appeared as architectural distortion and the other focal asymmetry. On MRI which were available in 7 LN, five were visualized, showing 3 nonmasses and 2 masses. All ten lesions were excised surgically, and pathology results led to an upgrade in two lesions (2/10, 20%).

CONCLUSION: LN diagnosed at ultrasound-guided breast biopsy did not show any specific imaging features and were associated with a 20%

underestimation rate. Therefore, LN diagnosed at ultrasound-guided biopsy should be managed by prompt surgery.

SE 034**Efficacy of Doppler Ultrasonography to Detect and Differentiate MR-Detected Breast Lesions**

Hankyul Kim, Boo-Kyung Han, Eun Young Ko,
Eun Sook Ko, Ji Soo Choi, Joo Hyun Park
Department of Radiology, Samsung Medical Center, Korea

PURPOSE: To evaluate the presence of vascularity of MR-detected Breast Lesions on Doppler US and to compare the vascularity grade between benign and malignant lesions.

METHODS: Ninety seven patients with breast cancer who had 101 MR-detected additional lesions were enrolled in this study. Reference standard was histologic results by core or surgical biopsy. The size of US lesions, MR and US BI-RADS category, Doppler grade from 1 to 3 (1; no vascularity, 2; perilesional, scattered or traversing vascularity, 3; intralesional, centripetal, or concentrated vascularity) were recorded. MR category, US category and Doppler grade were compared with final results.

RESULTS: Sixty were malignant (n = 43) or high risk lesions (n = 17) and 41 were benign. Doppler vascularity was seen in 66 of 101 total lesions (65.3%) and 49 of 60 risky lesions (81.6%). While 11 of 35 Doppler grade 1 lesions (31.4%) were risky lesions, among the 51 Doppler grade 3 lesions, 39 (76.4%) were risky lesions. The difference was statistically significant (p = 0.0001). Benign lesions with Doppler grade 3 vascularity were fibroadenomas (n = 6), sclerosing adenosis (n = 2), intramammary lymph nodes (n = 2) or columnar cell change (n = 2). Malignant lesions with Doppler grade 1 vascularity were invasive ductal cancer (n = 3), invasive lobular cancer (n = 1), ductal carcinoma insitu (n = 2) and mucinous cancer (n = 1), and all except mucinous cancer showed US BI-RADS category 4B or more. Low suspicion category lesions on both MR and US with grade 1 or 2 vascularity showed no malignancy.

CONCLUSION: Doppler US is useful to identify US abnormality concordant with MR enhancement.

High Doppler vascularity could raise a malignancy potential and low Doppler vascularity with non-suspicious morphologic features could exclude a malignancy.

SE 035

Contrast-Enhanced US Parameters in Breast Cancer: Correlations with Prognostic Factors

Youn Joo Lee¹, Sung Hun Kim², Bong Joo Kang², Yun Ju Kim³

¹Department of Radiology, The Catholic University of Korea, Daejeon St. Mary's Hospital, Korea

²Department of Radiology, The Catholic University of Korea, Seoul St. Mary's Hospital, Korea

³Department of Radiology, National Cancer Center, Korea

PURPOSE: To correlate the value of contrast-enhanced ultrasound (CEUS) with prognostic factors and subtypes of invasive carcinoma.

METHODS: The study included 24 breast cancer patients who were treated with NAC. All patients conducted CEUS, using three different region of interest (ROI). ROI 1 was placed on the hotspot area, ROI 2 on the enhanced total tumor, ROI 3 on the entire tumor area of gray-scale US. The parameter peak enhancement, wash-in (Wi) area under curve (AUC), wash-out (Wo) AUC, WiWoAUC, wash-in rate, wash-out rate, rise time, falltime, mean transit time, time to peak, wash-in perfusion index, ROI area, quality of fit were measured. The status of estrogen receptor (ER), progesterone receptor, human epidermal growth factor receptor 2 gene amplification, and Ki-67 proliferative index were assessed by immunohistochemistry.

RESULTS: No quantitative CEUS parameters using three different ROIs showed significant difference between low grade (grade 1, 2) and high histologic grade (grade 3). Neither do qualitative parameters. While, a statistically significant difference between ER negative (21522.37 ± 14352.96 a.u) and ER positive group (42205.15 ± 23876.65 a.u) was detected in the mean WiAUC values of ROI3 ($P=0.022$). The mean WiAUC, WoAUC, WiWoAUC, Wi perfusion index values of ROI3 also differentiated between the ER-positive group and the ER negative

group, and between non-triple-negative group and triple-negative group ($P<0.05$).

CONCLUSION: The CEUS parameters were helpful in differentiating subtypes, but could not predict the histologic grade.

SE 036

Doppler Ultrasonography Features of Breast Cancer

Fatima Kakhkharova¹, Jamoliddin Kahhorov¹, Alisher Kakhkharov²

¹Department of Radiology, National Oncologic Scientific Center, Uzbekistan

²Department of Oncology and Radiology, Tashkent Medical Academy, Uzbekistan

BACKGROUND: Ultrasound picture of breast cancer is very variable one. Doppler ultrasound provides useful information about blood flow in tumor and peritumoral area, which diseases can help to distinguish malignant from benign breast masses.

AIM: To determine doppler specific features of breast cancer.

MATERIALS AND METHODS: 28 Doppler ultrasounds of breast cancer and 32 benign tumors were analyzed. The following parameters were studied: maximal systolic speed, minimal diastolic speed, index of pulsation, resistant index, quantity of tumor vessels, type of vascularization.

RESULTS: Doppler features of breast cancer were: peak systolic blood speed 35,5 cm/s, absence of final diastolic blood speed in mass, mixed type of vascularization, increased number of tumor vessels. Different sides of tumor vascularization were noticed in breast cancer: in central part of tumor-53,6%, in peripheral part- 28,5%, avascular tumors were found in 17,9%. Benign tumors mostly were avascular one (71,9%), and with peripheral vascularization (28.1%). Index of pulsation and index of resistance were higher in malignant ($IP=1,43 \pm 0,02$, $IR=0,71 \pm 0,03$) than in benign ($IP=1,18 \pm 0,05$, $IR=0,61 \pm 0,03$).

CONCLUSION: Doppler sonography should be used routinely in daily practice of breast radiologist, due to high sensitivity and specificity.

SE 037**Breast Diseases Involving the Whole Breast: Clinicopathologic and Imaging Features**Gi Won Shin¹, Young Mi Park¹, Suk Jung Kim², Hyun Kyung Jung²¹Department of Radiology, Inje University Busan Paik Hospital, Korea²Department of Radiology, Inje University Haeundae Paik Hospital, Korea

Some breast diseases can sometimes grow tremendously and lead to involve the entire breast. These diseases can be benign or malignant. We present benign diseases such as huge hamartomas involving both breasts and left axilla, rapidly growing giant fibroadenoma with infarction, extensive mastitis, diffuse breast edema caused by non-mammary origin, and malignant ones such as advanced breast carcinoma, malignant phyllodes tumor, multiple myeloma involving both entire breasts, and diffuse bilateral infiltrative metastases from signet ring cell gastric cancer. It is helpful for the exact diagnosis and proper management to know these diseases and their imaging findings.

SE 038**Silicone Injection of Breasts and Gluteal Region: Correlation of Ultrasound and Computed Tomography Scan Findings**

Ming Huan Cheng, Yin Eie Teo

Department of Radiology, Keningau Hospital, Malaysia

Over many decades silicone injections have been used globally for cosmetic breast and buttock augmentations. We present a case report on ultrasound and Computed Tomography (CT) scan findings in a 39-year-old woman. She initially presented with history of gestational trophoblastic disease, underwent CT Thorax and Abdomen for staging. CT scan showed multiple isodense soft tissue nodules of various sizes with surrounding fat streakiness, evenly distributed in both breasts and both gluteal regions. Ultrasound images demonstrated multiple anechoic cystic lesions surrounded by extensive echogenic regions with

acoustic shadowing, giving rise to “snowstorm” appearance. On further clinical history, she claimed to have approached an aesthetic practitioner and received silicone injections in both breasts and gluteal region 10 years ago. This case report emphasizes the importance of clinical history and radiological findings of silicone injections in order to avoid misinterpretation of images as tumor, which could cause patient discomfort and unnecessary biopsy procedure.

SE 039**Complication after Breast Implants**Otgontuya Tserenjav¹, Tumendemberel Danga², UI-Oldokh Sumya²¹Department of Radiology, National Second Hospital of Mongolia, Mongolia²Department of Radiology, Khovd Province Hospital, Mongolia

BACKGROUND: This complication occurs in 2%-4% of patients, and is usually from bacteria that normally live on the skin. Infected implants put the patient at additional risks including: scar contracture, wound separation, and (in very rare cases) a severe illness called Toxic Shock Syndrome.

KEY WORDS: breast implantation, complications after surgery

A 34-year old female. Had a breast implantation in foreign country. After some time came to hospital with symptoms such as pain, redness, swelling, and fever.

Ultrasound of both breasts: Linear hypoechoic area in 3-4 o'clock direction of right breast. Large irregular margined hypoechoic portion in right parasternal region s/o abscess formation.

MDCT of chest: Large sized, irregular hypo densities internal gas bubbles with slight peripheral enhancement in right parasternal chest wall. No significant bone (sternal) destruction. Impression was of right sided parasternal elongated fluid infiltration, abscess internal gas bubbles with s/o stochondritis.

Laboratory test: Chemistry test showed us that CRP was 5.4 which is really high.

CBC Routine showed us that W.B.C was 15 which is

elevated.

In MIC tests: WBC was elevated and No bacteria test results were RBC-many.

CONCLUSION: Breast and Parasternal abnormalities such as abscess formation are identifiable by Breast sonography. However, extension of abnormalities such as costal abnormalities are proved by CECT.

SE 040

Spontaneous Infarction of Phyllodes Tumor of the Breast in a Postpartum Woman:

A Case Report

Yoogi Cha, Hye Won Kim

Department of Radiology, Wonkwang University School of Medicine & Hospital, Korea

Phyllodes tumor of the breast in a pregnant woman is rare, and spontaneous infarction of this tumor has not been reported to date. Infarction could usually develop in malignant tumors of the breast in different mechanism and pathogenesis. Breast tumor infarction in pregnant women is uncommon, except for fibroadenomas. The authors report a case of spontaneous infarction of a benign phyllodes tumor in a 30-year-old postpartum woman that exhibited rapid growth during late pregnancy, and discuss imaging findings.

SE 041

Benign Skin Lesion in Premammary Zone of the Breast Mimicking Malignant Breast Parenchymal Lesion: A Case Report

Jae Hong Yoon¹, Jin Hwa Lee¹, Eun Cho¹, Sujin Kim²

¹*Department of Radiology, Dong-A University Hospital, Korea*

²*Department of Pathology, Dong-A University Hospital, Korea*

Various benign and malignant lesions occur in premammary zone, as a primary lesion or secondary involvement by systemic disease. Although relatively uncommon, benign and malignant breast parenchymal lesions arising from anterior terminal duct lobular units are encountered within the premammary layer, and differential diagnosis

between skin and superficial parenchymal lesions is necessary. The anatomic structures of the nipple-areolar complex (NAC) are somewhat specialized, and we should understand its anatomy. Herein, we report a case of trichoblastoma which is detected in premammary zone of the NAC area, mimicking breast parenchymal lesion in a 48-year-old female patient.

SE 042

A Rare Case of Solitary Fibrous Tumor of the Breast: Radiologic Findings and a Brief Review

So Yeon Park¹, Ok Hee Woo¹, Hye Seon Shin¹, Kyu Ran Cho², Bo Kyoung Seo³

¹*Department of Radiology, Korea University Guro Hospital, Korea*

²*Department of Radiology, Korea University Anam Hospital, Korea*

³*Department of Radiology, Korea University Ansan Hospital, Korea*

Solitary fibrous tumor (SFT) is a rare group of spindle cell neoplasm, categorized under intermediate fibroblastic tumor having rarely metastasis. It usually occurs in the pleura (1), but extrapleural SFT has been reported including the retroperitoneum, deep soft tissues of the proximal extremities, abdominal cavity and head and neck. However, SFT is very rare in the breast, with less than 20 cases reported in the English literature without any case involving local recurrence or metastases. To our knowledge, there are few case reports of recurrent solitary fibrous tumor of the breast with imaging findings, and the analysis of radiologic findings is limited. Herein, we present mammography, sonography and MRI findings of SFT in the breast of a 63-year-old female patient with recurrence of the tumor twice.

This patient represents with the history of right breast enlargement since 2 months. The mammography and the breast ultrasonography (US) showed a large oval circumscribed mass, which has heterogeneous echogenicity in US. Five months after mass excision, the patient complained of palpable mass at the previous operative site. Breast MRI revealed a 9.0 × 5.7 × 5.0 cm-sized bilobulated oval shaped mass with circumscribed margin with low

SI on T1WI and heterogeneously high SI on T2WI showing a homogeneously enhancing pattern with internal necrotic portion with a type III kinetic curve.

SE 043

Breast Cancers with Unusual Site Presentation

Hye Seon Kang, Bo Bae Choi

Department of Radiology, Chungnam National University Hospital, Korea

Breast cancer has been the second leading cause of all cancers since 2004. Breast cancer is most commonly originated from the terminal ductolobular Unit in glandular tissues. Among breast cancer types, IDC accounts for about 90% of all breast cancers. Others are invasive lobular carcinoma, medullary carcinoma, tubular carcinoma, mucinous carcinoma, papillary carcinoma, adenocarcinoma, apocrine carcinoma, adenocystic carcinoma, secretory carcinoma, papillary lesions of the nipple and malignant follicular tumor.

Breast cancer is often metastasized to the bone, lung, liver, and central nervous system in order. It is rare that tumor cells metastasis from other organs to the breast tissue. Clinically, 0.3% to 2.7% of breast cancers are reported to have metastasized from other organs to the breast tissue. Cancers of other organs that metastasize to the breast include melanoma, lung cancer, Ovarian cancer, kidney cancer, Gastro-Intestinal cancer.

In this exhibition, at first we illustrate mammography and ultrasonography findings of Breast cancer showing at unusual site presentation.

Invasive ductal carcinoma in pectoralis muscle, Invasive tubular and cribriform carcinoma in axillary,

Invasive ductal carcinoma only in axillary except breast glandular tissue

At second, We introduce mammography, ultrasonography and MRI findings of Breast cancer showing at Unusual metastasis.

Cutaneous metastatic breast cancer, Metastatic breast cancer from gastric adenocarcinoma, Metastatic breast cancer from leukemia.

This exhibition shows very unusual and rare case of breast cancers.

It will be very help to study specific breast cancer.

SE 044

Breast Cancer

Tumenjargal Lkhagvasuren,

Gonchigsuren Lkhagvasuren

Department of Radiology, National Trauma Center, Mongolia

INTRODUCTION: Invasive breast cancer is a heterogeneous disease regarding its clinical presentation, pathological classification and clinical course. Most tumors are derived from mammary ductal epithelium, mainly the terminal duct-lobular unit and up to 75% of the diagnosed infiltrating ductal carcinoma are defined as invasive ductal carcinoma. Invasive lobular carcinoma, which comprises up to 15%, is the second most common epithelial type. Many risk factors for the development of breast cancer have been identified through epidemiological studies. Gene profiling led to the discovery of different molecular subtypes with phenotypic diversity concerning clinical outcome, including response to treatment, disease-free survival and overall survival. Nowadays, local advanced disease is not frequently seen as in the past because of the availability of information and the widespread use of screening mammography. However, advanced local disease may be found as in the present report.

SE 045

Diagnostic Benefits of Ultrasonography-Guided Biopsy Compared with Mammography-Guided Biopsy for Suspicious Microcalcifications without Definite Mass

Ji Youn Kim, Min Jae Yoon, Keum Won Kim,

Yoong Joong Kim, Jae Young Seo, Chul Mok Hwang

Department of Radiology, Konyang University Hospital, Korea

PURPOSE: To compare the diagnostic benefits of ultrasonography-guided core needle biopsy (US-CNB), rather than USG-guided localization with excisional biopsy (US-LEB), mammography-guided localization excisional biopsy (MG-LEB) and

stereotactic-guided vacuum assisted biopsy (S-VAB) for diagnosing suspicious breast microcalcifications without definite mass.

MATERIALS AND METHODS: We retrospectively reviewed 178 cases of suspicious breast microcalcification lesions without a definite mass on mammography. We enrolled patients who underwent image-guided biopsies. US-CNB (n=47) and US-LEB (n=72) were performed for almost US-visible microcalcification. MG-LEB (n=32) and S-VAB (n=27) were performed for mammogram-only visible lesions. Mammographic findings and false negative rates were analyzed. Histological diagnosis and Breast Imaging Reporting and Data System (BI-RADS) category were evaluated.

RESULTS: Among the total lesions associated with microcalcifications, 119 of 178 cases (66.9%) were identified sonographically. US-visible microcalcifications were more likely to be malignant (27.7% vs. 11.9%, $p=0.012$) and higher BI-RADS category (32.8% vs. 15.3%, $p=0.019$). The false negative rate was 10.0% (4/40) among the 40 lesions confirmed as malignant. Three false negative cases were detected in US-CNB and one case in S-VAB. The presence of microcalcifications within a mass or a ductal dilation on ultrasonography showed a significant higher malignant rate (72.7% vs. 17.5%, $p<0.001$).

CONCLUSION: Ultrasonography-guided core needle biopsy is an accurate and acceptable biopsy method for US-visible microcalcification lesions. US-visible microcalcifications are higher in BI-RADS category and higher malignant rate than US-invisible microcalcifications.

Cardiovascular

SE 046

The Correlation of Epicardial Adipose Tissue by Echocardiography to Acute Coronary Syndrome

Uranzaya Ganbold, Enkhbold Sereejav

Department of Radiology, The First Central Hospital of Mongolia, Mongolia

PURPOSE: The purpose of this article is to describe an echocardiography protocol optimized for correlation of epicardial adipose tissue and acute coronary syndrome.

MATERIALS AND METHODS: One hundred and sixty patients (135 males and 25 females with mean age of 54.94 ± 8.87 , respectively) admitted for coronary angiogram underwent assessment of epicardial adipose tissue thickness by echocardiography. Epicardial adipose tissue thickness was measured on the free wall of right ventricle in parasternal long- and short-axis views at end-systole for 3 cardiac cycles. Subjects were segregated into the acute coronary syndrome group and control group.

RESULTS: Mean epicardial adipose tissue thickness was higher in patients with acute coronary syndrome than in the control group (5.46 ± 0.70 vs. 3.02 ± 0.68 mm, $p<0.001$). Epicardial adipose tissue thickness was larger in patients with myocardial infarction than in patients with unstable angina (5.59 ± 0.72 vs. 5.14 ± 0.56 , $p<0.005$). EF was lower in patients with myocardial infarction than in patients with unstable angina (53.4 ± 8.07 vs. 58.5 ± 6.57 , $p<0.006$).

CONCLUSION: Increased epicardial adipose tissue is strongly associated with acute coronary syndrome. Mean epicardial adipose tissue thickness was higher in patients with myocardial infarction than in patients with unstable angina.

KEY WORDS: Acute coronary syndrome, Echocardiography; Epicardial adipose tissue

SE 047**Sonographic Evaluation of Caval Index(C.I) for Prevention of Volume Overload Induced Lung Edema in Intensive Care Unit; Noninvasive Examination of Intravascular Volume Status**

Heung Cheol Kim, Ko Eun Yang, Sook Namkung, Myung Sun Hong

Department of Radiology, Chuncheon Sacred Heart Hospital, Korea

OBJECTIVE: As evaluation of IVC, to prevent lung edema caused by inappropriate intravascular volume management.

METHODS: 15 patients admitted to ICU were enrolled. All patients underwent chest X-ray, routine laboratory tests and ultrasound examination. The caval index (C.I) was determined by transabdominal ultrasonography in supine position; measuring the IVC diameter and collapsibility during inspiratory and expiratory phases of the respiratory cycles.

$C.I(\%) = (\text{expiratory IVC diameter} - \text{inspiratory IVC diameter}) / \text{expiratory IVC diameter} \times 100$.

We divide the C.I into 3 groups: lower in <20%, intermediate in 21~50%, high in >50%.

RESULTS: In all patients, the vital signs were stable. The mean IVC diameter and C.I were 1.48 cm (range from 0.74 to 2.77 cm) and 27.76%(range from 8.5 to 60%). The lower, intermediate and higher C.I groups were 4, 9 and 2 patients, respectively. Of intermediate and high C.I group, there weren't any patients of renal dysfunction on laboratory tests and lung edema on chest X-ray. 3 patients showed lung consolidations, representing lung edema on chest X-ray and they all were below 10% of C.I (lower C.I group). Of them, 1 patient had signs of renal dysfunction and 1 patient was suspicious combined pneumonia. But we couldn't clear differentiate consolidations by pneumonia from edema on chest X-ray alone. Depending on results of C.I, intravascular volume was controlled and lung edema has subsided rapidly but pneumonia induced consolidation still remained.

CONCLUSION: Ultrasonic examination of the IVC is to aid in assessment of the intravascular volume status of patients. Particularly, this may be useful in ICU patients who need for more careful volume regulation, such as renal dysfunction and in case of

poor differentiation whether pneumonia is combined or not in patient with lung edema on chest X-ray.

Genitourinary

SE 048**First Trimester Biometric Differences in Ethnic Mongolian Population**

Bayanjargal Ochirpurev, Mendsaikhan Gochoo, Erdembileg Tsegmed, Munkhtsetseg Davaasuren
Department of Obstetrics and Gynecology,
Mongolian National University of Medical Science,
Mongolia

PURPOSE: First trimester fetal biometric assessment is very important for the accurate estimation of gestational age to conduct optimal antenatal care. This is the first study to construct the first trimester Mongolian fetal standard biometry which is to answer the following questions; Which widespread first trimester fetal nomogram is similar to Mongolian fetal biometry, are there any unique fetal characteristics in Mongolian ethnic groups?

MATERIALS AND METHODS: In accordance with inclusion and exclusion criteria 658 healthy women between 11-14⁺⁶ weeks of gestation examined on the following fetal biometric measurements: biparietal diameter (BPD), head circumference (HC), abdominal circumference (AC) and femur length (FL). The study occurred between Jan 2013 to April 2014 Combined measurement of abdominal and vaginal examination was done. Physicians who worked for more than 10 years in the field of obstetrical ultrasound are required to do at least three measurements to get correct results. Statistical analysis was performed with SPSS-21, E-View, and Windows Excel. A regression model was developed with biometric measurements and was compared to widespread nomograms in the world.

RESULTS: The obtained Mongolian first trimester standard fetal biometry was compared to Hadlock from Europe, M.A.Esetov from the same geographic region, Osaka from Asia, ASUM from the reference of Australia. BPD was 4-6 mm longer, HC was 20-

13 mm longer than Hadlock but it was the same as others. FL was a bit shorter than Hadlock and ASUM but it was the same as Osaka and M.A.Esetov at 12-14⁺⁶ weeks of gestation.

CONCLUSION: Difference with the obtained nomograms may be due to ethnic differences of the Mongolian fetal development. Current study shows that there are needs to use separate growth chart to estimate accurate gestational age for Mongolian population.

SE 049

Retrospective Comparison of Renal Ultrasonographic and Clinical Findings in Patients with Rhabdomyolysis

Jae-Joon Chung, Eun-Suk Cho, Joo Hee Kim, Jeong-Sik Yu

Department of Radiology, Gangnam Severance Hospital, Korea

PURPOSE: To retrospectively compare the ultrasonographic and clinical findings between two groups with abnormal and normal ultrasonographic findings of kidneys who clinically diagnosed as rhabdomyolysis.

MATERIALS AND METHODS: A total of 78 patients were divided into two groups: A group with abnormal renal ultrasonographic findings and B group with normal renal ultrasonographic findings. Blood urea nitrogen, creatinine, potassium, prothrombin time, activated partial thromboplastin time (aPTT), creatine kinase, myoglobin in serum and urine, dark urine and microscopic hematuria were assessed, which were checked within 3 days before or after renal ultrasonography. All data were statistically analyzed using student's t-test or Mann-Whitney U test.

RESULTS: The most common cause of the rhabdomyolysis in this study was intense exercise, followed by general weakness, muscle ache, intense shivering from generalized tonic seizure, drug intoxication, burn, and operation or trauma, etc. On renal ultrasonography of group A (n=26; M:F=19:7; mean age, 48.7 years), both kidneys show enlarged size, increased cortical thickness and diffusely decreased cortical echogenicity, suggestive of acute

and diffuse renal disease. Group A showed elevated blood urea nitrogen, creatinine, potassium, and prolonged aPTT compared with those in Group B (n=52; M:F=36:16; mean age, 41.6 years), which were statistically significant (p value < 0.01). Other parameters including prothrombin time, creatine kinase, myoglobin in serum and urine, dark urine and microscopic hematuria showed no statistical difference between two groups.

CONCLUSION: The patients with elevated blood urea nitrogen, creatinine, potassium, and prolonged aPTT showed the renal ultrasonographic findings of acute and diffuse renal disease, but other parameters showed no statistical difference between two groups with rhabdomyolysis.

SE 050

Ultrasonographic Appearance of Tumors of the Testis; Radiologic-Pathologic Correlation

Yongsoo Kim, Young Seo Cho, Sanghyeok Lim
Department of Radiology, Hanyang University Guri Hospital, Korea

INTRODUCTION: Ultrasound of the scrotum is the primary and comfortable image modality and highly accurate in differentiation between extratesticular and intratesticular, and differentiation between solid and cystic lesions. We analyzed correlation of sonographic and pathologic finding of the various testicular tumors.

METHOD: The purpose of this exhibit is to correlate the US imaging features of tumors of the testis with their pathologic findings. Illustrative cases will include seminoma, mature teratoma, immature teratoma, yolk sac tumor, mixed germ cell tumor, leukemia, lymphoma, and Leydig's cell tumor.

DISCUSSION: Testicular tumors are divided into two categories; germ cell and non-germ cell tumor. Those of germ cell origin make up 90% to 95% of primary testicular tumors and are generally highly malignant. By contrast, non-germ cell tumors are generally benign.

CONCLUSION: The typical US imaging features along with the corresponding microscopic and gross pathology can be seen here. Seminoma, leukemia, and lymphoma revealed homogeneous hypoechoic

mass. Leydig's cell tumor, teratoma, and mixed germ cell tumors contained cystic lesion. Teratoma, yolk sac tumor, and mixed germ cell tumor contained calcifications. Differential diagnoses will be presented as well as the role of US imaging in characterization of these tumors.

SE 051

Value of Renal RFA with CEUS as a Problem Solving Tool for a RCC in a Solitary Kidney and with Chronic Renal Disease

Shenaz Momin¹, Asif Momin¹, Avinash Gutte²

¹Department of Radiology, Prince Aly Khan Hospital, Mumbai, India

²Department of Radiology, Sir J J Hospital, Mumbai, India

Use of CEUS to delineate renal masses prior and after RF ablation is an effective and desirable tool in patients with renal failure or those with a solitary kidney thus avoiding use of CECT.

RFA was done in both cases using multipronged monopolar RF ablator (RITA -Angiodynamics).

The subcapsular location of these renal lesions allowed us to avoid CECT and easily use ultrasound (Siemens S 3000).

Additional hydro dissection was used with 5% DW to separate right lobe of liver and colon away from the lesion. For better visualisation colour doppler imaging and US contrast (Sonovue, Bracco) was used during and immediately after the procedure, deciding the end point of ablation during single session. This technique was effective in treating these lesions; preserving renal parenchyma without the risk of post operative co-morbidities or prolonged hospital stay.

One year follow-up in both our cases showed excellent response satisfactory loco-regional control. The surgeon's acceptance level also was also encouraging. No complications were noted in our cases. US guided Renal RFA with contrast enhancement can be an option for partial nephrectomy or CECT with iodinated contrast in CRF or single kidneys.

SE 052

US of Prostate Masses

Dong Won Kim, Seong Kuk Yoon

Department of Radiology, Dong-A University Hospital, Korea

Ultrasonography is a first line imaging technique for evaluation of the prostate because it is almost universally available, in noninvasive, does not require ionizing radiation. Transrectal US (TRUS) is the most widely used imaging method for prostate masses because it is readily available, repeatable, and relatively inexpensive.

Prostate tumors are subdivided into epithelial, neuroendocrine, prostatic stromal, mesenchymal, hemolymphoid, miscellaneous, and metastatic tumors. More than 95% of malignant tumors of the prostate are adenocarcinomas arising from the prostatic epithelium. Focal masses or diffuse involvement may be neoplastic or non-neoplastic disorders with inflammatory, hyperplasia, and infectious causes. Clinical, macroscopic, and radiologic findings for these masses may overlap; thus, histologic evaluation is required.

SE 053

Contrast-Enhanced Ultrasonography (CEUS) Findings of Solid and Cystic Lesions in Kidney

Jung Hun Lee, Young Hwan Lee

Department of Radiology, Wonkwang University School of Medicine & Hospital, Korea

LEARNING OBJECTIVE: To identify the CEUS findings of various solid and cystic lesions in kidney. CEUS is widely used for a variety of disease in kidney, and it enables real-time detection of microvascular blood flow. So, CEUS is useful for evaluating focal solid hypovascular and atypical cystic masses, which are difficult to differentiate by contrast-enhanced CT. Also, CEUS have shown good diagnostic accuracy to classify cysts using the Bosniak classification. Furthermore, CEUS showed improved characterization of complicated cysts that were indeterminate on CT.

We retrospectively reviewed the imaging findings of CEUS in patients who underwent CEUS from

March 2012 to March 2017 at our hospital. We evaluated variable parameters such as cystic and solid component, internal septation, thick wall, calcification, and enhancement pattern. And we included cases which were pathologically confirmed. Most of these cases were diagnosed as renal cell carcinoma (RCC) (n=32). Other cases were oncocytoma (n=1), angiomyolipoma (n=4), benign cyst (n=9), metastasis (n=1), and tuberculosis (n=1). **CONCLUSION:** CEUS is very helpful for characterizing cystic and solid masses which were difficult to differentiate on CECT and classifying complex renal cysts by Bosniak system.

SE 054

Intratesticular Focal Hypoechoic Lesions: Sonographic and Clinical Findings

Dal Mo Yang, Hyun Cheol Kim, Sang Won Kim, Ji Su Kim

Department of Radiology, Kyung Hee University Hospital at Gangdong, Korea

Sonography with a high frequency transducer is the imaging modality of choice for the scrotum. Most intratesticular lesions are seen as hypoechoic lesions. The differentiation of intratesticular hypoechoic lesions as either malignant or benign lesion is important because the treatment of these lesions is different. In this paper, we review the sonographic and clinical features of different types of intratesticular focal hypoechoic lesions, such as testicular cysts, benign and malignant testicular tumors, testicular inflammatory lesions, segmental testicular infarction and testicular trauma.

SE 056

Prenatal Ultrasound of Multiple Gestations: Check Points and Common Abnormalities

Seonghwan Byun, Boem Ha Yi, Hae Kyung Lee, Min Hee Lee, Seo-Youn Choi, Ji Eun Lee

Department of Radiology, Soonchunhyang University Bucheon Hospital, Korea

Multiple gestations are getting more common because of increasing assisted conception, and in multiple gestation, perinatal mortality is higher than singleton. We would like to show normal ultrasound findings of multiple gestations in first and later trimester multiple gestation pregnancies, and present the check points we should keep in mind during the ultrasound examination of multiple gestation. Common abnormal findings of fetuses and maternal organs will be demonstrated as well.

SE 057

Churg-Strauss Syndrome Involving Testis and Epididymis

Yongsoo Kim, Young Seo Cho, Sanghyeok Lim

Department of Radiology, Hanyang University Guri Hospital, Korea

Churg-Strauss syndrome (CSS), or allergic granulomatous angiitis, is a rare syndrome that affects small- to medium-sized arteries and veins. CSS involves mainly lungs, skin, nerves, and gastrointestinal tract. Here, we report a case of CSS involving testis.

A 47-year-old male presented with painful left scrotal swelling. Scrotal ultrasonography shows diffuse enlargement of left epididymis with several cysts and prominent left scrotal wall thickening, and increased vascularity in left epididymis and both testicle. He was treated with antibiotics and analgesics under impression of epididymitis for 4 weeks. Scrotal pain was constant and follow up ultrasonography shows fluid collection in left scrotal sac. So, left orchiectomy and epididymectomy was performed and pathological analysis reveals Churg-Strauss syndrome involving left testis.

SE 058**Cellular Angiofibroma of the Scrotum**

Young Seo Cho

Department of Radiology, Hanyang University Guri Hospital, Korea

To review clinical presentation and ultrasonographic finding of cellular angiofibroma of the scrotum with radiologic and pathologic correlation.

Head & Neck**SE 059****Superficially Palpable Masses in Head and Neck: Sonographic Features and Pathologic Correlations**

Hyoung Seop Kim, Jin Kyung An, Jeong Joo Woo, Yoon Young Jung, Myung Won You, Eui Chul Jung
Department of Radiology, Eulji Hospital, Eulji University, Korea

Palpable lesions of head and neck are the common symptoms of patients visiting the hospital. Ultrasonography is often used as the first screening method for the palpable lesions. It is useful for radiologist to be familiar with these conditions and imaging findings. We divided these lesions as follows: cutaneous and subcutaneous lesions, lesions in fascia and muscle, lesions from lymph node, and lesions in salivary gland. The lesions included epidermal cyst, trichilemmal cyst, trichoepithelioma, steatocystoma, pilomatricoma, lipoma, hemangioma, tuberculosis, lymphoma, pleomorphic adenoma, and Warthin's tumor.

SE 060**Ultrasonographic Features of Pyriform Sinus Fistula-Related Suppurative Thyroiditis**Dongbin Ahn¹, Jeong Kyu Kim²*¹Department of Otorhinolaryngology, Kyungpook National University Hospital, Korea**²Department of Otorhinolaryngology, Daegu Catholic University Medical Center, Korea*

Diagnosis of pyriform sinus fistula (PSF) presenting as suppurative thyroiditis after infection is always challenging and mainly relies on CT scan and esophagography rather than ultrasonography (US). However, considering that PSF is congenital anomaly and most of PSF-related suppurative thyroiditis develop in pediatric patients, radiation exposure of CT scan and poor compliance of esophagogram could be important issue in diagnostic process. Therefore, we attempt to find diagnostic US characteristics of PSF-related suppurative thyroiditis.

During 10-year period, we experienced with 20 cases of PSF-related suppurative thyroiditis where PSF were confirmed by suspension laryngoscopic examination under general anesthesia. Among these, 13 patients completed US examination in the diagnostic process. We reviewed their US images and found several characteristics that indicate presence of underlying PSF.

In approximately in 70%, PSF-related suppurative thyroiditis involved upper 1/3 of the thyroid gland, where the cricothyroid muscle or pharyngeal constrictor muscle is located. Layered echogenic/hypoechoic rim of the lesion showed in 92.3% of cases and was considered as a distinctive feature of PSF-related suppurative thyroiditis, which represents layer of dilated pyriform sinus fistula tract.

US can be useful diagnostic modality that indicates presence of underlying PSF in suppurative thyroiditis. Therefore, in pediatric patients with suspicious PSF-related suppurative thyroiditis, US should be used as a first diagnostic image to avoid CT scan and esophagogram that are associated with radiation exposure and poor compliance.

SE 061**Comparison of Ultrasonography (US) and Computed Tomography (CT) Features of Calcified Thyroid Nodules (CTNs): Histopathologic Correlation**

Yoo Jin Lee, Dong Wook Kim

*Department of Radiology, Busan Paik Hospital, Korea***OBJECTIVES:** To compare the patterns and types of CTNs examined by preoperative neck US and CT.**METHODS:** From January to June 2011, 224 patients who underwent neck US and CT before thyroid surgery were included. Of the 224 patients, 165 had a CTN showing a clear match on US and CT. The CTN patterns were classified as follows: peripheral, central, and combined. The CTN types were classified as follows: micro-, nodular, eggshell, curvilinear, pure, and mixed. The patterns and types of CTNs examined by preoperative neck US and CT were compared and correlated with histopathologic findings.**RESULTS:** Of the 165 CTNs in 165 patients, 143 were papillary thyroid carcinomas, 2 follicular thyroid carcinomas, 7 follicular adenomas, and 13 nodular hyperplasias. The most common CTN pattern on US and CT was combined and central, respectively, and a statistical difference was observed in the CTN patterns between US and CT ($p < 0.0001$). In the type of CTNs, the most common type on US was microcalcification (64.2%, 106/165), whereas the prevalence rate of punctate calcification on CT was only 9.1% (15/165). A statistical difference was observed in the type of CTNs between US and CT ($p < 0.0001$). In addition, eggshell calcification on US and CT showed a low malignancy rate (37.5% and 28.6%), whereas nodular and pure calcifications on CT showed a high malignancy rate (77.6% and 87.5%).**CONCLUSION:** US is superior to CT in the evaluation of microcalcifications, whereas macrocalcifications showed the different features between US and CT. Recognizing the different features of CTNs on US and CT may be helpful in the evaluation of thyroid nodules.**SE 062****Life Saving Chemical Ablation of Large Acute Onset Parotid Space Neck Lymphangioma**

Asif Momin, Shenaz Momin

Department of Radiology, B Y L Nair Hospital, Mumbai, India

4 year old village girl presented with acute onset right parotid space soft swelling with difficulty in swallowing and respiratory discomfort since 2 days. She had this swelling since one year with Neck MRI revealing multiseptate lymphovenous malformation. During prior ENT consultation wait and watch policy was adopted due to her young age.

Due to acute distress, initial ultrasound guided 5F pigtail drainage with negative pressure suction was done to reduce the mass effect and restore airway. Iodinated Contrast study was done to know the exact extent and to rule out venous leak.

Decision was taken to treat this SOL with Sclerotherapy using sodium tetradesyl sulphate under ultrasound and fluoroscopy control. Possible facial nerve involvement was checked by using lignocaine instillation in the cavity.

Under endotracheal tube control to prevent post treatment airway edema; further Sclerotherapy was achieved using additional ethanol alcohol chemical ablation.

Patient did benefit dramatically with significant reduction in size of the lesion. Additional Sclerotherapy was done after one month to treat residual superficial residual cavities. Follow up after six months showed more than 90% reduction in the size with no refilling. Alcohol and other sclerosants when used with caution can be the effective treatment even for large multiseptate lymphangiomas of the neck spaces in an emergency setting; thus surgery and resultant scar could be avoided in the young child.

SE 063**Merkel Cell Carcinoma, a Potential Mimicker of Lymphoma on Ultrasonography**

Soo Young Chae, Jung Hye Na, Inseon Ryoo,
Sangil Suh, Hae Young Seol

*Department of Radiology, Korea University Guro
Hospital, Korea*

Merkel cell carcinoma (MCC) is a rare and aggressive neuroendocrine tumor of the skin. MCC typically manifests as a small, firm, fast-growing, non-tender, dome-shaped red, violaceous, or purple nodule located on areas of the body that have been exposed to sunlight. Since its common affected area is head and neck, ultrasonography has been an initial imaging modality of the primary lesion and neck areas and a guidance to percutaneous needle biopsy. Due to the rarity of this highly aggressive disease, only a few imaging reports on MCC were published. Herein, we report two cases of MCC mimicking lymphoma on ultrasonography.

Musculoskeletal**SE 064****Botulinum Toxin A Injection with Radial Extracorporeal Shock Wave Therapy in Spastic Cerebral Palsy**

Dong Rak Kwon, Gi-Young Park

*Department of Rehabilitation Medicine, Daegu
Catholic University Medical Center, Korea*

OBJECTIVE: To investigate the combined effect of botulinum toxin A (BTA) injection with radial extracorporeal shock wave therapy (ESWT) for spasticity in children with spastic cerebral palsy (CP)

MATERIALS AND METHODS: A total seven patients with spastic CP were recruited. They received repeated BTA (Meditoxin; Medytox Inc.) injection in the gastrocnemius (GCM) muscle under ultrasound guidance. All children received one ESWT (BTL-5000 unit, using the following parameters: energy of 0.15 mJ/mm²; total shot dose 1500 shocks; frequency 4 Hz) session for GCM immediately after BTA injection

and two consecutive ESWT sessions with weekly intervals. In addition, all children received outpatient rehabilitation treatment during and after ESWT treatment. Clinical assessments including Modified Ashworth Scale (MAS), passive range of motion (PROM) of ankle dorsiflexion with the knee extended were performed before BTA injection (base line), 1 month, and 3 months after treatment. Shear wave velocity (SWV) of the GCM using Acoustic Radiation Force Impulse (ARFI) imaging was measured before, at 1 and 3 months after BTA injection.

RESULTS: The mean PROM of ankle dorsiflexion with knee extension before treatment (-14.1-14.1°) was significantly increased at 1 month (6.2-14.1°) and 3 months (0.2-14.1°) after BTA injection with ESWT. The mean MAS of the ankle plantar flexor before treatment (3.2) was significantly decreased at 1 month (2.0) and 3 months (2.5) after BTA injection with ESWT. The mean SWV of the GCM before treatment (2.7 m/sec) was significantly decreased at 1 month (1.8 m/sec) and 3 months (2.1 m/sec) after BTA injection with ESWT.

CONCLUSION: This study showed that clinical and imaging parameters of spasticity were improved and maintained at 3 months after combined treatment of BTA injection with ESWT in children with spastic CP.

SE 065**Do the Findings of Magnetic Resonance Imaging, Arthrography, and Ultrasonography Reflect Clinical Impairment in Patients with Adhesive Capsulitis of the Shoulder?**

Gi-Young Park¹, Dong Rak Kwon¹, Dae-Gil Kwon¹,
Jung Hyun Park²

¹*Department of Rehabilitation Medicine, Daegu
Catholic University Medical Center, Korea*

²*Department of Rehabilitation Medicine, Severance
Hospital, Korea*

OBJECTIVE: To investigate the correlation between arthrography, magnetic resonance imaging (MRI), and ultrasonography (US) findings in patients with adhesive capsulitis (AC) of the shoulder and their clinical presentation as well as functional impairment.

SUBJECTS AND METHODS: Seventy-five patients (27 males, 48 females; mean age 55.3 ± 9.8 years) who were clinically diagnosed as unilateral AC were recruited. A visual analog scale (VAS), passive shoulder range of motion (ROM), Cyriax stage, and Constant-Murley score (CMS) were measured for clinical parameters. The thickness of axillary recess, coracohumeral ligament (CHL), and the enhanced portion in the rotator cuff interval were measured by using contrast-enhanced MRI. Single contrast arthrography as used to calculate the total score of shoulder arthrographic criteria. US was used to measure the thickness of the inferior glenohumeral ligament (IGHL) and CHL, and the IGHL ratio and CHL ratio were calculated by comparing with the unaffected side.

RESULTS: None of MRI parameters was correlated with clinical assessment scores. The total score of shoulder arthrographic criteria was negatively correlated with the total shoulder motion ($p < 0.05$), ROM of shoulder flexion ($p < 0.05$), and abduction ($p < 0.05$). The total CMS score was well correlated with the total score of shoulder arthrographic criteria ($p < 0.05$). The total shoulder joint capacity was positively correlated with the total shoulder motion ($p < 0.05$), and ROM of shoulder flexion ($p < 0.05$). The IGHL thickness, IGHL ratio, CHL thickness, and CHL ratio were negatively correlated with the shoulder external rotation ($p < 0.05$), respectively.

CONCLUSION: The findings of US and arthrography in patients with AC of the shoulder were correlated with the clinical assessment scores. However, all measuring parameters on MRI were not correlated with clinical impairments. US is recommended as the preferred option for diagnosing AC of the shoulder.

SE 066

Variable Sonographic Findings of the Subungual Glomus Tumor

Ga Young Lee¹, Sun Joo Lee¹, Hye Jung Choo¹, Sung Moon Lee²

¹Department of Radiology, Inje University Busan Paik Hospital, Korea

²Department of Radiology, Keimyung University Dongsan Medical Center, Korea

PURPOSE: The purposes of this study are to review the variable sonographic features of the subungual glomus tumor and to correlate with other imaging modality.

CONTENTS ORGANIZATION: 1. Normal anatomy and imaging appearance of nail apparatus and subungual space

2. Variable sonographic findings of the subungual glomus tumor including several cases and correlate with other imaging modality

- Typical finding
- Atypical findings

SUMMARY: Glomus tumor is a rare benign soft tissue tumor, originated in systemic fine glomus in arteriovenous anastomoses. Although glomus tumors may affect any area of the body, up to 75% occur in the hand, and approximately 65% of these are in the fingertips, particularly in the subungual space. Clinical manifestations include excruciating pain, intense tenderness that may be provoked by mild trauma, and temperature sensitivity. Ultrasonography is sensitive for tumors as small as 3 mm in diameter. At US, a subungual glomus tumor typically manifests as a well-circumscribed solid, hypoechoic mass with hypervascularity. If the size of the tumor is large enough, most of them accompany erosion of the underlying phalangeal bone. However, it can also be seen focal bony indentation despite the small size. Sometimes, the glomus tumor can be seen variable internal echogenicity and vascularity depending on the thickness of the patient's nail. At MRI, glomus tumor manifests as low signal intensity on T1-weighted image and high signal intensity on T2-weighted image with marked contrast enhancement. Through the review of this exhibit, radiologists can recognize the variable ultrasonographic findings of the subungual glomus

tumor and can correlate clinical features and radiologic findings for an exact diagnosis.

SE 067

Ultrasonographic Finding of Joplin's Neuroma: a Case Report

Sumin Lee¹, Sunjoo Lee¹, Hyejung Choo¹,
Sung Moon Lee²

¹Department of Radiology, Inje University Busan Paik Hospital, Korea

²Department of Radiology, Keimyung University Dongsan Medical Center, Korea

PURPOSE: Joplin's neuroma refers to an entrapment neuropathy of the plantar proper digital nerve, which results from perineural fibrosis. It is a rare disease and not fully described in the previous radiologic literature. The purpose of this study is to characterize the sonographic features of the Joplin's neuroma in the foot.

MATERIALS AND METHODS: A 24-years-old female complains pricking sensation on medial side of the great toe and 1st MPJ for 6 months. She was hospitalized and radiologic studies were performed to identify the location and characterize the lesion. Then sonography-guided injection was done to treat the symptom.

RESULTS: In our case, ultrasound (US) images showed the lesion was located on the pathway of medial proper plantar digital nerve and compressed at 1st MPJ & plantar aspect of hallux. On gray-scale US images, a focal, hypoechoic and fusiform swelling of the medial proper plantar digital nerve was seen. Relief of the pain after sonography-guided injection was observed, which may serve as a therapeutic solution as well as a diagnostic test.

CONCLUSION : On this case, the ultrasonographic findings of Joplin's neuroma reveals a focal, hypoechoic, and fusiform swelling, proximal to 1st MPJ, which is typical alteration of peripheral nerves entrapment, regardless of entrapment site. The normal medial proper plantar digital nerve is typically difficult to identify on US. But when focal irritation of the nerve is seen on US with symptom of entrapment neuropathy, Joplin's neuroma should be considered as a possible diagnosis.

SE 068

Sonoelastography Findings in Evaluation of Various Benign Soft Tissue Lesions

Eunjin Hwang, Eun-Kyung Khil, Seun-Ah Lee,
Jung-Ah Choi

Department of Radiology, Dongtan Sacred Heart Hospital, Korea

We evaluated conventional B-mode US and compression type sonoelastography (SE) for 31 soft tissue lesions of 31 patients, from January to October 2016. Both quantitative and qualitative grading were done for each examination using the color-code grading system and the tissue-elasticity ratio by semi-automatic range of interest (ROI) at least 3 times by one experienced radiologist. The color pattern was graded into three major patterns: blue-hard, green-soft and red-softer. The range of tissue-elasticity ratio was from 0.35 to 6.13. There were 18 masses of blue, 1 green, 4 reds, 2 blue/green, 2 green/red and 3 blue/red. Fourteen lesions were assessed on US as epidermal inclusion cysts, six of which were pathologically confirmed. Twelve of epidermal inclusion cysts showed relatively lower tissue-elasticity (mean value: 1.66, from 0.35 to 6.13) and half of epidermal inclusion cysts showed blue color. We assessed 2 neurogenic tumors, 3 nodular fasciitis, 2 hemangioma, 2 fibromatosis coli of pediatrics, 2 benign fibrous histiocytoma, 1 lipoma and 1 lymph node. They all showed blue and the mean value of tissue-elasticity ratio was 3.39, ranging from 1.23 to 5.73. We assessed 2 ganglions, 1 abscess and 1 TGDC. They showed mostly red and the tissue-elasticity ratio was 0.89, ranging from 0.59 to 1.14. Sonoelastography demonstrated variable findings of benign soft tissue lesions and may be useful in characterizing these lesions.

SE 069**Imaging Findings of Digital and Extradigital Glomus Tumor**

Jungwon Park¹, Sunjoo Lee¹, Hyejung Choo¹,
Sung Moon Lee²

¹Department of Radiology, Inje University Busan Paik Hospital, Korea

²Department of Radiology, Keimyung University Dongsan Medical Center, Korea

PURPOSE: The aim of this exhibit is to review digital and extradigital glomus tumors with emphasis on ultrasound and MR imaging findings.

CONTENTS ORGANIZATION: Various locations of glomus tumor will be described with ultrasound and MR imaging findings.

- Digital
- Extradigital: upper & lower extremities, stomach

SUMMARY: Glomus tumors are rare vascular neoplasm arising from the neuromyoarterial glomus body, a highly specialized arteriovenous anastomosis responsible for thermoregulation. This is typically benign tumor, but locally aggressive form, malignant and metastatic potential have been reported. The most common site is the distal extremity, particularly in subungual region of the finger, atypical locations such as GI tract, lung, trachea, intraosseous, and intraneural areas have been identified. Patients usually present with a prolonged history of solitary painful lesion with tenderness to palpitation, skin discoloration, and sensitivity to cold. Ultrasonographic finding of typical glomus tumor is a well-circumscribed solid, hypoechoic mass with hypervascularity on color Doppler. On MRI, it is depicted as low to intermediate signal intensity on T1-weighted image, marked high signal intensity on T2-weighted image, and strong contrast enhancement. Through this exhibit, imaging findings of digital and extradigital glomus tumors including ultrasonography and MRI are reviewed, and it may be helpful to make an exact diagnosis.

SE 070**High-Resolution Sonography of Cutaneous Branches: Upper Extremity**

Sung Kwan Kim¹, Sun Joo Lee¹, Hye Jung Choo¹,
Sung Moon Lee²

¹Department of Radiology, Inje University Busan Paik Hospital, Korea

²Department of Radiology, Keimyung University Dongsan Medical Center, Korea

PURPOSE: To review detailed anatomy and specific anatomic landmarks for cutaneous nerves of the upper extremity.

CONTENTS ORGANIZATION: Sonographic anatomy and specific landmarks of the important upper extremity cutaneous nerves

1. Cutaneous nerves around shoulder and elbow
 - Superolateral brachial cutaneous nerve
 - Posterior brachial cutaneous nerve
 - Posterior antebrachial cutaneous nerve
 - Medial antebrachial cutaneous nerve
 - Lateral antebrachial cutaneous nerve
2. Cutaneous nerves of wrist and hand
 - Dorsal cutaneous branch of the ulnar nerve
 - Palmar cutaneous branch of the median nerve
 - Superficial branch of the radial nerve
 - Interdigital nerve

SUMMARY: Advances in scanner and transducer have enabled high-quality peripheral nerve imaging. High-resolution sonography has some advantages over MRI to evaluate the cutaneous nerves, such as high spatial resolution, the possibility of a dynamic examination, and evaluation of long segments in a real time. Because the sensory distribution of the main nerve and the cutaneous branch overlap, it is important to perform the focused sonographic evaluation based on clinical signs or symptoms through meticulous history taking from the patient. Accurate anatomical knowledge of course and landmarks of cutaneous nerves help in their identification and selection for appropriate nerve injection. Thus, sonography can be the ideal imaging tool of peripheral nerve disease, especially in small cutaneous nerve.

SE 071**Musculoskeletal Ultrasound Finding in Disseminated Tuberculosis**

Maria Goretti Ametembun

Department of Internal Medicine, Lukas Government Hospital, Stella Maris Hospital, Fanayama Health Centre South Nias, North Sumatera, Indonesia

PURPOSE: To describe ultrasound finding of musculoskeletal manifestation in disseminated tuberculosis.

MATERIALS AND METHODS: This descriptive study was conducted as a public-private mix approach at some least health facilities: Fanayama Community Health Centre, Lukas Government Hospital, Stella Maris Hospital, under coordination of South Nias Ministry of Health, Teluk Dalam, North Sumatera during May-July 2015. All patients had musculoskeletal sign and symptoms, in addition to disseminated tuberculosis including peritoneal (dry type)/small bowel tuberculosis, chronic cough (lung tuberculosis suspected), neck lymph nodes enlargement and mild fever. The only available portable black and white ultrasound with convex probe 3,5 MHz was performed on musculoskeletal affected area and tympanic and dullness abdominal pain area according to 'dam board phenomenon' of peritoneal dry type/small bowel tuberculosis.

RESULTS: N =2, (9 and 11 y) boys. Musculoskeletal ultrasound finding were thickening of the muscle and synovial of painful affected area in addition to several ovale/round nodular structures (patchy hyper-echoic non-shadowing with an irregular rim of lower echo-density). Small bowel ultrasound showed hypoperistaltic, irregular thickening heterogenic hypo-echoic of the small bowel wall in addition to similar several ovale/round nodular structures (patchy hyper-echoic non-shadowing with an irregular rim of lower echo-density); loss differentiation of the wall layers, irregular margin and narrowing of the lumen were examined on the dullness pain area. No X-ray available. Follow-up after anti tuberculosis treatment showed improvement both clinically with ultrasound.

CONCLUSION: Ultrasound of musculoskeletal manifestation in disseminated tuberculosis cases has some characteristics.

SE 072**Fibroma of Tendon Sheath of the Hand: Ultrasonographic and MRI Findings**Yeon Soo Lee¹, Hae Joung Sul²

¹*Department of Radiology, The Catholic University of Korea, Daejeon St. Mary's Hospital, Korea*

²*Department of Pathology, The Catholic University of Korea, Daejeon St. Mary's Hospital, Korea*

Fibroma of the tendon sheath (FTS) is a rare, benign, soft tissue lesion. Clinically, FTS presents similarly to the more common giant cell tumour of the tendon sheath (GCTTS). FTS can be distinguished histologically from GCTTS by the lack of giant cells and hemosiderin-laden macrophage. The authors present a case of FTS in the ulnovolar side of the fourth metacarpophalangeal joint level adjacent to the flexor digitorum tendon. A 61- year old man presented with a month history of painful palpable mass in the right palm. Examination demonstrated 1.6×1.4×1.3 cm sized, soft, movable, nodular superficial mass and radiating pain. Radiographs revealed soft tissue mass. Ultrasound showed a mixed heterogeneous mass adjacent to 4th flexor digitorum tendon. MRI demonstrated that the mass showed heterogenous low T1, intermediate to high T2 signal intensity with peripheral rim enhancement adjacent to flexor digitorum tendon at the fourth metacarpophalangeal joint level. Preoperative diagnosis was neurogenic tumor or GCTTS. The patient underwent excisional biopsy of the lesion with neurovascular adhesion. A diagnosis of FTS was made. The case report provided a rare case of the FTS and highlights the need to consider this entity in the differential diagnosis of any soft tissue lesion in the hand adjacent to tendon sheath

Pediatric

SE 073

Quantifying Sternocleidomastoid Muscle Intrinsic Stiffness Difference Using Dynamic Sonoelastography in Congenital Muscular Torticollis

Dong Rak Kwon, Gi-Young Park

Department of Rehabilitation Medicine, Daegu Catholic University Medical Center, Korea

PURPOSE: To quantify sternocleidomastoid muscle (SCM) stiffness using acoustic radiation force impulse (ARFI) sonoelastography in infants with congenital muscular torticollis (CMT).

MATERIALS AND METHODS: Twenty infants with an SCM thickness greater than 10 mm with or without involvement of the entire SCM length (limitation of neck rotation passive range of motion [PROM]: group 1S $>30^\circ$, group 1M = 15° - 30°) and 12 infants with an SCM thickness smaller than 10 mm with or without involvement of any part of SCM (group 2) were included. The SCM thickness was measured using B-mode ultrasound, and the local SCM shear wave velocity (SWV) and subcutaneous fat layer using ARFI sonoelastography.

RESULTS: The neck rotation PROM was significantly greater in group 1S ($36.5^\circ \pm 5.3^\circ$) than in group 1M ($18.8^\circ \pm 4.9^\circ$; $p < .01$); the SWV of the SCM in the affected side (2.87 ± 0.99 m/s) was significantly higher than that in the unaffected side (1.50 ± 0.30 m/s; $p < .01$). The SWV of the SCM was significantly higher in group 1S than in group 1M. In group 1, the SWV of the affected SCM was positively correlated with the degree of deficits in PROM of neck rotation in the affected side ($r = .77$; $p < .01$).

CONCLUSION: This study revealed a difference in the SWV of the affected SCM according to the limitation of neck rotation PROM in infants with CMT and SCM thickness greater than 10 mm, although no difference in SCM thickness was observed.

SE 074

Ultrasound Diagnosis of Development Dysplasia of the Hip and the Congenital Hip Dislocation in Children

Norjmaa Sereenendorj

Department of Radiology, Mongolian Radiological Society, Mongolia

SURVEY AIMS: To analyse and determine overall result upon diagnosis of developmental dysplasia of the hip and the congenital hip dislocation in 0 to 4 months old infants from family health centers of soums, provinces and districts who are suspicious of developmental dysplasia of the hip and the congenital hip dislocation at the Department of Radiology of National Trauma and Orthopedics Center of Mongolia.

Within our survey, of 0 to 4 months old total 560 infants suspicious of DDH and CDH, 497 ($88.75\% \pm 1.3$) were diagnosed as no hip injuries and 63 ($11.25\% \pm 1.3$) were diagnosed DDH and CDH.

Age and gender ratio among 63 infants diagnosed DDH and CDH was as male 14 ($22\% \pm 5.62$) and female 49 ($78\% \pm 5.62$). 17 ($27\% \pm 5.6$) of them were one month old infants, of which, 13 ($76.5\% \pm 10.6$) were female and 4 ($23.5\% \pm 10.6$) were male. 14 ($22\% \pm 5.2$) of infants were 2 months old, all 14 (100%) of them female. 26 ($41\% \pm 6.2$) were 3 months old infants, of which, 22 ($85\% \pm 7.0$) were female and 4 ($15\% \pm 7.0$) were male. 4 months olds are 6 ($10\% \pm 3.8$), all are (100%) male. 14 ($5.9\% \pm 1.5$) of 238 male infants, and 49 ($15.2\% \pm 2.0$) of 322 female infants were diagnosed developmental dysplasia of the hip and the congenital hip dislocation.

DDH and CDH is more prevalent in female infants rather than male infants which is proving the statistics ($\text{ĐE}, 0.001$).

SE 075**The Report about Ultrasonic Examination of a Hip Joint of Newborns in Delivery Room of a Hospital of Huvsgul Aimag**

Enkhtaivan Namuuntsetseg, Enkhbold Sereejav
Department of Radiology, The First Central Hospital of Mongolia, Mongolia

PURPOSE: The report and assessment about ultrasonic examination of a hip joint of newborns in delivery room of a hospital of Huvsgul aimag.

MATERIALS AND METHODS: 600 newborns with age from 1 to 7 days for ultrasonic examination of a hip joint were chosen, among them 48 cases with pathology of this joint were revealed, they were subjected to careful examination.

RESULTS: Among 600 newborn children chosen for examination at assessment on Graff's classification (A - 92%, B - 7,8%, C - 0,16%, D - 0%). If to consider by gender among 48 newborns with an pathology of a hip joint: a male - 27%, a female - 73%. Among female newborns such pathology change happens more, than among newborns is a male ($p < 0.05$). Pathological change on the right - 12,5%, on the left - 37,5%, on both parties - 50%. If to compare by the number of pathological changes and on weight: 2500g - 29,16%, 2500-3600g - 27,8%, 3601g - 43,75% ($r=0.20$, $p < 0.01$).

CONCLUSION: On a research of the International Organization of health care dislocation of a hip joint among 1000 live-born is observed 0,7-2,5, on our research among 1000 live-born there were 1,6, pathological change of a hip joint in female newborns had 3 times more, than in male newborns.

SE 076**Is it Acceptable Not to Perform Voiding Cystourethrography in Infants with Low-Grade Hydronephrosis?**

Sun Kyoung You, Seongsu Kang
Department of Radiology, Chungnam National University Hospital, Korea

PURPOSE: The purpose of our study was to determine the value of vesicoureteral reflux (VUR) screening using postnatal ultrasonography and voiding cystourethrography (VCUG) in infants with prenatal/postnatal hydronephrosis.

MATERIALS AND METHODS: We retrospectively reviewed the medical records of infants with prenatal/postnatal hydronephrosis who underwent VCUG before 6 months of age, between March 2014 and December 2016. We excluded those with renal/bladder anomalies and urinary tract infections. Each kidney was considered as a separate renal unit (RU). The severity of postnatal hydronephrosis was recorded using the Society for Fetal Urology (SFU) grade and the anteroposterior diameter (APD) of the renal pelvis. We evaluated the relationship between postnatal hydronephrosis and VUR.

RESULTS: Overall, 103 RUs from 58 patients were analyzed in this study (boys:girls, 48:10; mean gestational age, 37.2 ± 2.8 weeks; range, 27.7-41.5 weeks; mean birth weight, 2970.1 ± 715.7 g). APDs were statistically significant different among the four SFU grades of hydronephrosis ($p < 0.05$, one-way ANOVA). Four RUs from four infants showed VUR (4/103, 3.8%; Grade 1(1), Grade 2(2), Grade 5(1)). Of 23 infants with high-grade hydronephrosis (SFU 3 and 4), one (4.3%) had grade 5 VUR. Of 80 infants with low-grade hydronephrosis (SFU 1 and 2), 3 (3.7%) had low-grade VUR. There were no significant differences in SFU grades of hydronephrosis and APD between the VUR and non-VUR groups (all $p > 0.05$).

CONCLUSION: Our results indicate that in order to avoid missing a case of high-grade VUR (grades 3-5), VCUG should be implemented in infants with high-grade postnatal hydronephrosis (SFU grades 3-4).

SE 077**The Vomiting Neonates and Infants: Operation or Observation? - the Decision Algorithm Navigating the Radiologic Diagnosis of a Surgical Emergency**

Yongsang Kim, Myung Won You, Yoon Young Jung
Department of Radiology, Eulji University Hospital, Korea

Vomiting in the neonates and infants, usually occurs because of intestinal obstruction and needs surgical intervention. However, various forms and presentations of vomiting would be diagnostic challenging for clinicians and radiologists. In this presentation, we attempted to review various cause of vomiting in the neonates and infants along with applicable imaging modality and diagnostic work up procedures to define concise algorithm guiding to appropriate decision making.

1. Plain radiographic pattern; obstructive vomit vs. non obstructive vomit

Obstructive vomiting: proximal obstruction or distal obstruction

Non obstructive vomiting: GER, functional disorder, necrotizing enterocolitis etc.

2. Bilous vs. non bilous vomit

Non bilous vomit: pyloric stenosis, functional disorder, GER etc.

Bilous vomit: mostly intestinal obstruction

3. High level (proximal) obstruction vs. Low level (distal) obstruction

Proximal obstruction: duodenal atresia, jejunal atresia, midgut volvulus, malrotation etc.

Distal obstruction: ileal atresia, colonic atresia, meconium plug ileus, Hirschsprung disease etc.

4. Review of individual obstructive diseases with appropriate diagnostic modality

Small bowel atresia; UGI/barium edema findings

Midgut malrotation; US exam, UGI study findings

Midgut volvulus; US exam, UGI study findings

Meconium plug syndrome, meconium ileus; US exam, UGI study findings

Colonic atresia; barium edema finding

Hirschsprung disease; barium edema finding

Others;

5. Decision algorithm navigating the appropriate radiologic diagnosis for a surgical emergency.

1) check for X- ray pattern: non obstructive vs. obstructive

2) determine level of obstruction with plain radiograph and clinical finding

- bilous vs. non bilous vomit

- high level vs. low level obstruction

3) define individual disease with US exam

- pyloric stenosis

- midgut volvulus, malrotation

4) define individual disease with UGI study/ colon edema.

- small bowel atresia; jejunal or ileal atresia

- intestinal malrotation, midgut volvulus

- meconium plug syndrome

- colon atresia, Hirschsprung disease

SE 078**Cervical Thymus Mimicking Metastatic Recurrence on PET/CT: Diagnosis with Ultrasound**

Saelin Oh, So-Young Yoo, Ji Hye Kim,
 Tae Yeon Jeon

Department of Radiology, Samsung Medical Center, Korea

OBJECTIVE: To evaluate the utilization of ultrasound (US) scan to diagnose cervical thymus mimicking metastatic recurrence on PET/CT.

MATERIALS AND METHODS: Four patients (M:F 1:3, age range 6-13 years) who underwent neck US scan for suspected metastatic relapse on PET/CT after chemotherapy with a final diagnosis of cervical thymus were included. US features of cervical thymus including location, size, shape and presence of continuity with the mediastinal thymus were analyzed as well as PET/CT findings and clinical features.

RESULTS: There were two lymphomas, one alveolar sarcoma and one ganglioneuroblastoma with variable intervals between chemotherapy and PET/CT (mean 6.9 months). Standardized uptake value (SUV) max of the cervical thymus showed no significant difference with that of the mediastinal thymus. On US, the lesion showed identical echogenicity with the mediastinal thymus; location was infrathyroidal in all patients (right: left 3:1); size ranging from 1.9

cm to 4.0 cm; slightly angular contour in the shape; continuity with the mediastinal thymus was noted in two patients.

CONCLUSION: Cervical thymus may manifest as a focal uptake on PET/CT after chemotherapy related with thymic hyperplasia, simulating metastatic recurrence. US provides a rapid and confident diagnosis, obviating further imaging studies or invasive procedure.

Physics

SE 079

A New High Definition Voxel Based Reconstruction Method for Three-Dimensional Ultrasound MPR Imaging

Sungchan Kim, Jinbum Kang, Ilseob Song, Yangmo Yoo

Department of Medical Solution Institute, Sogang University, Korea

In medical 3-D ultrasound (US), multiplanar reconstruction (MPR) imaging is useful in obstetrics and gynaecology. The 2-D MPR imaging simultaneously shows three perpendicular planes (e.g., transverse, sagittal, and coronal view) from the stored volume data. This technique makes it possible to obtain the desired anatomical views and to provide clinical detail (e.g., distances or areas) from a selected volume of tissue or specific organs. To produce the 2-D MPR imaging from the acquired 3-D volume data, the 3-D scan conversion (SC), which transforms the acquired ultrasound data in the 3-D polar coordinate system to the 3-D Cartesian coordinate system, is performed for display. Recently, direct 3-D SC and separable 3-D SC method were introduced that they are followed by interpolation (e.g., trilinear or bilinear) using neighboring pixels. However, the direct 3-D SC and separable 3-D SC methods suffer from blurring artifact that may cause the deterioration of image quality. In this study, We propose a new high resolution 3-D SC method using voxel based beamforming (VBF). In this method, dynamic receive focusing is directly performed on each voxel

in 3-D Cartesian coordinate without interpolation. In addition, the beamformed data corresponding to adjacent four scanlines are compounded to avoid blocking artifact. To evaluate the performance of the proposed method, the phantom study was conducted using the research ultrasound acquisition system with 3-D curved probe. As a result, the proposed method showed improved results compared to the 3-D SC methods direct and separable in terms of conspicuity and margin sharpness without blurring artifact. Moreover, it showed higher the information entropy contrast (IEC) value, i.e., 97.02 vs. 113.6 vs. 130.22, respectively. These results indicate that the proposed MPR imaging method provides high quality images without blurring artifacts.

SE 080

An Efficient Transmit Delay Calculation Method for Coherent Plane-Wave Compounding in Convex Array Transducer

Dooyoung Go, Jinbum Kang, Yangmo Yoo

Department of Medical Solution Institute, Sogang University, Korea

Ultrafast ultrasound imaging based on coherent plane-wave compounding was recently introduced to achieve high frame rate imaging without compromising spatial resolution or SNR. In addition, the coherent compounding method using convex array transducer may be used to obtain larger field of view with increased penetration depth. However, the transmit delay operation for plane-wave excitation is typically increased in proportion to the number of plane-wave angles. In this paper, we propose an efficient transmit delay calculation method for convex plane-wave compound imaging. In the proposed method, unlike the conventional approach, only a single transmit delay for a defined steering angle is calculated and its transmit delay is then shifted along the element of the transducer to acquire other transmit delays for different plane-wave angles. To evaluate the performance of the proposed method, the computational complexity (i.e., the number of operation of multiplication) was measured in the simulation study. The result showed that the number of operation was substantially

decreased compared to the conventional method, e.g., 8192 vs. 192 (42 times less) with the shift of 32 at 64 angles. In addition, there is no difference between the reconstructed images by conventional and proposed method. These results indicate that the proposed method can effectively reduce the computational complexity for convex plane-wave excitation without degrading of image quality.

SE 081

A Modified Homographic Transform-Based Image Registration Method for 3-D Automatic Breast Ultrasound System with Dual Wide Field-of-View Imaging

Hojung Lee, Ilseob Song, Jinbum Kang, Yangmo Yoo
Department of Medical Solution Institute, Sogang University, Korea

Automated breast ultrasound system with dual wide field-of-view image acquisition can reduce a scanning time approximately half than existing systems. Subtle mechanical misalignment between dual transducers causes evident difference in axial plane reconstructed image and in that common image region for an image registration. Accurate registration of misaligned dual wide field-of-view ultrasound images is important for decrease scanning time and precise diagnosis. Since axial plane image acquired by misaligned dual transducers represent slightly different features, homography estimation using RANSAC has lower probability in accuracy. In this paper a modified homography-based RANSAC algorithm is presented for improving probability of RANSAC and accuracy of feature-based homographic transform image stitching. Perspective projection based on homography estimation can be applied for axial plane reconstructed image registration. In the modified method, x-axis scale factor S_x and y-axis scale factor S_y and perspective degree P in homography parameters are analyzed. Since misalignment of transducer is limited to some extent, analyzed homography parameters are updated to fit the predictable (reasonable) range (degree) and iterate to RANSAC step. To evaluate the performance of the proposed method, phantom studies were conducted by an ultrasound research platform

(Vantage, Verasonics Inc., Kirkland, WA, USA) using a L12-5 linear array transducer. In the phantom study, pork phantom was built and a programmable step motor stage system (SHOT-304GS, OptoSigma) was used to apply intended degree of misalignment image acquisition. For the quantitative assessment, the correlation coefficients between an non-registrated image and the registrated image with original image in common region were measured, i.e., 0.762.03, and 0.920.84, respectively. These results indicate that the modified method based on homographic transform-based image registration can improve the probability of precise image registration for automated breast ultrasound system with dual wide field-of-view image.

SE 082

Characteristic Responses of Neuronal Cells to Ultrasound Under the Variable Heights of Culture Medium in the Well

Gwansuk Kang¹, Tsengel Bayarsaikhan¹,
Su-Yong Eun², Min Joo Choi²

¹*Department of Interdisciplinary Postgraduate Program in Biomedical Engineering, Jeju National University, Korea*

²*Department of Medicine, Jeju National University, Korea*

Ultrasound has a potential for the clinical treatment of nerve regeneration in both central and peripheral nervous system. Many in vitro studies which use cell lines cultivated in culture wells often lack reproducibility and successful transfer to other experimental conditions. The standing waves formed in the well is suspected to cause the problems, which was not clarified yet. The acoustic pressure in the standing wave field is sensitive to the amount of the culture medium. The present study was to look into the dynamic response of neuronal cells exposed to ultrasound under the various heights of culture medium.

HT-22 cell lines were cultured in Dulbecco's Modified Eagle Medium and the four different heights of the medium were considered, for which the pressures predicted on the bottom of the well by a simple standing wave theory were equally

divided from zero to the maximum value. The cells were exposed to 1 MHz ultrasound with an nominal intensity of 50 mW/cm² for 10 min. Optical images of the cell were recorded for 14 min from 5 min before US irradiation. It was shown that the expansion of neurites was observed when ultrasonic irradiation began. Temporal morphological changes and area of the cell were measured to quantify the degree of the morphological response. The variation of the acoustic peak pressure against the medium height was found to be characteristically similar to the morphological cell responses.

The experimental results indicate that the ultrasonic exposure will be significantly different even if the ultrasonic device output setting remains the same. The present study claims that the parameter such as the culture medium height closely associated with standing wave effects must be monitored when in vitro ultrasonic cell experiments are performed. Further investigation including the physiological responses of cells is suggested to underpin the present observations.

Thyroid

SE 083

Detection of Malignancy among Suspicious Thyroid Nodules Less than 1 cm with Various Thyroid Image Reporting and Data Systems

Su Min Ha¹, Jae Kyun Kim¹, Jung Hwan Baek²

¹Department of Radiology, Chung-Ang University Hospital, Korea

²Department of Radiology, Asan Medical Center, Korea

PURPOSE: In patients undergoing active surveillance of papillary thyroid microcarcinoma (PTMC), definitive therapy-usually preceded by a definitive diagnostic procedure-is not recommended until evidence of disease progression is obtained, as stated in the American Thyroid Association (ATA) guidelines. This is because the deferring of definitive diagnosis and therapy until disease progression has no impact on the disease-specific survival.

Here, we evaluated the malignancy rate of thyroid nodules, which was further stratified based on the size cut-off value of 1 cm, with suspicious findings on ultrasonography (US), by using various malignant stratification systems.

MATERIALS AND METHODS: The data were retrospectively collected between January 2003 and June 2003 from 9 university hospitals that had previously participated in the Korean Society of Thyroid Radiology (KSThR) multicenter study on the ultrasonographic differentiation between benign and malignant thyroid nodules. In total, 829 thyroid nodules from 711 patients were included. We calculated the malignancy rate of thyroid nodules, which was further stratified by size, by using 4 different types of malignant risk stratification systems. We assessed the factors that could differentiate benign from malignant nodules using the χ^2 test.

RESULTS: In the suspicious thyroid nodules <1 cm in size on US, the malignancy rates ranged from 77.4% to 82.8%; the lowest rate was from the KSThR, whereas the highest rate was noted in the Web-based system. Thus, the rate of benign nodules among suspicious thyroid nodules <1 cm in size on US was 17.2-22.6%.

CONCLUSION: A biopsy should be considered before active surveillance to exclude benign nodules with suspicious US features, and could thus prevent unnecessary active surveillance and patient anxiety.

SE 084**Columnar Cell Variant of Papillary Thyroid Carcinoma; Differentiation between Indolent and Aggressive Types**

Jooyeon Cho¹, Jung Hee Shin¹, Soo Yeun Hahn¹,
Young Lyun Oh²

¹Department of Radiology, Samsung Medical Center, Korea

²Department of Pathology, Samsung Medical Center, Korea

PURPOSE: The columnar cell variant of papillary thyroid carcinoma (CCV-PTC) is regarded as a rare subtype of PTC that is classified into one of aggressive variants with early dissemination and short survival periods. However, the prognosis of the columnar cell variant is still controversial, as cases of CCV- PTC with indolent behavior have also been reported.

MATERIALS AND METHODS: Seven cases of CCV-PTC were identified from surgical pathology at Samsung Medical Center from 1994 to 2016. The histological, architectural, and cytological features fulfilled the diagnostic criteria of the CCV-PTC. We reviewed the US features and clinicopathological findings of 7 cases.

RESULTS: Four young female patients aged from 27 to 34 years (mean, 31.25 years) were proven as indolent clinical course, two old patients aged 55 and 70 years were presented as aggressive clinical course. The remaining one old patient was incidentally found and not followed up. All patients underwent total thyroidectomy and radioiodine therapy. Indolent group had T1 staging without nodal metastasis and no disease during follow-up (range 8-17 years). While aggressive group showed greater tumor size (1.8 cm and 6 cm), gross extrathyroidal extension to muscle, lymph node and distant metastasis. One male patient who recurred immediately after operation died four years after the diagnosis of thyroid cancer. At US, indolent group revealed smooth margin except for one. All two cases of aggressive group had microlobulated margin.

CONCLUSION: CCV-PTC has a good prognosis in young patients with T1 staging. Early recognition and complete treatment prevent aggressive course of this tumor.

SE 085**Efficacy and Safety of Ethanol Ablation for Branchial Cleft Cysts**

Eun Ju Ha¹, Seon Mi Baek², Jung Hwan Baek³,
Su Young Shin², Miran Han¹, Chul-Ho Kim⁴

¹Department of Radiology, Ajou University Hospital, Korea

²Department of Radiology, Sharing and Happiness Hospital, Korea

³Department of Radiology, Asan Medical Center, Korea

⁴Department of Otolaryngology, Ajou University Hospital, Korea

PURPOSE: Branchial cleft cyst (BCC) is a common congenital lesion of the neck. This study evaluated the efficacy and safety of ethanol ablation (EA) as an alterBranchial cleft cyst (BCC) is a common congenital lesion of the neck. This study evaluated the efficacy and safety of ethanol ablation (EA) as an alternative treatment to surgery for BCC.native treatment to surgery for BCC.

MATERIALS AND METHODS: Between September 2006 and October 2016, EA was performed in 22 patients who refused surgery for a second BCC. After the exclusion of two patients who were lost to follow-up, the data of 20 patients were retrospectively evaluated. All index masses were confirmed as benign before treatment. Ultrasound-guided aspiration of the cystic fluid was followed by injection of absolute ethanol (99%) into the lesion. The injected volume of ethanol was 50-80% of the volume of fluid aspirated. Therapeutic outcome, including volume reduction ratio (VRR), therapeutic success rate (VRR > 50% and/or no palpable mass), and complications, were evaluated.

RESULTS: The mean index volume of the cysts was 26.4 ± 15.7 mL (range: 3.8-49.9 mL). After ablation, the mean volume of the cysts decreased to 1.2 ± 1.1 mL (range: 0.0-3.5 mL). The mean VRR at last follow-up was $93.9 \pm 7.9\%$ (range: 75.5-100.0%, $P < 0.001$). Therapeutic success was achieved in all nodules (20/20; 100%), and the symptomatic ($P < 0.001$) and cosmetic ($P < 0.001$) scores had improved significantly by the last follow-up. In one patient, intracystic hemorrhage was developed during the aspiration; however, no major complications

occurred in all patients.

CONCLUSION: EA is an effective and safe treatment for patients with BCC who refuse, or are ineligible for, surgery.

SE 086

The Relationship between Thyroid Nodule Size and Malignancy Risk

Saerom Chung, Jung Hwan Baek, Young Jun Choi, Jeong Hyun Lee

Department of Radiology, Asan Medical Center, Korea

PURPOSE: Several studies have examined the value of thyroid nodule size as a predictor of malignancy, however, results are conflicting. The aim of this study was to evaluate the association between size of thyroid nodule and malignancy risk.

MATERIALS AND METHODS: From January 2013 to December 2013, 3970 thyroid nodules which underwent US-guided fine needle aspiration (FNA) or core needle biopsy (CNB) were retrospectively reviewed. We assessed the relationship between nodule size and malignancy risk. And subgroup analysis according to the pathology of malignant nodule was done.

RESULTS: Of 3970 thyroid nodules, 1170 nodules were malignant. Of those nodules with less than 1 cm in diameter, 42.7% were malignant. In contrast, of those nodules with 1.0 to 1.9 cm, 2.0 to 2.9 cm, 3.0 to 3.9 cm, and 4.0 to 4.9 cm were malignant in 21.35, 18.2%, 17%, and 16.4%. About papillary thyroid carcinoma (n=1009), the thyroid nodule size is inversely related to malignancy risk (Spearman $r = -0.311$, $p < 0.001$), while nodules with follicular carcinoma (n=51) or follicular variant papillary thyroid carcinoma (n=85) shows positive relation to malignancy risk (Spearman $r = 0.127$, Spearman $r = 0.088$, $p < 0.001$).

CONCLUSION: Thyroid nodule size is inversely related to malignancy risk, as larger nodules have lower malignancy rates. However, the risk of follicular carcinomas or follicular variant papillary thyroid carcinomas increases as nodules enlarge.

SE 087

Safety of Radiofrequency Ablation of Benign Thyroid Nodules and Recurrent Thyroid Cancers: A Systematic Review and Meta-Analysis

Saerom Chung, Chong Hyun Suh, Jung Hwan Baek, Hye Sun Park, Young Jun Choi, Jeong Hyun Lee

Department of Radiology, Asan Medical Center, Korea

PURPOSE: Ultrasound-guided RFA has shown good results for benign thyroid nodules and recurrent thyroid carcinoma. Although the types and incidence rates of complications have been assessed, previous studies were limited by their retrospective designs, small numbers of patients, and lack of systematic evaluation. We performed a systematic review and meta-analysis to evaluate the safety of radiofrequency ablation (RFA) for the treatment of benign thyroid nodules and recurrent thyroid cancers.

MATERIALS AND METHODS: Ovid-MEDLINE, EMBASE, and Library of Cochrane databases were searched up to July 12, 2016 for studies on the safety of RFA for treating benign thyroid nodules or recurrent thyroid cancers. Pooled proportions of overall and major complications were assessed using random-effects modeling. Heterogeneity among studies was determined using the χ^2 statistic for the pooled estimates and the inconsistency index I^2 .

RESULTS: A total of 24 eligible studies were included, giving a sample size of 2421 patients and 2786 thyroid nodules. Forty-one major complications and 48 minor complications of RFA were reported, giving a pooled proportion of 2.38% for overall RFA complications [95% confidence interval (CI), 1.42%-3.34%] and 1.35% for major RFA complications (95% CI, 0.89%-1.81%). There were no heterogeneities in either overall or major complications ($I^2 = 1.24\%$ -21.79%). On subgroup analysis, the overall and major complication rates were significantly higher for malignant thyroid nodules than for benign thyroid nodules ($p = 0.0011$ and 0.0038 , respectively).

CONCLUSION: RFA was found to be safe for the treatment of benign thyroid nodules and recurrent thyroid cancers.

SE 089**Ultrasound in Non Palpable Thyroid Masses
Diagnostics**

Nozima Khodjaeva

*Department of Radiology, Mediofarm Private Clinic,
Uzbekistan*

BACKGROUND: Implementation of thyroid ultrasound in daily practice caused the increase of small thyroid lesions detection, which cannot be detected with palpation. Clinical significance of diagnostics of non palpable small thyroid masses is the subject of debates. Nowadays early thyroid microinvasive carcinoma detection are possible, but ultrasound signs of it still has not been systemized.

AIM: To improve early diagnostics of microinvasive thyroid carcinoma.

MATERIALS AND METHODS: Ultrasounds of 45 patients with non palpable thyroid masses were analyzed. In all cases biopsy or surgery were done.

RESULTS: Colloid proliferative goiters were diagnosed in 82,2% of cases, follicular adenomas- in 6,6% of cases, microinvasive cancer- in 11,2% cases. Papillar microcarcinoma had following ultrasound signs: hypoechogenic mass with indistinct wavy shapes (55,5%), hypoechogenic mass with indistinct rounded shapes (26,6%), hypoechogenic mass with clear contours (17,8%).

CONCLUSION: Ultrasound should be included in thyroid cancer screening program, because of possibility of early thyroid lesions detection.

SE 090**Intra- and Inter-Observer Variability in Ultrasound
Measurements of Thyroid Nodules**Hyung Jin Lee, Dae Young Yoon, Young Lan Seo,
Jin Ho Kim, Sora Baek, Kyoung Ja Lim,
Young Kwon Cho, Eun Joo Yun*Department of Radiology, Kangdong Sacred Heart
Hospital, Korea*

OBJECTIVE: The purpose of this study was to assess the intra- and inter-observer variability in ultrasound (US) measurements of thyroid nodules.

METHODS: We performed a prospective study of the US examinations of 73 patients with 122 thyroid

nodules greater than 5 mm in size. US measurements in four dimensions (anteroposterior, transverse, longitudinal, and the maximum diameters) and measurement of the estimated volume (using the ellipsoid formulae) of each thyroid nodule were performed twice by two independent radiologists (A and B, with 10 years and 6 months of experience, respectively). The intra- and inter-observer variability in measurements of thyroid nodules was assessed with Bland-Altman analysis of agreement. The absolute values of intra- and inter-observer variability were compared using Student's t-test.

RESULTS: The 95% limits of intra- and inter-observer agreement for the anteroposterior, transverse, longitudinal, and maximum diameters and estimated volume of thyroid nodules were $\pm 18.2/14.3/21.0\%$, $\pm 17.2/17.3/18.2\%$, $\pm 14.6/15.5/22.3\%$, $\pm 13.8/15.5/19.6\%$, and $\pm 30.2/27.7/44.1\%$, respectively. The absolute values of intra-observer variability were lower than those of inter-observer variability for all measurements.

CONCLUSION: There was considerable intra- and inter-observer variability in US measurement of thyroid nodules, which must be taken into account during the follow-up US of patients with thyroid nodules.

SE 091**US-Guided Ablations of Primary and Recurrent
Thyroid Cancers**Soyeong Jeong, Jung Hwan Baek, Young Jun Choi,
Jeong Hyun Lee*Department of Radiology, Asan Medical Center,
Korea*

Papillary thyroid carcinoma (PTC) is the most common subtype of thyroid malignancy with a good prognosis and a low mortality rate. Surgery is the standard treatment for patients with primary and recurrent thyroid cancer patients. Although patients with PTC show an excellent outcome, the cancer recurrence in the neck ranged from 20% to 59%. When surgery is not available for recurrent thyroid cancers, current guidelines suggest a radioactive iodine therapy, external beam radiation therapy, chemotherapy and image guided ablations. In

primary thyroid cancers, active surveillance has been suggested as a first-line management especially for low-risk PTC (less than 1cm) instead of immediate surgery.

Although surgery is the standard treatment, complications can be increased because distortion of neck anatomy by scar tissue formation, especially in patients with repeated neck dissections. Active surveillance for low risk PTC also has several problems. For these patients, ultrasound (US)-guided ablations such as ethanol ablation (EA) and radiofrequency ablation (RFA) have been suggested as alternatives. The goal of this poster is to evaluate the possible indications, devices, techniques, clinical outcomes and complications of US-guided EA and RFA based on the scientific evidence available and an expert opinion regarding the use of ablations for the primary and recurrent thyroid cancers.

SE 092

Diagnostic Efficacy of Core Needle Biopsy as a First-Line Diagnostic Tool for Low or Intermediate Suspicion Thyroid Nodules: Comparison with Fine Needle Aspiration Using Propensity Score Analysis

Hye Shin Ahn¹, Inyoung Youn², Dong Gyu Na³,
Soo Jin Kim⁴

¹Department of Radiology, Chung-Ang University Hospital, Korea

²Department of Radiology, Kangbuk Samsung Medical Center, Korea

³Department of Radiology, GangNeung Asan Hospital, Korea

⁴Department of Radiology, New Korea Hospital/ Human Medical Imaging and Intervention Center, Korea

PURPOSE: To retrospectively compare the diagnostic efficacy of fine needle aspiration (FNA) and core-needle biopsy (CNB) as a first-line diagnostic tool for low or intermediate suspicion thyroid nodules.

MATERIALS AND METHODS: From January, 2010 to May 2015, consecutive 408 thyroid nodules (≥ 1 cm) with low or intermediate suspicion US patterns were selected from a database of patients who initially underwent CNB at one institution. For the

comparison of CNB, another dataset of consecutive 433 thyroid nodules (≥ 1 cm) were included from patients who initially underwent FNA at two institutions. Adjustments for significant differences in patients' characteristics were facilitated via propensity score matching (PSM). The rate of inconclusive results including nondiagnostic or atypia/follicular lesion of undetermined significance (AUS/FLUS) was compared. Diagnostic values for malignancy and the complication rate of FNA and CNB were evaluated.

RESULTS: A 1:1 matching of 299 patients via PSM yield no significant differences between two groups for any covariate. After PSM, CNB showed lower rates of nondiagnostic result (1.0% vs. 7.0%, $P<0.001$), AUS/FLUS (9.7% vs. 29.4%, $P<0.001$), and inconclusive result (10.7% vs. 36.5%, $P<0.001$) than FNA. A total of 208 FNA and 253 CNB nodules were finally diagnosed. With the criteria of Bethesda category 4, 5, and 6, CNB showed a significantly higher sensitivity (100% vs. 48.0%, $P=0.001$) for malignancy than FNA, while the specificities of those were similar (99.2% vs. 98.4%, $P=0.450$). There were only several cases of mild hemorrhage in both groups. However, the complication rate showed no statistical difference (CNB: 1.47% vs. FNA: 0.23%, $P=0.065$).

CONCLUSION: CNB may be more effective for the diagnosis of malignancy than FNA as a first-line diagnostic tool in low or intermediate suspicion thyroid nodules.

SE 093**Comparison of Diagnostic Efficacy with 18-Gauge and 20-Gauge Ultrasound-Guided Core Needle Biopsy for Thyroid Nodules**

Hye Shin Ahn¹, Mirinae Seo², Su Min Ha¹,
Hee Sung Kim³

¹Department of Radiology, Chung-Ang University
Hospital, Korea

²Department of Radiology, Kyung Hee University
Medical Center, Korea

³Department of Pathology, Chung-Ang University
Hospital, Korea

PURPOSE: To compare the diagnostic efficacy of 18-gauge and 20-gauge ultrasound (US)-guided core needle biopsy (CNB) for diagnosis of the thyroid nodules.

MATERIALS AND METHODS: We included consecutive 81 thyroid nodules of 80 patients who underwent US-guided biopsy with 20-gauge core needle, from September 2014 to November 2015, and consecutive 86 thyroid nodules of 85 patients who underwent US-guided biopsy with 18-gauge core needle, from December 2015 to September 2016 at one tertiary-hospital. The diagnostic results of CNB were categorized into 6 categories based on the six-tier CNB pathology reporting system. The rate of inconclusive results including nondiagnostic or atypia/follicular lesion of undetermined significance (AUS/FLUS) and diagnostic values of CNB for malignancy was compared. The number and type of complication were also described in included patients.

RESULTS: 18-gauge CNB showed lower rate of nondiagnostic result (1.2% vs. 8.6%, $P = 0.026$) than 20-gauge CNB, however AUS/FLUS (27.9% vs. 28.4%, $P = 0.176$) and inconclusive result (29.1% vs. 37.0%, $P = 0.540$) were not significantly different. A total of 43 nodules of 20-gauge CNB and 46 nodules of 18-gauge CNB were finally diagnosed. With the criteria of category 5 and 6, 18-gauge CNB showed a significantly higher sensitivity (75% vs. 66.7%), higher negative predictive value (83.9% vs. 75.9%), and higher accuracy (89.1% vs. 83.7%) for malignancy than 20-gauge CNB. There was no major complication in all patients and mild hematoma was reported in 3 patients of 18-gauge CNB (3.5%) and 2

patients of 20-gauge CNB (2.5%).

CONCLUSION: The CNB with 18-gauge core needle will be more effective for the diagnosis of malignancy in thyroid nodules than CNB with 20-gauge core needle.

SE 094**Comparison of Core Needle Biopsy and Fine Needle Aspiration as a First-Line Diagnostic Tool in High Suspicion Thyroid Nodules Using Propensity Score Analysis**

Inyoung Youn¹, Hye Shin Ahn², Dong Gyu Na³,
Soo Jin Kim⁴

¹Department of Radiology, Kangbuk Samsung
Medical Center, Korea

²Department of Radiology, Chung-Ang University
Hospital, Korea

³Department of Radiology, GangNeung Asan
Hospital, Korea

⁴Department of Radiology, New Korea Hospital/
Human Medical Imaging and Intervention Center,
Korea

To compare the core needle biopsy (CNB) and fine needle aspiration (FNA) as a first-line diagnostic tool in high suspicion thyroid nodules. We included consecutive high suspicion nodules (> 5 mm) in which CNB was performed at one institution ($n=419$) and in which FNA was performed at other two institutions ($n=405$) as a first-line diagnostic tool. With propensity score matching (PSM), we facilitated the adjustments for significant differences in patients' baseline characteristics. The rate of inconclusive results and diagnostic values were compared between the results of CNB and FNA. Each 57 CNB and FNA group nodules were extracted using PSM analysis from a total of 824 nodules. CNB showed a lower rate of inconclusive results (8.1% vs. 32.8%, $p<0.001$) including nondiagnostic (1.7% vs. 7.4%) and AUS/FLUS (6.4% vs. 25.4%) results compared with FNA, and PSM analysis also showed a significantly lower rate of inconclusive results ($P<0.001$). With the criteria of Bethesda category 4, 5, and 6, CNB showed significantly higher sensitivity for malignancy in total nodules (99.3% vs. 87.5%, $P<0.001$) and PSM nodules (100% vs.

85.7%, $P=0.019$) regardless of the nodule size. With the criteria of Bethesda category 6, CNB also showed significantly higher sensitivity for malignancy in total nodules (93.7% vs. 67.6%, $P<0.001$) and PSM nodules (91.7% vs. 71.4%, $P=0.033$) regardless of the nodules size. The specificity for malignancy was similarly high in both CNB and FNA group nodules ($P>0.05$). CNB showed lower inconclusive results and higher sensitivity for malignancy, and CNB may be more effective than FNA as a first-line diagnostic tool in high suspicion nodules.

SE 095

Tuberculosis in Thyroid

Munkhdul Altankhuyag

Department of Radiology, UB Songdo Hospital,
Mongolia

BACKGROUND: Tuberculosis (TB) of the head and neck commonly involved cervical lymph nodes, larynx, pharynx, and timely diagnosis of the disease is paramount. In this report, we describe a rare case of TB that involved thyroid only.

KEY WORDS: thyroid, tuberculosis

A 47-years-old lady noticed an enlargement in the anterior neck. Ultrasound revealed 2.6×3.3 cm sized isoechoic capsulated lesion with irregular margins and inhomogeneous structure in the left thyroid lobe. The right thyroid lobe measured 1.7×1.5×1.2 cm, showed a well-defined heterogeneous lesion with surrounding hypoechoic halo lesion. Cervical lymph nodes were unremarkable.

Laboratory test shows total T3 1.37 ng/ml, free T4 0.86 ng/dl, TSH 0.531 uIU/ml.

The US and laboratory findings were suspicious for a follicular adenoma. The FNA biopsy supported the presence of adenoma. Therefore, partial thyroidectomy had been performed, with the final histology of operative specimen revealed tuberculoma.

CONCLUSION: The isolated thyroid TB is rare, however, a thorough knowledge of head and neck TB is essential because early diagnosis and therapy can prevent a permanent loss of function or needless surgery.

SE 096

Radiofrequency Ablation for Nonfunctioning Benign Thyroid Nodules in Children and Adolescents

Jin Yong Sung

Department of Radiology, Daerim St. Mary's
Hospital, Korea

PURPOSE: To retrospectively evaluate efficacy and safety of radiofrequency (RF) ablation for nonfunctioning benign thyroid nodules in Children and Adolescents.

MATERIALS AND METHODS: We evaluated 14 pediatric patients (M:F ratio=4:10, mean age, 15.7±2.3 [range, 12-19]) with nonfunctioning benign thyroid nodules (mean longest diameter, 3.7±1.1 cm [range, 2.0-5.6 cm]) who were treated with RF ablation between 2005 and 2015. The inclusion criteria for RF ablation therapy were 1) benign cytological confirmation in at least two separate fine needle aspiration and/or core needle biopsy, 2) reports of pressure symptoms or cosmetic problems caused by thyroid nodules, 3) without spiculated/microlobulated margin, microcalcification, nonparallel shape, or evidence of lymph node metastasis on ultrasonography (US), 4) normal serum levels of thyroid hormone and thyrotropin, and 5) follow-up periods of more than 6 months. RF ablation was performed with using a RF generator and an 18-gauge internally cooled electrode. Changes in nodules on follow-up US and complication during and after RF ablation were evaluated.

RESULTS: The mean follow-up period was 36.9±21.7 (range, 6-69) months. At last follow-up, the longest nodule diameter and volume significantly decreased (3.7±1.1 cm vs. 1.4±0.9 cm and 14.6±13.3 mL vs. 1.7±4.4 mL, respectively; $p<0.05$). Both cosmetic and compressive symptoms significantly improved (3.8±1.0 vs. 1.4±0.4 and 3.4±1.0 vs. 0.1±0.4, respectively; $p<0.05$). Mean number of ablation sessions was 2.1±1.2. There was no major complication during and after RF ablation.

CONCLUSION: RF ablation could be a safe and effective treatment modality for nonfunctioning benign thyroid nodules in children and adolescents.

Author Index

A

Adiya, Altantsetseg: SE 027 (p171)
 Agrawal, Nitesh: SE 008 (p160), SE 014 (p163), SE 015 (p164)
 Ahn, Dongbin: SE 060 (p184)
 Ahn, Hye Shin: SE 092 (p200), SE 093 (p201), SE 094 (p201)
 Ahn, Kookjin: SS 1 THY-8 (p131)
 Ahn, Su Joa: SS 3 ABD-7 (p146), SE 018 (p166)
 Alhabshi, Sharifah Majedah Idrus: SC 2 BR-2 (p152)
 Altangerel, Bilegt: SE 009 (p161)
 Altankhuyag, Munkhdul: SE 095 (p202)
 Ametembun, Maria Goretti: SE 071 (p190)
 An, Jin Kyung: SE 059 (p184)
 An, Su Joa: YIA-1 (p140)
 Arora, Ankur: SE 015 (p164)
 Atakhanova, Nigora: SE 032 (p173)

B

Baek, Jung Hwan: SS 1 THY-3 (p128), SS 1 THY-5 (p129), SC 1 THY-4 (p133), SC 1 THY-6 (p134), SC 1 THY-7 (p134), SC 1 THY-8 (p135), YIA-3 (p141), SE 083 (p196), SE 085 (p197), SE 086 (p198), SE 087 (p198), SE 091 (p199)
 Baek, Seon Mi: SC 1 THY-8 (p135), SE 085 (p197)
 Baek, Sora: SE 090 (p199)
 Bang, Minseo: SE 025 (p169)
 Bayarsaikhan, Tsengel: SE 082 (p195)
 Betgeri, Somsharan: SS 3 ABD-5 (p144)
 Bhatia, Kunwar: MP 1 THY (p19), SC 1 THY-1 (p35)
 Bihari, Chhagan: SE 015 (p164)
 Bor, Amartuvshin: SE 011 (p162), SE 012 (p162)
 Byun, Jae Young: SS 3 ABD-2 (p142)
 Byun, Seonghwan: SE 056 (p183)

C

Cha, Jaehyung: SC 2 BR-8 (p155), SE 030 (p172)
 Cha, Joo Hee: SFS 4 BR-3 (p77)
 Cha, Yoogi: SE 040 (p177)
 Chae, Hee-Dong: CR -1 (p138)
 Chae, Soo Young: SE 063 (p186)
 Chai, Jee Won: CC 1 MSK-1 (p23)
 Chang, Jung Min: SC 2 BR-6 (p154)
 Chang, Won Chang: YIA-1 (p140)
 Chang, Won: SS 3 ABD-7 (p146), SE 018 (p166)
 Chang, Yun-Woo: CC 7 PED-3 (p102), SE 025 (p169)

Cheng, Ming Huan: SE 038 (p176)
 Cheon, Jung-Eun: SS 4 PED-1 (p148), SS 4 PED-5 (p150), SS 4 PED-7 (p151), CC 7 PED-1 (p95)
 Cho, Eun: SC 2 BR-5 (p154), SE 029 (p172), SE 041 (p177)
 Cho, Eun-Suk: SE 049 (p181)
 Cho, Jinhan: SE 006 (p159)
 Cho, Jooyeon: SE 084 (p197)
 Cho, Kyu Ran: SC 2 BR-8 (p155), SE 030 (p172), SE 042 (p177)
 Cho, Yeon Jin: SS 4 PED-7 (p151)
 Cho, Yoon Joo: SS 1 THY-7 (p130)
 Cho, Young Ah: SS 4 PED-6 (p151)
 Cho, Young Kwon: SE 090 (p199)
 Cho, Young Seo: SE 050 (p181), SE 057 (p183), SE 058 (p184)
 Choi, Bo Bae: SE 026 (p170), SE 043 (p178)
 Choi, Byung Ihn: MP 3 ABD-1 (p21)
 Choi, Chul Soon: SE 003 (p158), SE 017 (p165)
 Choi, Chung Hwan: SS 3 ABD-6 (p145)
 Choi, Dong Whan: SC 1 THY-7 (p134)
 Choi, Eun Jung: SE 022 (p168), SE 025 (p169)
 Choi, Gayoung: SE 005 (p159)
 Choi, Hyunsuk: SS 1 THY-8 (p131)
 Choi, Jae Woong: SE 005 (p159), SE 013 (p163)
 Choi, Ji Soo: YIA-2 (p141), SE 023 (p168), SE 034 (p174)
 Choi, Joon-Il: SS 3 ABD-2 (p142)
 Choi, Jung-Ah: SS 2 MSK-3 (p136), SE 068 (p188)
 Choi, Min Joo: SE 082 (p195)
 Choi, Moon Hyung: SS 3 ABD-2 (p142), CC 6 GU-1 (p84)
 Choi, Seo-Youn: SE 056 (p183)
 Choi, Young Hun: SS 4 PED-1 (p148), SS 4 PED-5 (p150), SS 4 PED-7 (p151)
 Choi, Young Jun: SS 1 THY-5 (p129), SC 1 THY-6 (p134), SE 086 (p198), SE 087 (p198), SE 091 (p199)
 Choo, Hye Jung: SE 028 (p171), SE 033 (p174), SE 066 (p187), SE 070 (p189)
 Choo, Hyejung: SE 067 (p188), SE 069 (p189)
 Chun, Eun Ju: CC 5 CV-4 (p74)
 Chung, Jae-Joon: SE 049 (p181)
 Chung, Saerom: SS 1 THY-5 (p129), SE 086 (p198), SE 087 (p198)

D

Danga, Tumendemberel: SE 039 (p176)
 Davaasuren, Munkhtsetseg: SE 048 (p180)
 Desai, Saloni: SS 3 ABD-5 (p144), SE 008

(p160), SE 014 (p163), SE 015 (p164)
 Dorjpalam, Undarmaa: SE 007 (p159)
 Duisyenbi, Zaya: SE 027 (p171)

E

Erdenebaatar, Soyolmaa: SE 009 (p161)
 Eun, Su-Yong: SE 082 (p195)

F

Fan, Xiaoming: SS 3 ABD-1 (p142)
 Ferraioli, Giovanna: MP 3 ABD-2 (p22), SFS 1 ABD-1 (p28)

G

Galbaatar, Chantsalsuren: SE 027 (p171)
 Ganbold, Urantzaya: SE 046 (p179)
 Ghimire, Ram Kumar: SS 4 GU-1 (p147)
 Go, Dooyoung: SE 080 (p194)
 Gochoo, Mendsaikhan: SE 048 (p180)
 Gutte, Avinash: SE 051 (p182)

H

Ha, Dong-Ho: SS 2 MSK-5 (p137)
 Ha, Eun Ju: SS 1 THY-7 (p130), SC 1 THY-4 (p133), CC 4 THY-3 (p47), SE 085 (p197)
 Ha, Ji Young: SS 4 PED-7 (p151)
 Ha, Sang Yun: SS 3 ABD-6 (p145)
 Ha, Seung Mi: YIA-2 (p141)
 Ha, Su Min: SC 1 THY-7 (p134), SE 083 (p196), SE 093 (p201)
 Hahn, Soo Yeon: SS 1 THY-4 (p129), SC 1 THY-5 (p133)
 Hahn, Soo Yeun: SE 084 (p197)
 Han, Boo-Kyung: YIA-2 (p141), SE 023 (p168), SE 034 (p174)
 Han, Joon Koo: SS 3 ABD-4 (p144), SS 3 ABD-7 (p146), SE 001 (p157), SE 018 (p166)
 Han, Kyunghwa: SC 1 THY-2 (p131), SC 1 THY-3 (p132)
 Han, Miran: SS 1 THY-7 (p130), SE 085 (p197)
 Han, Sang Won: SS 4 PED-3 (p149)
 Hashimoto, Beverly: MP 6 BR (p66), SFS 4 BR-1 (p75)
 Holland, Christy: JS 1 (p63)
 Hong, Doran: SS 4 PED-2 (p149)
 Hong, Eun Kyoung: SS 4 PED-1 (p148)
 Hong, Hanh Tuong Thi: SE 002 (p157)
 Hong, Hyun Sook: CC 7 PED-2 (p98)
 Hong, Min Ji: SS 1 THY-3 (p128)
 Hong, Myung Sun: SE 047 (p180)
 Huy, Hoang Nguyen: SE 002 (p157)

Author Index

Hwang, Chul Mok: SE 045 (p178)
 Hwang, Eunjin: SS 2 MSK-3 (p136), SE 068 (p188)
 Hwang, Ik Jung: SE 033 (p174)
 Hwang, Mi Soo: SE 021 (p167)
 Hwang, Sung Il: SFS 6 GU-2 (p112)

J

J., Tsetsegee: SE 011 (p162), SE 012 (p162)
 Jang, Hyeon Ji: SE 026 (p170)
 Jang, Jinhee: SS 1 THY-8 (p131)
 Jantsansengee, Baigalmaa: SE 009 (p161)
 Je, Bo-Kyung: SS 4 PED-2 (p149)
 Jeon, Tae Yeon: SFS 5 PED-2 (p80), SE 078 (p193)
 Jeong, Hae Woong: SE 028 (p171), SE 033 (p174)
 Jeong, Soyeong: SE 091 (p199)
 Jeong, Sun Hye: SE 025 (p169)
 Jin, Tiefeng: SE 019 (p166)
 Jo, Jeonghyun: CC 5 CV-2 (p68)
 Jun, Jae Kwan: SE 022 (p168), SE 025 (p169)
 Jung, Ah Young: SS 4 PED-6 (p151)
 Jung, Eui Chul: SE 059 (p184)
 Jung, Hyun Kyung: SE 037 (p176)
 Jung, Kyoonsun: SC 2 BR-8 (p155)
 Jung, Na Young: SC 2 BR-7 (p155)
 Jung, So Lyung: SS 1 THY-8 (p131)
 Jung, Won-Bin: SS 2 MSK-2 (p136)
 Jung, Yoon Young: SE 059 (p184), SE 077 (p193)

K

Kahhorov, Jamoliddin: SE 031 (p173), SE 032 (p173), SE 036 (p175)
 Kakkhkharov, Alisher: SE 031 (p173), SE 032 (p173), SE 036 (p175)
 Kakkhkharova, Fatima: SE 031 (p173), SE 036 (p175)
 Kang, Bong Joo: SC 2 BR-1 (p94), SC 2 BR-4 (p153), SC 2 BR-7 (p155), SE 024 (p169), SE 035 (p175)
 Kang, Gwansuk: SE 082 (p195)
 Kang, Hye Seon: SE 043 (p178)
 Kang, Hyo-Jin: YIA-1 (p140), SS 3 ABD-4 (p144), SS 3 ABD-7 (p146), SE 001 (p157), SE 018 (p166)
 Kang, Jinbum: SE 079 (p194), SE 080 (p194), SE 081 (p195)
 Kang, Seongsu: SE 076 (p192)
 Kang, Sun Young: SS 4 PED-1 (p148)
 Kang, Tae Wook: SS 3 ABD-6 (p145)
 Kang, Yusuhn: CC 1 MSK-2 (p24)
 Khanal, Umesh: SS 4 GU-1 (p147)
 Khil, Eun-Kyung: SS 2 MSK-3 (p136), SE

068 (p188)
 Khodjaeva, Nozima: SE 089 (p199)
 Khurelsukh, Khulan: SE 027 (p171)
 Kim, Bum-Soo: SS 1 THY-8 (p131)
 Kim, Chul-Ho: SE 085 (p197)
 Kim, Dong Won: SE 052 (p182)
 Kim, Dong Wook: SE 028 (p171), SE 033 (p174), SE 061 (p185)
 Kim, Eun Sil: SC 2 BR-8 (p155)
 Kim, Eun-Kyung: SC 1 THY-2 (p131), SC 1 THY-3 (p132), SC 2 BR-3 (p153), SC 2 BR-5 (p154)
 Kim, Hankyul: SE 034 (p174)
 Kim, Hee Sung: SE 093 (p201)
 Kim, Heung Cheol: SE 047 (p180)
 Kim, Hoe Suk: SE 019 (p166)
 Kim, Hye Won: SE 025 (p169), SE 040 (p177)
 Kim, Hyoung Seop: SE 059 (p184)
 Kim, Hyun Cheol: SE 054 (p183)
 Kim, Hyung Ham: CC 2 PHY-3 (p34)
 Kim, In-One: SS 4 PED-1 (p148), SS 4 PED-5 (p150), SS 4 PED-7 (p151)
 Kim, Jae Kyun: SE 083 (p196)
 Kim, Jeong Kyu: SS 1 HN-1 (p127), SE 060 (p184)
 Kim, Jeong Rye: SS 4 PED-6 (p151)
 Kim, Jeong Woo: SE 005 (p159), SE 013 (p163)
 Kim, Ji Hye: SE 078 (p193)
 Kim, Ji-Hoon: SS 1 THY-3 (p128), SS 1 THY-6 (p130), SC 1 THY-4 (p133), SC 1 THY-7 (p134),
 Kim, Ji Su: SE 054 (p183)
 Kim, Ji Youn: SE 045 (p178)
 Kim, Jin Ho: SE 090 (p199)
 Kim, Joo Hee: SE 049 (p181)
 Kim, Jung Hoon: SS 3 ABD-4 (p144), SE 001 (p157)
 Kim, Keum Won: SE 025 (p169), SE 045 (p178)
 Kim, Kyeong Ah: SE 005 (p159), SE 013 (p163)
 Kim, Min Jung: SC 2 BR-3 (p153), SC 2 BR-5 (p154)
 Kim, Myung-Joon: SS 4 PED-3 (p149), SS 4 PED-4 (p150)
 Kim, Sang Won: SE 054 (p183)
 Kim, Soo Jin: CC 3 ABD-2 (p38), SE 092 (p200), SE 094 (p201)
 Kim, Soo-Yeon: SC 2 BR-6 (p154)
 Kim, Sujin: SS 2 MSK-5 (p137), SE 029 (p172), SE 041 (p177)
 Kim, Suk Jung: SE 037 (p176)
 Kim, Sung Hun: SFS 4 BR-2 (p76), SC 2 BR-4 (p153), SC 2 BR-7 (p155), SE 022 (p168), SE 024 (p169), SE 035 (p175)

Kim, Sung Kwan: SE 070 (p189)
 Kim, Sungchan: SE 079 (p194)
 Kim, Tae Hyuk: SS 1 THY-4 (p129)
 Kim, Tae-Yoon: SS 2 MSK-4 (p137)
 Kim, Woo Sun: SS 4 PED-1 (p148), SS 4 PED-5 (p150), SS 4 PED-7 (p151)
 Kim, Yeun-Yoon: SC 1 THY-3 (p132)
 Kim, Yongsang: SE 077 (p193)
 Kim, Yongsoo: SE 050 (p181), SE 057 (p183)
 Kim, Yoong Joong: SE 045 (p178)
 Kim, You Me: SE 022 (p168), SE 025 (p169)
 Kim, Youngseon: SE 021 (p167)
 Kim, Yumi: SC 2 BR-4 (p153), SC 2 BR-7 (p155)
 Kim, Yun Ju: SE 024 (p169), SE 035 (p175)
 Kim, Yura: CR -4 (p140)
 Ko, Eun Sook: YIA-2 (p141), SE 023 (p168), SE 034 (p174)
 Ko, Eun Young: YIA-2 (p141), CC 8 BR-2 (p122), SE 023 (p168), SE 034 (p174)
 Koh, Esther: CR -3 (p139)
 Kwak, Jin Young: SC 1 THY-2 (p131), SC 1 THY-3 (p132)
 Kwon, Dae-Gil: SS 2 MSK-2 (p136), SE 065 (p186)
 Kwon, Dong Rak: SS 2 MSK-2 (p136), SE 064 (p186), SE 065 (p186), SE 073 (p191)
 Kwon, Heejin: SE 006 (p159)
 Kwon, Myoungae: SS 4 PED-2 (p149), SE 030 (p172)

L

Lee, Ahwon: SE 024 (p169)
 Lee, Chang Hee: SE 005 (p159), SE 013 (p163)
 Lee, Dong Ho: SS 3 ABD-8 (p146), SS 3 ABD-9 (p147)
 Lee, Ducky: SC 1 THY-7 (p134)
 Lee, Eun Hye: SE 022 (p168), SE 025 (p169)
 Lee, Eunsol: YIA-3 (p141)
 Lee, Ga Young: SE 066 (p187)
 Lee, Gun Woo: SS 3 ABD-6 (p145)
 Lee, Hae Kyung: SE 056 (p183)
 Lee, Hojung: SE 081 (p195)
 Lee, Hyung Jin: SE 090 (p199)
 Lee, Jae Young: SS 3 ABD-8 (p146), SS 3 ABD-9 (p147), SFS 3 KSTU-2 (p59)
 Lee, Jeong Hyun: SS 1 THY-5 (p129), SC 1 THY-6 (p134), SE 086 (p198), SE 087 (p198), SE 091 (p199)
 Lee, Jeong Min: YIA-1 (p140), SS 3 ABD-7 (p146), SE 018 (p166)
 Lee, Jeong-Hoon: YIA-1 (p140)
 Lee, Jeonghoon: YIA-3 (p141)

Author Index

Lee, Ji Eun: SE 056 (p183)
 Lee, Ji Hye: SC 1 THY-2 (p131)
 Lee, Jin Hwa: SE 025 (p169), SE 029 (p172), SE 041 (p177)
 Lee, Jin Seong: SS 4 PED-6 (p151)
 Lee, Jong Hyon: SS 3 ABD-6 (p145)
 Lee, Jongmee: SE 005 (p159), SE 013 (p163)
 Lee, Ju-Han: SE 030 (p172)
 Lee, Jung Hun: SE 053 (p182)
 Lee, Jung Hyun: SS 3 ABD-6 (p145)
 Lee, Jung Min: SC 2 BR-4 (p153), SC 2 BR-7 (p155)
 Lee, Mi-Jung: SS 4 PED-3 (p149), SS 4 PED-4 (p150), SFS 5 PED-1 (p78)
 Lee, Min Hee: MP 2 MSK (p20), SE 056 (p183)
 Lee, Sang Min: YIA-1 (p140), SS 3 ABD-4 (p144), SS 3 ABD-7 (p146), SE 001 (p157), SE 018 (p166)
 Lee, Sangyun: SE 006 (p159)
 Lee, Seun-Ah: SS 2 MSK-3 (p136), SE 068 (p188)
 Lee, Seunghyun: SS 4 PED-7 (p151)
 Lee, Song: SS 1 THY-8 (p131)
 Lee, Sumin: SE 067 (p188)
 Lee, Sun Joo: SE 028 (p171), SE 033 (p174), SE 066 (p187), SE 070 (p189)
 Lee, Sung Moon: SE 066 (p187), SE 067 (p188), SE 069 (p189), SE 070 (p189)
 Lee, Sunjoo: SE 067 (p188), SE 069 (p189)
 Lee, Yedaun: CC 3 ABD-3 (p39)
 Lee, Yeon Soo: SE 072 (p190)
 Lee, Yong Seung: SS 4 PED-3 (p149)
 Lee, Yoo Jin: SE 028 (p171), SE 033 (p174), SE 061 (p185)
 Lee, Yoon Jin: CC 3 ABD-4 (p41)
 Lee, Youn Joo: SE 035 (p175)
 Lee, Young Hwan: SE 053 (p182)
 Lee, Young Jonn: SS 3 ABD-2 (p142)
 Lim, Hyun Kyung: SC 1 THY-8 (p135)
 Lim, Kyoung Ja: SE 017 (p165), SE 090 (p199)
 Lim, Sanghyeok: SE 050 (p181), SE 057 (p183)
 Lkhagvasuren, Gonchigsuren: SE 044 (p178)
 Lkhagvasuren, Tumenjargal: SE 044 (p178)

M

Martinoli, Carlo: SFS 2 MSK-1 (p49), SFS 2 MSK-2 (p50)
 McCarville, M Beth: MP 4 PED (p64), SFS 5 PED-3 (p83)
 Momin, Asif: SE 051 (p182), SE 062 (p185)
 Momin, Shenaz: SE 051 (p182), SE 062 (p185)

Moon, Hee Jung: SC 1 THY-2 (p131), SC 1 THY-3 (p132), SC 2 BR-3 (p153), SC 2 BR-5 (p154)
 Moon, Ji Yoon: SE 003 (p158)
 Moon, Sung Kyoung: CC 6 GU-4 (p93)
 Moon, Woo Kyung: SC 2 BR-6 (p154), SE 019 (p166)
 Mukund, Amar: SS 3 ABD-5 (p144), SE 008 (p160)
 Munkhbat, Sarnaitsetseg: SE 009 (p161), SE 027 (p171)

N

Na, Dong Gyu: SS 1 THY-3 (p128), SC 1 THY-4 (p133), SC 1 THY-7 (p134), CC 4 THY-2 (p45), SE 092 (p200), SE 094 (p201)
 Na, Jung Hye: SE 063 (p186)
 Namkung, Sook: SE 047 (p180)
 Namuuntsetseg, Enkhtaivan: SE 075 (p192)
 Nguyen, Anh: SS 3 ABD-3 (p143)
 Nguyen, Hung: SS 3 ABD-3 (p143)
 Nyamkhuu, Narantungalag: SE 004 (p158)

O

Ochirpurev, Bayanjargal: SE 048 (p180)
 Oh, Jongyoung: SE 006 (p159)
 Oh, Saelin: SE 078 (p193)
 Oh, Sueyoung: YIA-3 (p141)
 Oh, Young Lyun: SS 1 THY-4 (p129), SE 084 (p197)

P

Paeng, Dong-Guk: SFS 3 KSTU-4 (p62)
 Pahk, Ki Joo: SFS 3 KSTU-3 (p60)
 Panta, Om Biju: SS 4 GU-1 (p147)
 Pargewar, Sudheer: SS 3 ABD-5 (p144), SE 008 (p160), SE 014 (p163), SE 015 (p164)
 Park, Ah Young: SC 2 BR-8 (p155), CC 8 BR-1 (p119)
 Park, Byung Kwan: MP 5 GU (p65)
 Park, Cheol Min: SE 005 (p159), SE 013 (p163)
 Park, Eun Hae: CC 1 MSK-3 (p26)
 Park, Eun-Ah: CC 5 CV-1 (p67)
 Park, Gi-Young: SS 2 MSK-2 (p136), SE 064 (p186), SE 065 (p186), SE 073 (p191)
 Park, Hee Jin: SE 016 (p165)
 Park, Hye Sun: SE 087 (p198)
 Park, Ji Eun: SS 4 PED-5 (p150)
 Park, Jinhyung: CC 2 PHY-2 (p33)
 Park, Joo Hyun: SE 034 (p174)
 Park, Jung Hyun: SE 065 (p186)

Park, Jungwon: SE 069 (p189)
 Park, Mi-Suk: SFS 1 ABD-2 (p29)
 Park, Sae Jin: SS 3 ABD-7 (p146)
 Park, Sekyoung: CR -2 (p139)
 Park, So Yeon: SE 042 (p177)
 Park, Youngjean: CC 8 BR-3 (p126), SC 1 THY-2 (p131), SC 1 THY-3 (p132), SC 2 BR-3 (p153), SC 2 BR-5 (p154)
 Park, Yang Shin: SE 005 (p159), SE 013 (p163)
 Park, Yangshin: CC 3 ABD-1 (p36)
 Park, Young Mi: SE 028 (p171), SE 033 (p174), SE 037 (p176)
 Phan, Hai: SS 2 MSK-1 (p135), SS 3 ABD-3 (p143)

Q

Quang, Trong Nguyen: SFS 6 GU-1 (p106), SFS 6 GU-3 (p114)

R

Rajesh, S: SS 3 ABD-5 (p144), SE 008 (p160), SE 014 (p163), SE 015 (p164)
 Rentsensambuu, Saruulzaya: SE 010 (p161)
 Rha, Sung Eun: SS 3 ABD-2 (p142)
 Roh, Sang Soo: SE 028 (p171)
 Roh, Younghoon: SE 006 (p159)
 Roh, Yun Ho: SS 4 PED-3 (p149)
 Ryoo, Inseon: SE 063 (p186)
 Ryu, Jeong Ah: SS 2 MSK-4 (p137)
 Ryu, Young Jin: SS 4 PED-5 (p150)

S

Seo, Bo Kyoung: SC 2 BR-8 (p155), SE 030 (p172), SE 042 (p177)
 Seo, Dong Wan: SFS 1 ABD-3 (p30)
 Seo, Jae Young: SE 045 (p178)
 Seo, Jongbum: SFS 3 KSTU-2 (p51)
 Seo, Mirinae: SE 020 (p167), SE 093 (p201)
 Seo, Young Lan: SE 017 (p165), SE 090 (p199)
 Seol, Hae Young: SE 063 (p186)
 Sereejav, Enkhbold: SE 007 (p159), SE 046 (p179), SE 075 (p192)
 Sereenendorj, Norjmaa: SE 074 (p191)
 Shim, Young Sup: CC 6 GU-3 (p92)
 Shin, Gi Won: SE 028 (p171), SE 033 (p174), SE 037 (p176)
 Shin, Hye Seon: SE 042 (p177)
 Shin, Hyun Joo: SS 4 PED-3 (p149), SS 4 PED-4 (p150)
 Shin, Ilah: SS 1 THY-2 (p128)
 Shin, Jung Hee: SS 1 THY-4 (p129), SC 1 THY-5 (p133), SC 1 THY-6 (p134), CC

Author Index

4 THY-1 (p43), SE 084 (p197)
 Shin, Su Young: SE 085 (p197)
 Sim, Ki Choon: CC 6 GU-2 (p91)
 Singh, Harsh: SS 4 GU-1 (p147)
 Sinn, Dong Hyun: SS 3 ABD-6 (p145)
 Sohn, Yu-Mee: SE 020 (p167)
 Son, Ho-Jin: SS 1 HN-1 (p127)
 Song, Byung Joo: SE 024 (p169)
 Song, Ilseob: SE 079 (p194), SE 081 (p195)
 Song, You Seon: CC 5 CV-3 (p72)
 Suh, Chong Hyun: SE 087 (p198)
 Suh, Sangil: SE 063 (p186)
 Sul, Hae Joung: SE 072 (p190)
 Sumya, Ul-Oldokh: SE 039 (p176)
 Sung, Jin Yong: SS 1 THY-3 (p128), SC 1
 THY-4 (p133), SC 1 THY-7 (p134), SE
 096 (p202)

T

Tayade, Kalpana: SS 1 THY-1 (p127)
 Tayade, Prakash: SS 4 GU-2 (p148)
 Teo, Yin Eie: SE 038 (p176)
 Tran, Chau: SS 2 MSK-1 (p135)
 Tsegmed, Erdembileg: SE 048 (p180)
 Tsendjav, Tuvshinjargal: SE 011 (p162), SE
 012 (p162)
 Tserendorj, Badamsed: SE 004 (p158), SE
 010 (p161)

Tserenjav, Otgontuya: SE 039 (p176)
 Tsevegmid, Erdembileg: SE 011 (p162), SE
 012 (p162)

V

Van, Riep Tran: SE 002 (p157)
 Vo, Quyen: SS 2 MSK-1 (p135)

W

Wong, Yi Li (Grace): SC 2 BR-2 (p152)
 Woo, Jeong Joo: SE 059 (p184)
 Woo, Ok Hee: SC 2 BR-8 (p155), SE 030
 (p172), SE 042 (p177)

Y

Yang, Dal Mo: SE 054 (p183)
 Yang, Hyun Kyung: SS 3 ABD-4 (p144), SS
 3 ABD-7 (p146), SE 001 (p157), SE
 018 (p166)
 Yang, Ko Eun: SE 047 (p180)
 Yeoh, Hyun Jung: SS 2 MSK-4 (p137)
 Yi, Boem Ha: SE 056 (p183)
 Yoo, Hyunju: SC 1 THY-7 (p134)
 Yoo, Roh-Eul: SS 1 THY-6 (p130)
 Yoo, So-Young: SE 078 (p193)
 Yoo, Yangmo: SE 079 (p194), SE 080

(p194), SE 081 (p195)

Yoo, Young Jin: SS 1 THY-7 (p130)
 Yoon, Changan: CC 2 PHY-1 (p32)
 Yoon, Dae Young: SE 003 (p158), SE 017
 (p165), SE 090 (p199)
 Yoon, Haesung: SS 4 PED-3 (p149), SS 4
 PED-4 (p150)
 Yoon, Hee Mang: SS 4 PED-6 (p151)
 Yoon, Jae Hong: SE 029 (p172), SE 041
 (p177)
 Yoon, Jeong Hee: SS 3 ABD-7 (p146)
 Yoon, Jung Hyun: SC 1 THY-2 (p131), SC 1
 THY-3 (p132), SC 2 BR-3 (p153), SC
 2 BR-5 (p154)
 Yoon, Min Jae: SE 045 (p178)
 Yoon, Seong Kuk: SE 052 (p182)
 You, Myung Won: SE 059 (p184), SE 077
 (p193)
 You, Sun Kyoung: SE 076 (p192)
 Youn, Inyoung: SE 092 (p200), SE 094
 (p201)
 Yu, Jeong-Sik: SE 049 (p181)
 Yun, Eun Joo: SE 003 (p158), SE 017
 (p165), SE 090 (p199)

Z

Zeng, Zeng: SS 3 ABD-1 (p142)
 Zhang, Meihua: SE 019 (p166)